Western Australian School of Mines

Early Strength of Shotcrete

Hla Aye Saw

This thesis is presented for the Degree of
Doctor of Philosophy
of
Curtin University

June, 2015

DECLARATION

To the best of my knowledge and belief this contains no materials previously published by any other person expect where due acknowledgement has been made.

This thesis contains no material which has been accepted for the award of any other degree or diploma in any university.

Signed:.....

Date:.....

ABSTRACT

Shotcrete is a designed material which comprises of cement, supplementary cementing mineral, fine and coarse aggregates, chemical admixtures, water and usually fibres. The physical, chemical and mechanical properties of each of these constituent materials affect the mechanical properties of the gelling, setting and hardening of the final shotcrete. The strength of a shotcrete is its ability to withstand an applied stress without failure.

Shotcrete for underground mine support often requires rapid setting and early strength development of the freshly sprayed shotcrete. In underground mining industry the early strength of the shotcrete generally refers to the strength developed from the time of spraying (0) to (4) hours curing. The early strength is usually determined by indirect methods and correlated to the strength development with time.

A total 248 shear strength tests (175 vane shear tests and 73 triaxial tests) were conducted for different mix designs of shotcrete paste in this research. The test results provide shear strength development with time for shotcrete paste with and without the influences of chemical admixtures, such as accelerator, superplasticiser, water reducing admixture and hydration stabiliser, as well as synthetic fibre and aggregates at the early age of hydration, which is between 10 minutes to 8 hours after mixing.

More than 100 electrical resistance developments with time were measured in the laboratory for the shotcrete paste with different mix design during the development of different version of a prototype electrical resistance measurement probe. The test results provide electrical resistance development with time for shotcrete paste with and without the influences of chemical admixtures, such as accelerator, superplasticiser, water reducing admixture and hydration stabiliser, as well as synthetic fibre and aggregates at the early age of hydration, which is between 0 minutes to 24 hours after mixing.

A total of 14 electrical resistance developments with time were measured in the field for in situ shotcrete. The correlation of electrical resistance to shear strength development provides a tool to determine safe re-entry time.

This research achieved its objectives and thus presented,

(1) Objective: The 'strength' developed in the shotcrete with time for worst, average and best conditions for the shotcrete mix and it's in situ curing environment,

Results : The shear strength increased exponentially during the first 4 and 8 hours of curing in all shotcrete paste mixes except for the shotcrete paste mixed with hydration stabiliser. The shear strength of shotcrete paste mixed with accelerator was significantly higher than that of shotcrete paste mixed without chemical admixture. Shear strength of shotcrete paste mixed with accelerator and synthetic fibres was slightly higher than that of shotcrete paste mixed with only accelerator. Similarly, shear strength of shotcrete paste mixed with accelerator, synthetic fibre and aggregates was slightly higher than that of shotcrete paste mixed with accelerator and synthetic fibres. Therefore early age strength of shotcrete is mainly control by the shear strength of shotcrete matrix only, not the strength of the fibres.

(2) Objective: The minimum strength required of the shotcrete to support itself and how much time is required for that strength to develop after application,

(3) Objective : The minimum strength required of the shotcrete to support the excavation,

Results: The shear strength required to be developed for a 50 mm thick layer of shotcrete to support 1 meter cube block of rock is about 100 kPa, in addition to supporting its own mass. That level of shear strength will develop at about 3 hours after spraying, for the shotcrete mix with 4 % accelerator and synthetic fibres and about 3:45 (hr:mm) after spraying, for the shotcrete mix without accelerator and synthetic fibres.

The shear strength required to be developed for a 50 mm thick layer of shotcrete to support a regular tetrahedral block of rock with 1.0 m side lengths is about 13.5 kPa, in addition to supporting its own mass. That level of shear strength will develop at about 40 minutes after spraying, for the shotcrete mix with 4 % accelerator and synthetic fibres and about 2.25 hours after spraying, for a mix without accelerator and synthetic fibres.

(4) Objective: a simple, robust, unambiguous field instrument was invented to indicate when re-entry conditions of the shotcrete have been met in situ.

Results: A wireless prototype probe with LED light indicator was invented during this research. The LED has been programmed to turn the light to indicate “Red” when the shear strength of the shotcrete is less than the minimum required strength to support its own weight and an unstable 0.4 or 2.7 tonne block of rock. The LED light turns to “Green” when the shear strength of the shotcrete reaches the minimum required strength to support its own weight and that of an unstable 0.4 or 2.7 tonne block of rock.

ACKNOWLEDGEMENTS

This thesis was completed with a great contribution from many people. I would like to acknowledge those who provided support technically, financially, intellectually, morally and most importantly spiritually.

The first one is my supervisor, Professor Ernesto Villaescusa. His guidance, inspiration and encouragement have trained me to be a confidence researcher in academics. Without his support, I would have never gained such a valuable experience and obtain this achievement at the Western Australian School of Mines, Curtin University. He is not just my thesis advisor, but also one of my best friends.

I would like to express my appreciation to Mr. Neil Warburton, the former the Chief Executive Officer of Barminco Limited, for his faith, confidence and endorsed a full financial sponsorship for the successful of this research. My appreciation also extends to all the management and technical staffs from Braminco Limited for their work in the process of patent application as well as underground mine access. I wish that Barminco Limited will continue to be a successful and Australia's largest underground mining contractor.

I would like to express my appreciation to Dr. Alan Thompson, associate supervisor of this research, for his countless wisdom and thorough proofreading ability.

I would like to acknowledge Mr. Chris Windsor, who has offered a great technical advice including help with the initial research proposal, experimental techniques and data analysis during this research. He also always supported me mentally and morally.

I would like to thank the rest of the Western Australian School of Mines (WASM) Rock Mechanics team: Mr. Luis Machuca, Mr. Pat Hogan, Mr. Lance Fraser, Mr. Anupam Tanchangea and Mr. Chris Ho for all their help in the field work, laboratory testing and development of the prototype electrical resistance measurement. I appreciate their great friendships and I am really grateful to be a part

of WASM Rock Mechanics research team. I am also would like to thank to Mr. James Langdon (JNetrix Pty Ltd) for his advice and helping in the development of an electronic measurement device.

A very special depth of deep gratitude is offer to my parents, (Saw Mountbatten), and Naw Ruth Hla, who are always a constant source of love and inspiration. I also would like to thanks my brother Peter Hla Min, sister Naw Mu Mu Aye for their love and kindness.

Last, but not the least I deeply thankful to my wife Kay Thwe Htwe for her love, support, understanding and encouragement throughout my study.

AUTHOR'S STATEMENT OF PREVIOUS PUBLICATION

Some results of data analyses and approaches discussed in this thesis have been previously published by the author during the time of thesis preparation. No references to these publications have been made in the body of the thesis, as the ideas and analysis techniques were developed as part of the thesis background work by the author prior to publication. The following list details the previous publication by the author at the time of submission of this thesis.

Saw, H., Villaescusa, E., Windsor, C. R., & Thompson, A. G. (2009), "Non-linear, elastic - plastic response of steel fibre reinforced shotcrete to uniaxial and triaxial compression testing", International Conference on Shotcrete for Underground Support XI, Davos, Switzerland. http://services.bepress.com/eci/shotcrete/

Saw, H., Villaescusa, E., Windsor, C. R., & Thompson, A. G., (2013). "Laboratory testing of steel fibre reinforced shotcrete", International Journal of Rock Mechanics and Mining Sciences, Volume 57, pp. 167-171.

TABLE OF CONTENTS

LIST OF FIGURES

LIST OF TABLES

CHAPTER 1

INTRODUCTION

1.1 Background of the research

The use of shotcrete in Australian mines has continued to grow since the late 80s due to its success in supporting excavations where other methods have failed. The current practice in Australia is now close to the International State-of-the-Art. Future use of shotcrete will continue and is likely to increase further as mines attempt development within the higher stress regimes and more difficult conditions that generally accompany mining at depth.

In terms of economics, there is also the necessity to economise on development costs, in particular, faster development rates are required with lower ground support costs and increased safety. All of these objectives may be achieved in certain rock conditions using In Cycle Shotcrete (ICS).

ICS in the true engineering sense, involves precise mark up and drilling of face holes (using modern drilling Jumbos, blasting (using careful blasting techniques), water jet scaling (using specialised hydro-jetted machines), State of the Art shotcrete (using modern shotcrete machines) with a timed re-entry into the excavation followed by rock bolting.

ICS may be suitable for many sites that possess good rock mass conditions, stress conditions below the strength of the rock mass and excavations created using the appropriate equipment. Given such circumstances the key remaining issue is the re-entry time after shotcrete application.

Re-entry time presents a conflict between increased productivity and workplace safety. The current literature does not sufficiently address the issue of re-entry time and some suggestions indicate it should be based on the shotcrete reaching a compressive strength of 1 MPa (Clements, 2004). This is somewhat illogical for it is the shear strength of the shotcrete and possibly its adhesive strength that is critical. These are the measures of strength to be considered in this research.

1.2 Objectives of the research

The objectives of the research are,

1. To accurately define the ‘strength’ developed in the shotcrete with time for worst, average and best conditions for the shotcrete mix and it’s in situ curing environment.

2. To adequately define the minimum strength required of the shotcrete to support itself and how much time is required for that strength to develop after application.

3. To adequately define the minimum strength required of the shotcrete to support the excavation.

4. To determine approximately, by some form of simple, robust, unambiguous field test when re-entry conditions of the shotcrete have been met in situ.

1.3 Structure of the thesis

1.3.1 Chapter 2: Literature review

Chapter 2 provides a comprehensive review of the different aspects of shotcrete technology which includes shotcrete mix design and spray process, materials properties and their influences on the strength development, and early strength and existing test methods.

1.3.2 Chapter 3: Mechanical and physical properties of shotcrete paste at early age

Chapter 3 provides the laboratory test methods used in this research and the results for the mechanical and physical properties of shotcrete paste at early age. The mechanical properties include Uniaxial Compressive Strength (UCS) and shear strength. The physical properties include heat of hydration and electrical resistance. The electrical resistance measurement was conducted simultaneously while conducting shear strength. But, only shear strength of shotcrete paste and the influences of chemical admixture, fibres and aggregates on the shear strength development are presented in Chapter 3. The details shear strength test results for shotcrete paste are presented in Appendix B. The electrical resistance measurement results are presented in Chapter 4.

1.3.3 Chapter 4: Development of early age strength evaluation apparatus

Chapter 4 describes the development of early age strength evaluation apparatus invented in this research. The apparatus measure the electrical resistance to infer the development of shear strength to determine safe re-entry time. The prototypes probes were tested in the laboratory for different mixes, sample geometry, voltage input, electrodes, electrodes layout and geometry, and penetration depth before implementation in the field for in situ shotcrete use in underground mine. The electrical resistance development with time for shotcrete paste without and with the influences of chemical admixtures, synthetic fibres and aggregates are presented in this chapter.

1.3.4 Chapter 5: Correlation of shear strength and electrical resistance

Chapter 5 describes the correlation and concept of measuring electrical resistance to infer the development of shear strength with time to determine safe re-entry time in an underground excavation. Shear strength of shotcrete paste at early age presented earlier in Chapter 3 and electrical resistance development with time presented in Chapter 4 are correlate in this Chapter. The correlation is then implemented into developing the theory and tool for calculation of safe re-entry time after shotcrete application in an underground excavation.

1.3.5 Chapter 6: Mechanical properties of hardened shotcrete

Chapter 6 provides the mechanical properties such as UCS, shear and tensile strength of hardened shotcrete, that is, after 24 hours curing. The results include both the peak and post-peak (elastic and plastic) regions under uniaxial and triaxial loading in order, to predict the shear strength in terms of cohesion, friction and dilation angle and, to examine how these parameters vary with 1, 3 , 7 and 28 days curing. A procedure to estimate the dilation angle is also suggested in this Chapter.

1.3.6 Chapter 7: Conclusions

Chapter 7 details the original contributions by this research. This research has made many scientific contributions to the fields of both civil and mining industries related to the mechanics of materials such as, concrete, shotcrete and rock. Limitations of the research are discussed as well as proposed future work and applications of the research outcomes in the civil and mining industries.

CHAPTER 2

LITERATURE REVIEW

2.1 Introduction

This chapter reviews different aspects of shotcrete technology which includes shotcrete mix design, materials properties and their influences on the strength development, early strength and existing test methods. This research was focused on the fundamental of shear strength development of shotcrete with time at early age, especially 0 to 4 hours. Therefore, a continuous literature search related to "the shear strength development of shotcrete with time at early age" was conducted from the beginning to the end of this research, which was from July, 2006 to October, 2014. With the best knowledge of the researcher, no literature on "the shear strength development of shotcrete with time at early age" was published during this period.

2.2 Shotcrete mix design

Shotcrete is a designed material which comprises of cement, supplementary cementing mineral, fine and coarse aggregates, chemical admixtures, water and usually fibres. It begins as a separated heterogeneous mixture of solids and fluids which are combined, mixed, pumped and sprayed to form a heterogeneous but uniform layer of solids and fluids that harden into a solid concrete layer. The mechanical properties of shotcrete change as the material hydrates from a fluid to a paste and then hardens to a solid. The physical, chemical and mechanical properties of each of these constituent materials affect the mechanical properties of the gelling, setting and hardening of the final shotcrete. Generally, the principles of conventional concrete technology can be applied to the mix design of shotcrete, particularly in the wet-mix process (AuSS, 2008). Table 2.1 shows typical range of constituent material in a shotcrete mix. The properties of the constituent materials and their resulting physical and mechanical properties on the fresh and hardened shotcrete are described in the section 2.3.

The two common processes are dry-mix and wet-mix processes.
The dry-mix process consists of:

1. Cement, coarse and fine aggregates, mineral additives and (with or without) fibres which are thoroughly mixed,
2. The cementitious mixture is fed into the delivery equipment, carried by compressed air through the delivery hose to a nozzle,
3. The nozzle is fitted inside with a water ring, through which water is introduced under pressure and mixed with the other ingredients, and sprayed at high velocity onto a rock mass surface.

The equipment used for dry-mix consists of two distinct types, pressure vessels and rotary or continuous-feed guns. The detailed mechanics of dry-mix equipment is described in Guide to Shotcrete (ACI 506R-05). Today, dry-mix shotcrete is mainly used in projects with relatively small volumes where and/or high flexibility are required (Melbye, 1994).

The wet-mix process consists of:

1. Cement, coarse and fine aggregates, mineral additives, (with or without) fibres and mixing water which are thoroughly mixed the same as conventional concrete,
2. The mixture is fed into a delivery equipment or agitation truck, conveyed by compressed air to a nozzle and sprayed at high velocity onto a rock mass surface.

The development of concrete technology and advances in robotic shotcrete systems enhances the application of wet-mix shotcrete process. The robotic shotcrete system consists of carrier vehicle, conveyance system, spraying manipulator (manual, semi-auto or fully automatic), dosage unit for set accelerator control unit and compressor for compressed air supply. Girmscheid & Moser (2001) described the development of a fully automated shotcrete robot for rock support. A fully automatic system can be used not only for spraying, but also for the final profile control. The final profile

control is done by scanning the excavated tunnel profile by a laser system and calculations of the required shotcrete layer thickness out of the excavated profile and the design profile. The desired layer thickness is achieved by controlling the spraying velocity (Girmscheid & Moser, 2001).

Table 2.1. Typical range of constituent material in a shotcrete mix.

Constituents		Dry mix	Wet mix	Unit
Cement		400 - 420	400 - 450	kg/m^3
Fine aggregate (Fine to coarse sand)		1380 - 1510	1110 - 1180	
Coarse aggregate (Maximum 9 - 12.5 mm)		235 - 400	500 - 535	
Water		150 - 200	175 - 200	
[1]Mineral additive (Supplementary cementing materials)	Silica fume	20 - 50		
	Fly ash	20 - 75		
	Granulated blast-furnace slag	20 - 50		
[1 & 2]Chemical admixture	Air-entraining	0.3 - 0.5		Litre/m^3
	Accelerator	20 - 22		
	Hydration stabiliser	-	1- 2	
	Water reducer	-	1 - 2	
	Superplasticiser	-	3 -7	
[3]Steel fibres		30 - 40		kg/m^3
[4]Synthetic fibres		5 -8		kg/m^3

1. All types of mineral additive and chemical admixture may or may not be use in a particualr mix.
2. Chemical admixture dosage shall follow to a manufacturer's guide line.
3. For steel fibres reinfoced shotcret.
4. For synthetic fibres reinforced shotcrete.

2.3 Materials properties

2.3.1 Cement

Generally, cement can be described as a material with adhesive and cohesive properties which make it capable of bonding minerals fragments into a compact mass. The first modern prototype of cement was made in 1845 by Isaac Johnson,

who burnt a mixture of clay and chalk until clinkering, so that the reactions necessary for the formation of strongly cementitious compounds took place. The fundamentals of producing cement have not changed until this day. The cement is produced by intimately mixing together calcareous and argillaceous, or other silica, alumina and iron oxide-bearing materials, burning them at a clinkering temperature and grinding the resulting clinker (Naville, 1995). It is well known as Portland cement. That name is derived from the similarity of hardened cement to Portland stone, which was quarried on the Isle of Portland in Dorset, England.

The raw materials used in the manufacture of cement mainly consist of lime, silica, alumina and iron oxide. These compounds interact with one another at clinkering temperature and forming a series of more complex chemical compounds. Based on the chemical analysis with X-ray diffraction method, Bogue (1929) observed that,

1. Portland cement is mainly composed of Lime (CaO), Silica (SiO_2), Alumina (Al_2O_3), Ferric oxide (Fe_2O_3) and Magnesia (MgO)
2. Fe_2O_3 reacts with Al_2O_3 and CaO to form $4CaO.Al_2O_3.Fe_2O_3$ (Tetracalcium aluminoferrite)
3. MgO remains uncombined
4. Al_2O_3 remaining from combinations as $4CaO.Al_2O_3$., react with CaO to form $3CaO.Al_2O_3$ (Tricalcium aluminate)
5. CaO remaining from in the above combinations reacts with SiO_2 to form $2CaO.SiO_2$ (Dicalcium silicate)
6. Any CaO not consumed in the formation of $2CaO.SiO_2$, then react with it to form $3CaO.SiO_2$ (Tricalcium silicate)
7. CaO remaining after converting all of the Dicalcium silicate to Tricalcium silicate will be present as uncombined CaO (Fee lime)

In addition, Bogue (1929) suggested a method to calculate the proportions of those cementing compounds. It is often referred as “Bogue composition” and included in ASTM C150, Standard Specification for Portland cement.

It is well accepted that, all cements are mainly composed of the four compounds, Tricalcium silicate (C_3S), Dicalcium silicate (C_2S), Tricalcium aluminate (C_3A) and Tetracalcium aluminate (C_4AF). The rate of hydration of each compound is different. Based on these facts, different types of cement are produced for a wide range of application. This is done primarily by altering the proportions of each compound through the compositions of the raw material and manufacturing process. In addition, supplementary cementing materials may be blend with the main constituents. Cement is classified into different types or classes based on its chemical constituents and performance. The three major standards of specifications are ASTM C150, European standard EN-197 and Australian standard AS 3972. The standards contain specifications for chemical compositions and physicals properties of Portland and blended cements. The important physical and mechanical properties are fineness, soundness, consistency, time of setting, heat of hydration, specific gravity, air content and compressive strength. Tables 2.2 to 2.5 present a summary of different types and classes of Portland and blended cements classified based on the chemical compositions. A summary of required physical and mechanical properties are presented in Tables 2.6 to 2.7. Although chemical composition is important for manufacturing, the physical and mechanical properties provide more direct information concerning the performance of a cement (Popovics, 1992).

Table 2.2. Standard types and composition of Portland cements (ASTM C 150/C 150 M – 09).

Type	Application	Al_2O_3 max %	Fe_2O_3 max %	MgO max %	SO_3, max %		Loss of ignition max %	Insoluble residue, max %	C_3S max %	C_2S min %	C_3A, max %	$C_3S + 4.75C_3A$, max %	$C_4AF + 2(C_3A)$, or solids solution $(C_4AF + C_2F)$, as applicable max %
					When (C_3A) is 8% or less	When (C_3A) is more than 8%							
Type I	For use when the special properties specified for any other type are not required.	-	-	6	3	3.5	3	0.75	-	-	-	-	-
Type IA	Air entraining cement for the same sues as Type I, when air-entrainment is desired.	-	-	6	3	3.5	3	0.75	-	-	-	-	-
Type II	For general use, more especially when moderate sulfate resistance is desired.	6	6	6	3	-	3	0.75	-	-	8	-	-
Type IIA	Air entraining cement for the same uses as Type II, where air-entrainment is desired.	6	6	6	3	-	3	0.75	-	-	8	-	-
Type II (MH)	For general use, more especially when moderate heat of hydration and moderate	6	6	6	3	-	3	0.75	-	-	8	100	-
Type II (MH)A	Air entraining cement for the same uses as Type II (MH), where air-entrainment is	6	6	6	3	-	3	0.75	-	-	8	100	-
Type III	For use when high early strength is desired.	-	-	6	3.5	4.5	3	0.75	-	-	15	-	-
Type IIIA	Air entraining cement for the same uses as Type III, where air-entrainment is desired.	-	-	6	3.5	4.5	3	0.75	-	-	15	-	-
Type IV	For use when a low heat of hydration is desired	-	6.5	6	2.3	-	2.5	0.75	35	40	7	-	-
Type V	For use when high sulfate resistance is desired.	-	-	6	2.3	-	3	0.75	-	-	5	-	25

Table 2.3. The 27 products in the family of common cements (EN 197-1:2000).

Main types	Notation of the 27 products (Types of common cement)		Composition (Percentage by mass)										
			Main constituents										
			Clinker	Blast furnace slag	Silica fume	Pozzolana		Fly ash		Burnt shale	Limestone		Minor additional constituents
						Natural	Natural calcined	Siliceous	Calcareous				
			K	S	D	P	Q	V	W	T	L	LL	
CEM I	Portland cement	CEM I	95-100	-	-	-	-	-	-	-	-	-	0-5
CEM II	Portland-slag cement	CEM II/A-S	80-94	6-20	-	-	-	-	-	-	-	-	0-5
		CEM II/B-S	65-79	21-35	-	-	-	-	-	-	-	-	0-5
	Portland-silica fume cement	CEM II/A-D	90-94	-	6-10	-	-	-	-	-	-	-	0-5
	Portland-pozzolana cement	CEM II/A-P	80-94	-	-	6-20	-	-	-	-	-	-	0-5
		CEM II/B-P	65-79	-	-	21-35	-	-	-	-	-	-	0-5
		CEM II/A-Q	80-94	-	-	-	6-20	-	-	-	-	-	0-5
		CEM II/B-Q	65-79	-	-	-	21-35	-	-	-	-	-	0-5
	Portland-fly ash cement	CEM II/A-V	80-94	-	-	-	-	6-20	-	-	-	-	0-5
		CEM II/B-V	65-79	-	-	-	-	21-35	-	-	-	-	0-5
		CEM II/A-W	80-94	-	-	-	-	-	6-20	-	-	-	0-5
		CEM II/B-W	65-79	-	-	-	-	-	21-35	-	-	-	0-5
	Portland-burnt shale cement	CEM II/A-T	80-94	-	-	-	-	-	-	6-20	-	-	0-5
		CEM II/B-T	65-79	-	-	-	-	-	-	21-35	-	-	0-5
	Portland-limestone cement	CEM II/A-L	80-94	-	-	-	-	-	-	-	6-20	-	0-5
		CEM II/B-L	65-79	-	-	-	-	-	-	-	21-35	-	0-5
		CEM II/A-LL	80-94	-	-	-	-	-	-	-	-	6-20	0-5
		CEM II/B-LL	65-79	-	-	-	-	-	-	-	-	21-35	0-5
	Portland-composite cement	CEM II/A-M	80-94	<----------6-20---------->									0-5
		CEM II/B-M	65-79	<----------21-35---------->									0-5
CEM III	Blastfurnace cement	CEM III/A	35-64	36-65	-	-	-	-	-	-	-	-	0-5
		CEM III/B	20-34	66-80	-	-	-	-	-	-	-	-	0-5
		CEM III/C	5-19	81-95	-	-	-	-	-	-	-	-	0-5
CEM IV	Pozzolanic cement	CEM IV/A	65-89	-	<----------11-35---------->					-	-	-	0-5
		CEM IV/B	45-64	-	<----------36-55---------->					-	-	-	0-5
CEM V	Composite cement	CEM V/A	40-64	18-30	-	<----------18-30---------->			-	-	-	-	0-5
		CEM V/B	20-38	31-50	-	<----------31-50---------->			-	-	-	-	0-5

Table 2.4. Cement types and compositions (AS 3972 – 2010).

Cement type			Portland cement	Type GP (Note 1)	Mineral additions and minor additional constituents (7.5 % combined maximum for Type GP and 20% combined maximum for Type GL)			Supplementary cementitious materials (SCM) (Note 4)	
					Mineral additions (Note 2)		Minor additional constituents (Note 3)	Fly ash and/or slag	Amorphous silica
					Fly ash or slag	Limestone			
General purpose cement		GP	92.5 to 100	-	0 to 7.5		0 to 5	-	-
General purpose limestone cement		GL	80 to 92	-	-	8 to 20	0 to 5	-	-
Blended cement		GB	-	<92.5	-	-	-	>7.5	0 to 10
Special purpose cement	High early strength cement	HE	(Note 5)						
	Low heat cement	LH							
	Sulfate resisting cement	SR							
	Shrinkage limited cement	SL							

Notes:

1. If Type GB cement consists of Type GP and amorphous silica only, the proportion of Type GP shall be 90% or above.
2. For Type GP the 'mineral additions' may comprise limestone, fly ash for slag, or a combination of these materials, at the discretion of the cement manufacturer.
3. The "minor additional constituents" addition forms part of the allowable amount of "mineral addition" in the cement.
4. Type GB cement may contain supplementary cementitious materials (SCMs) comprising either or both fly ash and slag at combined levels above 7.5 % and amorphous silica at a level not exceeding 10%.
5. Special purpose cement may be general purpose cement or blended cement that complies with the requirement for special purpose cement.

Table 2.5. Standard and optional required physical and mechanical properties (ASTM C 150/C 150 M – 09).

Type	Fineness (Specific surface) m^2/kg				Soundness (Autoclave expansion) Max %	Time of setting , Minute				Air content of mortar, volume, %		Heat of hydration, kJ/kg		Compressive strength, MPa			
	Turbidimeter test		Air Permeability			Vicat test		Gillmore test									
	Min	Max	Min	Max		Not less than	Not more than	Initial set, not less than	Final set, not more than	Max	Min	7 days, Max	28 days, Max	1 day	3 days	7 days	28 days
Type I	150	-	260	-	0.8	45	375	60	600	12	-	-	-	-	12	19	28
Type IA	150	-	260	-	0.8	45	375	60	600	22	16	-	-	-	10	16	22
Type II	150	-	260	-	0.8	45	375	60	600	12	-	-	-	-	10	17	28
Type IIA	150	-	260	-	0.8	45	375	60	600	22	16	-	-	-	8	14	22
Type II (MH)	150	245	260	430	0.8	45	375	60	600	12	-	290	-	-	10	17	28
Type II (MH)A	150	245	260	430	0.8	45	375	60	600	22	16	290	-	-	8	14	22
Type III	-	-	-	-	0.8	45	375	60	600	12	-	-	-	12	27	-	-
Type IIIA	-	-	-	-	0.8	45	375	60	600	22	16	-	-	10	19	-	-
Type IV	150	245	260	430	0.8	45	375	60	600	12	-	250	290	-	-	7	17
Type V	150	-	260	-	0.8	45	375	60	600	12	-	-	-	-	8	15	21

Table 2.6. Mechanical and physical requirements for all 27 products. (EN 197-1:2000).

Strength class	Compressive strength, MPa				Initial setting time, Minute	Soundness (Expansion) mm
	Early strength		Standard strength			
	2 days	7 days	28 days			
32.5 N (Ordinary early strength)	-	≥ 16	≥ 32.5	≤ 52.5	≥ 75	≤ 10
32.5 R (High early strength)	≥ 10	-				
42.5 N (Ordinary early strength)	≥ 10	-	≥ 42.5	≤ 62.5	≥ 60	
42.5 R (High early strength)	≥ 20	-				
52.5 N (Ordinary early strength)	≥ 20	-	≥ 52.5	-	≥ 45	
52.5 R (High early strength)	≥ 30	-				

Table 2.7. Physical and mechanical properties of General and Special purpose cements (AS 3972 – 2010).

Cement type			Setting time		Soundness, Maximum %	Peak temperature rise, maximum °C	Expansion, maximum microstrain at 16 week exposure	Shrinkage, maximum microstrain at 28 days	Compressive strength, minimum, MPa		
			Minimum (min)	Maximum (min)					3 days	7 days	28 days
General purpose cement		GP	45	6	5	-	-	-	-	35	45
General purpose limestone cement		GL	45	10	5	-	-	-	-	20	35
Blended cement		GB	45	10	5	-	-	-	-	20	35
Special purpose cement	High early strength cement	HE	45	6	5	-	-	-	25	40	-
	Low heat cement	LH	45	10	5	23	-	-	-	10	30
	Sulfate resisting cement	SR	45	10	5	-	750	-	-	Note 1	Note 1
	Shrinkage limited cement	SL	45	10	5	-	-	750	-	Note 1	Note 1

Notes:
1. Type SL and Type SR cemments shall comply with the strength requirements of either Type GP or Type GB, depending on the nature of the cement.

2.3.1.1 Hydration of cement

When cement is mixed with water a series of simultaneous and consecutive reactions take place between water and the constituents of cement. These reactions are covered by the term “hydration of cement”. There are two ways in which the constituents of cement can react with water. First, where direct addition of some molecules of water takes place, this being a true reaction of hydration. The second type of reaction with water is hydrolysis (Neville, 1995). The progress or kinetics of hydration can be followed by different measurements such a, x-ray quantitative analysis (Gard, 1964), infrared spectroscopy (Farmer, 1964), differential thermal analysis (Mackenzie, 1964), silylation through the measurement of the size and quantity of the formed oligomers (Tamas, 1976), determination of the non-evaporable water (Glasser, 1964), thermal gravimetric analysis of the liberated calcium hydroxide (Tamas, 1966), heat evolution, specific surface of the cement gel (Kantro, 1964). In additional to these traditional methods, more recent advances techniques, such electron microscopy, nuclear magnetic resonance spectroscopy, MÖssbauer spectroscopy has allowed the systematic examination of cement chemistry and the complex processes during its hydration. Bogue (1955), Lea (1956), Kuhl (1961), Lea (1970) and Taylar (1990) published their book on more chemistry details of cement and its hydration. A review on chemistry and mechanism of cement hydration is briefly described below.

2.3.1.1.1 Chemistry of cement hydration

All the compounds present in cement are anhydrous. When mixed with water they are decomposed to form hydrated compounds. At first, supersaturated and unstable solutions are formed and these solutions gradually deposit their excess solids and tend to come into equilibrium (Lea, 1970). Le Chaterier (1882) observed that the products of hydrations of cement are chemically the same as the products of hydrations of the individual compounds under similar conditions. In addition, the products of reaction may influence one another or may themselves interact with the

other compounds in the system (Bogue and Lerch 1934, Steinour 1952). The hydration of the individual compound is described in more details below.

Tricalcium silicate ($3CaO.SiO_2$) or *(C_3S)*- The hydration of C_3S commences quickly and both lime and silica pass into solution initially in the same molecular ratio 3:1 as in the anhydrous compound. The concentration of lime in solution increases steadily while that of silica rapidly decreases. Crystals of calcium hydroxide ($Ca(OH)_2$) soon appear together with gelatinous or nearly amorphous calcium silicate hydrated (CSH-gels) (Lea, 1970). This process begins with the dissolution of C_3S. Oxygen ions on the surface of C_3S lattice react with protons in the water and form hydroxide ions, which in turn combine with Ca^{2+} to form $Ca(OH)_2$.

$$O^{2-}\ (\text{lattice}) + H^{+}\ (aq) \rightarrow OH^{-}\ (aq) \qquad (2.\ 1)$$

$$2OH^{-}\ (aq) + Ca^{2+}\ (aq) \leftrightarrows Ca(OH)_2\ (aq) \qquad (2.\ 2)$$

At the same time, silicate material from surface of C_3S lattice enters the liquid phase (Older, 1998).

$$SiO_4^{4-}\ (\text{lattice}) + nH^{+}\ (aq) \rightarrow H_nSiO_4^{4n-}\ (aq) \qquad (2.\ 3)$$

The immediate product formed in pastes has a $CaO : SiO_2$ ratio near to 3.This forms as a coating on the C_3S surfaces and retards the reaction. After a few hours, dissolution or splitting off of this initial products results in an acceleration of the hydration and the formation as the second product of a CSH gel (I) of lower $CaO:SiO_2$ ratio, 1.5 or less. This is followed by formation of a third stable product CSH gel (II). The completely hydrated silicate contains both products with $CaO:SiO_2$ ratio 1.4 to 1.6. The molar ratio increases as the water:solid ratio of the original paste decreases.

The hydration reaction of C_3S is represented in a generalised form by the equation,

$$C_3S + (2.5+n)H \rightarrow C_{1.5+m}SH_{1+m+n} + (1.5 - m)CH \quad (2.4)$$

Where,

n = Amount of substance
m = Molar mass
C_3S = Tricalcium Silicate
H = Water
CSH = Calcium Silicate Hydrated
CH = Calcium Hydroxide

Dicalcium silicate ($2CaO.SiO_2$) or *(C_2S)*- The reaction of C_2S is considerably slower compared to the reaction of C_3S and substantially less calcium hydroxide is produced. It is not detectable under microscope until after many weeks. The calcium silicate hydrated gels (CSH- gels) produced are the same type as those from C_3S. However, the course of reactions is different. In a C_2S paste the initial product formed as a surface coating with $CaO:SiO_2$ ratio close to 2. Within twelve hours or so, this converts into a low-lime product related to CSH gel (I) and the molar ratio drops to 1.1 to 1.2. A stable final product related to CSH gel (II) is gradually formed. The molar ratio gradually increases to 1.65 to 1.8 after a year or so.

A generalised equation applicable at any age of water:solid ratio for hydration of C_2S is,

$$C_2S + (1.5+n)H \rightarrow C_{1.5+m}SH_{1+m+n} + (0.5 - m)CH \quad (2.5)$$

Where,

C_2S = Dicalcium silicate
H = Water
CSH = Calcium Silicate Hydrated
CH = Calcium Hydroxide

Tricalcium aluminate($3CaO.Al_2O_3$) or *(C_3A)*- The reaction of C_3A with water take place very rapidly. In the present of excess water, hexagonal plate or needles crystals began to form within a few minutes and increase rapidly in size and amount. They consist of a mixture of the hydrate $4CaO.Al_2O_3.19H_2O$ and $2CaO.Al_2O_3.8H_2O$ or closely-related solid solutions. No calcium hydroxide or hydrated alumina is precipitated. The hexagonal plate crystals are metastable and they can eventually transform into the less soluble and more stable isometric compound $3CaO.Al_2O_3.6H_2O$. Some lime in C_3A may be replaced to give the compound $Na_2O.8CaO.3Al_2O_3$. At complete hydration, the reaction can approximately be represented by the equation,

$$3CaO.Al_2O_3\,(s)+6H_2O\,(l) \rightarrow 3CaO.Al_2O_3.6H_2O\,(s) \qquad (2.\ 6)$$

Tetracalcium aluminoferrite($4CaO.Al_2O_3.Fe_2O_3$) or *(C_4AF)*- When C_4AF is mixed with water, hexagonal plate crystals are rapidly formed. Those crystals occur mostly as foliated masses. The rate of reaction increases with the proportion of alumina. However, its reaction is less rapid than C_3A. The residual unhydrated C_4AF and a hydrated iron oxide or amorphous Fe_2O_3 (hematite) deposited around it forms a dark mass. At temperature about 15°C the hexagonal plate crystals converts into a cubic C_3AH_6-C_3FH_6 solid solution. C_4AF also react with calcium hydroxide ($Ca(OH)_2$), which is some of the hydration product of C_3S. At complete hydration the reaction can approximately be represented by the equation,

$$4CaO.Al_2O_3\,.Fe_2O_3\,(s) +2Ca(OH)_2(aq) +10H_2O\,(l) \rightarrow$$

$$3CaO.Al_2O_3.6H_2O\,(s) + 3CaO.Fe_2O_3.6H_2O\,(s) \qquad (2.\ 7)$$

Efffect of Gypsum ($CaSO_4.2H_2O$) - The hydration products of C_3S and C_2S are slightly modified by Gypsum. Some of the sulphates can enter the structure of CSH-gels and change its morphology. The hydration products of C_3A change significantly

with the presence of Gypsum. These are needles of a calcium sulphoaluminate hydrate ($3CaO.Al_2O_3.3CaSO_4.32H_2O$), which are referred to as Ettringite. In the case of C_4AF, the reaction yields a solid solution of sulphoaluminate and sulphoferrite hydrate. The reaction of Gypsum and C_3A can approximately be shown by the equation,

$$3CaO.Al_2O_3(s) + 3CaSO_4(s) + 31H_2O\ (l) \rightarrow 3CaO.Al_2O_3.\ 3CaSO_4.32H_2O\ (s) \quad (2.\ 8)$$

2.3.1.1.2 Mechanism of cement hydration

The mechanism of cement hydration comprises two stages, namely setting and hardening. Generally, setting refers to the change from a fluid to a rigid state and hardening refers to the gain in strength of a cement paste that has set. In fact, the setting and hardening mechanism is very complex, due to the present of several chemical compounds and the physical nature of their hydration products (Lea, 1970). Various theories have been advanced to explain the mechanism of cement hydration. The two important theories, which are considered as the foundation for modern theories, were the crystalline theory explained by Le Chatelier (1882) and colloidal theory by Michaelis (1893). Crystalline theory states that, "*the development of cementing action to the passage of the anhydrous cement compounds into solutions and the precipitation of the hydration products as interlocking crystals*". In the colloidal theory, "*cohesion was considered to results from the precipitation of a colloidal gelatinous mass which hardened as it lost water by external drying or by inner suction caused by hydration of the inner unhydrated cores of the grains*." Baikov (1926) suggested three stages of setting and hardening based on Le Chatelier and Michaelis theories. First a solution stage; second; a colloidal stage and third; a crystallisations stage. Rebinder (1954) explains the mechanism of setting and hardening based on his theory of coagulation in suspension of a finely divided solid dispersed in a liquid. Two types of three-dimensional networks can be formed, a coagulation network and crystalline network. In 1965, Si'lchenko et.al. explained

that when Portland cement and water are mixed there is an immediate rapid reaction with the formation of a supersaturated solution. Then, the reaction rapidly slows down and this is ascribed to the formation of a film of micro-crystalline or gel-like calcium sulphoaluminate around the cement particles. A period of slow reaction period then follows. During that time, the amount of hydration products gradually builds up with time and slowly increases the plastic viscosity of the paste (Lea, 1970). Several detailed reviews have been written about the mechanisms. Those are Taylor, et al, 1984, Gartner and Gaidis, 1989, Gaidis and Gartner, 1989 and Gartner, et at., 2002.

A recent review written by Bullard, et al., (2010) suggested that, cement hydration involves a collection of coupled chemical processes, which occur at a rate determined by the nature of the process and by the state of the system at that instant. These processes fall into one of the following categories and occur in series, in parallel or in some more complex combination.

1. *Dissolution/dissociation* involves detachment of molecular units from the surface of a solid in contact with water (Dove et at., 2005 and 2007).
2. *Diffusion* describes the transport of solution components through the pore volume of cement paste (Glasstone et al., 1941, Mills et al., 1989) and/or along the surfaces of solids in the adsorption layer (Somorjai, 1994, Adamson and A.P. Gast, 1997).
3. *Growth* involves surface attachment, the incorporation of molecular units into the structure of a crystalline or amorphous solid within its self-adsorption layer (Burton, 1951).
4. *Nucleation* initiates the precipitation of solids heterogeneously on solid surfaces or homogeneously in solution, when the bulk free energy driving force for forming the solid outweighs the energetic penalty of forming the new solid–liquid interface (Kaschiev and van Rosmalen, 2003).

5. *Complexation,* involves reactions between simple ions to form ion complexes or adsorbed molecular complexes on solid surfaces (Stumm and Morgan, 1972, Morel, 1983).
6. *Adsorption,* involves the accumulation of ions or other molecular units at an interface, such as the surface of a solid particle in a liquid (Powers and Brownyard, 1946, Somorjai, 1994, Adamson and Gast, 1997 and Morel, 1983).

2.3.1.1.2.1 Mechanism of C_3S hydration

C_3S constitutes about 50% to 70% of cement by weight. It tends to dominate the early hydration period that comprises setting and early strength development. In addition, it is the component most responsible for the formation of the calcium silicate hydrate gel (CSH), the principle product of hydration (Bullard, et al., 2010). Figure 2.1 shows a typical curve relating the fraction of C_3S consumed with time as determined by quantitative X-ray diffraction analysis (after Taylor et al., 1984). Taylor et al., suggested two stages of reactions which can be divided into four periods. The first stage reaction occurs primarily in pre-induction period and continues very slowly into the induction period. The second stage reaction begins at the end of induction period and continues through acceleratory, in which the main reaction first begins to occur rapidly and post-acceleratory periods, where slow and continuing reaction take place. The beginning and ending of these periods are still difficult to pinpoints precisely.

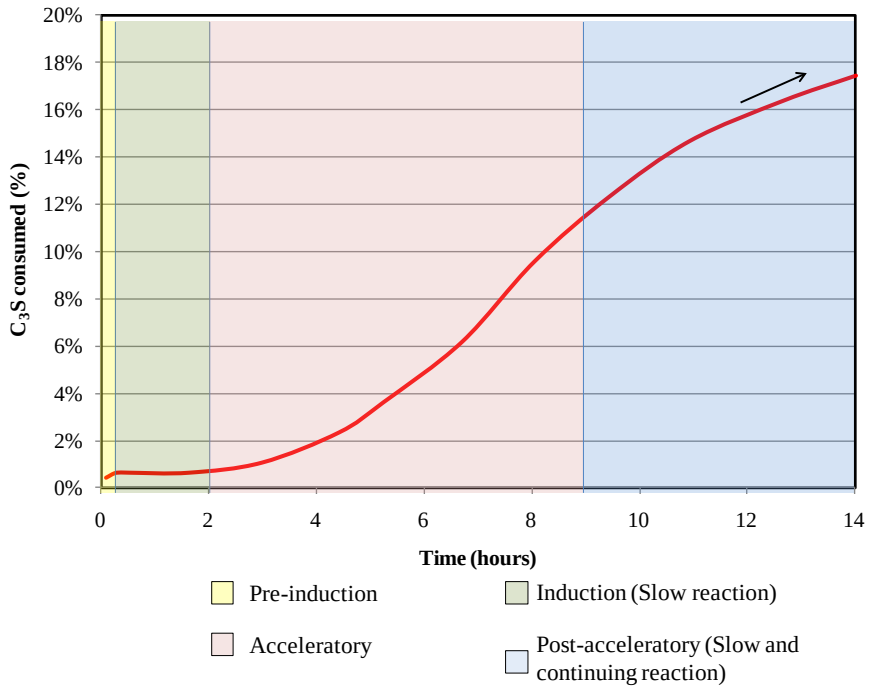

Figure 2.1.Typical curve of C_3S hydration as a function of time (Modified after Taylor et al., 1984).

Diamond (1976), proposed a system of nomenclature based on scanning electron microscope (SEM) observations. Jennings et al., (1981) later modified and extended the system using transmission methods. Figure 2.2 represents a summarised flowchart for such systems.

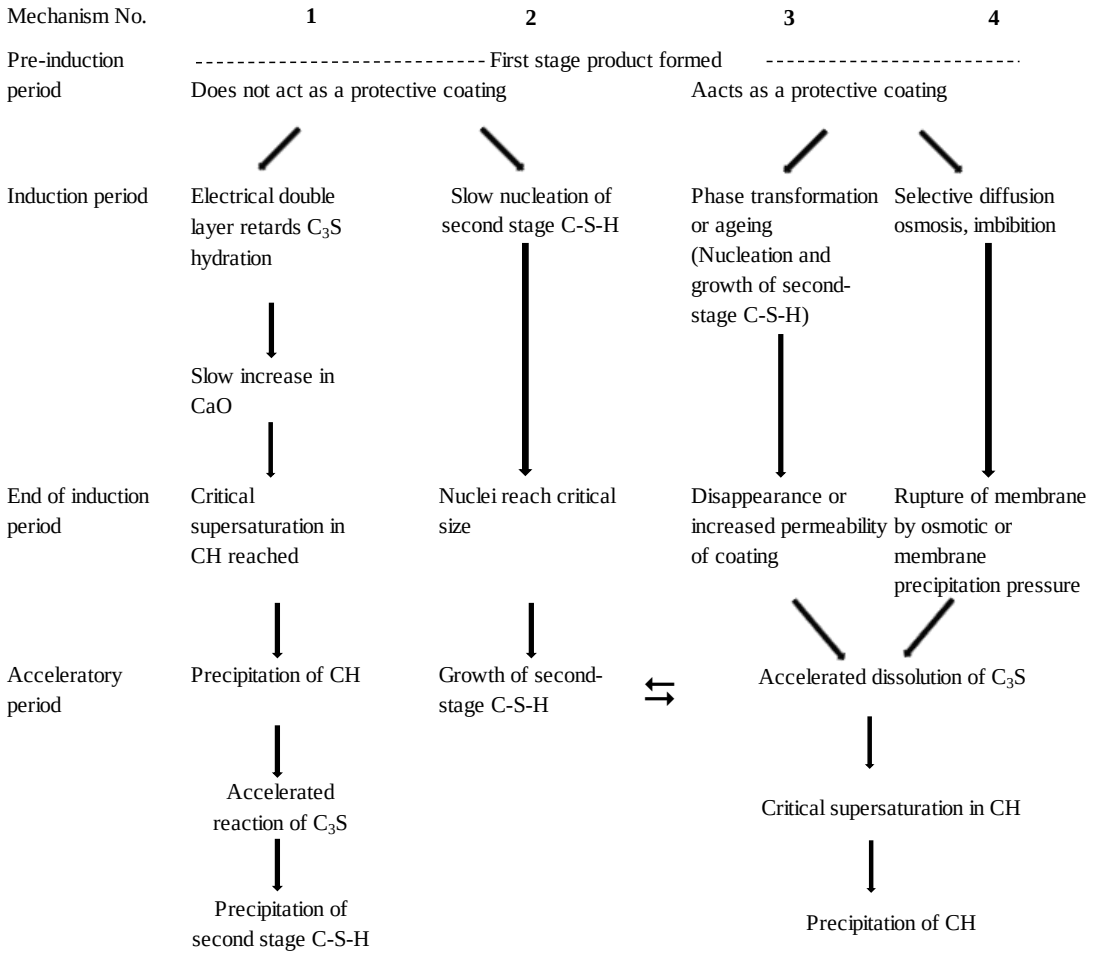

Figure 2. 2. Flowchart for C_3S hydration mechanisms (After Jawed et al., 1984).

2.3.1.1.2.2 Mechanism of C_2S hydration

The kinetics and mechanism of C_2S are similar to those for C_3S , but with a much lower rate of reaction .The products are also similar apart from much smaller content of CH (Taylor, 1997).

2.3.1.1.2.3 Mechanism of C_3A hydration

The reaction of C_3A is very fast. There is no period of slow reaction and setting is almost instantaneous. As described in the previous section, this quick setting is undesirable in concrete or cement grout. Therefore, calcium sulphate (Gypsum – $CaSO_4.2H_2O$) is added to the cement to control the reaction of C_3A. With the presence of calcium sulphate the reaction of C_3A is significantly changed. There is an initial period of rapid reaction, after which the rate decreases rapidly within a few minutes. During the initial reaction, ettringite ($3CaO.Al_2O_3.3CaSO_4.32H_2O$) is the main hydrate phase formed. The reaction can approximately be represented by the equation,

$$3CaO.Al_2O_3+3CaSO_4+32H_2O \rightarrow 3CaO.Al_2O_3.3CaSO_4.32H_2O \quad (2.\ 9)$$

$$\text{Tricalcium aluminate+Gypsum+Water} \rightarrow \text{Etringite (Trisulfate)} \quad (2.\ 10)$$

This initial period of rapid reaction quickly gives way to a period of low heat output. The duration depends on the quantity of calcium sulphate in the system. When the added calcium sulphate has been consumed, the rate of reaction is rapidly increased again. The main hydration product is calcium monosulfoaaluminate.

2.3.1.1.2.3 Mechanism of C_4AF hydration

Generally, the hydration mechanism of C_4AF is similar to that of C_3A. However, differences in hydration behaviour may occur depending on the ability of the hydrate to accommodate ferric ion in their structure (RILEM Technical Committees, 1986). The hydrous ferric hydroxide is produced as a separate phase (Fukuhara et al., 1981). In 1980, Fukuhara et al, observed the formation of amorphous, iron rich pseudomorphs of C_4AF grains in the system of C_4AF-$CaSO4.2H_2O$-H_2O.

2.3.2 Supplementary cementing materials

2.3.2.1 Silica fume

Silica fume, as defined in ASTM C1240 is a "very fine pozzolanic material, composed mostly of amorphous silica produced by electric arc furnaces as a by-product of the production of elemental silicon or ferrosilicon alloys". It may be added directly to concrete (shotcrete) as an individual material or in a blend of Portland cement and silica fume. The silica fume generally contains more than 90 % silicon dioxide (SiO_2). It consists primarily of very fine smooth spherical glassy particles with a surface area ranging from 13, 000 to 30, 000 m^2/kg measured by nitrogen-absorption method (Malhotra et al, 1987). Individual silica fume particles have a diameter of less than 1 micron, which is approximately 1/100 of the size of an average cement particle. However, they are usually found in agglomerations with size ranging from 1 to 100 microns. The specific gravity ranges from 2.21 to 2.33 according to the study conducted by Aïtcin et al., (1984).

The use of silica fume in high strength and high performance concrete has become an increasingly accepted practice. Silica fume enhances the properties of concrete by both physical and chemical mechanisms. The physical mechanisms include reduced bleeding water, provision of nucleation sites and more efficient packing of the solid particles. The reduced bleeding water increases cohesiveness and thus reduced segregation (Sellevold, 1987). Silica fume accelerates the hydration of cement during early stages by providing nucleation sites where the products of cement hydration can more readily precipitate from solution (Sellevold et al., 1987). In hydrating, cement paste, silica fume react with Calcium Hydroxide (CH) to form Calcium Silicate Hydrate (CSH). Morgan (1988) also reported that the use of silica fume in shotcrete enhances adhesion and cohesion of the mixture and reduced rebound. The ACI 506.5R-9 "Guide for specifying underground shotcrete" recommended the use

of Silica fume in shotcrete because it can improve the shotcrete performance with respect to rebound and maximum achievable build-up. The ACI 243R provides a comprehensive guide for use of silica fume in concrete.

2.3.2.2 Fly ash

According to ASTM C618 - 08a, fly ash is "the finely divided residue that results from the combustion of ground or powdered coal and this is transported by flue gasses". It is primarily the inorganic portion of the source coal in a particulate form (Popovics, 1992). According to ASTM 618 – 08a, fly ash is classified into class "F" and "C" by its chemical composition and physical properties. Table 2.8 present chemical and physical requirements for fly ash.

Table 2. 8. Chemical and physical requirements for fly ash (ASTM C618 -08a).

Chemical and physical requirements		Class F	Class N
Silicon dioxide (SiO_2) + aluminum oxide (Al_2O_3) + iron oxide (Fe_2O_3), minimum, %		70	50
Sulfur trioxide (SO_3), maximum, %		5	5
Moisture content, maximum, %		3	3
Loss of ignition, maximum, %		6	6
Fineness: Amount retained when wet-sieved on 45 micron sieve, maximum, %		34	34
Strength activity index:	With Portland cement, at 7 days, minimum percent of control	75	75
	With Portland cement, at 28 days, minimum percent of control	75	75
Water requirement, maximum, percent of control		105	105
Soundness: Autoclave expansion or contraction, maximum, %		0.8	0.8
Uniformity requirement: The density and fineness of individual samples shall not vary from the average established by the ten preceding test, or by all preceding tests if the number is less than ten, by more that:	Density, maximum variation from average, %	5	5
	Percent retained on 45 micron, maximum variation, percentage points from average	5	5

Fly ash consists of 60 to 90 % amorphous (glassy) spheres and 10 to 40 % crystalline phase. Its reaction depends largely on breakdown and dissolution of glassy structure by hydroxide ions and the heat generated during the early hydration of the hydraulic cement fraction (ACI 232.2R-03). The reaction of the fly ash continues to consume $Ca(OH)_2$ to form additional CSH. The amount of heat evolved as a consequence of the reactions is usually reduced when fly ash is proportioned together with Portland cement in the concrete. If the Portland cement content is reduced, fly ash can extend the setting time of concrete. When fly ash is used to replace a portion of cement in a unit volume of concrete, the amount of paste increases. Lane (1983) reported that an increase in paste volume produces a fresh concrete with greater plasticity and better cohesiveness.

The compressive strength and the rate of strength gain in the hardened concrete are affected by the chemical and physical properties of a particular type of fly ash and the cement. A Class F fly ash can develop lower strength in 7 days or less when the concrete is cured in room temperature. When concrete is cured in a moist condition, the continued pozzolanic activity of fly ash provides strength development at later ages (Abdun-Nur, 1961). Class C fly ashes often show higher rate of reaction at early ages than Class F fly ashes. However, certain Class C fly ashes may not show the later stage strength gain. The ACI 232.2R-03 provides a comprehensive guide for use of fly ash in concrete. The ACI 506.5R-9 “Guide for specifying underground shotcrete” suggests that the use of fly ash is acceptable only if all shotcrete performance requirements can be demonstrated during preconstruction testing.

2.3.2.3 Slag cement

According to ASTM C219-07a, slag cement is defined as “hydraulic cement consisting predominantly of ground granulated blast-furnace slag”. The granulated blast-furnace slag (GBFS) is a glassy granular material formed when molten blast-furnace slag is rapidly chilled by immersion in water. The blast-furnace slag is the non-metallic product developed in molten condition simultaneously with iron in the

blast furnace. The composition of blast-furnace slag is determined by that of the ores, fluxing stone and impurities in the coke charged into the blast furnace. The major oxides of silica, alumina, lime and magnesia constitute 95% or more of the total oxides (ACI 232.2R.03). ASTM C989 – 10 provides three grades of Slag cements, depending on their respective mortar strengths when blended with an equal mass of Portland cement. The classification and other physical requirements for Slag cement is presented in Table 2.9. The classifications are Grades 80, 100 and 120, based on Slag Activity Index:

$$\text{Slag activity index, \%} = \left(\frac{\text{SP}}{\text{P}}\right) \times 100 \qquad (2.\ 11)$$

Where,

SP = Average compressive strength of slag cement – reference cement mortar cubes at designated ages

P = Average compressive strength of reference cement mortar cubes at designated ages

Table 2.9. Physical requirements for Slag cement (ASTM C989 - 10).

Physical requirements				
Fineness : Amount retained when wet screened on a 45 micron sieve, maximum %			20	
Air content of Slag mortar, maximum %			12	
Slag Activity Index, minimum, %	-		Average of last five consecutive samples	Any Individual samples
	7 days Index	Grade 80	-	-
		Grade100	75	70
		Grade 120	95	90
	28 days Index	Grade 80	75	70
		Grade100	95	90
		Grade 120	115	110

The hydration of slag cement in combination with Portland cement at normal temperature is a two-stage reaction (Regourd, 1980, Roy and Idorn, 1982). Initially

and during the early hydration, the predominant reaction is with alkali hydroxide, but subsequent reaction is predominantly with calcium hydroxide. The principal hydration product is the same as that formed when Portland cement hydrates, that is, calcium-silicate hydrate (Smolczyk, 1978). Wood (1981) reported that the workability of concrete containing slag cement was improved when compared with concrete without slag cement. The compressive strength and rate of strength gain in concrete containing slag cement varies depending upon the slag activity index of a particular slag cement. Hogan and Meusel, (1981) reported that, compared with Portland cement concrete, the use of Grade 120 slag cement typically results in reduced strength at 1 to 3 days and increased strength beyond 7 days curing. The use of Grade 100 results in lower strength at 1 to 21 days, but equal or greater strength after 21 days. Grade 80 typically gives reduced strength at all ages. ACI 506.5R-9 "Guide for specifying underground shotcrete" suggested that the use of slag cement is acceptable only if all shotcrete performance requirements can be demonstrated during preconstruction testing. This is especially relevant to early strength gain.

2.3.3 Mixing water

The mixing water is the free water encountered in freshly mixed shotcrete. It has three main functions: (1) it reacts with the cement powder, thus producing hydration (2) it acts as a lubricant, contributing to the workability the fresh mixture and (3) it secures the necessary space in the cement paste for the development of hydration products (Popovics, 1992). The two important aspects are quantitative and qualitative. The quantitative aspect is how much water should be added to the batch. It is indicated by water to cement ratio (W/C). The W/C ratio is given by the mass of free water relative to the mass of cement powder comprising the shotcrete mix. The W/C ratio is known to affect most of the chemical and mechanical properties of the fresh and hardened shotcrete (Windsor, 2004). Thompson & Windsor (1998) derived

a theoretical W/C ratio value of 0.42 in order to achieve complete hydration of GP cement. The theoretical range of effects of the W/C ratio on compressive strength of cement grout presented by Thompson & Windsor (1998) are shown together with test data given by Hyett et al (1992) in Figure 2.3. The scatter in experimental results below W/C ratio 0.42 can be attributed to the increased presence of air voids resulting from mixing and variability of the curing process effectiveness (Thompson & Windsor, 1998).

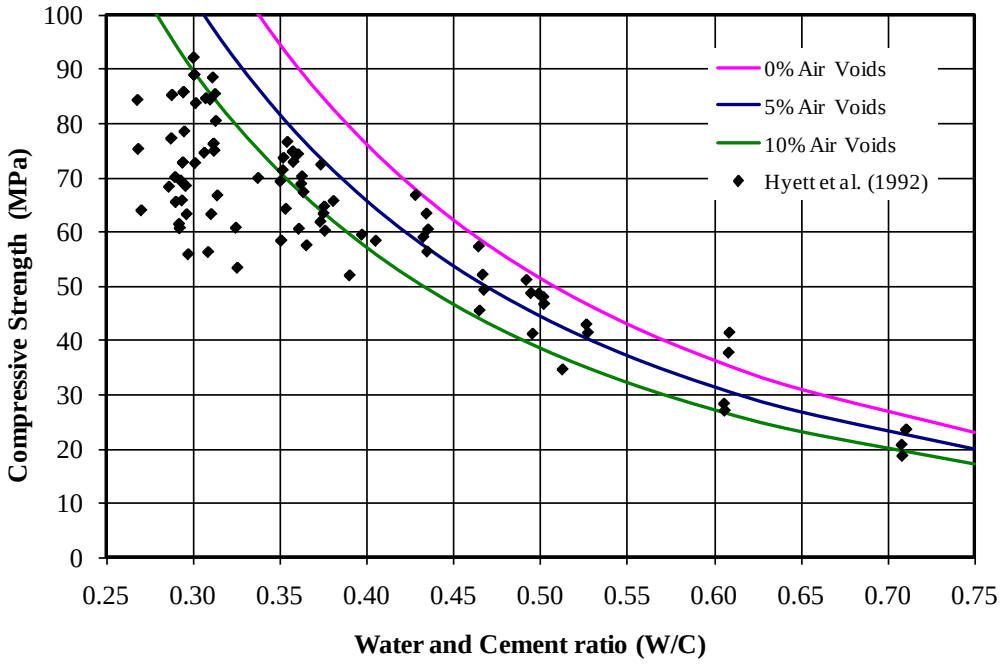

Figure 2.3. Variation in theoretical and experimental compressive strength of cement grout for different water and cement ratios. (Reproduced from Thompson & Windsor, 1998)

The qualitative aspect is the question of what quantities of impurities may make the water unsuitable for shotcrete mixing. The ACI 506.5R-9 “Guide for specifying underground shotcrete” suggested that mixing water used for underground shotcrete shall comply with the ASTM C1602/C1602M. In general, potable water is permitted to be used without testing for conformance with the ASTM standard. Non-potable

water is permitted to be used in any proportions to the limits qualified to meet the required performance and chemical limits as shown in Table 2.10 and 2.11.

Table 2.10. Concrete performance requirements for mixing water (ASTM C1602/C1602M- 06).

	Limits	**Test methods**
Compressive strength, minimum % control at 7 days	90	ASTM C31/ C31 M, C39/C39 M
Time of set, deviation from control, hour:minute	From 1:00 early to 1:30 later	ASTM C403/C403M

Table 2.11. Chemical limits for combined mixing water (ASTM C1602/C1602M- 06).

Maximum concentration in combined mixing water		**Limits (ppm)**	**Test methods**
A. Chloride as Cl^-	1. in prestressed concrete, bridge decks or otherwise designed	500	ASTM C114
	2. Other reinforced concrete in moist environments or containing aluminum embedments or dissimilar or with stay-in-place galvanized metal from	1000	ASTM C114
B. Sulfate as SO_4		3000	ASTM C114
C. Alkalies as (Na_2O+0.658 K_2O)		600	ASTM C114
D. Total solids by mass		50,000	ASTM C 1603

2.3.4 Aggregate

Aggregate is granular material, such as sand, gravel, crushed stone, or iron blast-furnace slag, used with a cementing medium to form hydraulic-cement concrete or shotcrete (ASTM C125 – 10a). It occupies at least three quarters of the total volume

of a given shotcrete mix and thus, its properties greatly affect the properties of the concrete or shotcrete mix. Generally, aggregates can be classified in several ways: according to their petrography, specific gravity, particles size distribution (PSD), natural or manufactured, crushed or naturally processed and chemically inert or reactive (Popovics, 1992). Among those, PSD is the most frequently used classification. Based on PSD analysis it can be divided into coarse and fine aggregate. Generally, aggregate predominantly retained on the 4.75 mm sieve is defined as coarse aggregate and passing 4.75 mm sieve and retained on the 75 micron sieve is defined as fine aggregate. Aggregates consisting of both coarse and fine particles are called combined for mixed aggregates (ASTM: C125 -10a). ASTM:C125 does not define the upper limit of coarse aggregate. Based on Australian standard AS 1289.3.6.1-2009: *"Methods of testing soils for engineering purposes - Soil classification tests - Determination of the particle size distribution of a soil - Standard method of analysis by sieving"* fine aggregate ranges from fine sand to fine gravel and coarse aggregate ranges from medium to cobles. Figure 2.4 shows a graphical representation of coarse and fine aggregate with different combined grading limits to produce shotcrete for underground application. According to ACI 506.5R-09, combined grading No. 1 aggregates are sometimes used in finishing coats and other thin layers and No. 2 are normally preferred for ground support and linings. American Concrete Institute suggested that, coarse aggregate shall have 9.5 mm maximum size for underground shotcrete application (ACI 506.5R-09). This limitation is based on the pumping and/or spraying equipment and in order to avoid too much rebound (Melbye, 1994). According to Armelin and Banthi (1998), the kinetic energy of the incoming particle and the mechanical properties of the substrate and its cohesion are all key parameters to predict if a particle will either be trapped in the in-place shotcrete or rebound.

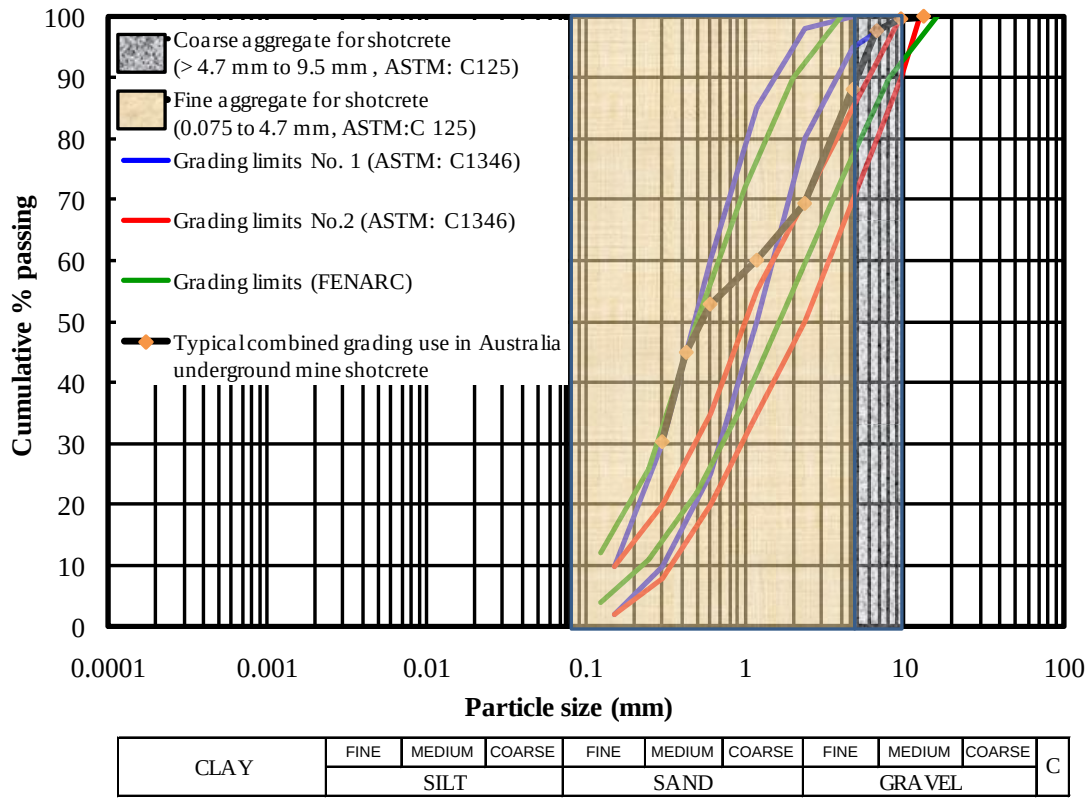

Figure 2.4. Grading limits for combined aggregate for shotcrete (ASTM:C125, C1436, ACI 506.5R-09 & AS1289.3.6.1).

The research from the conventional cast in place concrete industry suggested that, extending the grading of aggregate to a larger maximum size lowers the water requirement of the mix, so that the water and cement ratio can be lowered with a consequence of increased in strength (Higginson, et al , 1963). Reny & Jolin (2011) suggested that, the use of coarse aggregate in shotcrete mixture will provide a wide range of benefits to both plastic and hardened properties. The question is “what is the optimum maximum aggregate size”. Based on the knowledge from the design of “Cyclopean concrete” where large stones or ‘Plums” are used, the maximum aggregate size should not be greater than one-third of the thickness of concrete (Neville, 1995). A typical thickness of shotcrete use for underground mine ground support is ranging from 50 to 75 mm. Therefore, the maximum aggregate size can be up to 17 mm for a 50mm thick shotcrete layer.

In addition to a PSD, the particle shape and texture, specific gravity, bulk density, moisture content, mineral and chemical properties and the strength of aggregate also influence the properties of shotcrete. Nevertheless, more research need to done to understand more about the effects of aggregate on shotcrete properties.

2.2.5 Fibres

Fibres are the slender filaments, which may be discrete or in the form of bundles, networks, or strands of natural or manufactured materials, which can be distributed uniformly throughout a fresh cementitious mixture (ASTM C125 – 10a). Since ancient times, fibres have been used to reinforce brittle materials. For examples, straw was used to reinforce bricks and horsehair was used to reinforce mortar and plaster. In most recent times, large scale commercial use of asbestos fibres in a cement paste matrix began with the invention of Hatschek process in 1898. However, alternate fibres were introduced in the 1960s and 1980s, due to the health hazard associated with asbestos fibres (ACI 544.1R-96). In the early 1960s, the first major investigation was made to evaluate the potential of steel fibres as a reinforcement for concrete (Romualdi and Batson, 1963). Since then, a substantial amount of research, development experimentation, and industrial application of fibres reinforced concrete has occurred. There are numerous fibres types available for commercial and experimental use. The basic categories are steel, glass, synthetic and natural fibre materials, though, ACI 506-5R suggested that only steel and synthetic fibre shall be used for underground shotcrete application. The physical and mechanical properties of fibre reinforced shotcrete (FRS) are influenced by the fibres types and dimension (length to diameter ratio), geometry, dosage, distribution and bond characteristics between fibre and shotcrete matrix. Figure 2.5 shows that fibres with various orientations actually respond in different failure modes. The responses are predominantly shear, tensile and compression in nature. The most common response is a combination of these modes. The force-displacement relationship of the individual fibres can be described with characteristic diagram as shown in Figure 2.6 (Saw, et. al., 2009).

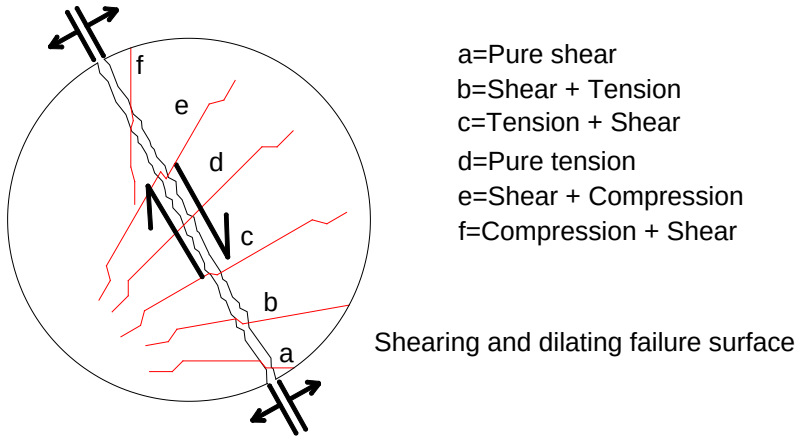

Figure 2.5. Fibre with various response modes for different fibre orientation (Modified from Windsor, 1996).

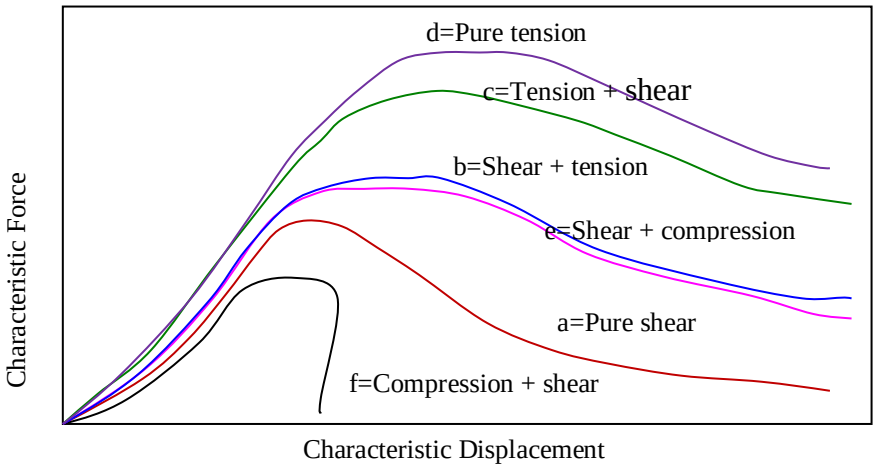

Figure 2.6. Force-displacement characteristic diagram for different fibre orientation.

Windsor (2009) suggested that, the adhesive, frictional and mechanical bond strength between the fibre and the cementitious matrix control the mechanical performance of the failure surface (or cracked shotcrete), not the strength of the fibre. Figure 2.7 (Windsor, 2009) shows cracked surfaces in a synthetic fibre reinforced shotcrete surface on a mine excavation wall shown in “A” with magnifications at crack points “B” and “C”. Collectively, views “A”, “B” and “C” show:

- The fibres lie in the plane of the layer, oriented approximately normal to crack.
- The orientations of fibres across the crack indicate the geometry of crack displacement.
- Some fibres remain bonded in each crack face depending on crack displacement (A)
- Some fibres have pulled out of each crack face depending on crack displacement (B).
- There are very few broken fibres.
- There are little if any, fibres projecting from the layer surface.

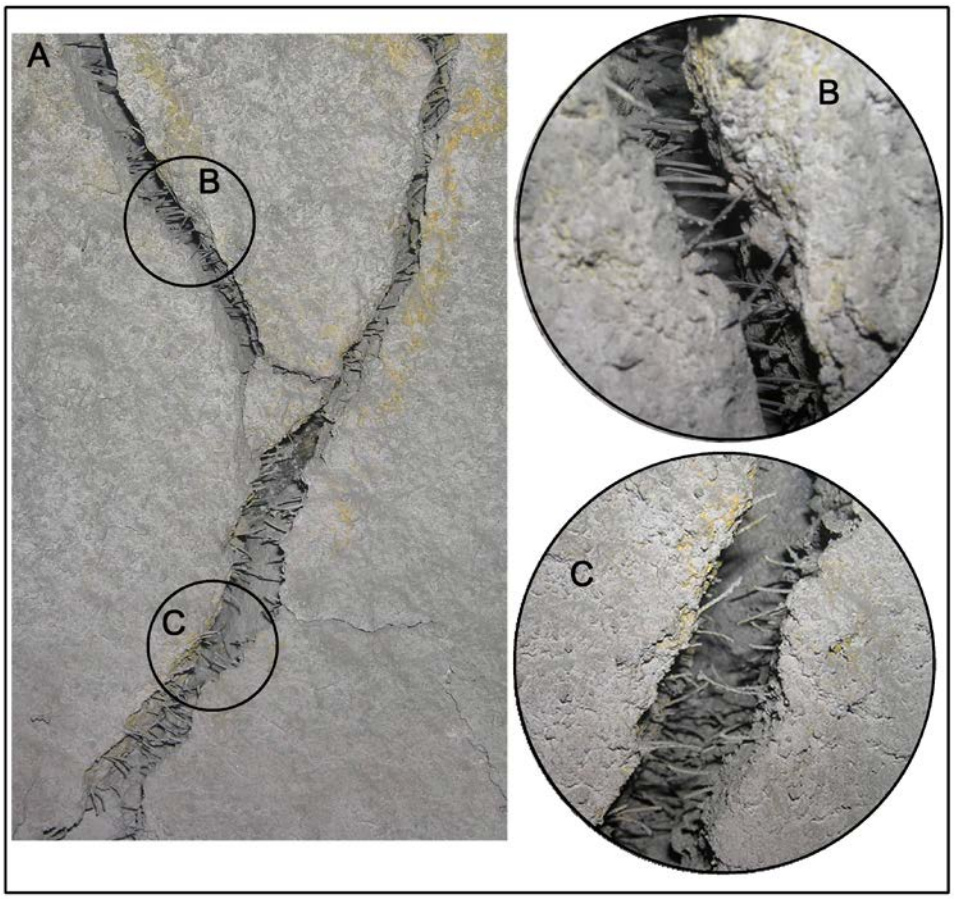

Figure 2.7. Cracked surfaces in a synthetic fibre reinforced shotcrete surface on a drive wall shown in "A" with magnifications at crack points "B" and "C" (Windsor, 2009).

2.3.5.1 Steel fibres

Steel fibres are defined as short, discrete lengths of steel which are sufficiently small to be randomly dispersed in an unhardened concrete mixture (ACI 544.1R-96). Basically, there are five general types of steel fibres used based on the process or product. They are cold-drawn wire (Type – I), cut sheet (Type – II), melt-extracted (Type –III), mill cut (Type –IV) and modified cold-drawn wire (Type – V). These steel fibres can be either straight or deformed (ASTM A820/A 820M, 2006). The ASTM A820 specified the standard for steel fibres for reinforced concrete or shotcrete. A typical steel fibre dosage is between 30 and 40 kg/m^3 of shotcrete.

2.3.5.2 Synthetic fibres

Synthetic fibres are made from polymers such as acrylic, aramid, carbon, nylon, polyester, polyethylene and polypropylene. Table 2.12 summarises the range of physical properties of selected synthetic fibre types. Polypropylene base synthetic fibre is currently the most widely used fibre for shotcrete application. The fibre length, width and thickness of macro synthetic fibre are typically 48, 1.28 and 0.5 mm, respectively. A typical macro synthetic fibre dosage is between 5 and 8 kg/m³ of shotcrete. A typical length of micro synthetic fibre is 6 to 20 mm and 0.015 to 0.03 mm in diameter. Addition rate of micro synthetic fibre is typically 0.9 kg/m³ of shotcrete.

Table 2.12. Selected synthetic fibre types and properties (ACI 544.1R-96).

Base material	Specific garvity	Tensile strength (MPa)	Youngs modulus (GPa)	Melting point (°C)	Ignition point (°C)	Water absorption per ASTM D570, % by weigth
Acrylic	1.16 - 1.18	369 - 1000	14 - 19	221 - 455	-	1 -2.5
Aramid	1.44	2930	62	482	high	4.3
Carbon, Polyacrylonitrile based, high modulus	1.6 - 1.7	2482 - 3034	380	400	high	nil
Carbon, Polyacrylonitrile based, high tensile strength	1.6 - 1.7	3448 - 3999	230	400	high	nil
Carbon, Isotropic pitch based, general purpose	1.6 - 1.7	483 - 793	28 - 34	400	high	3 - 7
Carbon, Mesopase pitch based, high performance	1.80 - 2.15	1517 - 3103	152 - 483	500	high	nil
Nylon	1.14	965	5	200 - 430	-	2.8 - 5.0
Polyester	1.34 - 1.39	228 - 1103	17	257	593	0.4
Polyethylene	0.92 - 0.96	76 - 586	5	134	-	nil
Polypropylene	0.90 - 0.91	138 - 690	3 - 5	166	593	nil

2.3.6 Admixtures

An admixture is defined as “A material other than water, aggregate, hydraulic cement and fibre reinforcement used as an ingredient of concrete or mortar and added to the batch immediately before or during its mixing” (ASTM C125). It includes mineral and chemical admixtures, minerals admixture such as silica fume, fly ash and slag which were described in section 2.2.2 as supplementary cementing materials. Admixture described in this section refers to chemical admixtures. The admixtures may remain in a free state as a solids or solution, may interact at the surface or be chemically combined with the constituents of cement or cement paste. The type and extent of interaction may influence the physico-chemical and mechanical properties of concrete such as water demand, hydration kinetic, composition of the products, setting times, microstructure, strength and durability (Ramachandran, 1995). ASTM C1141/C1141M provides a standard specification for admixtures for shotcrete. A summary of shotcrete admixture requirements is presented in Table 2.13. Admixtures used in underground shotcrete application mainly fall into four categories: (a) accelerator, (b) superplasticiser or high range water reducer (c) hydration stabiliser and (d) air-entraining admixture. The following sections described the effects of those admixtures and chemistry underlying those effects.

Table 2.13. Shotcrete admixture requirement (ASTM :C 1141/C 1141M - 08).

Type I - Dry mix shotcrete			
Grade	**Admixture**	**ASTM standard**	**Other limits**
1	Accelerating, conventional	D98, C494/C494M Type C or E	
2	Retarding	D98, C494/C494M Type B or D	
3	Pozzolanic	C618, C989, C1240	
4	Metallic iron	Not established	The metallic particles shall be ground iron free from rust, oil, foreing materials, and nonferrous metal particles. The grading of the metallic aggregates shall be as follows when tested according to C136:
			US Sieve No. / % Passing
			4.75 mm (No.4) / 100
			2.36 mm (No. 8) / 90 - 100
			1.18 mm (No. 16) / 70 - 85
			600 μm (No. 30) / 20 - 35
			300 μm (No. 50) / 0 - 10
			150 μm (No. 100) / 0 - 5
5	Coloring	C 979	Even when using materials conforming to C 979, it may be difficult to obtain uniformity of coloring because of the placement
6	Organic polymer	C 1438	
9	Accelerating, quick setting	C 1398	Initial time of setting 1 to 3 minutes and fianl time of setting not more than 12 minutes in two of every three est and chloride limits of ACI 318 shall not be exceeded.
Type II - Wet mix shotcrete			
1	Accelerating, conventional	D 98, C494/C 494M Type C or E	
2	Retarding	C 494/C 494M, types B, D or G	
3	Pozzolanic	C 618, C 989, C1240	
4	Metallic iron	Not established	See Type I, Grade 4
5	Coloring	C 979	
6	Organic polymer	C 1438	
7	water reducing	C 494/C 494M, Types A, D, E, F or G	
8	Air-entraining	C 206	
9	Accelerating, quick setting	C 1398	See Type I, Grade 9

2.3.6.1 Accelerator

Most of the accelerators used for shotcrete in underground civil and mining applications mainly contain aluminium sulphate as a liquid state (Myrdal, 2007). The accelerator is added to a shotcrete mix as a separate component at the nozzle during spraying. That type of accelerator is widely known as alkali-free accelerator. The term “alkali-free” means the accelerator has no (or below 1%) alkali cations such as Na^+, K^+ and Li^+. Those alkali cat-ions can react with dissolvable silica SiO_2 that are sometimes present in aggregates. Such reactions are known as alkali-silica reaction which can fracture the aggregate due to expansion. That reaction may have a damaging effect on the concrete matrix (Garshol & Melbye, 1996). Addition of alkali-free accelerators changes the course of the chemical reactions especially at early stages. Burge (2001) found that Aluminium sulphate reacts with calcium

hydroxide ($Ca(OH)_2$) and produce additional ettringite and aluminium hyroxide. The reaction can approximately be represented by the equation,

$$Al_2(SO_4)_3+6Ca(OH)_2+32H_2O \rightarrow 3CaO.Al_2O_3.3CaSO_4.32H_2O+Al(OH)_3 \quad (2.\ 12)$$

Aluminium sulphate+Calcium hydroxide+water→Etringite+Aluminium hydroxide (2. 13)

The aluminium sulfate components of these accelerators promote the crystallisation of ettringite at a very early stage. Within 4 hours of hydration, these crystals grow and fill most of the capillary pores. Usually, the formation of ettringite within the first 30 minutes is largely sufficient to set a shotcrete mix (Paglia, et, al., 2001).

Alkali-free accelerator may also contain;

1. Amine and glycolic acid (Angelskaar, 2003)
2. Hydrofluoric acid, diethanolamine, methyldiethanolamine and ethylenediamine tetraacetic acid (complex binder) (Sommer, 2000)
3. Magnesium sulphate, phosphorous acid, oxalic acid, maleic anhydride and diethanolamine (Angelskaar, 2004)
4. Citric and malic acids and their alkali metal salts (farrington, et al, 1996)
5. $Al(OH)_xR_y$, where x+y=3, R=organic acid (formic, acetic, 4-toluenesulphonic, lactic or oxalic) or nitric acid (Valenti, 1996)

Generally, addition of alkali-free accelerator is also known to reduce the shotcrete durability with respect to chloride resistance, permeability, sulphate attack, and freezing and thawing action (ACI 506-5R). Most accelerators results in lower 28 days strength when compared with a non-accelerated shotcrete. Complex factors that may cause low strength are: formation of C-S-H with higher C/S ratio, retardation of C_3S hydration, rapid initial setting followed by large heat development, and a more porous structure (Ramachandran, 1995). Table 2.14 shows examples of commercial accelerator for shotcrete.

Table 2.14. Examples of commercial accelerator for shotcrete (Myrdal, 2007).

Name of product	Information on ingredients given in MSDS		
	Type of chemical ingredient	% by weight	Manufacturer
Meyco SA 160	Aluminum sulphate	30 – 45	BASF Chemical
	Diethanolamine	1 – 4	
Meyco SA 163	Aluminum sulphates/fluorides	15 – 30	
	Diethanolamine	1 – 5	
	Oxalic acid di-hydrate	1 – 6	
Meyco SA 164	Aluminum sulphates/fluorides	20 – 40	
Meyco SA 170	Aluminum sulphate, hexadecahydrate	25 – 50	
Meyco SA 172	Aluminum sulphate	30 – 50	
	Formic acid	0.5 – 2.5	
	Meyco SA 170	30 – 50	
Meyco SA 175	Aluminum sulphate	20 – 30	
	Maleic anhydride	1 – 4.5	
	Oxalic acid di-hydrate	1 – 4.5	
	Phosphorous acid	1 – 4.5	
Meyco SA 180	Aluminum sulphate	20 – 30	
	Diethanolamine	1 – 4.5	
	Phosphorous acid	1 – 5	
Sigunit–L 50 AF	Aluminum sulphate	No information	Sika Construction Chemical
Sigunit–L 53 AF S	Aluminum salts	No information	
Sigunit–L 5450 AF	Aluminum salts	No information	
Sigunite–L 72 AF VP	Aluminum sulphate	35 – 50	
	Formic acid	2 – 10	
	2,2”-iminodiethanol (diethanolamine)	1 – 3	
	Glycerin (propane-1,2,3-triol)	1 – 5	
Mapequick AF 2000	Aluminum sulphate	20 – 25	Mapei Chemical
	Aluminum fluoride	5 – 9.99	
Mapequick AF D 02	Aluminum sulphate	25 – 34.99	
	Manganese sulphate	0.5 – 0.99	
Mapequick AF 400	Aluminum sulphate	12.5 – 19.99	
	Inorganic fluoride	2.5 – 2.99	
	Manganese sulphate	1 – 2.49	
Sure-Shot AF	Aluminum sulphate (anhydrous)	> 60.0	Euclid Chemical
	Diethanolamine	3.0 – 7.0	

2.3.6.2 Superplasticiser

Superplasticiser is used within shotcrete for three different purposes or a combination of these; (1) to increase workability (pumpability and shootability) at a given mix composition, (2) to reduce the mixing water, at a given cement content and workability, in order to reduce the water and cement ratio, (3) to reduce both water and cement quantity (Collepardi, et. at, 1999). Superplasticisers belong to a class of water reducers which are capable of reducing water content about 30 - 40 %. According to ASTM C494/C494M most of the commercial superplasticisers can be classified as “type F – high range water reducing admixture”.

The chemical compounds for manufacturing superplasticiser are broadly classified into four groups: (1) fonated melamine-formaldehyde condensate (SMF); (2) sulfonated naphthalene-formaldehyde condensate (SNF); (3) modified lignosulfonates (MLS); and (4) others including sulfonic acid esters, polyacrylates, polystyrene sulfonate, etc., (Ramachandran & Malhotra, 1995). More recently, new superplasticisers have been developed based on acrylic polymers (AP). Superplasticisers based on SMF, SNF and MLS cause dispersion into smaller agglomerates of cement particles. Dispersion of cement particles occurs due to absorption and electrostatic repulsion. This process reduces the formation of entrapped water and surface interaction of particles causing the fluidising effect in a cement mixture. In AP based suerplasticisers dispersion of cement particles is not related to the electrostatic repulsion but the polymer adsorption itself (Collepardi, et. at, 1999). Collepardi (1999) also investigated that, the superplasticising effect also depends on the chemical composition of the cement and addition procedure. Some of the superplasticier also can retard the cement hydration up to 4 hours (Bracher, 2005). Table 2.15 shows examples of commercial superplasticiser for shotcrete.

Table 2.15. Examples of commercial superplasticiser for shotcrete.

Name of product	Information on ingredients given in MSDS		
	Type of chemical ingredient	% by weight	Manufacturer
Rheobuild 1000	Naphthalene sulfonates in water	No information	BASF Chemical
Glenium 27	Polycarboxylate solution	15 - 30%	
Sikament NN	Aqueous solution of anionic formaldehyde-polycondensate, naphthalene sulphonic acid, sodium salt	No information	Sika Construction Chemical
Sika Viscocrete PC HRF1	Salts of thiocyanic acid	0.1 - <1	
	mixture of: 5-chloro-2-methyl-4-isothiazolin-3-one and 2-methyl-2H-isothiazol-3-one	0 - <0.1	
ViscoCrete 20HE	Aqueous polymer solution	No information	
ADVA 190		No information	Grace Construction Products
Catexol 1000 SP-MN	Combination of melamine formaldehyde condensate, and other proprietary ingredients	No information	AXIM Concrete Technologies Inc
	Triethanolamine	1-5%	
	Formaldehyde	0.10%	
Superflux 2100 PC	Polycarboxylate	No information	
CentroxTM SH	Aqueous polymer solution	No information	Australian Industrial Additives Pty Ltd
	Mixture of 5-chloro-2methyl-2H-isothiazal-3-one and 2-methyl-2Hisothazaol-3-one (3:1)	20-40 ppm to 100%	

2.3.6.3 Air-entraning

An air-entraning admixture is “an admixture that causes the development of a system of microscopic air bubbles in concrete, mortar, or cement paste during mixing” usually used to increase workability and resistance to freezing and thawing .(ACI 212.3R-10). An air-entraning admixture does not generate air voids. It stabilise the air voids entrapped into the concrete during the mixing process (Powers, 1968). As the air entraining admixture molecules are inserted between adjacent water molecules at the water surface, the mutual attraction between the separated water molecules is reduced. Lowering the surface tension stabilises the bubbles againstmechanical deformation and rupture, making it easier for bubbles to be formed. Without the presence of an air-entraining agent, the smaller bubbles, which

have higher internal pressure, coalesce to form larger bubbles that have a greater tendency to escape to the surface and burst (Nagi, et. at., 2007). Materials used for air entrainment admixtures have been traditionally been based on water soluble compounds such as; salts of wood resins, synthetic detergents, salts of petroleum acids, salts of proteinaceous acids, fatty and resinous acids and their salts, and organic salts of sulfonated hydrocarbons (Dolch, 1995). These have now been largely replaced with synthetic surfactants based on blends of: alkyl sulphates, olefin sulphonates diethanolamines, alcohol ethoxylates and betains (Cement Admixture Association, 2006).

Air-entraining admixtures have no appreciable effect on the rate of hydration of cement or on the heat evolved by that process. Apparently they also have no effect on the chemical composition of the hydration products (Dolch, 1995). Beaupre (1994) suggested, the workability of the fresh shotcrete mix is increased to meet the pumpability requirement by introducing a large amount of entrained air bubbles (10% to 30%) in to the fresh mix. The initial large amount of air will be lost during pumping and shooting due to the compaction process. In addition, it can improve accelerator distribution within the shotcrete. This results in uniformly higher early strength achievement (Hauck & Kristiansen, 2010). Table 2.16 shows examples of commercial air-entraning admixture for shotcrete.

Table 2.16. Examples of commercial air-entraning admixture for shotcrete.

Name of product	Information on ingredients given in MSDS		
	Type of chemical ingredient	% by weight	Manufacturer
Micro -Air 940	Aqueous solution based on Alkylarylsulfonate	No information	BASF Chemical
	Dodecylbenzenesulphonic acid	1 % - < 10 %	
	Sodium hydroxide	0.1 % - < 1 %	
	Formaldehyde	0.01 % - < 0.19 %	
Micro - Air 905	Aqueous solution based on Alkylarylsulfonate	No information	
	Dodecylbenzenesulphonic acid	>= 0.1 % - < 2.5 %	
	Formaldehyde	0.1 % - < 1 %	
Sika Air	Aqueous solution based on synthetic surfactants	No information	Sika Construction Chemical
CATEXOL A.E. 260	Aqueous solution of a unique, synthetically manufactured non-Hazardous Ingredients	95-100%	AXIM Concrete Technologies Inc
	Alpha Olefin Sulfonate	1-5%	
	Diethylene Glycol	<2%	
Darex II AEA	Alkaline Solution of Fatty Acid Salts	No information	Grace Construction Products

2.3.6.5 Hydration stabiliser

Hydration stabilisers are used to limit prehydration of shotcrete and to extend the retention time of batched shotcrete when the handling and logistical constraint typically associated with underground construction causes prolonged transport and discharge time (ACI 506.5R-11). It is also commonly referred as hydration controlling admixture or retarder (ASTM C494). The stabiliser can suspend cement hydration up to 72 hours. Usually, an activator or accelerator is added to the shotcrete mix at the nozzle when it is sprayed.

The most widely used compounds to manufacture stabiliser are organic compounds such as Na, Ca or HN4 salts of lignosulfonic acids, hydroxyl-carboxylic acid and carbohydrates. Inorganic compound such as phosphates, borates and salts of Pb, Zn, Cu, As and Sb may also act as stabilisers (Ramachandran, et. al., 1995). The organic

stabiliser is adsorbed on to the surfaces of growing particles of hydration products and complexing calcium ions (Ca^{2+}) ions in aqueous solution (Taylor, 1997). The adsorption causes the precipitation of low-permeability coating film on the cement particles which slow down further hydration (Edmeades and Hewlett, 2008). Table 2.17 shows examples of commercial hydration stabiliserfor shotcrete.

Table 2.17. Examples of commercial hydration stabiliser for shotcrete.

Name of product	**Information on ingredients given in MSDS**		
	Type of chemical ingredient	**% by weight**	**Manufacturer**
Recover	Aqueous Solution of Hydroxycarboxylic Acid Salts and Compound Carbohydrates	No information	Grace Construction Products
Delvocrete stabiliser	Amino-tris (methylene phosphonic acid)	10 - < 30%	BASF Chemical
	Citric acid anhydrous	< 10%	
	Water	60%	
SikaTard -930	Liquid solution of polycarbonic acid salts	No information	Sika Construction Chemical
CentroxTM SS	Aqueous polymer solution	No information	Australian Industrial Additives Pty Ltd
	Mixture of 5-chloro-2-methyl-2H-isothiazal-3-one and 2-methyl-2Hisothazaol-3-one (3:1)	20-40 ppm	

2.4 Early strength of shotcrete

The strength of a shotcrete is related to its ability to withstand an applied stress without failure. The applied stress may be compressive, tensile or shear. In reality, an infinite variety of applied stress may possible. However, the total response and total strength can be a limited number of fundamental strength such as compression, tension, shear, torsion, flexure and combinations of those (Windsor, 1998). Many of the sampling and testing methods for shotcrete are similar to those used for concrete and can be broadly categorised as destructive and non-destructive testing. The sampling and testing of shotcrete are usually conducted on in situ or test panel (ACI 506-2 and ASTM C1140).

Shotcrete for underground mine support often requires rapid setting and early strength development of a freshly sprayed shotcrete. The final setting of shotcrete usually occurres within 10 minutes when accelerator is added at the nozzle with a defined dosage. The strength rapidly develops after the final setting. In underground mining industry the early strength of the shotcrete generally refers to the strength developed from the time of spraying (0) to (4) hours curing. The early strength is usually determined by indirect methods and correlated to the strength development with time. It is not possible to core the standard test specimen of shotcrete to perform conventional laboratory strength test within those curing times. Hence, the measured properties include; penetration resistance, pull out force, temperature, electrical conductivity and resistivity and ultrasonic wave velocity. The measurement methods can be broadly categorised as destructive and non-destructive determination. Although compression, tension, shear, torsion or flexure strength are possible to be correlated to an indirectly measured parameter, current literature shows that uniaxial compressive strength (UCS) is the most commonly used method.

The following sections review the early strengths and test methods of shotcrete.

2.4.1 Destructive methods

2.4.1.1 Penetration resistance test

Penetration resistance is the force required to press a steel needle or probes with defined dimensions into a sprayed concrete**.** The test method is an adaption of two test methods. The first method is pocket penetrometer test used to evaluate consistency and approximate unconfined compressive strength of soils. The second method is ASTM C403 "standard test method for time of setting of concrete mixtures by penetration resistance". Many early strength of shotcrete data using this method have been published by Jolin et al., 1999; Heere et al., 2002, Rispin, 2003, Clemets, 2004; Knight et al., 2006, O'Toole & Pope, 2006 and Bernard, 2009. Figure 2.8 shows early compressive strengths of shotcrete determined by penetration resistance method published in different literatures.

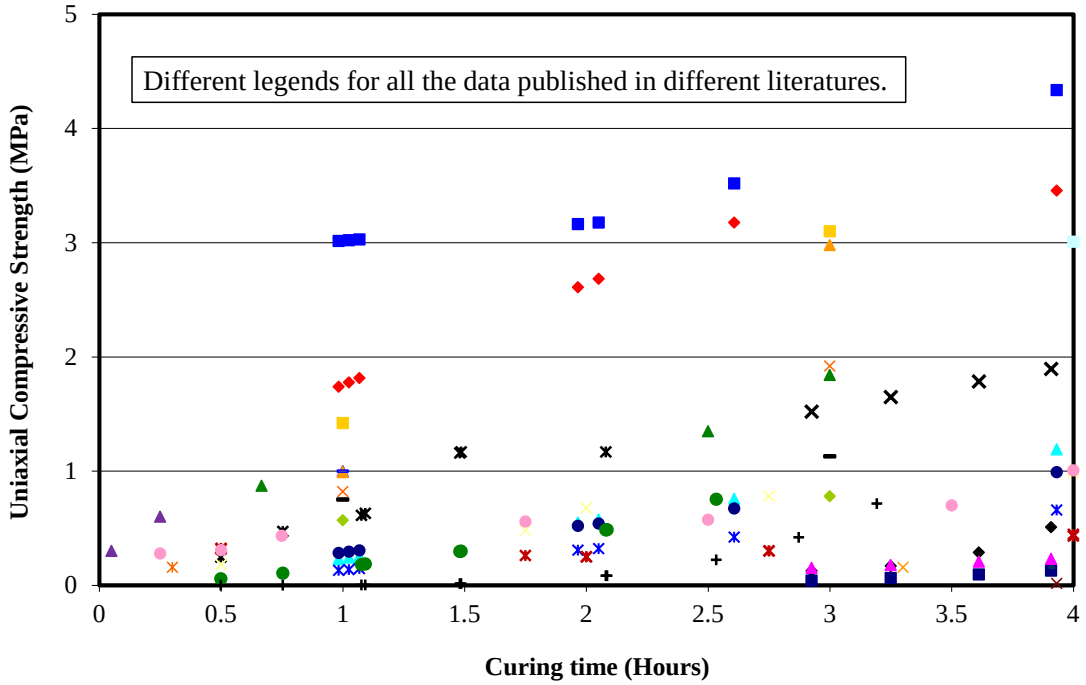

Figure 2.8.Typical compressive strength of shotcrete determined by penetration resistance.

2.4.1.2 Bolt firing and pull-out test

The method was originally developed by Kusterle and Lukas (1990). In this method a standardised nails are fired into the shotcrete with a Hilti DX 450L gun. The depth of penetration and pull-out force are determined to estimate the compressive strength. The change in strength can be allowed for by using different nails and ammunition. Bracher (2005) simplified this method by correlating the depth of penetration and compressive strength as shown in Figure 2.9.

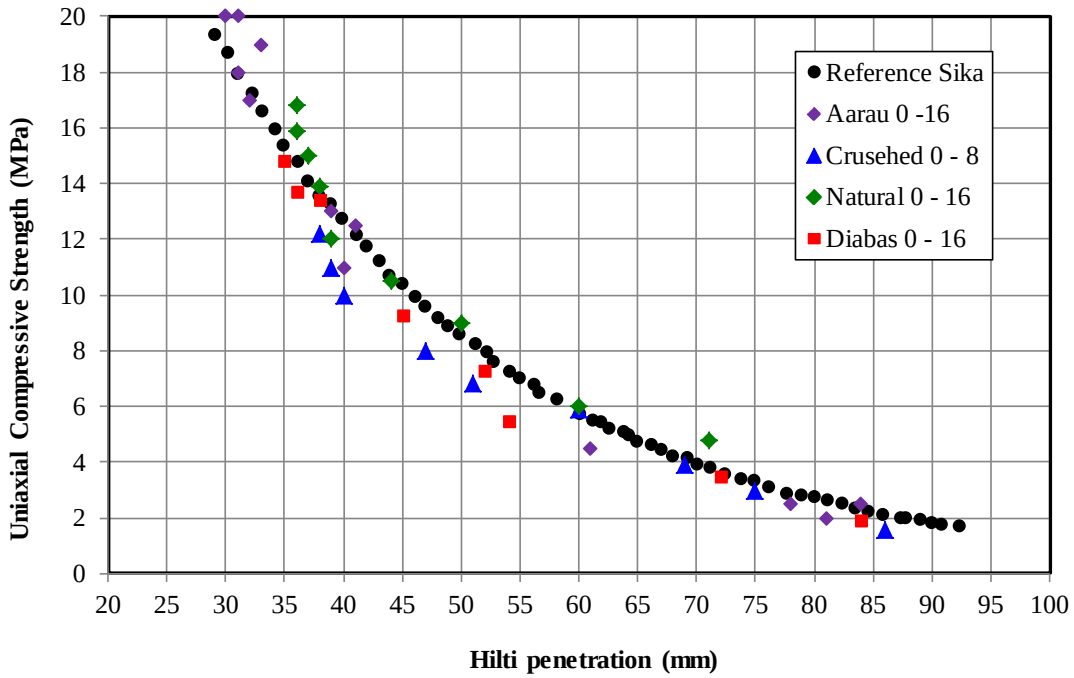

Figure 2.9.Compressive strength of shotcrete determined by penetration depth (Reproduced from Bracher, 2005).

2.4.1.3 Sprayed beam compression test

This method is an adaption of the ASTM C116; “Standard test method for compressive strength of concrete using portions of beams broken in Flexure”. In this method shotcrete samples is sprayed into a set of three or four moulds. The internal

dimensions of each mould are 350 x 75 x 75 mm (Length x Width x Height). The specimen is removed from the mould prior to the test. The test is usually conducted on site with a potable compression machine. The machine consist of a top loading plate with the dimensions 75 x 75 x 20 mm which transfer the load from the loading head to the specimen. The specimen is supported on two bottom plates. The first bottom plate is 75 mm long, 80 mm wide and 20 mm deep. The second plate is 200 mm long, 80mm wide and 20 mm deep. The gap between the two bottom plates is 75 mm. Therefore, the loaded section of the beam specimen is 75 long, 75 wide and 75 mm deep (Morgan et al., 1999). A sketch of Ganged 3 beams steel mould, portable compression test machine and beam support and loading plate is shown in Figure 2.10. Example of early strength development of wet mix shotcrete determined with sprayed beam compression test is presented in Figure 2.11.

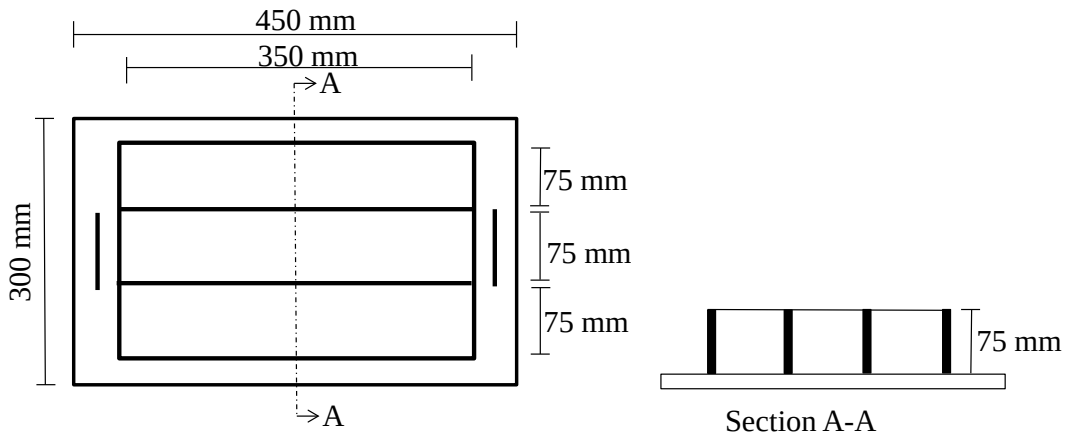

(a) Sketch of 3 beams steel mould.

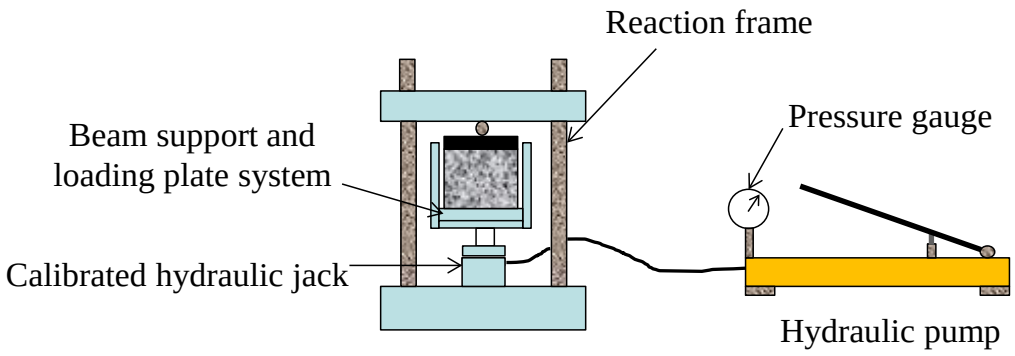

(b) Portable compression test machine.

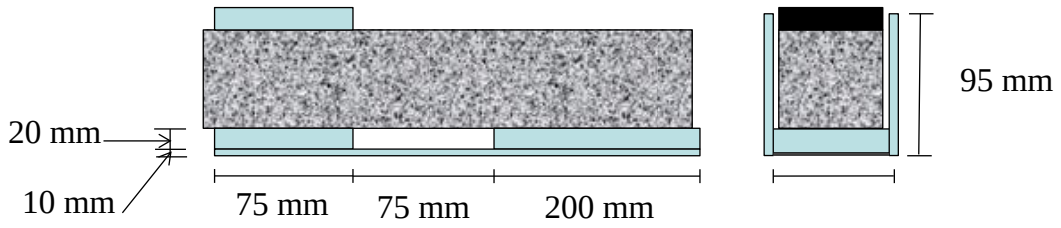

(C) Beam support and loading plate.

Figure 2.10.(a) Sketch of 3 beams steel mould, (b) portable compression test machine and (c) beam support and loading plate (Morgan et al., 1999).

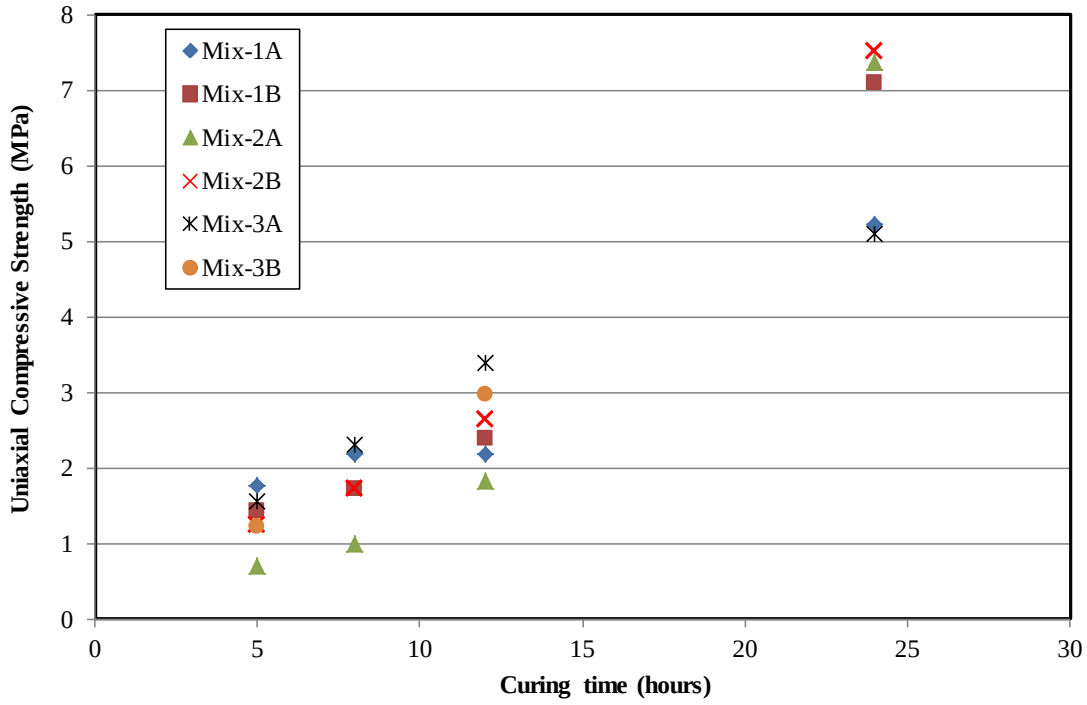

Figure 2.11. Early strength development of wet mix shotcrete determined with sprayed beam compression test (Reproduced from, Morgan et al., 1999).

2.4.1.4 Shear strength of fresh (immediately after sprayed) shotcrete

Shear strength is the strength of a material or component to resist a structural failure or yield where the material or component is subjected to shear load. A shear load is a force that tends to produce a sliding failure on a material along a plane that is parallel to the direction of the force (Gere & Timoshenko, 1990). Therefore, shear strength a fresh (immediately after sprayed) shotcrete is the strength that can resist sliding or yielding when it is subjected to shear loading. Figure 2.12 shown a sketch of shotcrete layer failed under shear, combination of shear and compression, and combination of shear and tension load (Windsor, 1999).

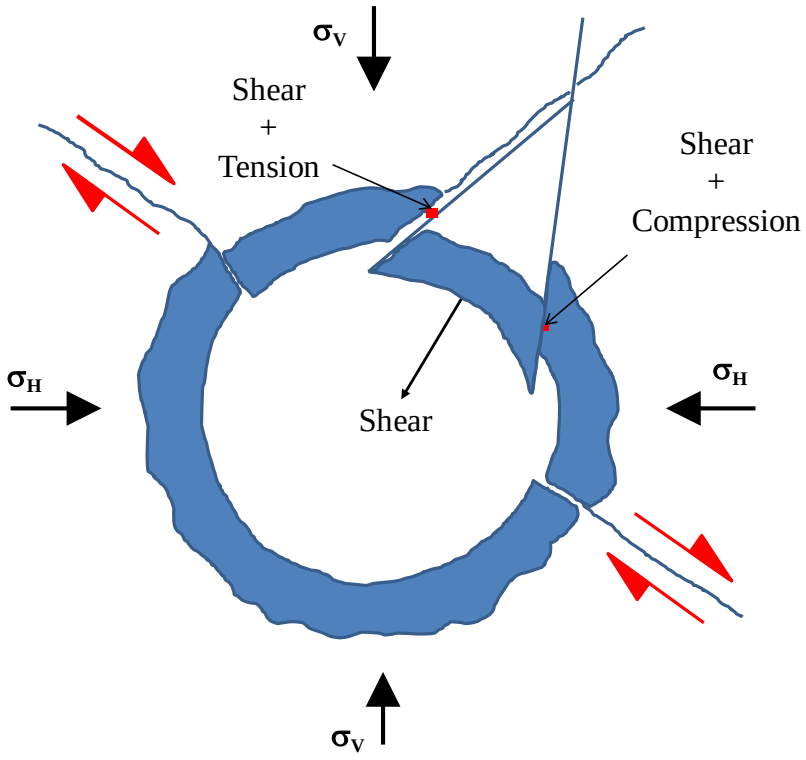

Figure 2.12. Shotcrete layer failed under shear load, combination of shear and compression, and combination of shear and tension load (Windsor, 1999).

The shear strength of shotcrete immediately after sprayed (Dry mix method) was studied by Jolin (1999) using vane shear test method. Before spraying the shotcrete the vane was embedded in the circular mould. The torque was applied to the vane within a minute after the sample was shot until failure occurred. The shear strength of shotcrete immediately after sprayed for different shotcrete mix conducted by Jolin (1999) is shown in Table 2.18. The result shows that the shear strength of fresh shotcrete ranges from 19.8 to 84.4 kPa.

Table 2.18. Shear strength of dry mix fresh shotcrete - 1 minute after spraying (Jolin, 1999).

Mix ID	Composition					Consistency	Curing time (Minute)	Shear strength of fresh shotcrete (kPa)
	Binder		Sand	Coarse aggregates	Air entrain admixture			
	Type	(%)	(%)	(%)	ml/l			
T10	10	20	64	16	-	Dry	1	60.6
						Normal	1	44.3
						Wet	1	28.0
T10+SF	10+10% silica fume	20	64	16	-	Dry	1	77.8
						Normal	1	59.2
						Wet	1	40.6
T30	10	20	64	16	-	Dry	1	84.4
						Normal	1	62.4
						Wet	1	40.5
T10@25%	10	25	60	15	-	Dry	1	67.5
						Normal	1	50.5
						Wet	1	33.4
T10+Agg	10	20	56	24	-	Dry	1	59.2
						Normal	1	46.8
						Wet	1	34.3
T10+AEA	10	20	64	16	15	Dry	1	68.8
						Normal	1	54.6
						Wet	1	40.3
T10+Predamp	10	20	64	16	-	Dry	1	-
						Normal	1	32.3
						Wet	1	19.8

2.4.2 Non - destructive methods

2.4.2.1 Temperature monitoring

During hydration, heat evolves due to exothermic chemical reactions in the mix predominantly associated with cementitious materials and water. The temperature rise can be converted into calories per gram (J/g) of cement. There are basically three measurement techniques for determining the heat of hydration. The first technique is using an isothermic calorimeter (Kuhl, 1961). In this technique, the heat of hydration of cement is directly measured by monitoring the heat flow from the specimen when both the specimen and the surrounding environment are maintained at approximately isothermal conditions. The second technique was suggested by Berman (1963) for the determination of heat evolution based on placing a concrete sample in an adiabatic calorimeter, in which no heat loss can occur. The third technique is by

measuring the difference between the heat of solution of the dry cement powder and the heat of solution of a separate portion of cement that has been partially hydrated for a known period of time (ASTM C186). Based on the basic three methods described above numerous experimental investigations have been conducted to correlate the heat of hydration and the strength of concrete/shotcrete (eg. ACI SP-241, 2007). The ASTM C 1074 suggests a procedure for estimating concrete strength by the maturity method. The maturity method is based on recorded temperatures of the concrete and a model developed from the laboratory strength testing of a concrete sample of the same mix. Dight & Hulls (2009) investigated the strength of shotcrete using maturity method. Figure 2.13 shows a summary of published data on temperature development different concrete, shotcrete and cement paste mixes.

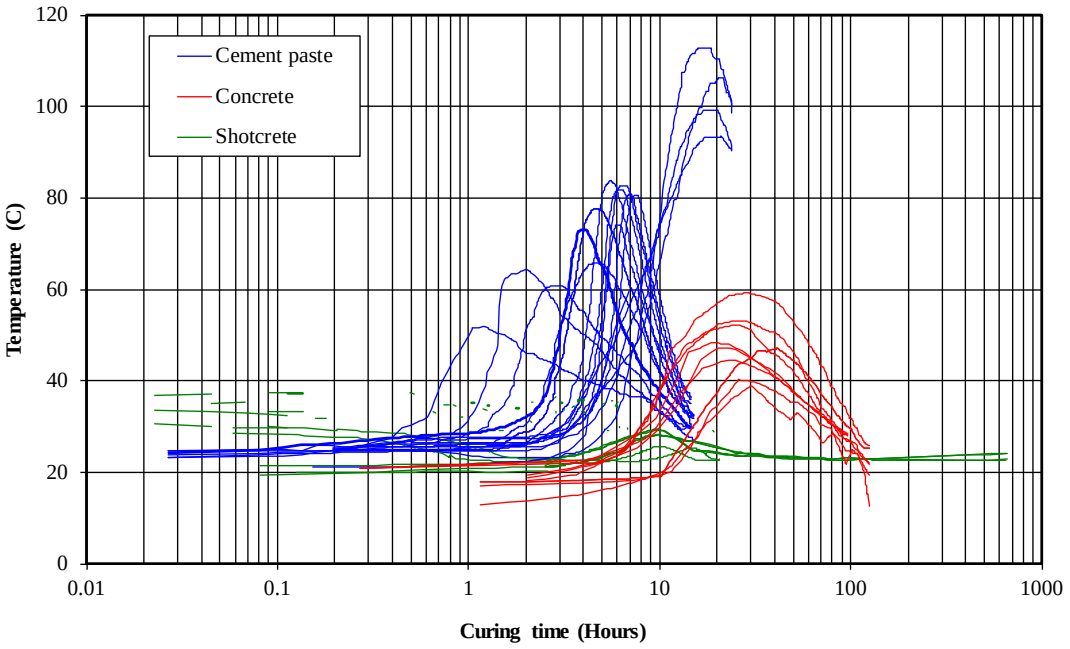

Figure 2.13. Temperature developments for different concrete, shotcrete and cement paste mixes (Data from various literatures).

2.4.2.2 Ultrasonic pulse velocity

The velocity of ultrasonic pulse travelling in a solid medium depends on the density and elastic properties of that material. In the ultrasonic pulse velocity (UPV) test, pulses of longitudinal stress waves are generated by an electro-acoustical transducer that is held in contact with one surface of the material under test. After travesing through the material, the pulses are received and converted into electrical energy by a second transducer located a distance "L" from the transmitting transducer. The transit time "T" is measured electronically. The pulse velocity "V" is calculated by dividing "L" by "T" (ASTM C597-09). A number of researchers have developed theoretical models to predict the relationship between UPV and the physical and mechanical properties of cement-based materials. Yildirim and Sengul (2011) investigated the effects of water:cement ratio, maximum size of aggregate, aggregate type, and fly ash addition on the dynamic modulus of elasticity of concrete. Their results indicate that the dynamic modulus values are approximately 30% higher than the static modulus obtained from unconfined compressive testing. This is due to the UPV test is conducted at low stress level (Yildirim & Sengul, 2011).

The correlation between unconfined compressive strength (UCS) of cement-based material and UPV depends on the mix design and the type of materials used (Neville, 1996). Therefore, the UPV may be used to estimate UCS with a calibration curve for each different mix. De Belie et al., (2005), investigated the influence of different accelerating admixtures and cement types for shotcrete on setting and hardening behaviour. The result from their investigation is shown in Figure 2.14. They suggested that, UPV measurements were sensitive to the effect of cement type, accelerator type and dosage on the setting behaviour of mortar. An increase of accelerator dosage results in an increasing UPV at early age. Mortar mixed without accelerator showed a dormant period of about 30 minutes before the UPV started to increase sharply. However, no such behaviour could be noticed in the mortar mixed with accelerator.

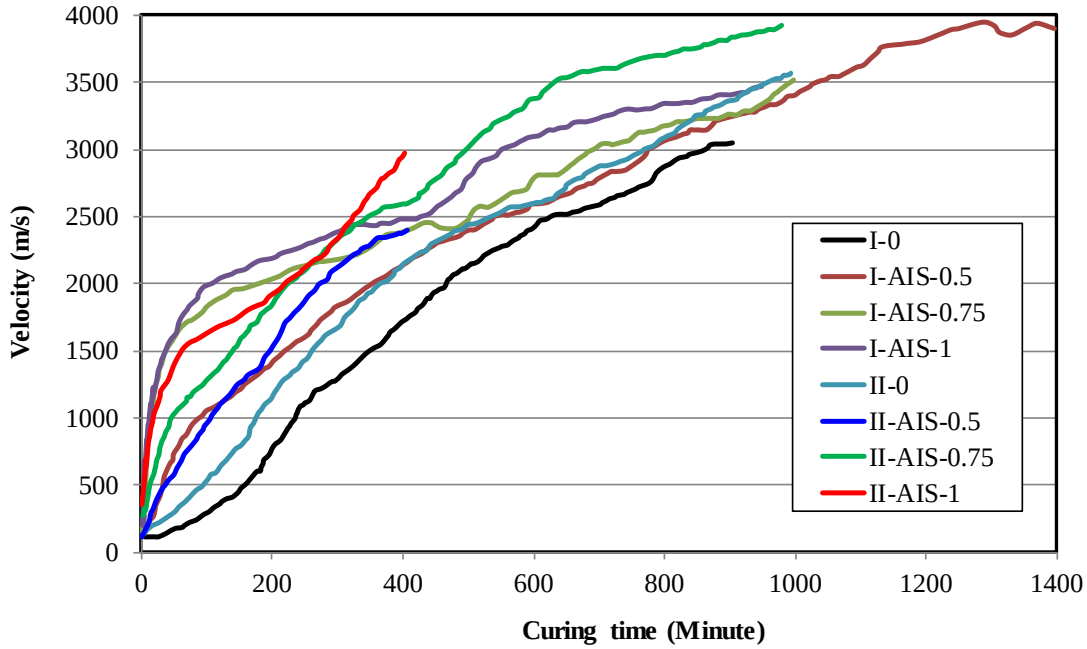

Figure 2.14. Ultrasound velocity vs. age for mortar with and without alkali-free accelerator AlS (numbers represent dosage), (Reproduce from De Belie et al., 2005).

Gibson & Bernard (2011) investigated the early age uniaxial compressive strength of fibre reinforced shotcrete with UPV measurement using an ultrasonic element embedded in shotcrete. The UCS were determined with existing destructive methods such as soil penetrometer, needle penetrometer, beam compression test and conventional UCS test on cored cylinder samples. Their research results are reproduced in Figure 2.15 and 2.16. The results show that the P-wave velocity of sprayed FRS significantly increased from about 1600 to 2500 m/s between 3:30 to 4:30 hours curing time. However, between 4:30 to 9:00 hours curing time the P-wave velocity of sprayed FRS remained around 2500 m/s. This reflects the effects of accelerator in the sprayed FRS as reviewed in section 2.3.5.1. The strength RFS increased significantly between 4:30 to 9:00 hours curing time.

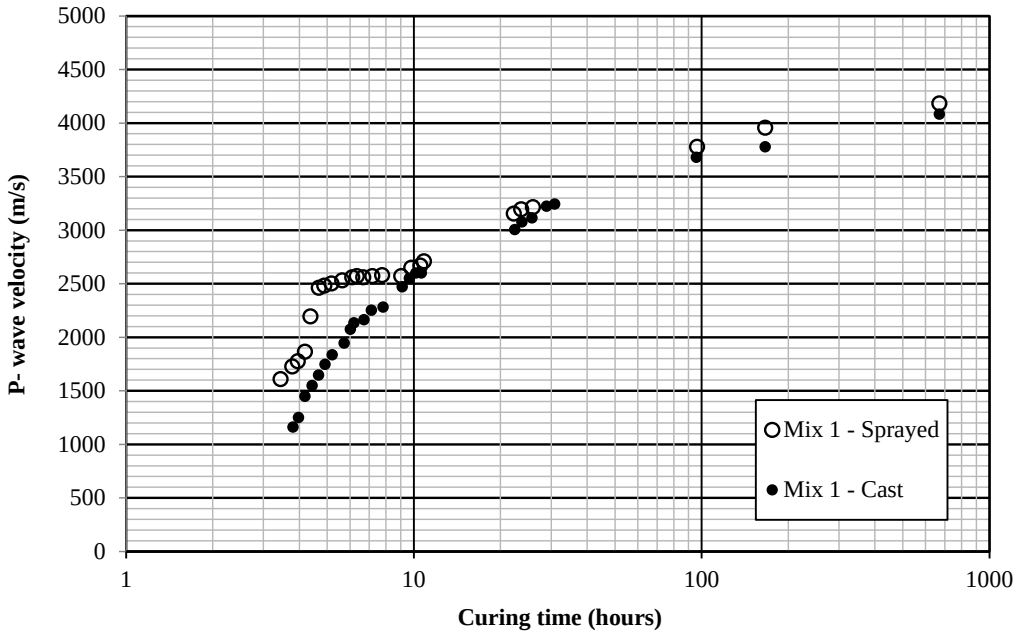

Figure 2.15. Development of P-wave velocity with curing time for fibre reinforced shotcrete (Reproduced from Gibson & Bernard, 2011).

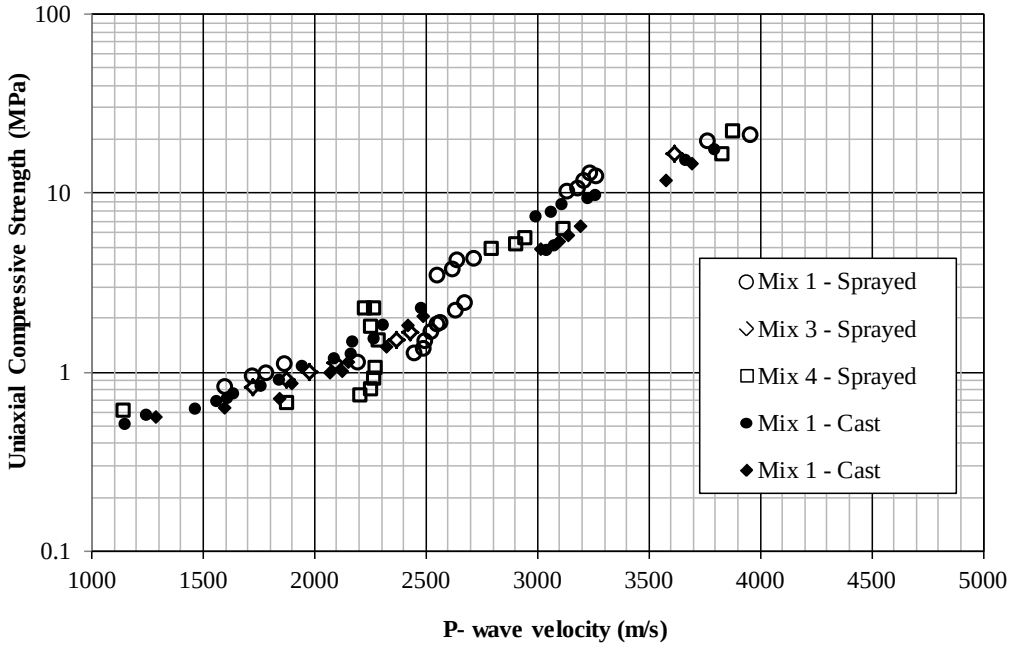

Figure 2.16. Relationship between UCS and P-wave velocity for different fibre reinforced shotcrete mixes (Reproduced from Gibson & Bernard, 2011).

2.4.2.3 Electrical method

Electrical method has been widely used to non-destructively determine the physical and mechanical properties of cement-based materials. The method is based on the application of direct or alternating current through the material and measuring the change in electrical properties, such as electrical resistance, dielectric constant, polarization resistance. Bogue (1947), mention the potential usefulness of electrical method, in which he referred to the work of Shimizu (1928). Sihmizu states that the electrical method is more accurate to investigate the setting of cement compared to mechanical and thermal methods. Baire (1932) suggested that the setting of cement starts as soon as there was a large drop in the electrical current. In 1939, Boast studied the setting phenomena during the first three hours and correlated conductivity with the 28 days UCS. Calleja (1952), suggested the electrical resistance of the heterogeneous system of the cement paste is due to two factors. One is the ionic conductivity of the solution, which depends on ionic concentration, temperature and type of ions present in the solution (such as, Na^{+}, K^{+}, Ca^{2+}, SO_4^{2-} and OH^{-}, etc.). The other factor is due to an increased mechanical resistance and cohesiveness as setting progresses. The concentration of these ions varies with initial water and cement ratio, degree of hydration, saturation and evaporation. Figure 2.17 show the test results of Calleja's early study. The upper curves show temperature changes with time and the lower curves show electrical resistance changes with time. Generally, the curves show that electrical resistance decreased with an increasing temperature. The development of electrical resistance for each mix is more differentiable than that of temperature development.

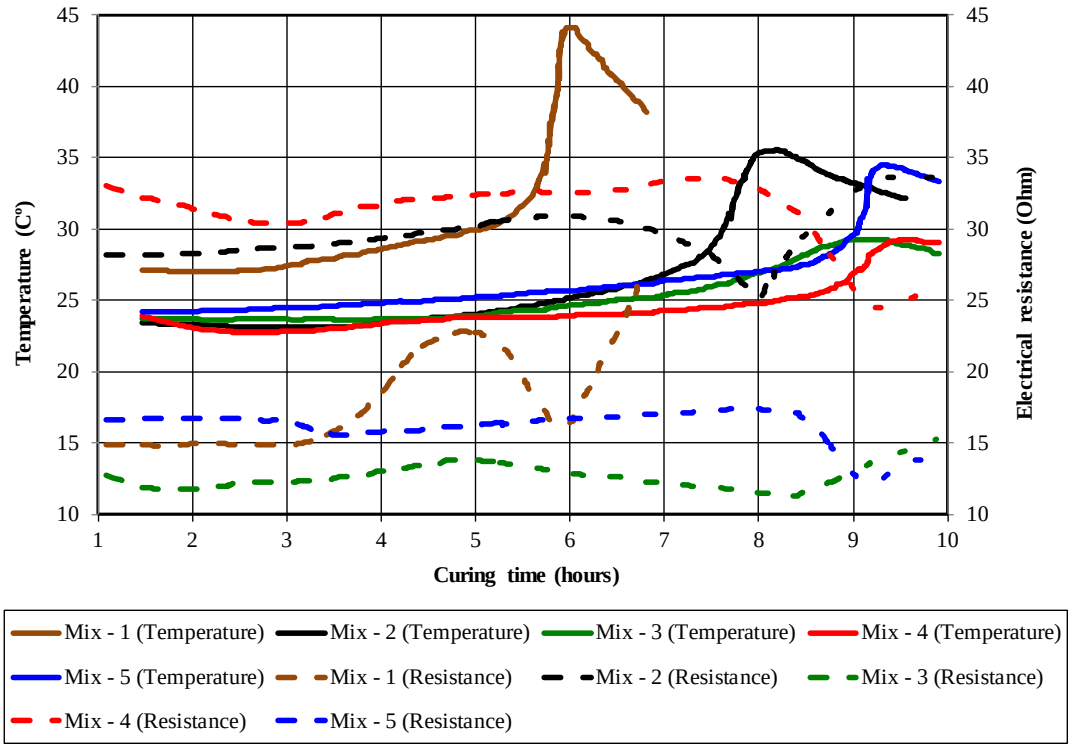

Figure 2.17. Temperature and electrical resistance development with curing time in cement paste (Reproduced from Calleja, 1952).

Monfore (1968) carried out research into the electrical properties of hardened concrete and identified the ions responsible for conduction and polarization within a concrete mix. McCarter and Curran (1984) investigated the electrical response characteristics (dielectric constant and resistivity) of cement paste during the first 24 hours. They concluded that the dielectric constant and resistivity depends upon different factors. The changes in dielectric constant and resistivity reflect chemical changes in the cement paste. The rate of change of these electrical parameters indicate rate at which chemical reactions are occurring. Khalaf and Wilson (1999) investigated the electrical properties of freshly mixed cement paste and concrete and the influences of different types of aggregate. Figures 2.18 and 2.19 show the electrical resistance of cement paste during hydration and electrical resistance of fresh concrete during hydration, respectively. They concluded that the cement paste is the primary governing factor in determining the electrical resistance of concrete.

However, both the fine and coarse aggregates are found to play a crucial role in the movement of water in fresh concrete.

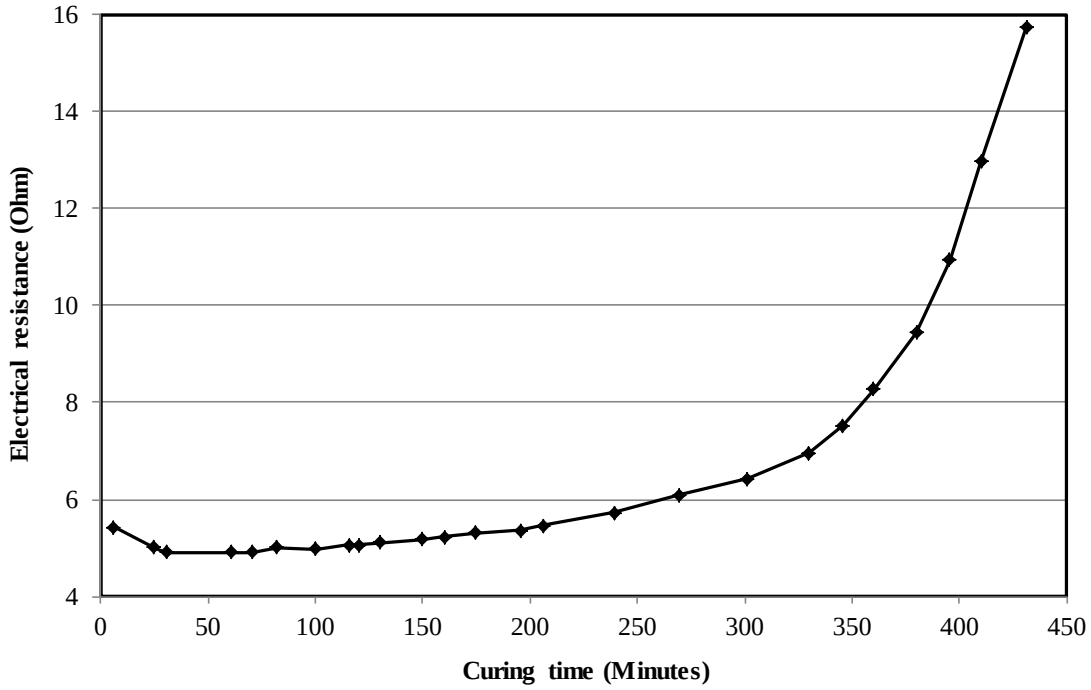

Figure 2.18. Electrical resistance of cement paste during hydration (Reproduced from Khalaf & Wilson, 1999).

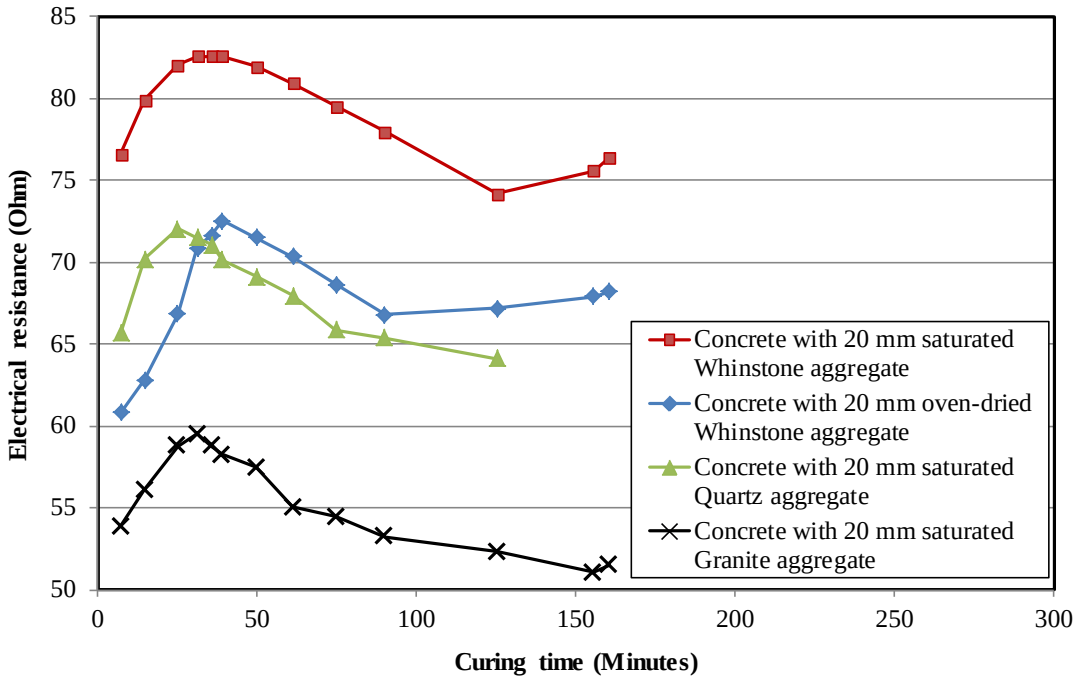

Figure 2.19. Resistance of fresh concrete during hydration (Reproduced from Khalaf & Wilson, 1999).

Van Beek (2000) studied the dielectric properties of young concrete in relation to the unconfined compressive strength development. He reported the influences of frequency, cement type, water:cement ratio, type and amount of aggregate on the dielectric properties. A prototype monitoring sensor called “Consensor” was developed to monitor the change in conductivity, which can be correlated to degree of hydration and strength development. Wen and Chung (2001) investigated the effect of admixtures, fibres, latex, and silica fume on the dielectric constant of cement paste. They concluded, the relative dielectric constant of cement paste is decreased by silica fume addition and by steel fibre addition, but is increased by latex addition and by carbon fibre addition. Topcu et al, (2012) studied the electrical conductivity of setting cement paste with different mineral admixtures such as fly ash, blast furnace slag and silica fumes. They found that, the electrical conductivity decreased by increasing the mineral additive. The rate of change of electrical conductivity is different with different types of mineral additive.

2.5 Conclusions and discussions

The literature review presented in Chapter 2 addresses the current State-of-the-Art shotcrete mix design, the constituent materials properties and their influences on the strength development, the early strength and existing test methods.

Shotcrete is a designed material, comprising cement, supplementary cementing mineral, fine and coarse aggregates, chemical admixtures, water and usually with fibres. The physical, chemical and mechanical properties of each of these constituent materials affect the mechanical properties of the gelling, setting and hardening of the final shotcrete.

All types of cement are mainly composed of four compounds namely, Tricalcium silicate (C3S), Dicalcium silicate (C2S), Tricalcium aluminate (C3A) and Tricalcium aluminate (C4AF). When cement is mixed with water a series of simultaneous and consecutive reactions take place between water and the constituents of cement. These reactions are known as “hydration of cement”. Various researchers studied the chemistry and mechanism of cement hydration. The key finding is C3S constitutes about 50% to 70% of cement by weight. It tends to dominate the early hydration period that comprises setting and early strength development. In addition, it is the component most responsible for formation of the calcium silicate hydrate gel (CSH), the principle product of hydration.

The two important aspects of mixing water are quantitative aspect and qualitative aspect. The quantitative aspect is that, how much water should be added to the batch. It is indicated by water and cement ratio (W/C). The W/C ratio is known to influence most of the chemical and mechanical properties of the fresh and hardened shotcrete.

Aggregates occupy at least three-quarters of the total volume of a given shotcrete mix and thus, their properties greatly affect the properties of the concrete or shotcrete mix.

Fibres are the slender filaments, which may be discrete or in the form of bundles, networks, or strands of natural or manufactured materials, which can be distributed uniformly throughout a fresh cementitious mixture. The basic categories are steel, glass, synthetic and natural fibre materials and used as reinforcement in shotcrete. The physical and mechanical properties of fibres reinforced shotcrete (FRS) are influenced by the fibres types and dimension (length to diameter ratio), geometry, dosage, distribution and bond characteristics between fibre and shotcrete matrix.

The chemical admixtures may remain in a free state as a solids or solution, may interact at the surface or be chemically combined with the constituents of cement or cement paste. The type and extent of interaction may influence the physico-chemical and mechanical properties of concrete such as water demand, hydration kinetic, composition of the products, setting times, microstructure, strength and durability. The chemical admixtures used in underground shotcrete application are accelerator, superplasticiser or high range water reducer, hydration stabiliser and air-entraining admixture.

Most of the accelerators used for shotcrete in underground civil and mining application mainly contain aluminium sulphate as a liquid state. Addition of accelerators changes the course of the chemical reactions especially at early stages. Aluminium sulphate reacts with calcium hydroxide ($Ca(OH)_2$) and produce additional ettringite and aluminium hyroxide. The aluminium sulfate components of these accelerators promote the crystallisation of ettringite at a very early stage. Within 4 hours of hydration, these crystals grow and almost fill the capillary pores. Usually, the formation of ettringite within the first 30 minutes is largely sufficient to set a shotcrete mix.

Superplasticiser is used within shotcrete for three different purposes such as, to increase workability, to reduce the mixing water, to reduce both water and cement quantity the chemical compounds included in the superplasticiser cause dispersion into smaller agglomerates of cement particles. This process reduces the formation of

entrapped water and surface interaction of particles causing a fluidising effect in the cement mixture.

An air-entraning admixture causes the development of a system of microscopic air bubbles in concrete, mortar, or cement paste during mixing. It stabilises the air voids entrapped within the concrete during the mixing process. Materials used for air entrainment admixtures are water soluble compounds or synthetic surfactants based on blends of: alkyl sulphates, olefin sulphonates diethanolamines, alcohol ethoxylates and betains. Air-entraining admixtures have no appreciable effect on the rate of hydration of cement and have no effect on the chemical composition of the hydration products.

Hydration stabilisers are used to limit prehydration of shotcrete. They are used to extend the retention time of batched shotcrete to hand and the logistical constraints typically associated with underground construction, such as prolonged transport and discharge times. The compounds included in stabiliser are organic such as Na, Ca or HN4 salts of lignosulfonic acids, hydroxyl-carboxylic acid and carbohydrates. Organic stabilisers are adsorbed on to the surfaces of growing particles of hydration products and complex calcium ions (Ca^{2+}) ions in aqueous solution. The adsorption causes the precipitation of low-permeability coating film on the cement particles which slow down further hydration.

The early strength of the shotcrete generally refers to the strength development from the time of spraying (0) to (4) hours curing. It is usually determined by indirect methods and correlated to the strength development with time. The measured properties include; penetration resistance, pull out force, temperature, electrical conductivity and resistivity and ultrasonic wave velocity. The measurement method can be broadly categorised as destructive and non-destructive determination. Although compression, tension, shear, torsion or flexure strength are possible to be correlated to the indirectly measured parameters, the current literature show uniaxial compressive strength (UCS) is the most commonly property used.

This research was focused on the fundamentals of shear strength development of shotcrete with time at early age, especially 0 to 4 hours. Therefore, a continuous literature search related to “the shear strength development of shotcrete with time at early age” was conducted from the beginning to the end of this research, which was from July, 2006 to October, 2014. With the best knowledge of the researcher, no specific literature on “the shear strength development of shotcrete with time at early age” was published during this period.

CHAPTER 3

MECHANICAL AND PHYSICAL PROPERTIES OF SHOTCRETE PASTE AT EARLY AGE

3.1 Introduction

There are two conflicting requirements of a shotcrete mix. Initially, it must have the rheological properties of a fluid in order to be mixed, pumped and sprayed. Finally it must have the mechanical properties of a solid to support rock. The rheology of the mix depends on the fluid/solid constituents, their particle sizes and proportions which in turn affect the mechanical properties of the in situ paste, its hardening and the mechanical properties of the final solid layer.

The mechanical properties of the solid layer that are significant in rock support action include its strength (compressive, tensile, shear and bond) its stiffness (flexural, biaxial and shear) and its density (void ratio and permeability). These are dictated by the rheology of the paste, the hardening mechanism of hydration and the environmental conditions (i.e. temperature and moisture) during hydration and curing.

Prior to hardening, the mechanical properties of the paste are dictated by the cementitious matrix comprising the cement, mineral additives, aggregates, chemical admixtures and the water. After hydration the shotcrete should possess the mechanical properties of the hardened matrix plus some additional, but fractional properties of the aggregates and fibres. It is important to note that these mechanical properties improve with hydration from that of the wet paste, to the stiff paste, to the hardened paste and finally to the fully hardened and cured shotcrete.

Consequently the early mechanical properties of shotcrete are those associated with the cementitious matrix and therefore it is predominantly the change in the cementitious matrix that will indicate the early mechanical response of shotcrete. This is an important characteristic. Many test methods and procedures have been developed for defining the rheology of concrete. These are essentially scaled up versions of the techniques developed for fine particle suspensions and gel systems. However, the range of particle sizes in shotcrete and the resulting heterogeneity

confuse the measurement of the rheological or flow properties of shotcrete. Given that the early mechanical properties of shotcrete are mainly those associated with the cementitious matrix, this research was restricted to testing of a shotcrete paste comprising the cementitious matrix only.

3.2 Shotcrete paste mix design

The shotcrete paste mix design used in this research was calculated following a typical range of constituent material in a shotcrete mix as presented in Chapter 2, Table 2.1. A typical shotcrete paste mix design use for laboratory test works in this research is shown in Table 3.1.

Table 3.1. Typical shotcrete paste mix design use for laboratory test works in this research.

Material		Shotcrete paste			
		Cement paste	Cement-sand mortar	Synthetic fibre reinforced	Synthetic fibre and aggregates (Fibre reinforced concrete)
General Purpose (GP) Cement (kg)		10	10	10	10
Water-cement ratio (by weight)		0.44	0.44	0.44	0.44
Cement-Sand ratio for mortar (by weight)		-	0.51	-	-
Water (kg)		4.38	4.38	4.38	-
Sand (kg)		-	19.61	-	19.50
Crushed dust aggregate (kg)		-	-	-	15.00
7 to 10 mm diameter coarse aggregate (kg)		-	-	-	9.50
Synthetic fibre (kg)		-	-	0.13	-
Chemical admixture	Accelerator	4 % of cement			
	Superplasticiser	1.5 % of cement			
	Hydration stabiliser	0.5 % of cement			
	Water reducing admixture	0.2 % of cement			

3.3 Test program

The test programs for this research consisted of 5 stages, such as, stage 1, stage 2, stage 3, stage 4 and stage 5. The details test program is presented in Appendix A. Stage 1 experiments were conducted as an initial study to identify the requirements and to set up the frame work of the research in order to complete the objectives as described in Chapter 1, Section 1.2. The mechanical properties of shotcrete paste, such as, UCS and shear strength tests were conducted with the Western Australian School of Mines (WASM) 50 ton Avery 50 universal test machine and a Haake VT550 rheorometer, respectively. The physical properties of shotcrete paste, such as heat of hydration (temperature) and electrical resistance were measured with IntelliRock II™ temperature measurement system and electrical multimeter, respectively. The research stage 2 was conducted based on the research outcome from stage 1. In the research stage 2, the shear strength was conducted with a Haake VT550 rheorometer and a Wykeham Farrance traixial test system WF4010. The electrical resistance was measured with the new device (Prototype v1) developed in this research. In the research stage 3 and 4, the method for determination of shear strength is the same research stage 2. The electrical resistance was measured with different versions of the prototypes developed with this research. Research stage 5 describes the in situ electrical resistance of shotcrete at early age.

The initial test results from stage 1 and shear strength test results from research stage 2, 3 and 4 are mainly presented in this Chapter. The details of the development of the electrical measurement device and the measurement results are described in Chapter 4.

3.4 Uniaxial compressive strength test

The uniaxial compressive strength test was performed on both shotcrete paste and shotcrete samples. The tests were conducted accordant with ASTM C39/C39 M-09a, “Standard test method for compressive strength of cylindrical concrete specimens”.

3.5 Shear strength of shotcrete paste

3.5.1 Vane shear test

Initial early strength measurement of shotcrete paste was conducted with a Haake VT550 viscometer combined with a FL100 vane which has a dimension 22 x 16 mm (diameter x height) to determine the vane shear strength. The vane shear strength test is described in Australian Standard AS1289.6.21. The test consists of insertion of the vane into a sample, followed by measurement of the torque required to rotate the vane. From the maximum torque and the dimensions of the vane the shear strength of the samples can be determined. This can be described by the following equation.

$$Su = \frac{10^9 \times 6}{\pi} \times \left(\frac{T}{D^2(3H+D)}\right) \quad (3.\ 1)$$

Where,

Su = Shear strength (kPa)
T = Maximum torque (kNm)
D = Vane diameter (mm)
H = Vane height (mm)

The setup of Haake VT550 viscometer is shown is Figure 3.1.

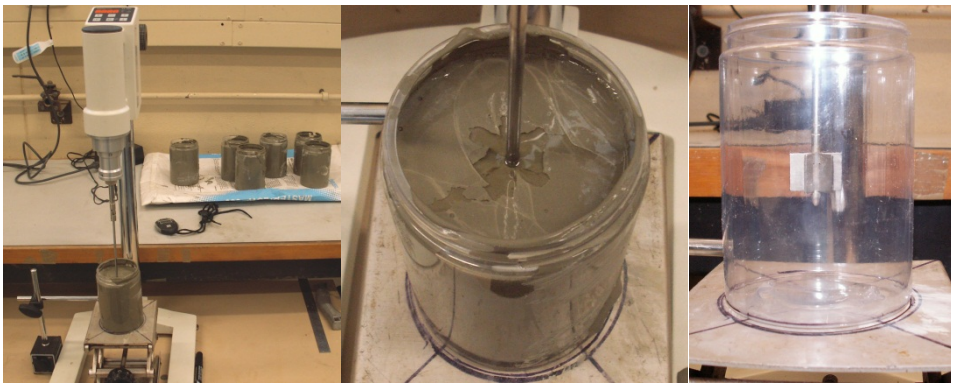

Figure 3.1. Setup of Haake VT550 viscometer.

After 3 hours curing it was be very difficult to measure shear strength with a Haake VT550 device. Therefore, a conventional uniaxial compressive strength (UCS) of the samples, measuring 50×100 mm (diameter x length) was determined using the WASM 50 ton Avery compression machine. The maximum shear strength was estimated as 50% of UCS. Table 3.2 shows UCS and estimated maximum shear strength of shotcrete paste at early age. Figure 3.2 Shotcrete paste shear strength development with curing time.

Table 3.2. UCS and estimated maximum shear strength of shotcrete paste.

Curing (hours)	**4**	**6**	**8**	**24**
UCS (MPa)	0.87	9.24	18.48	41.11
Estimated maximum shear strength (MPa)	0.44	4.62	9.24	20.56

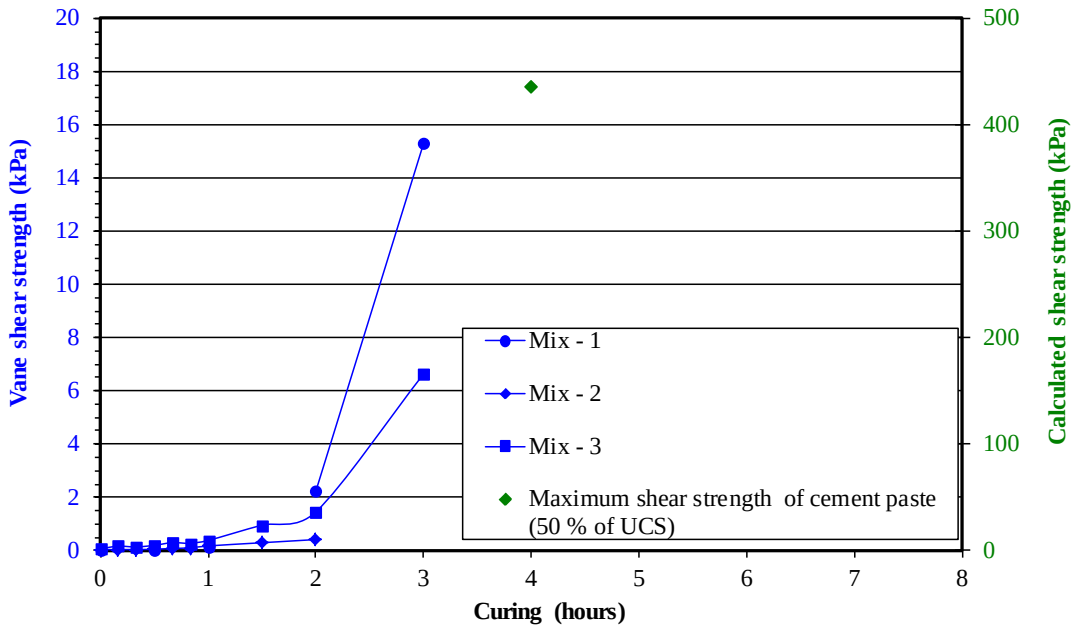

Figure 3.2. Shotcrete paste shear strength development with curing time.

The stage 1 initial experiments suggested that,

- The minimum shear strength of shotcrete paste with w/c ratio 0.44 is 33 Pa,
- After 3 hours curing the paste become very stiff and the yield stress cannot be measured with a VT550 viscomenter,
- At 4 hours curing the paste become hardened and the UCS is 0.87 MPa,
- The maximum shear strength of shotcrete paste without accelerator is estimated about 0.44 MPa at 4 hours curing,
- Development of a high capacity vane shear testing equipment may be required to measure after 3 hours,
- Such equipment must be able to measure the vane shear strength between 25 Pa to 500 kPa.

3.5.2 Shear strength test with triaxial compression

The determination of shear strength was undertaken using a conventional triaxial compression test method. A Wykeham Farrance traixial test system (WF4010) was used, when the paste was in solid gel state. The details of those apparatus are presented in Appendix I. The test was performed on a cylindrical shotcrete paste specimen enclosed in a rubber membrane, placed in a triaxial cell. The cell was filled with water and pressurised in order to apply a constant confining pressure. The specimen can be subjected to an axial stress through a loading ram in contact with the top of the specimen. The axial stress is continuously increased until a failure condition is reached. The axial stress acts as the total major principal stress (σ_1), in the axial direction. The isotropic confining pressure acts as the total minor principal stress (σ_3) in the lateral direction. The total intermediate principal stress (σ_2) is equal to the total minor principal stress (σ_3). Figure 3.3 illustrates the stress conditions associated with triaxial compression testing.

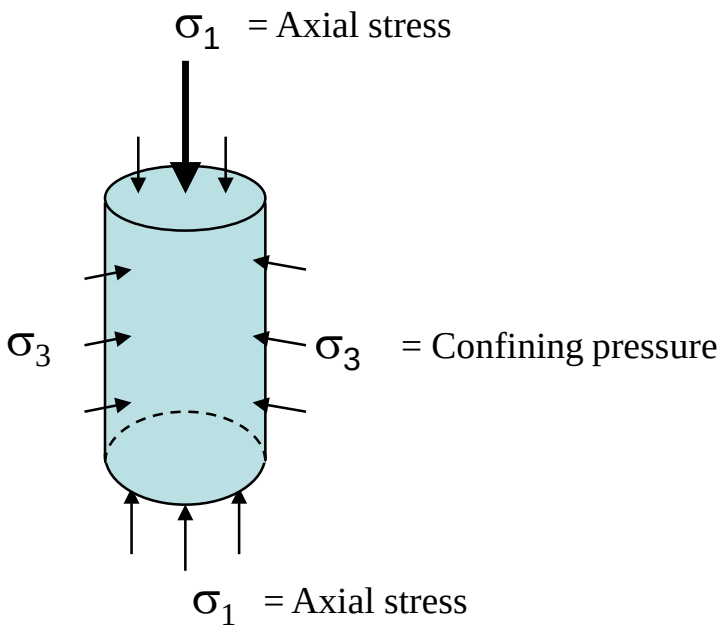

Figure 3.3. Stress conditions associated with triaxial compression test.

Basically, there are three procedures of triaxial compression test based on the drainage condition before shearing the specimen. They are: i. Unconsolidated Undrained (UU), ii. Consolidated Undrained (CU) and iii. Consolidated Drained (CD). The consolidation is used to describe the process whereby excess pore pressure due to the applied stress is allowed to dissipate, resulting in volume change. The consolidation process occurs subsequent to the application of the confining pressure if the pore fluids are allowed to drain. On the other hand, the consolidation process will not occur if the pore fluids are maintained in undrained condition (Fredlund & Rahardjo, 1993). In this research only UU triaxial compression test was performed to determine the shear strength.

The shear strength of can be formulated from any two of the three principal stress states. One of the most widely use shear failure criterion is the Coulomb criterion (1776),

$$\tau = c + \sigma_n \tan \phi \qquad (3.2)$$

Where, τ and σ_n represent shear stress and normal stress, respectively. The parameters c and ϕ are assumed to be constants called the cohesion and the angle of internal friction. In reality c and ϕ change with stress level. If we consider that normal stress (σ_n) is at zero condition, the minimum shear strength of a given material is equal to it cohesion (c) based on equation 3.2.

3.6 Temperature and degree of hydration

The degree of hydration (α) is defined as the fraction of individual cement compound such as C_3S, C_2S, C_3A and C_4AF consumed throughout the hydration process (Taylor, 1997). That is, the ratio of the amount of cement that has hydrated and the initial amount of cement. Their kinetics and mechanisms are described in section 2.3.1.1. The common parameters used to estimate the degree of hydration are liberated heat of hydration, amount of chemically bound water, chemical shrinkage, amount of $Ca(OH)_2$, specific surface of the cemented paste and uniaxial compressive strength (Breugel, 1991). In this research the degree of hydration was estimated from the temperature development with curing time suggested by Freiesleben-Hansen and Pedersen (1977). Figure 3.4 shows IntelliRock II™ temperature measurement system.

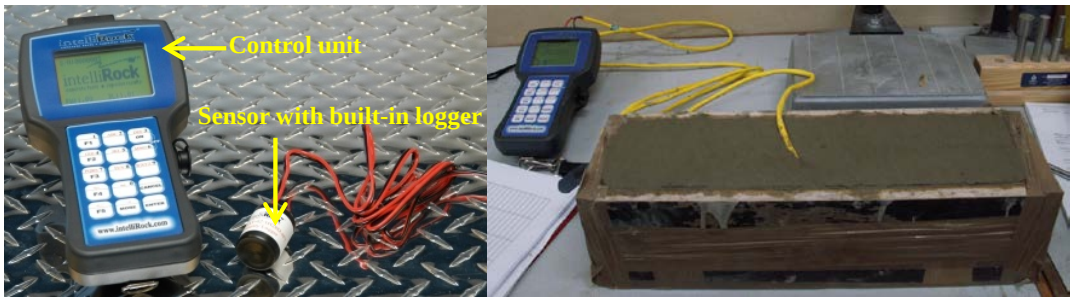

Figure 3.4. IntelliRock II™ temperature measurement system.

The equation suggested by Freiesleben-Hansen and Pedersen (1977) is as follows;

$$\alpha(t_e) = \alpha_u \times \exp\left[-\left(\frac{\delta}{t_e}\right)^{\beta}\right] \quad (3.3)$$

Where,

$\alpha(t_e)$ = Degree of hydration at equivalent age

α_u = Ultimate degree of hydration

δ = Hydration time parameter (hours)

β = Hydration shape parameter

t_e = Equivalent age at the reference curing temperature (hours)

In the equation (3.3), the ultimate degree of hydration (α_u) ranges from 60 to 100 % depend on the curing condition. The hydration time parameter (δ) and hydration shape parameter (β) are a constant valve derived from the test data. The equivalent age at the reference curing temperature (t_e) can be calculated with the equation also suggested by Freiesleben-Hansen and Pedersen (1977), which is shown in equation (3.4).

$$t_e = \sum_0^t \exp\left[\frac{E}{R}\left(\frac{1}{273+T_r} - \frac{1}{273+T_c}\right)\right] \times \Delta t \quad (3.4)$$

Where,

t_e = Equivalent age at the reference curing temperature (hours)

Δt = Time interval (hours)

T_c = Average temperature during the time interval (C°)

T_r = Constant reference temperature (C°)

R = Universal gas constant (8.3144/mol/K)

E = Activation energy (J/mol)

In the equation (3.4), the time interval (Δt) and the average temperature during the time interval (T_c) are the results from temperature measurement throughout the curing time. A constant reference temperature (T_r) is usually 20 C°. The activation energy (E) is a combination of the activation energies of all the cement components hydrating simultaneously (Pinto and Hover, 1999). Schindler (2002) suggested equation for estimation of activation energy based on weight ratio of cement compounds C_3A and C_4AF, and the specific area of the cement (Blaine value). The equation suggested by Schindler (2002) is shown Equation (3.5).

$$E = 22{,}100 \times p_{C3A}{}^{0.30} \times p_{C4AF}{}^{0.25} \times Blaine^{0.35} \quad (3.5)$$

Where,

p_{C3A} = Weight ratio of C3A in terms of the total cement content

p_{C4AF} = Weight ratio of C4AF in terms of the total cement content

Blaine = Blaine value, specific area of cement (m^2/kg)

Alternatively, the activation energy can be calculated with the method suggested in the ASTM C1074 – 04, “Standard practice for estimating concrete strength by the maturity method” (ASTM, 2001).

3.7 Electrical resistance

Instruments for measuring resistivity in materials are historically, well-established and available commercially. A typical resistivity meter for concrete is equipped with four, ‘post-like’ electrodes, in a straight line geometry known as the Wenner linear, four-point, electrode arrangement. A current is supplied to the material through the two outer electrodes and the potential difference is measured between the two inner electrodes. Knowing the potential difference and the supplied current, the resistance

for this configuration can be calculated using Ohm's Law and the so-called, 'Wenner Geometrical Factor', which assumes a homogeneous, infinite, isotropic material, symmetrical current flows and uniform current density (Keller and Frischknecht, 1966). Figure 3.5 shows 4 electrodes linear array and assumptions of current flow and density.

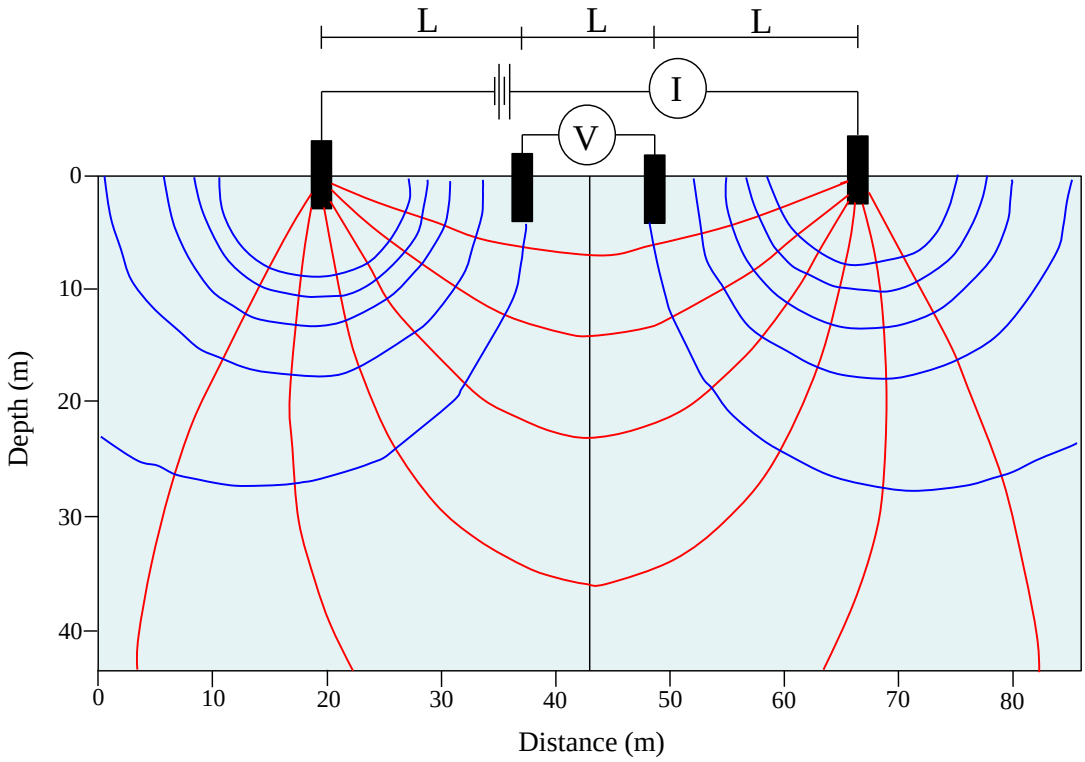

Figure 3.5. Schematic diagram 4 electrodes – linear array (Keller & Frischknecht, 1966).

The resistivity for a homogeneous, infinite, isotropic material, symmetrical current flows and uniform current density can be calculated with,

$$\rho = R \times k \tag{3.3}$$

$$R = \frac{\Delta V}{\Delta I} \tag{3.4}$$

$$k = 2\pi L \tag{3.5}$$

Where,

ρ = Resistivity

R = Electrical resistance

ΔV = Change in potential (Volt)

ΔI = Change in electrical current (Ampere)

k = Geometric factor

The geometric factor varies with the dimension of the sample and electrodes arrangement. For a rectangular resistive material with electrical electrodes on both ends as shown in Figure 3.6, the geometric factor is,

$$k = \frac{A}{L} \tag{3.6}$$

Where,

A = Cross sectional area

L = Distance between electrodes

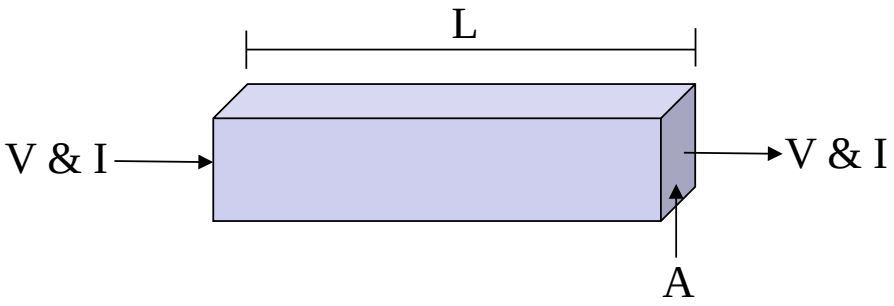

Figure 3.6. A rectangular resistive material with electrical electrodes on both ends.

Electrical resistivity is highly influenced by the geometric factor. On the other hand, electrical resistance is independent of the geometric factor. Therefore, in this research the electrical resistance was used to correlate with mechanical properties of a shotcrete paste. Figure 3.7 shows the set up for electrical current and potential measurement with multimeter in shotcrete paste sample.

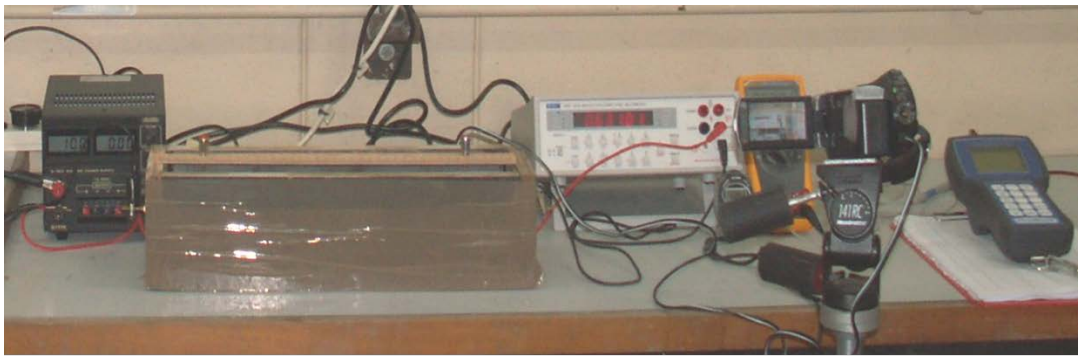

Figure 3.7. Set up for electrical current and potential measurement with a multimeter.

3.8 Results and discussions

3.8.1 UCS, temperature and degree of hydration

The UCS results for early strength paste are presented in Table 3.3. Figure 3.8 shows the development of temperature and UCS with curing time.

Table 3.3. Summary early age UCS test result.

Mix ID	UCS (MPa)								
	3 hours	4 hours	4.5 hours	5.5 hours	6 hours	8 hours	8.5 hours	12 hours	24 hours
Without Accelerator	0.04	-	-	0.81	-	8.55	-	-	28.74
Without Accelerator	0.03	-	-	0.86	-	8.47	-	-	33.70
Without Accelerator	-	-	-	0.90	-	6.50	-	-	34.41
4% Accelerator	-	-	0.19	-	2.58	-	6.16	14.87	25.91
4% Accelerator	-	-	0.19	-	2.55	-	6.10	17.17	27.63
4% Accelerator	-	-	0.16	-	2.66	-	6.85	15.26	25.20
5% Accelerator	-	3.28	-	-	9.97	14.52	-	23.17	21.59
5% Accelerator	-	2.75	-	-	10.03	12.68	-	22.20	21.28
5% Accelerator	-	3.13	-	-	10.70	11.03	-	20.40	23.40
6% Accelerator	-	2.71	-	-	4.31	9.35	-	12.54	26.67
6% Accelerator	-	3.22	-	-	3.89	9.29	-	13.65	26.67
6% Accelerator	-	3.10	-	-		8.08	-	11.53	24.58
6% Accelerator	0.24	3.23	-	-	4.39	8.32	-	13.45	29.41
6% Accelerator	0.24	3.16	-	-	4.59	8.79	-	13.45	24.98
6% Accelerator	-	-	-	-		9.19	-	12.54	

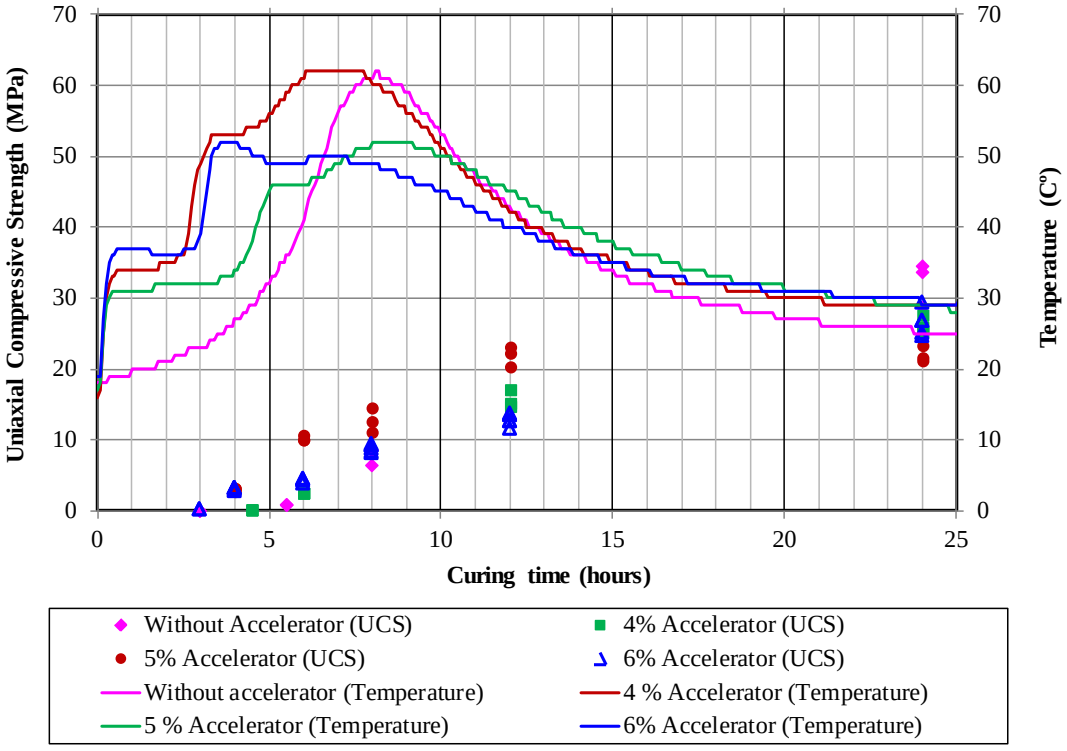

Figure 3.8. Development of temperature and UCS with curing time.

In order to correlate the degree of hydration and UCS correctly, the degree of hydration was firstly calculated with the equations suggested by Hansen and Pedersen (1977) as describe in Section 3.6. The constant value such as, hydration

time, shape parameters and activation energy were used from the value suggested by Poole et. al., (2007) for the preliminary calculation. The preliminary calculated degree of hydration was correlated with UCS. A relationship between UCS and degree of hydration was calculated based on the amount of chemically bound water for a shotcrete paste with w/c ratio (0.44). The relationship suggested by Thompson & Windsor (1998) was also plotted on the correlation graph. Finally, the best fit was determined by adjusting the constant value. Best fit correlation of UCS and degree of hydration is shown in Figure 3.9. Table 3.4 shows best fit activation energy, hydration time and shape parameters. Figure 3.10 shows development of temperature and best fit calculated degree of hydration with curing time.

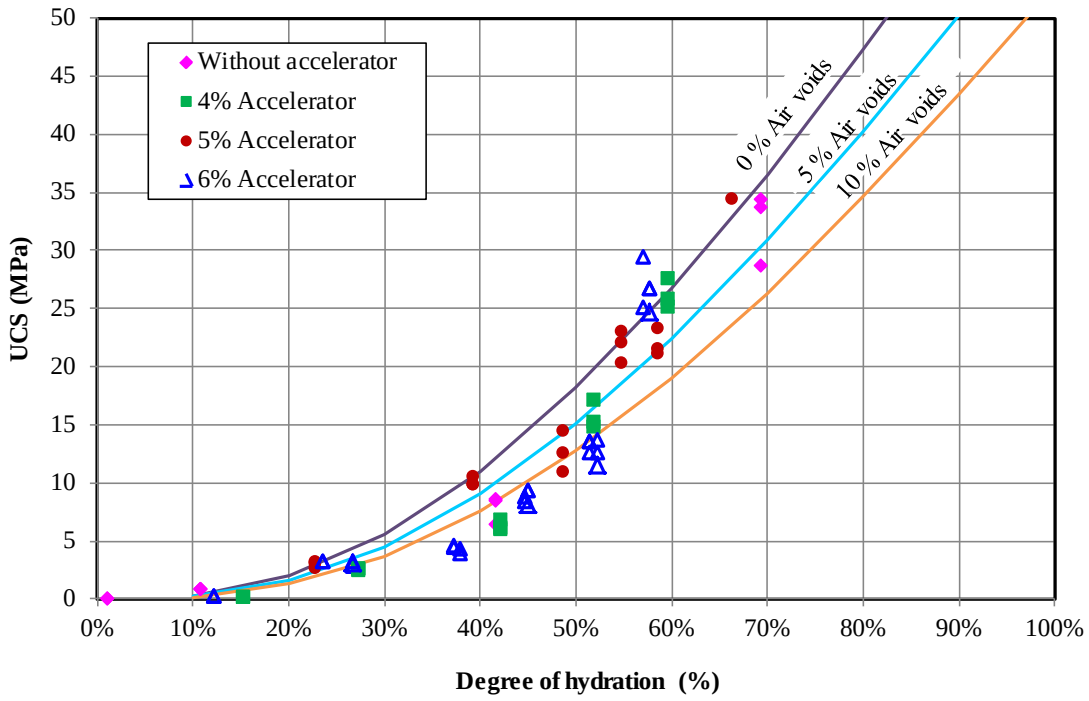

Figure 3.9. Correlation of UCS with calculated degree of hydration (Modified after Thompson & Windsor, 1998).

Table 3.4. Best fit activation energy, hydration time and shape parameters.

No.	Shotcrete paste ID	Activation Energy (J/mol)	Hydration time parameter (hours)	Hydration shape parameter	Ultimate degree of hydartion (%)
1	Without accelerator	39,078	16.5	1	100
2	4 % Accelerator	58,617	16.5	1	100
3	5 % Accelerator	60,570	16.52	1	100
4	6 % Accelerator	62,524	16.52	1	100

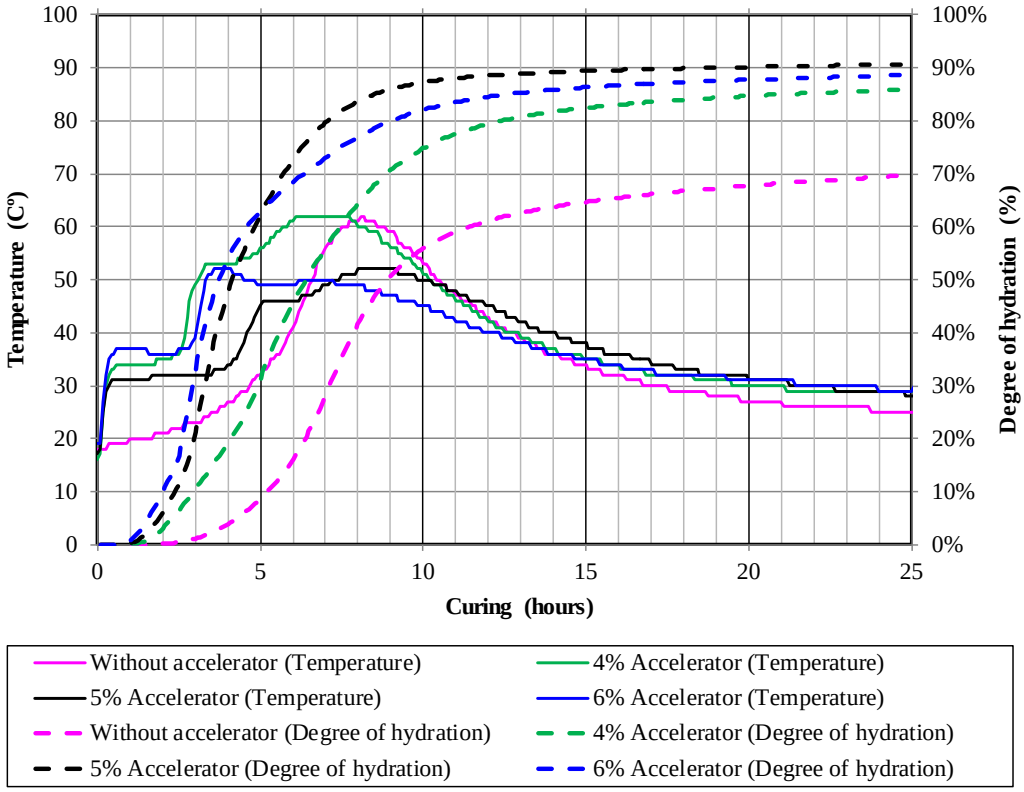

Figure 3.10. Correlation of temperature development in shotcrete paste (solid lines) and calculated degree of hydration with curing time (dotted lines).

Figure 3.11 shows the correlation of temperature development in underground shotcrete wall and calculated degree of hydration with curing time. In shotcrete, (usually with accelerator) the temperature increases immediately after spraying and does not change significantly within 1 to 4 hours. The calculation of degree of hydration from temperature measurement required many constant parameters which need to be calibrated correctly in a laboratory. The degree of hydration curves shown in Figure 3.11 were calculated based on the estimated parameters shown in Table 3.4. The degree of hydration does not change until 2 hours and gradually increases after 2 hours. Since the usual re-entry time is 4 hours (or less), it is concluded that the temperature does not provide a good indication of re-entry time.

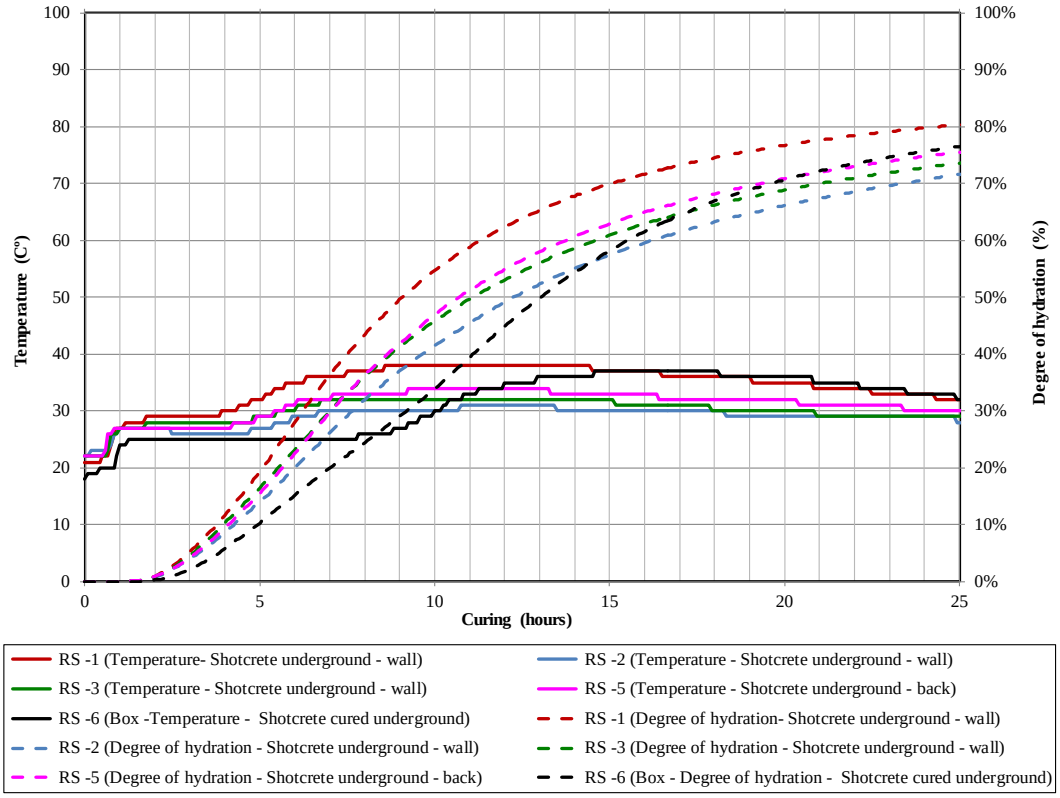

Figure 3.11. Correlation of temperature development in underground shotcrete wall and calculated degree of hydration with curing time.

3.8.2 Shear strength of shotcrete paste

The initial test from research stage 1 suggested that, the shear strength of shotcrete paste without chemical admixture can be determined with a vane shear method from 0 to 3 hours curing time. During that period the hydration products in the shotcrete paste are in the fluid gel state. After 3 hours the hydration products start transforming to a solids gel state and its shear strength cannot be determined with a standard vane shear test apparatus (VT550). Therefore, during research stage 2 and 3, the shear strength of shotcrete paste after 4 hours were determined with triaxial compression test method. The following sections describe the shear strength determinations of shotcrete paste at early age with and without the addition and different chemical admixture used for underground shotcrete application. The shear strength was estimated using a Coulomb shear failure criterion, as shown in Equation 3.2.

According to Coulomb's failure theory, shear strength consists of two constants, called cohesion (c) and angle of internal friction (ϕ). However, in this research, as described in Section 3.5.2, only minimum shear strength associated with cohesion (c) were used to correlated with electrical resistance with time.

3.8.2.1 Shear strength shotcrete paste without chemical admixture

Figures 3.12 to 3.19 show the triaxial test results conducted on the shotcrete paste samples mixed without chemical admixture. The test results were plotted on minor principle stress (σ_3) and major principle stress (σ_1) domain.The details test data are presented in Appendix – B. Generally, shear strength increased with curing time. The increased strength is mainly associated with cohesion (c). The angle of internal friction angle does not change significantly.

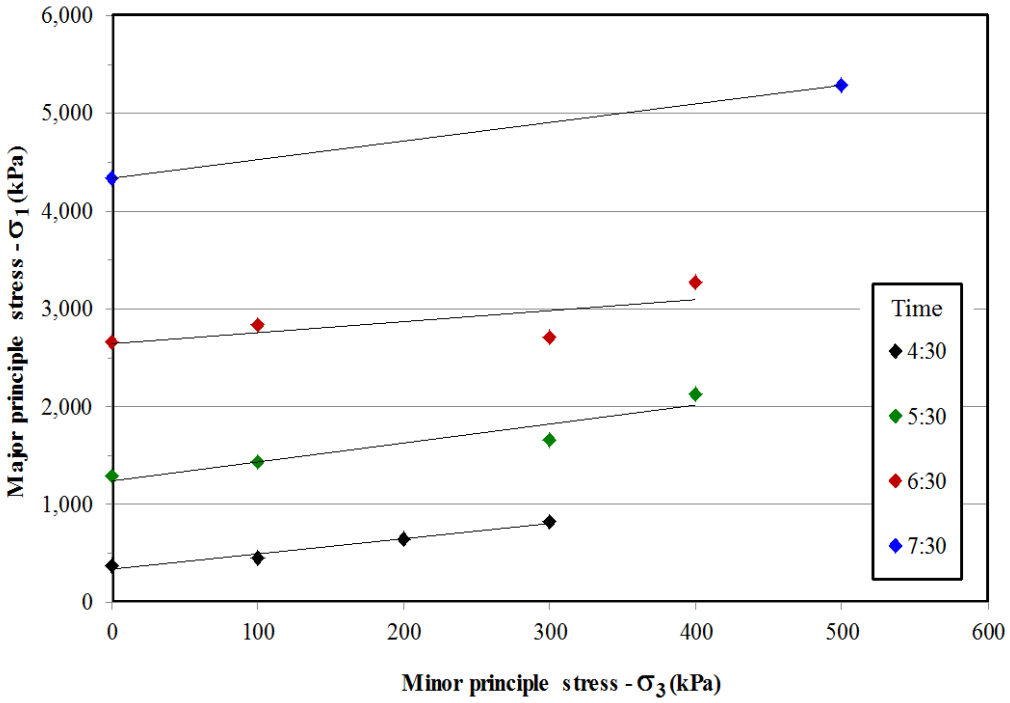

Figure 3.12. Triaxial test results for shotcrete paste batch No. SS_001.

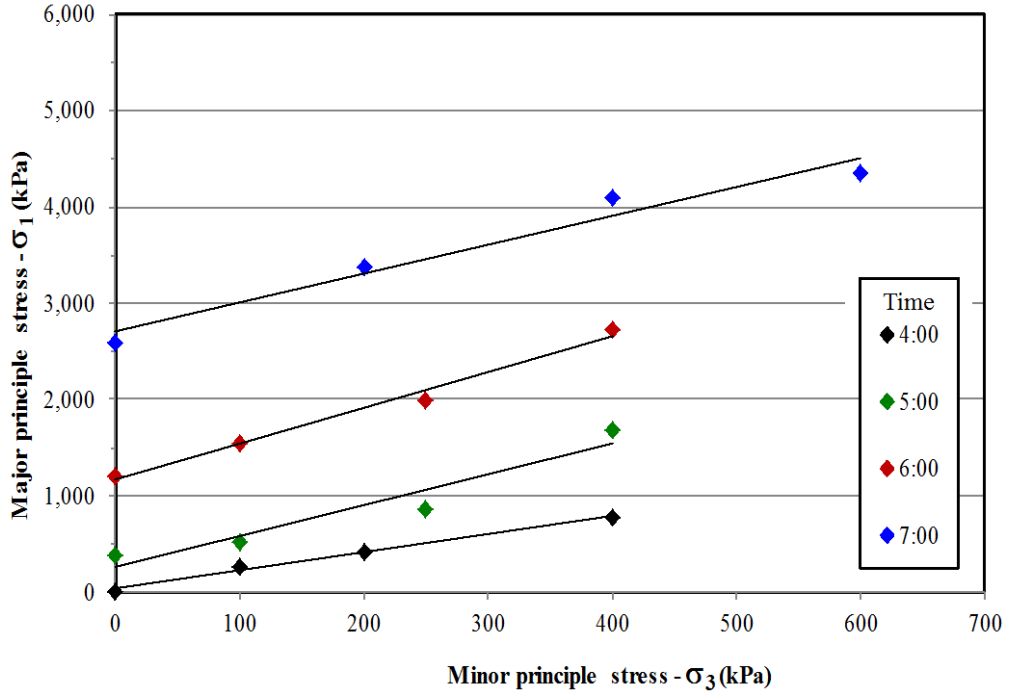

Figure 3.13. Triaxial test results for shotcrete paste batch No. SS_002.

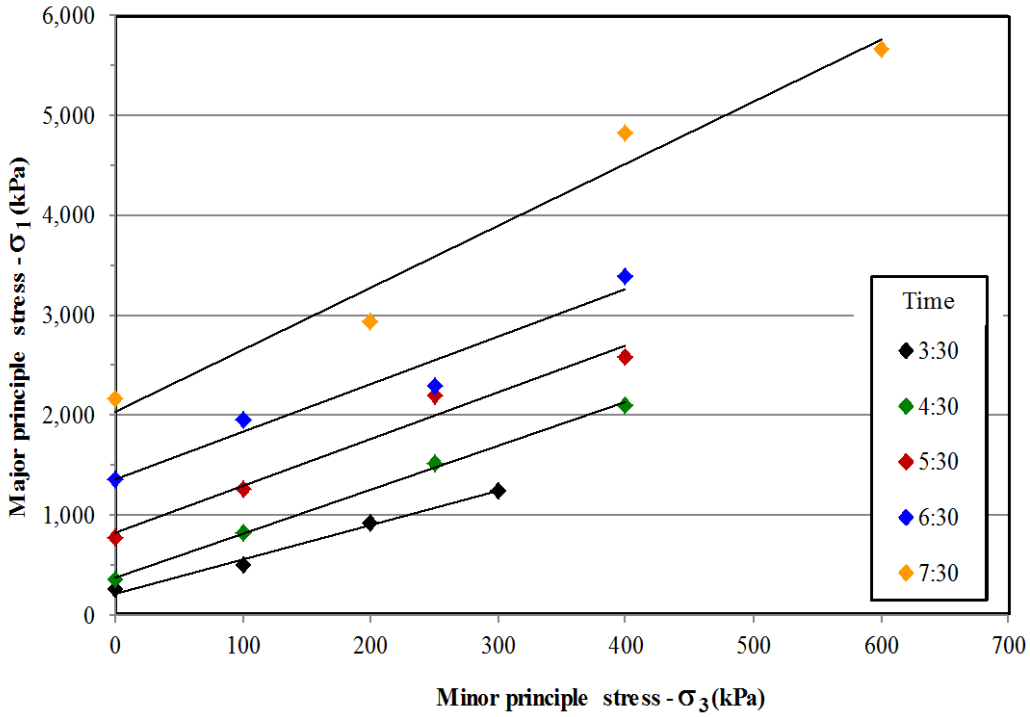

Figure 3.14. Triaxial test results for shotcrete paste batch No. SS_003.

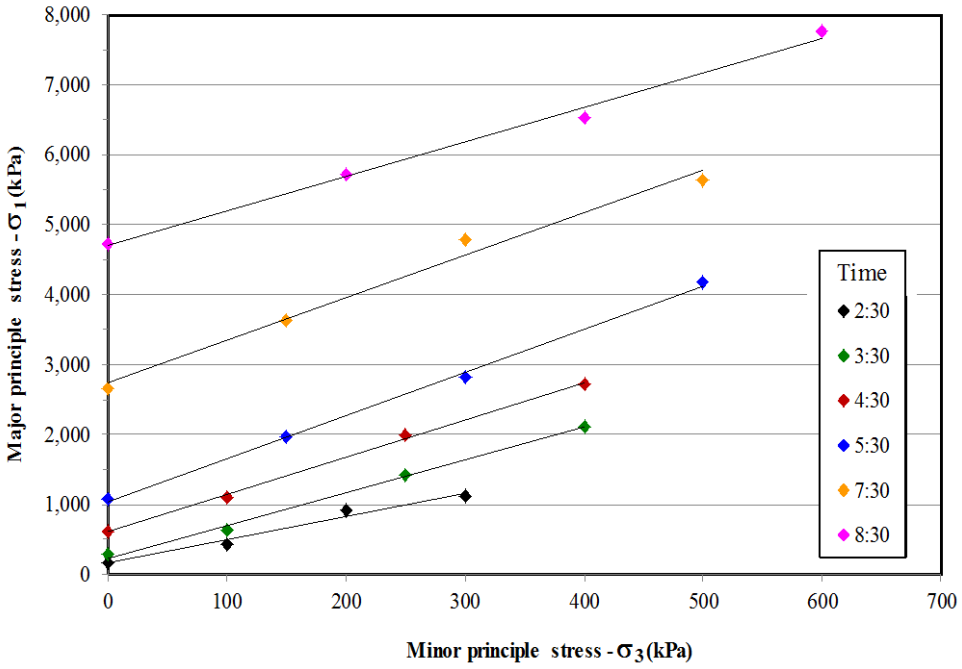

Figure 3. 15. Triaxial test results for shotcrete paste batch No. SS_004.

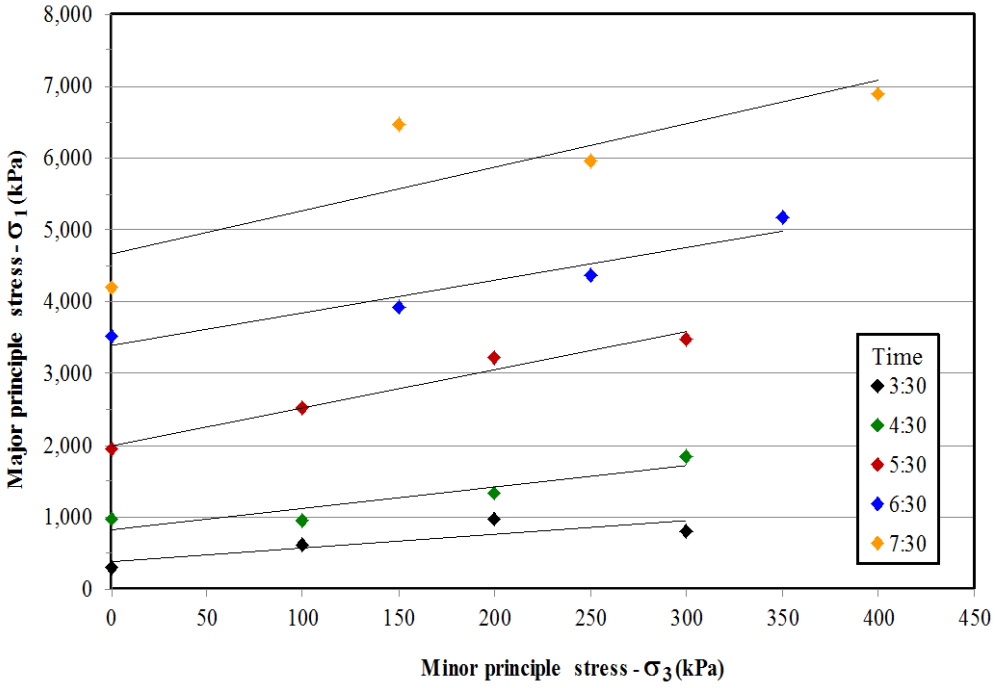

Figure 3.16. Triaxial test results for shotcrete paste batch No. SS_005.

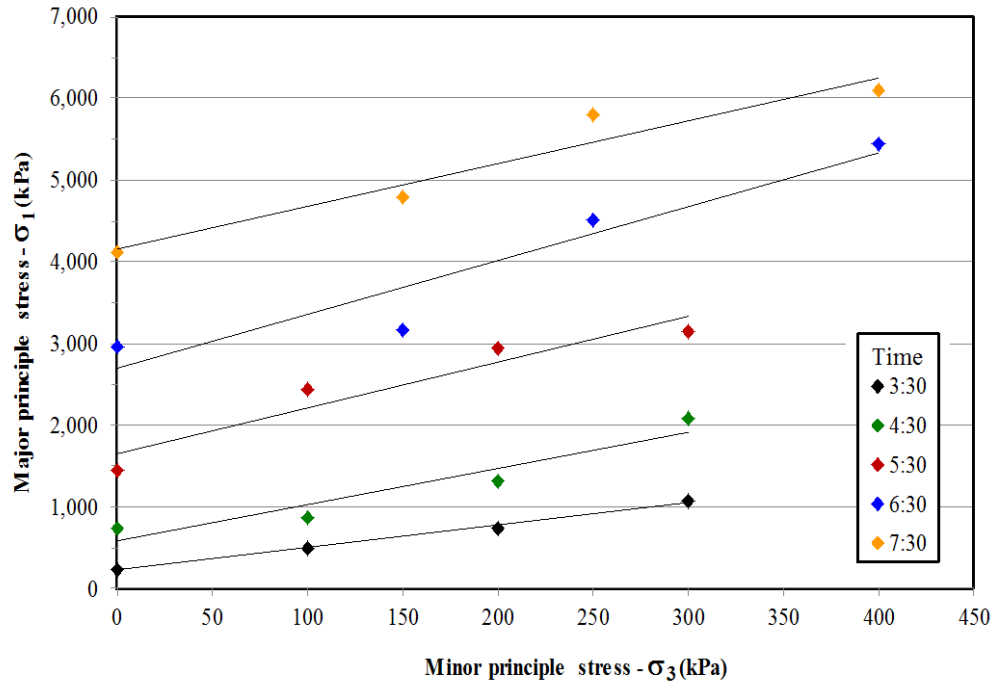

Figure 3.17. Triaxial test results for shotcrete paste batch No. SS_006.

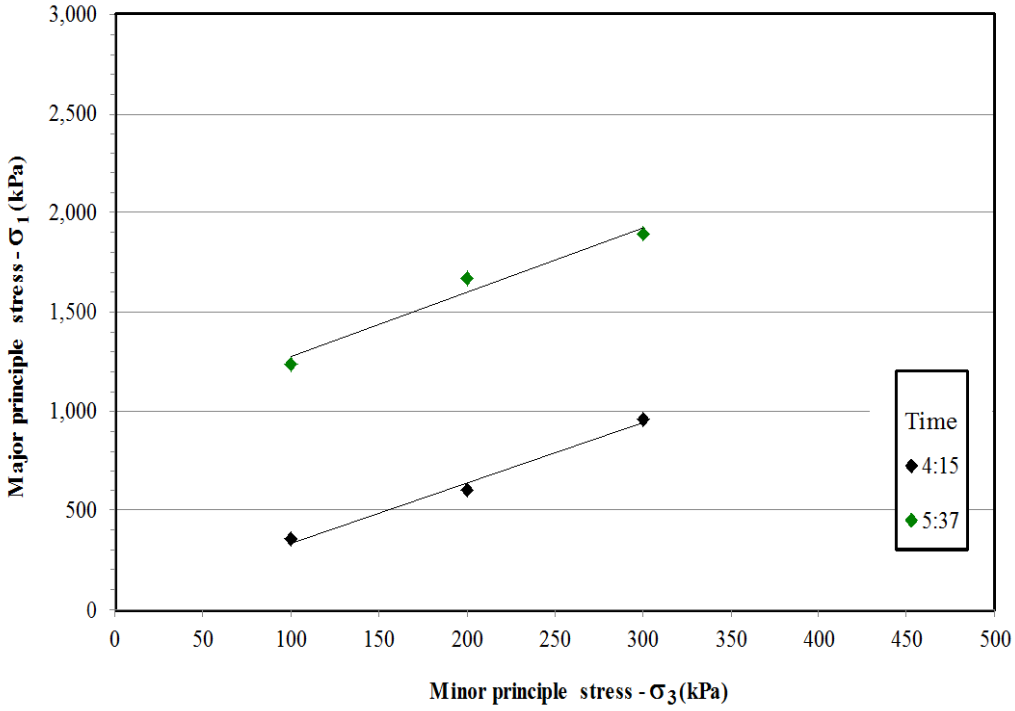

Figure 3.18. Triaxial test results for shotcrete paste batch No. GM_0011.

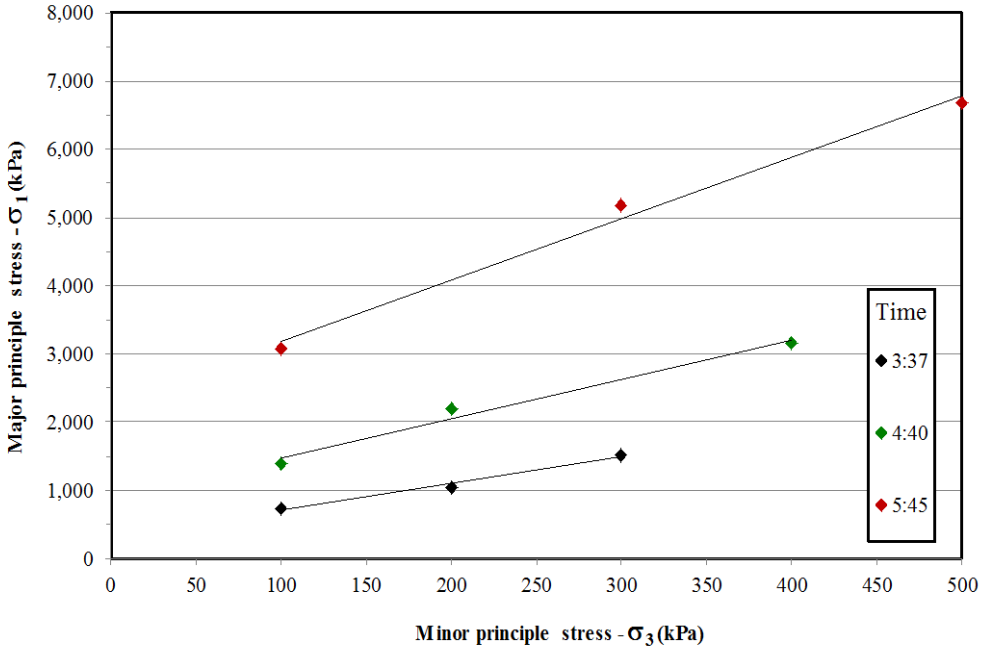

Figure 3.19. Triaxial test results for shotcrete paste batch No. GM_0012.

Tables 3.5 and 3.6 show the summary of shear strength test results for shotcrete paste without chemical admixture from research stages 1 to 3. Figures 3.20 and 3.21 show shear strength development of shotcrete paste without chemical admixture for 4 and 8 hours, respectively. Tables 3.5 and 3.6, Figures 3.20 and 3.21 suggested that, from 0 to 3 hours curing the shear strength ranges from 0.05 to 16 Pa. After 3 hours curing the shear strength increased significantly. The shear strength ranges from 36 to 80 kPa, 88 to 235 kPa, 189 to 432 kPa and 309 to 1265 kPa between 3.5 to 4 hours, 4.5 to 5:00 , 5.5 to 6 hours and 6.5 to 8.5 hours, respectively.

Table 3.5. Shear strength of shotcrete paste without chemical admixture.

Curing (hr:min)	Shear strength (kPa)								
	Stage 1	SS-001 to SS_006	GM_0001	GM_0002	GM_0003	GM_0004	GM_0005	GM_0011	GM_0012
0:00	0.05	-	-	-	-	-	-	-	-
0:10	0.06	-	-	-	-	-	-	-	-
0:15	-	-	-	-	-	0.28	0.14	0.08	0.08
0:20	-	-	-	-	-				-
0:30	0.07	-	0.23	0.18	0.31	0.36	0.17	0.12	0.17
0:45	-	-	-	-	-	0.48	0.31	0.21	0.38
1:00	0.43	0.38	1.08	0.47	1.96	1.23	0.68	0.50	0.79
1:00	-	0.22	-	-	-	-	-	-	-
1:10	0.64	-	-	-	-	-	-	-	-
1:15	-	-	-	-	-	2.59	1.35	1.35	2.28
1:20	1.02	-	-	-	-	-	-	-	-
1:30	1.60	1.16	3.68	6.35	8.48	3.25	3.60	2.12	6.14
1:30	-	1.16	-	-	-	-	-	-	-
1:30	-	0.77	-	-	-	-	-	-	-
1:45	1.70	-	-	-	-	6.41	7.07	4.80	15.94
1:50	-	-	-	-	-	-	-		-
2:00	1.93	4.30	14.83	14.52		-	-	9.03	-
2:10	3.97	3.97	-	-	-	-	-		-
2:15	-	-	-	-	-	-	-	13.30	-
2:30	-	-	-	-	-	-	-	-	-
2:45	8.72	-	-	-	-	-	-	-	-
3:00	10.04	-	-	-	-	-	-	-	-
3:30	-	58.00	-	-	-	-	-	-	-
3:30	-	69.00	-	-	-	-	-	-	-
3:30	-	54.00	-	-	-	-	-	-	-
3:30	-	-	-	-	-	-	-	-	-
3:37	-	-	-	-	-	-	-	-	80.00
4:00	-	36.00	-	-	-	-	-	-	-
4:15	-	-	-	-	-	-	-	-	-
4:30	-	88.00	-	-	-	-	-	-	-
4:30	-	138.00	-	-	-	-	-	-	-
4:30	-	235.00	-	-	-	-	-	-	-
4:30	-	105.00	-	-	-	-	-	-	-
4:40	-	131.00	-	-	-	-	-	-	-
4:45	-	-	-	-	-	-	-	-	188.00
5:00	-	-	-	-	-	-	-	-	-
5:30	-	189.00	-	-	-	-	-	-	-
5:30	-	354.00	-	-	-	-	-	-	-
5:30	-	349.00	-	-	-	-	-	-	-
5:30	-	210.00	-	-	-	-	-	-	-
5:30	-	432.00	-	-	-	-	-	-	-
5:37	-	-	-	-	-	-	-	263.00	-
5:45	-	-	-	-	-	-	-	381.00	-

Table 3.6. Shear strength of shotcrete paste without chemical admixture.

Curing (hr:min)	Shear strength (kPa)								
	Stage 1	SS-001 to SS_006	GM_0001	GM_0002	GM_0003	GM_0004	GM_0005	GM_0011	GM_0012
6:00	-	301.00	-	-	-	-	-	-	-
6:30	-	864.00	-	-	-	-	-	-	-
6:30	-	789.00	-	-	-	-	-	-	-
6:30	-	525.00	-	-	-	-	-	-	-
6:30	-	343.00	-	-	-	-	-	-	-
6:30	-	309.00	-	-	-	-	-	-	-
7:00	-	778.00	-	-	-	-	-	-	-
7:30	-	1265.00	-	-	-	-	-	-	-
7:30	-	946.00	-	-	-	-	-	-	-
7:30	-	906.00	-	-	-	-	-	-	-
7:30	-	407.00	-	-	-	-	-	-	-
7:30	-	555.00	-	-	-	-	-	-	-
8:30	-	1057.00	-	-	-	-	-	-	-

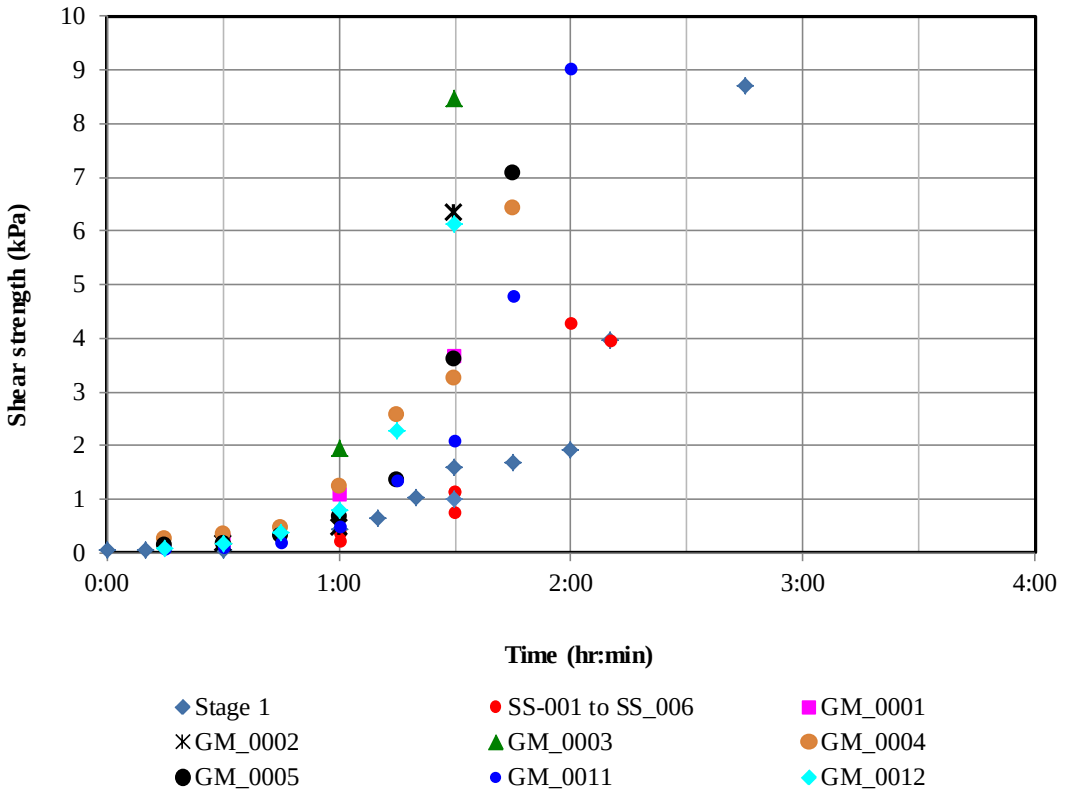

Figure 3.20. Shear strength development of shotcrete paste without chemical admixture (4 hours).

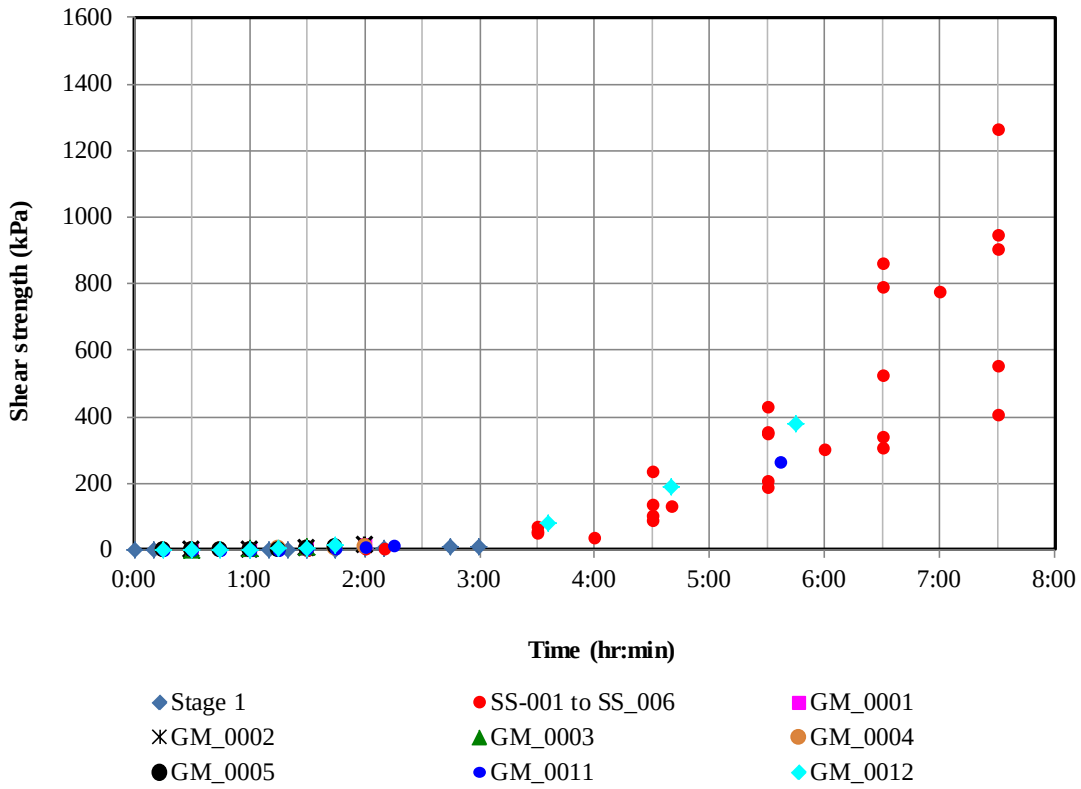

Figure 3.21. Shear strength development of shotcrete paste without chemical admixture (8 hours).

3.8.2.2 Shear strength of shotcrete paste with the influences accelerator

Figures 3.22 to 3.29 show the triaxial test results conducted on the shotcrete paste samples mixed with accelerator admixture. The results are plotted on minor principle stress (σ_3) ad major principle stress (σ_1) domain. The details test data are presented in Appendix – B. Tables 3.7 and 3.8 show the summary of shear strength test results for shotcrete paste with accelerator from research stages 1 to 3. Figures 3.30 and 3.31 show shear strength development of shotcrete paste with accelerator for 4 and 8 hours, respectively. Tables 3.7 and 3.8, Figures 3.30 and 3.31 suggested that, with the addition of accelerator the shear strength of shotcrete paste start increased after 15 minute curing and significantly increased after 2 hours curing. It ranges from 0.66

to 18 kPa, 17 to 496 kPa, 31 to 668 kPa, 131 to 2149 kPa, 240 to 1886 kPa and 737 kPa to 1756 kPa, between 0 to 2 hours, 2.5 to 3 hours, 3.5 to 4 hours, 4.5 to 5 hours, 5.5 to 6 hours and 6.5 to 7.5 hours, respectively.

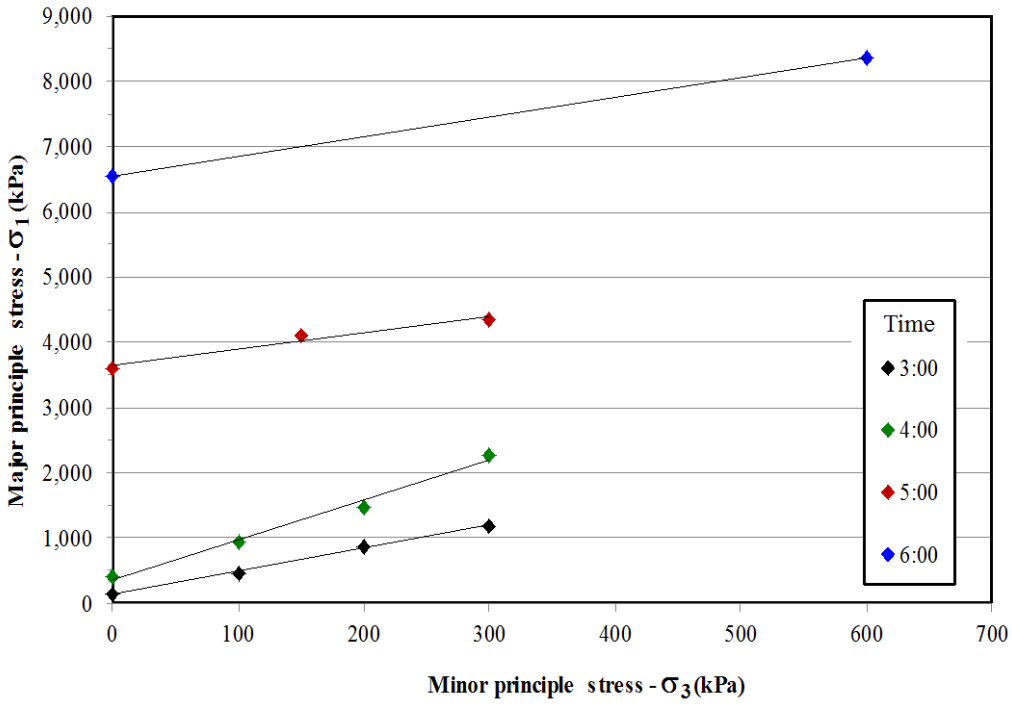

Figure 3. 22. Triaxial test results for shotcrete paste batch No. SS_007.

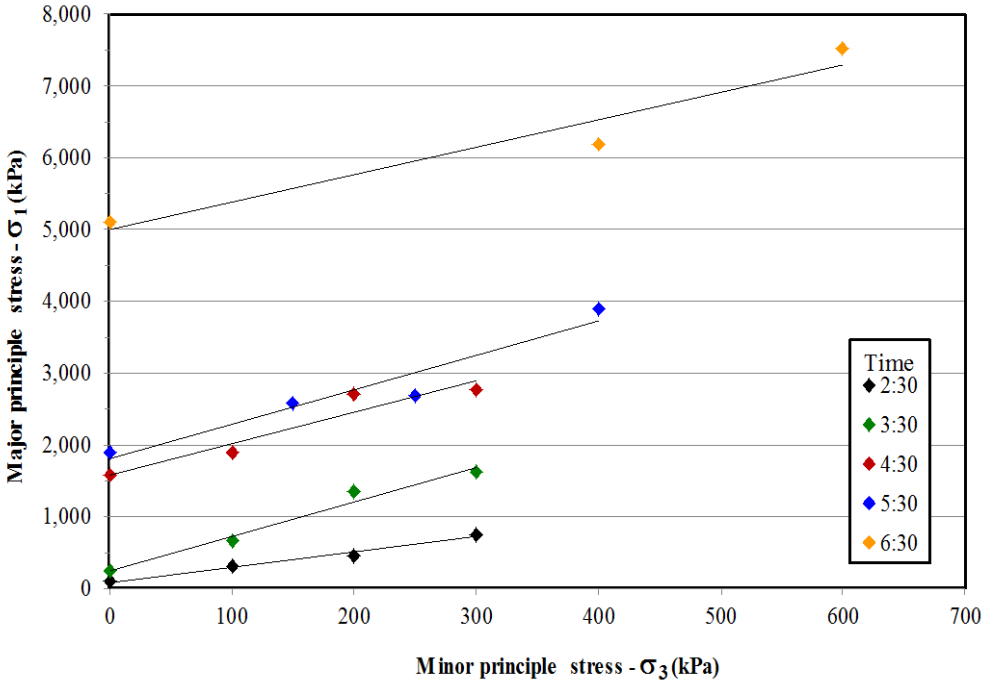

Figure 3.23. Triaxial test results for shotcrete paste batch No. SS_008.

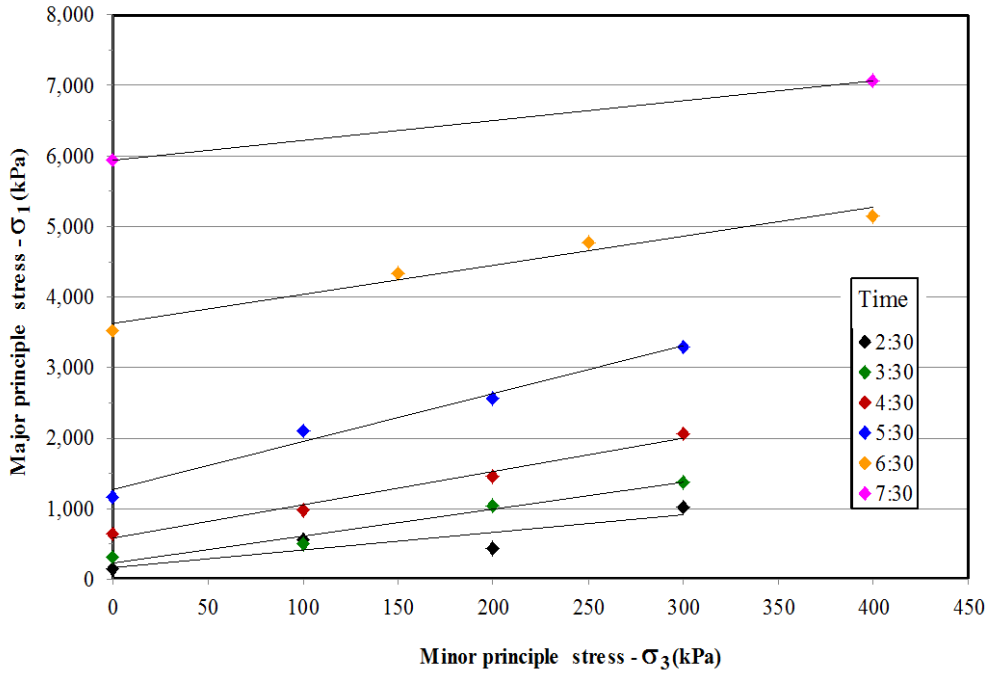

Figure 3.24. Triaxial test results for shotcrete paste batch No. SS_009.

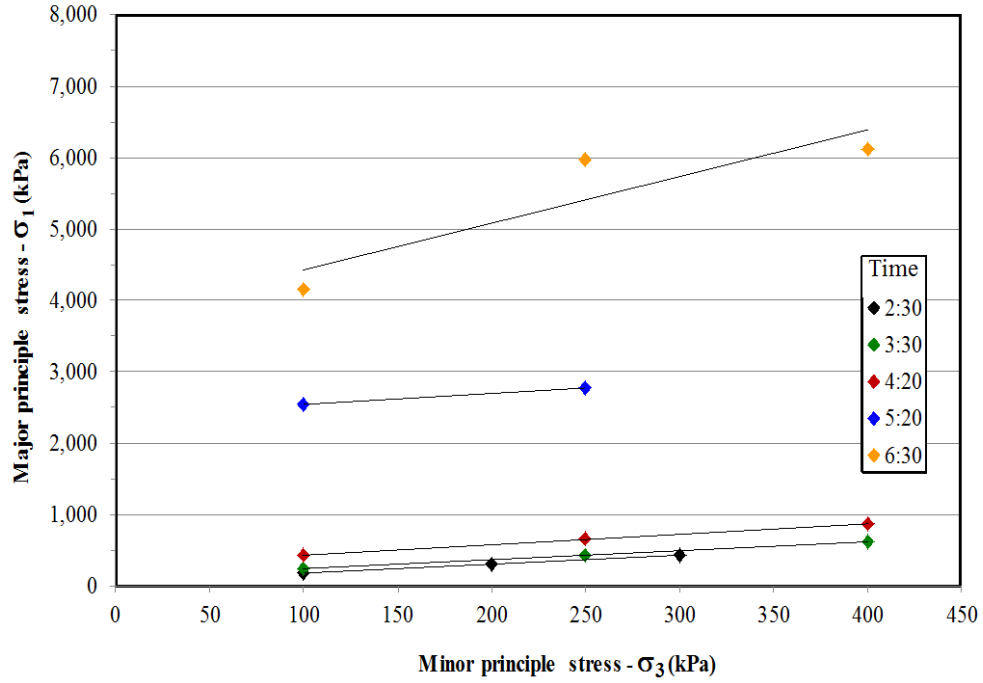

Figure 3.25. Triaxial test results for shotcrete paste batch No. SS_0010.

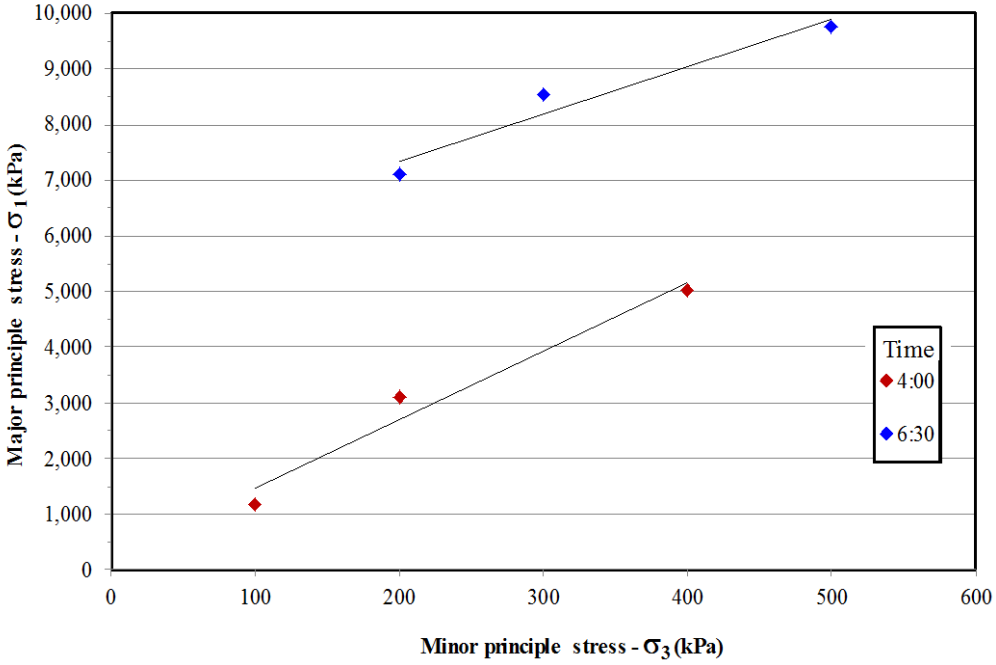

Figure 3.26. Triaxial test results for shotcrete paste batch No. SS_0011.

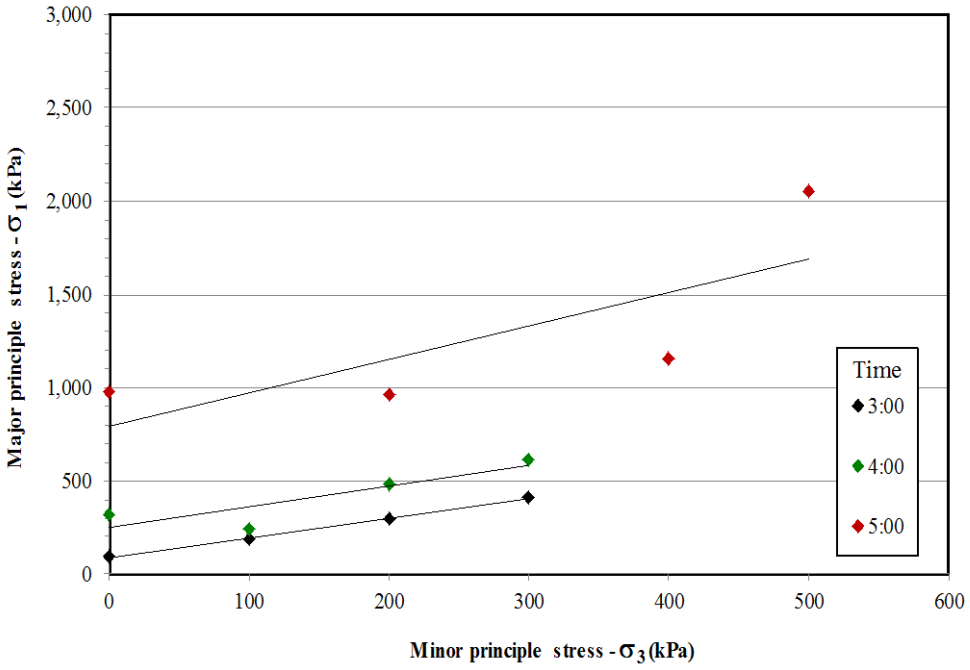

Figure 3.27. Triaxial test results for shotcrete paste batch No. SS_0012.

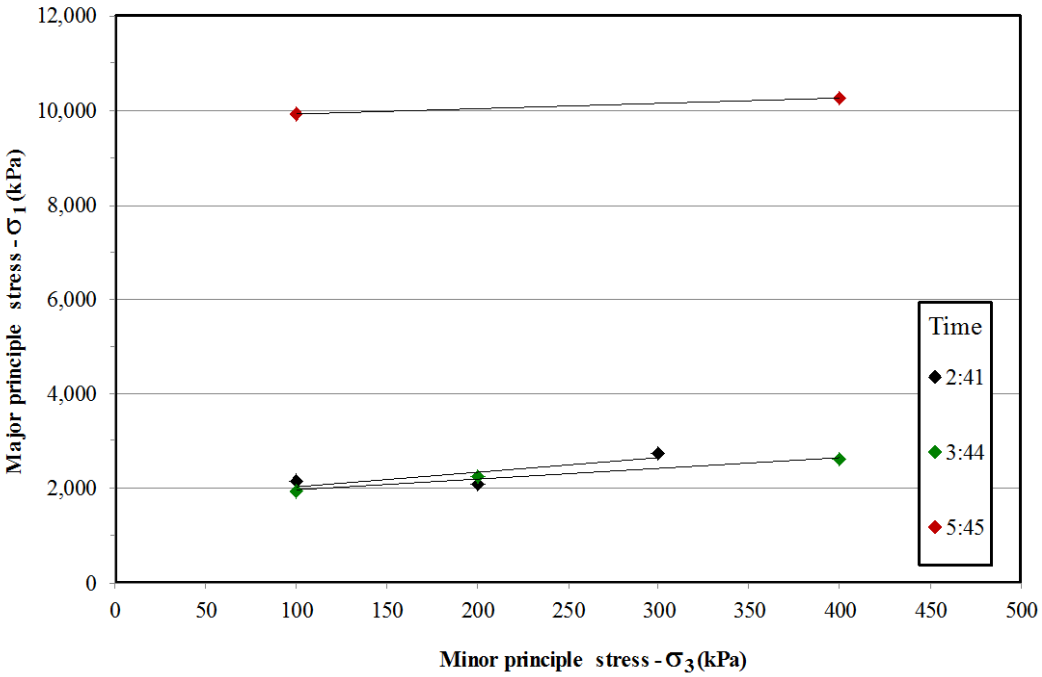

Figure 3.28. Triaxial test results for shotcrete paste batch No. GM_0014.

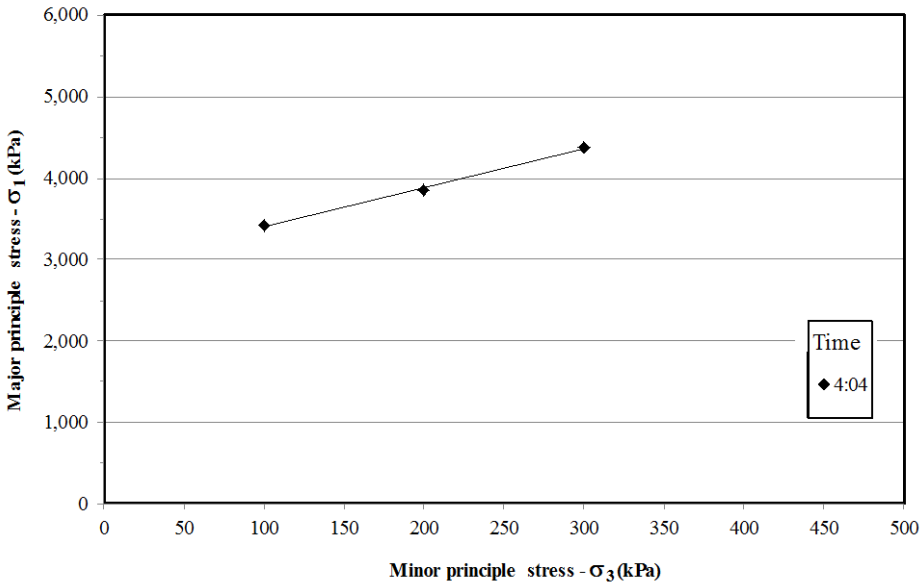

Figure 3.29. Triaxial test results for shotcrete paste batch No. GM_0015.

Table 3.7. Shear strength of shotcrete paste with accelerator.

Curing (hr:min)	Shear strength (kPa)		
	SS-007 to SS_012	GM_0014	GM_0015
0:10	0.66	-	-
0:10	1.06	-	-
0:15	-	6.30	3.56
0:20	2.22	-	-
0:20	2.14	-	-
0:30	2.87	16.64	5.45
0:30	2.42	-	-
0:40	2.84	-	-
0:40	3.34	-	-
0:45	-	14.84	6.75
0:50	3.66	-	-
0:50	3.68	-	-
1:00	4.20	-	10.47
1:00	4.00	-	-
1:10	4.41	-	-
1:10	4.27	-	-
1:15	-	-	18.01
1:20	6.01	-	-
1:20	5.70	-	-
1:30	6.16	-	-
1:30	6.72	-	-
1:40	10.51	-	-
1:40	10.72	-	-
1:50	13.04	-	-
1:50	14.81	-	-
2:00	17.80	-	-
2:00	16.61	-	-
2:30	26.00	-	-
2:30	48.00	-	-
2:30	17.00	-	-
2:41	-	496.00	-

Table 3.8. Shear strength of shotcrete paste with accelerator.

Curing (hr:min)	Shear strength (kPa)		
	SS-007 to SS_012	GM_0014	GM_0015
3:00	35.00	-	-
3:00	44.00	-	-
3:30	57.00	-	-
3:30	56.00	-	-
3:44	-	582.00	-
4:00	71.00	-	668.00
4:00	31.00	-	-
4:00	117.00	-	-
4:20	123.00	-	-
4:30	376.00	-	-
4:30	131.00	-	-
4:35	-	2149.00	-
5:00	1153.00	-	-
5:00	295.00	-	-
5:20	976.00	-	-
5:30	416.00	-	-
5:30	240.00	-	-
6:00	1886.00	-	-
6:30	1273.00	-	-
6:30	898.00	-	-
6:30	737.00	-	-
6:30	976.00	-	-
7:30	1756.00	-	-

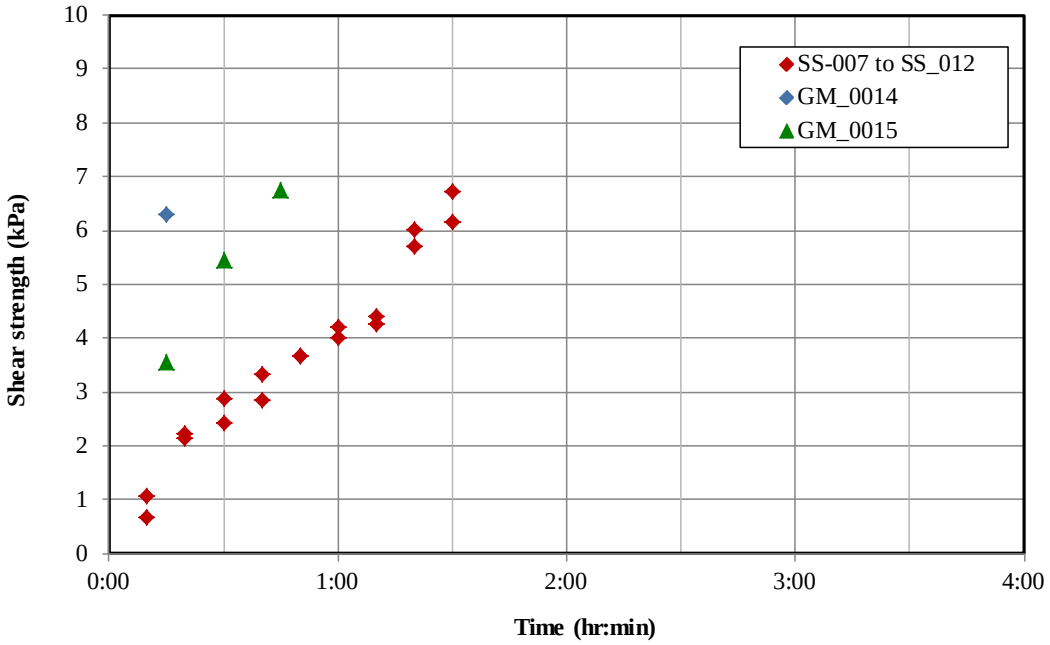

Figure 3. 30. Shear strength development of shotcrete paste with accelerator (4 hours).

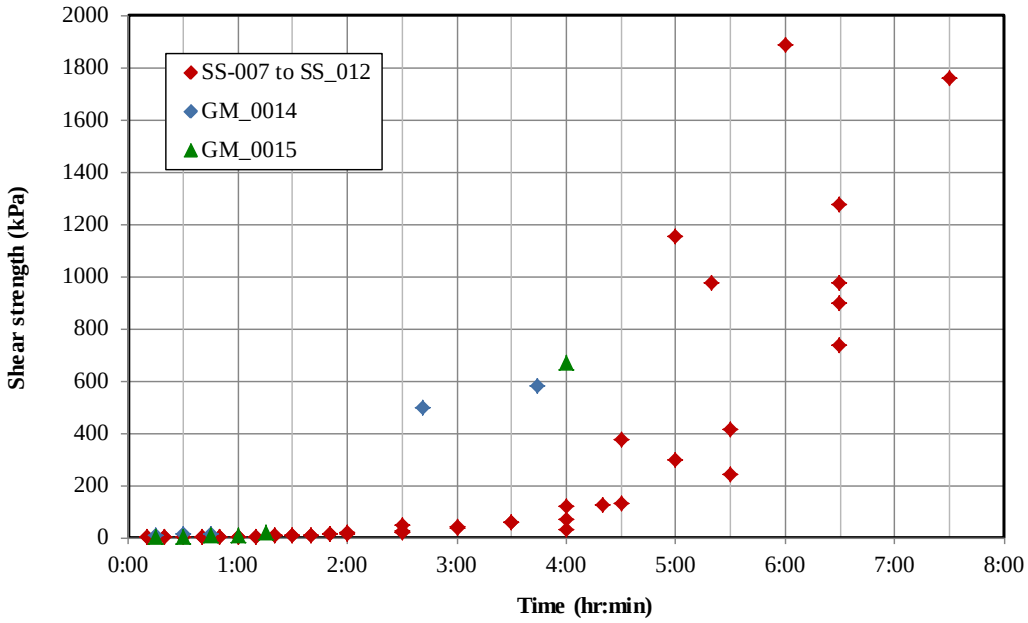

Figure 3.31. Shear strength development of shotcrete paste with accelerator (8 hours).

3.8.2.3 Shear strength of shotcrete paste with the influences of superplasticier

Figures 3.32 shows the triaxial test results conducted on the shotcrete paste samples mixed with superplasticier. The results are plotted on minor principle stress (σ_3) and major principle stress (σ_1) domain. The details test data are presented in Appendix – B. Tables 3.9 shows the summary of shear strength test results for shotcrete paste with superplasticier from research stages 2 and 3. Figures 3.33 and 3.34 show shear strength development of shotcrete paste with superplasticier for 4 and 8 hours, respectively. Table 3.9, Figures 3.33 and 3.34 suggested that, with the addition of superplasticier the shear strength of shotcrete paste start increased after 3.5 hours curing and significantly increased after 6 hours curing. It ranges from0.01 to 0.28 kPa, 0.02 to 3 kPa, 0.08 to 70 kPa and 118 to 369 kPa between 0 to 3 hours, 3.25 to 4 hours, 4 to 6 hours and 7 to 8 hours.

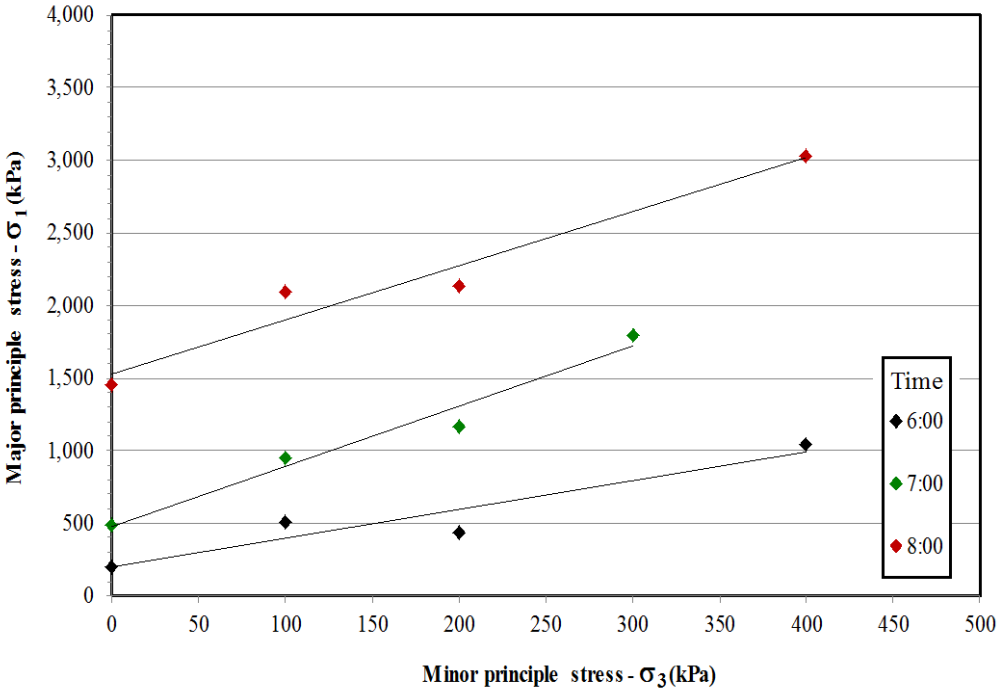

Figure 3.32. Triaxial test results for shotcrete paste batch No. SS_013.

Table 3.9. Shear strength of shotcrete paste with superplasticier.

Curing (hr:min)	Shear strength (kPa)		
	SS-013	GM_0026	GM_0027
0:30	-	-	0.01
0:45	-	-	0.01
1:00	-	0.01	0.01
1:15	-	-	0.02
1:30	-	0.01	0.01
1:45	-	0.01	0.02
2:00	-	-	0.03
2:15	-	0.01	0.06
2:30	-	0.01	0.18
2:45	-	-	0.20
3:00	-	0.01	0.28
3:15	-	0.02	0.45
3:30	-	0.07	1.12
3:45	-	0.04	2.31
4:00	-	0.08	3.14
4:15	-	0.12	7.45
4:30	-	0.24	10.87
4:45	-	-	17.22
6:00	70.00	-	-
7:00	118.00	-	-
8:00	369.00	-	-

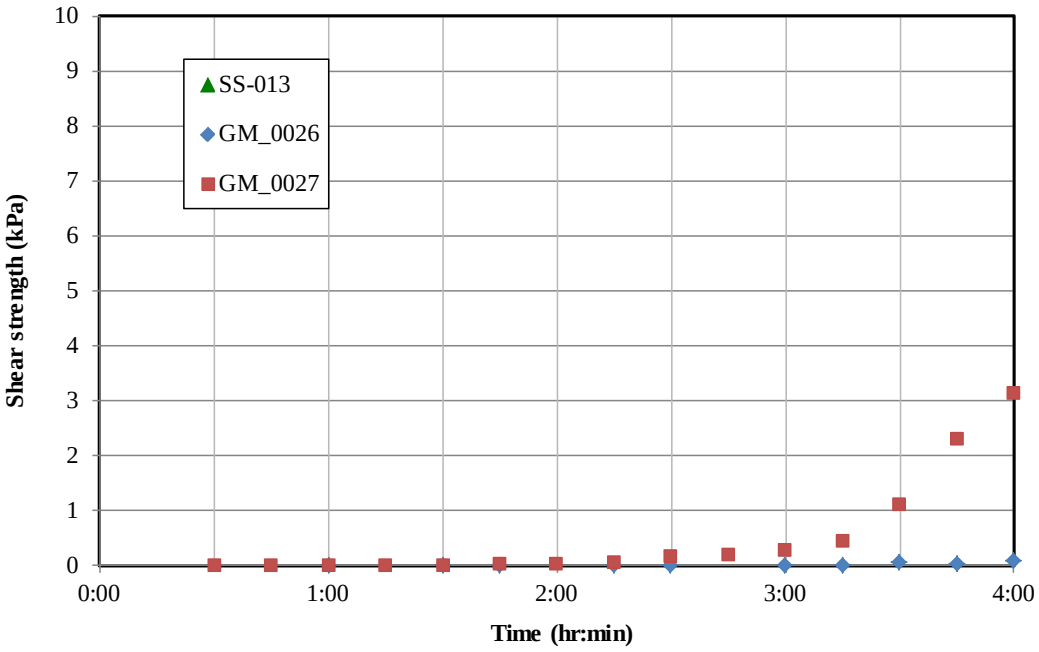

Figure 3.33. Shear strength development of shotcrete paste with superplasticier (4 hours).

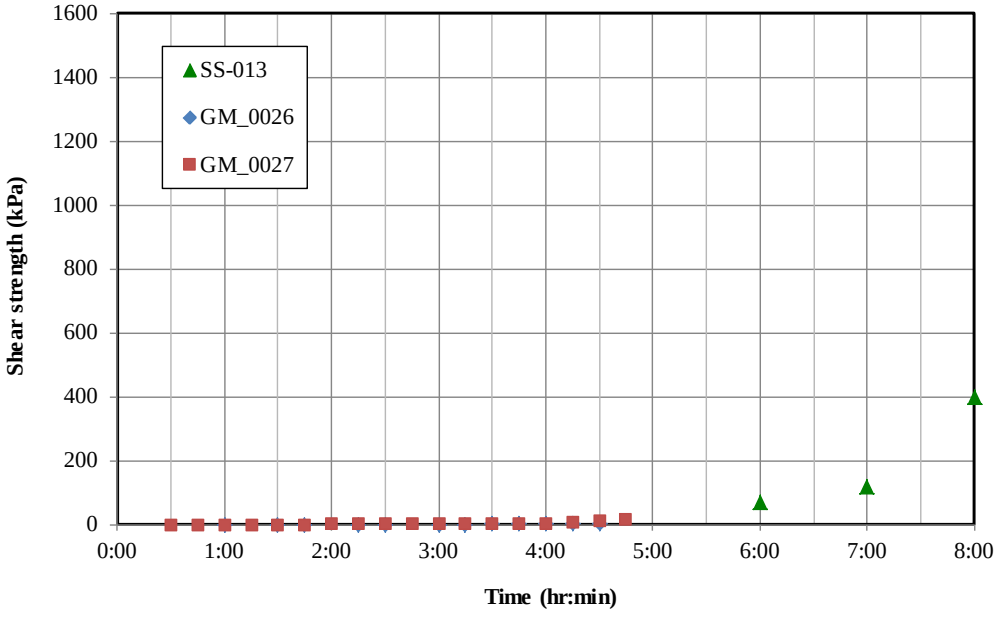

Figure 3.34. Shear strength development of shotcrete paste with superplasticier (8 hours).

3.8.2.4 Shear strength of shotcrete paste with the influences of water reducing admixture

Figures 3.35 to 3.37 show the triaxial test results conducted on the shotcrete paste samples mixed with water reducing admixture. The results were plotted on minor principle stress (σ_3) and major principle stress (σ_1) domain. The details test data are presented in Appendix – B. Tables 3.10 shows the summary of shear strength test results for shotcrete paste with water reducing admixture from research stages 2 and 3. Figures 3.38 and 3.39 show shear strength development of shotcrete paste with superplasticier for 4 and 8 hours, respectively. Table 3.10, Figures 3.38 and 3.39 suggested that, with the addition of water reducing admixture the shear strength of shotcrete paste start increasing after 2 hours cuing and significantly increased after 5 hours curing. It ranges from 0.04 to 0.63 kPa, 1 to 8 kPa, 8 to 101 kPa, 135 to 181 kPa and 475 to 711 kPa between 0 to 2 hours. 2.25 to 3 hours, 3.25 to 5 hours, 5 to 6 hours and 7 to 8 hours, respectively.

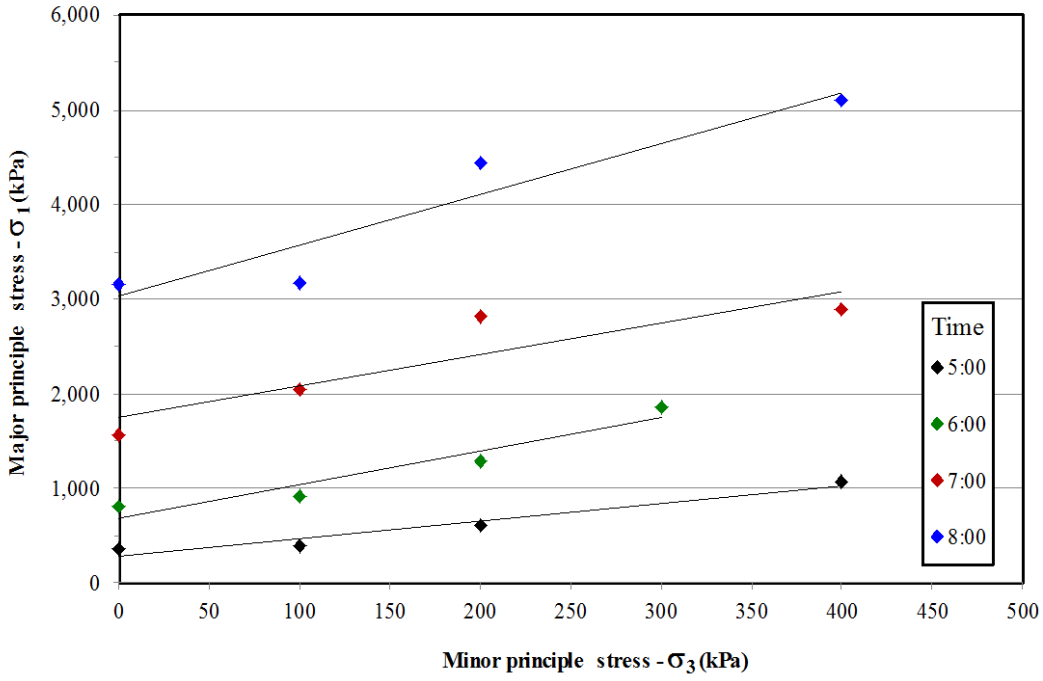

Figure 3.35. Triaxial test results for shotcrete paste batch No. SS_014.

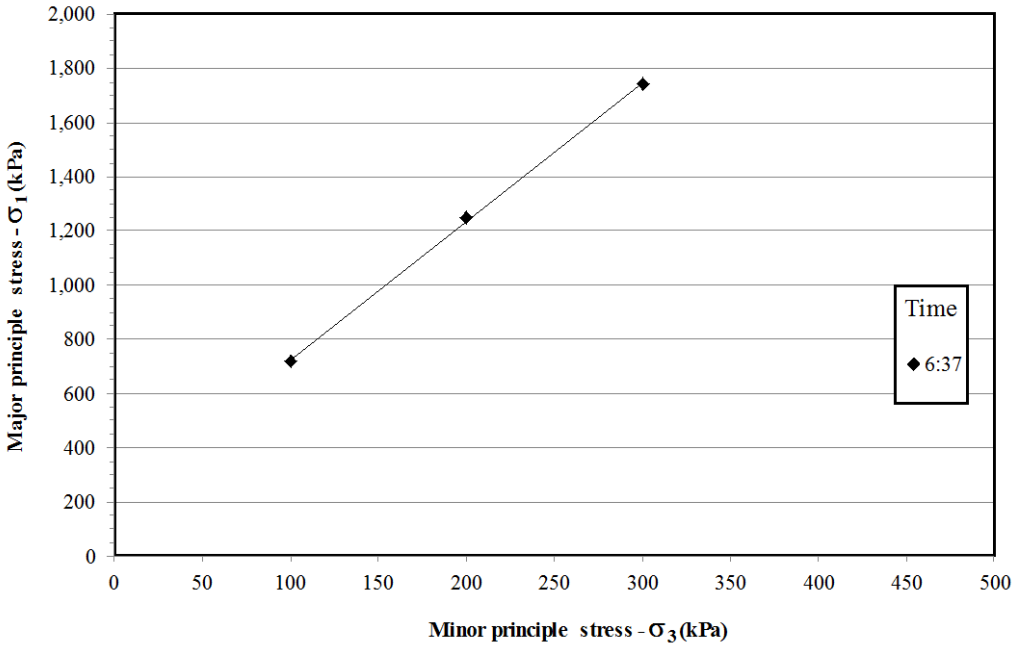

Figure 3.36. Triaxial test results for shotcrete paste batch No. GM_0022.

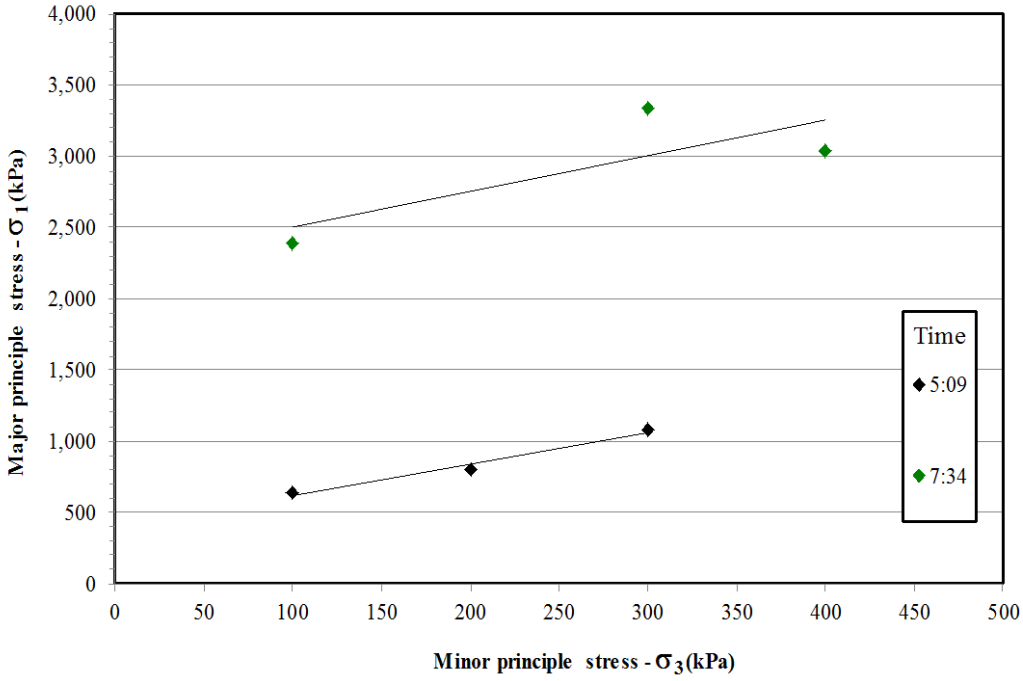

Figure 3.37. Triaxial test results for shotcrete paste batch No. GM_0025.

Table 3.10. Shear strength of shotcrete paste with water reducing admixture.

Curing (hr:min)	Shear strength (kPa)		
	SS_014	GM_0022	GM_0025
0:15	-	0.04	0.05
0:30	-	0.06	0.04
0:45	-	0.07	0.06
1:00	-	0.13	0.07
1:15	-	0.15	0.10
1:30	-	0.22	0.18
1:45	-	0.30	0.32
2:00	-	0.43	0.63
2:15	-	1.29	1.45
2:30	-	1.42	2.87
2:45	-	2.35	4.70
3:00	-	3.64	7.83
3:15	-	7.79	12.53
3:30	-	16.11	-
5:00	101.00	-	-
5:10	-	-	135.00
6:00	181.00	-	-
7:00	475.00	-	-
7:35	-	-	711.00
8:00	653.00	-	-

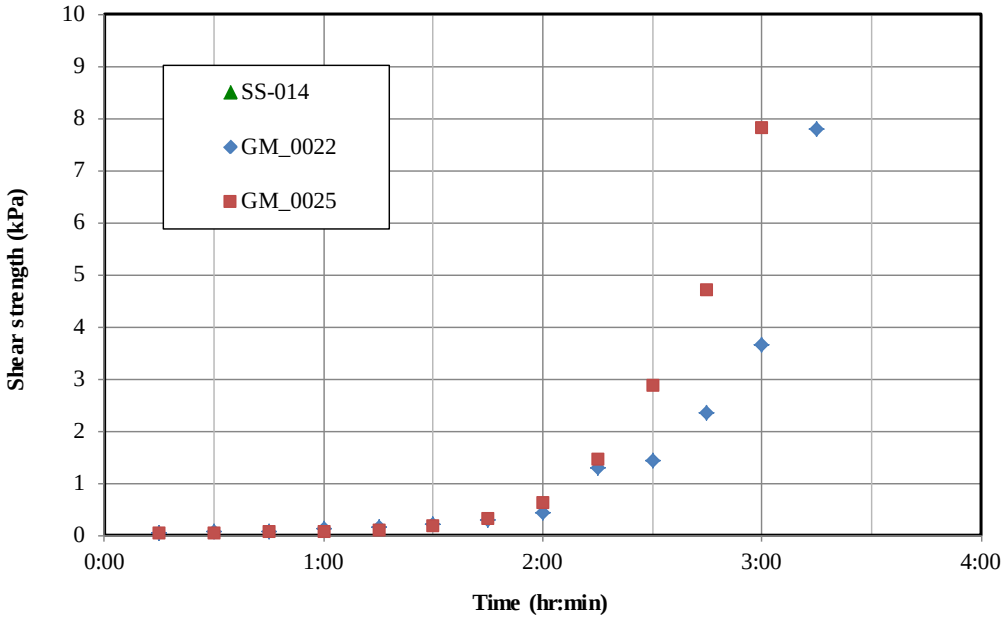

Figure 3.38. Shear strength development of shotcrete paste with water reducing admixture (4 hours).

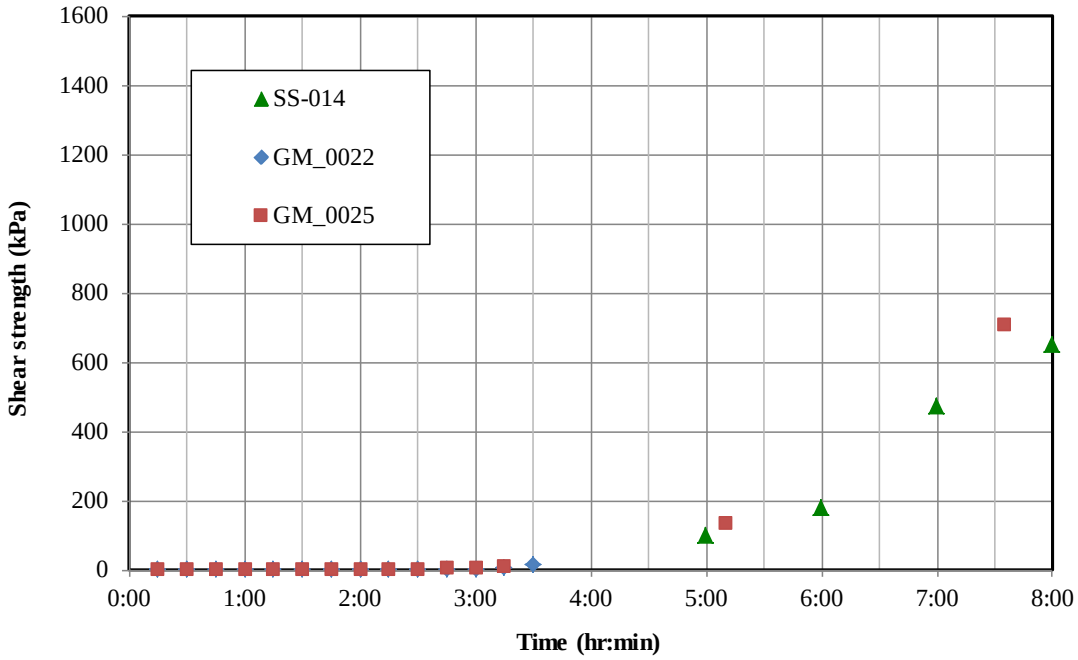

Figure 3.39. Shear strength development of shotcrete paste with water reducing admixture (8 hours).

3.8.2.5 Shear strength of shotcrete paste with the influences of a hydration stabiliser

Tables 3.11 shows the summary of shear strength test results for shotcrete paste with water reducing admixture from research stage 3. Figures 3.40 and 3.41 show shear strength development of shotcrete paste with a hydration stabiliser for 4 and 8 hours, respectively. Table 3.11, Figures 3.40 and 3.41 suggested that, with the addition of a hydration stabiliser, the cement hydration did not start until 4 hours. The cement hydration started after 4 hours curing. However, the shear strength was still very low ranging from 0.1 to 2 kPa between 2 hours 6.25 to 3 hours. The samples were still very soft to be able to conduct the shear strength test with triaxial test method until 8 hours curing.

Table 3.11. Shear strength of shotcrete paste with hydration stabiliser.

Curing (hr:min)	Shear strength (kPa)	
	GM_0018	GM_0019
0:15	0.06821	0.0892
0:30	0.09969	0.1023
0:45	0.1049	0.1784
1:00	0.1102	0.2414
1:15	0.1259	0.2886
1:30	0.1364	0.404
1:45	0.1443	0.5457
2:00	0.1784	0.5404
2:15	0.1469	0.6926
2:45	0.1836	-
2:45	0.1915	-
3:00	0.2151	-
3:15	0.2256	-
3:30	0.2204	-
3:45	0.2781	-
4:00	0.2571	0.8028
4:15	0.2886	0.7766
4:30	0.2519	1.049
4:45	0.3725	1.07
5:00	0.4617	1.613
5:15	0.5116	1.359
5:30	0.4985	2.382
5:45	-	1.868
6:00	-	2.429
6:15	-	2.015

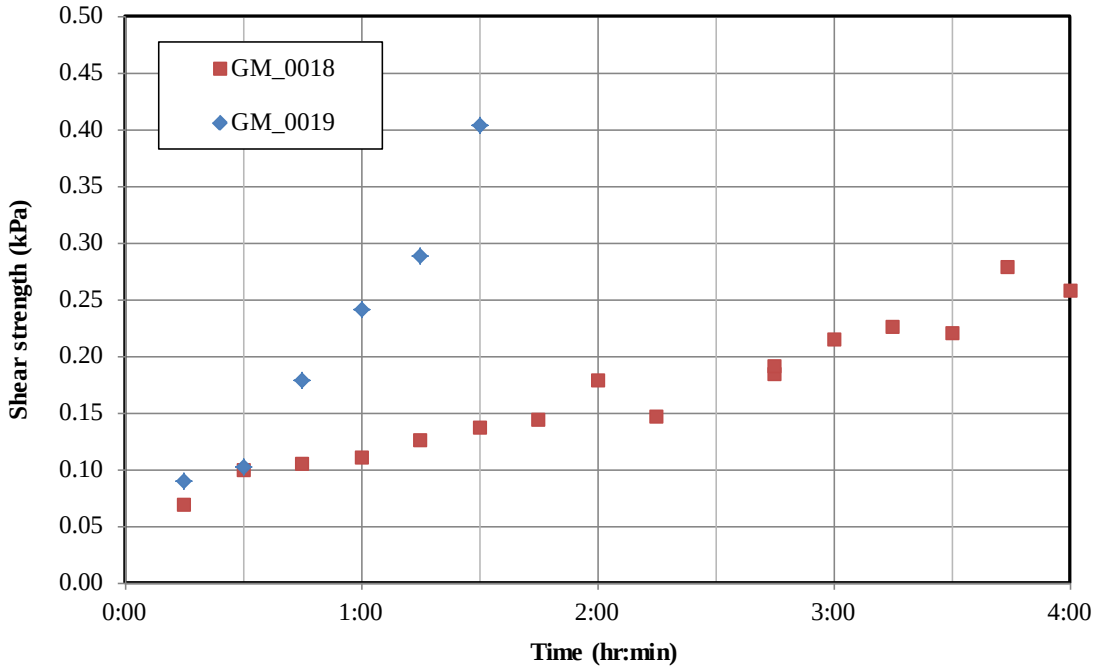

Figure 3.40. Shear strength development of shotcrete paste with hydration stabiliser (4 hours).

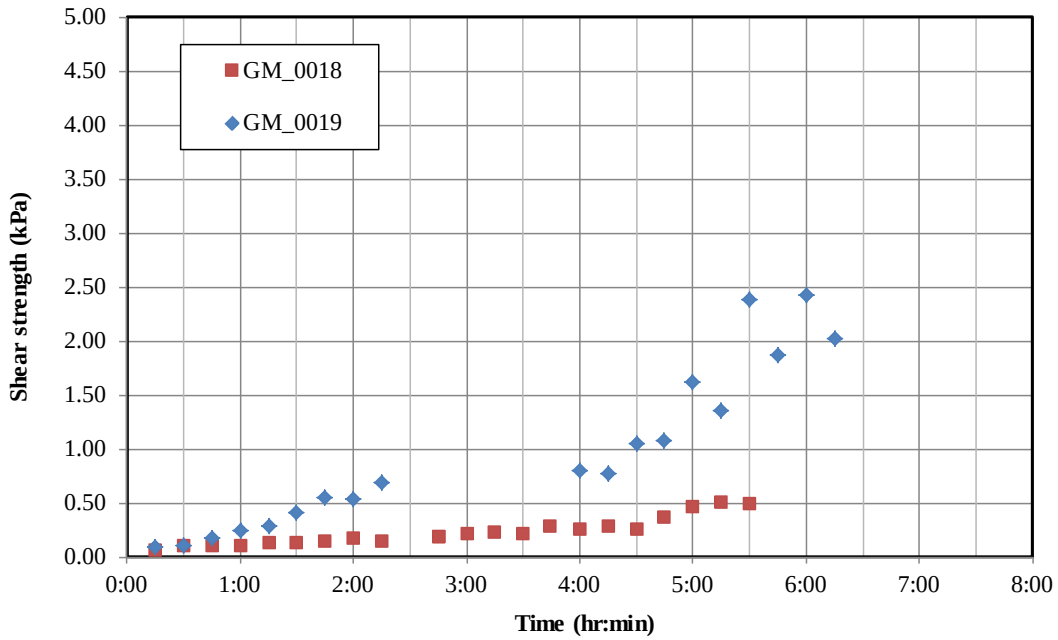

Figure 3.41. Shear strength development of shotcrete paste with hydration stabiliser (8 hours).

3.8.2.6 Summary - Shear strength of shotcrete paste with and without the influences of chemical admixture

The influences of chemical admixtures on the cement hydration and its chemistry are described in Chapter 2, Section 2.3.5. The previous Sections (3.8.2.2 to 3.8.2.5) shows the test results conducted within this research. A summary of shear strength development of shotcrete paste with and without the influence of chemical admixture for the first 4 and 8 hours of hydration are presented in Figures 3.42 and 3.43, respectively. The results show that, generally the shear strength increased exponentially during the first 4 and 8 hours of curing in all shotcrete paste mixes except for the shotcrete paste mixed with hydration stabiliser. The shear strength of shotcrete paste mixed with accelerator was significantly higher than that of shotcrete paste mixed without chemical admixture. The shear strength of shotcrete paste mixed with water reducing admixture was slightly lower than that of shotcrete paste mixed without chemical admixture. The shear strength of shotcrete paste mixed with superplasticer was significantly lower than that of shotcrete paste mixed without chemical admixture. The shear strength of shotcrete paste mixed with hydration stabiliser was extremely lower than that of shotcrete paste mixed without chemical admixture.

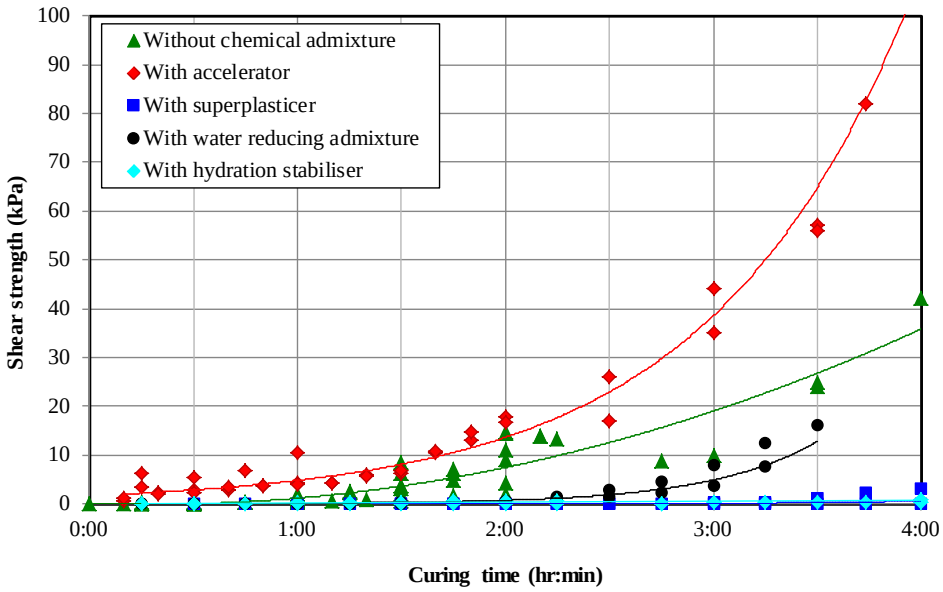

Figure 3.42. Shear strength developments of shotcrete paste with and without the influences of chemical admixture during the first (4) hours of hydration.

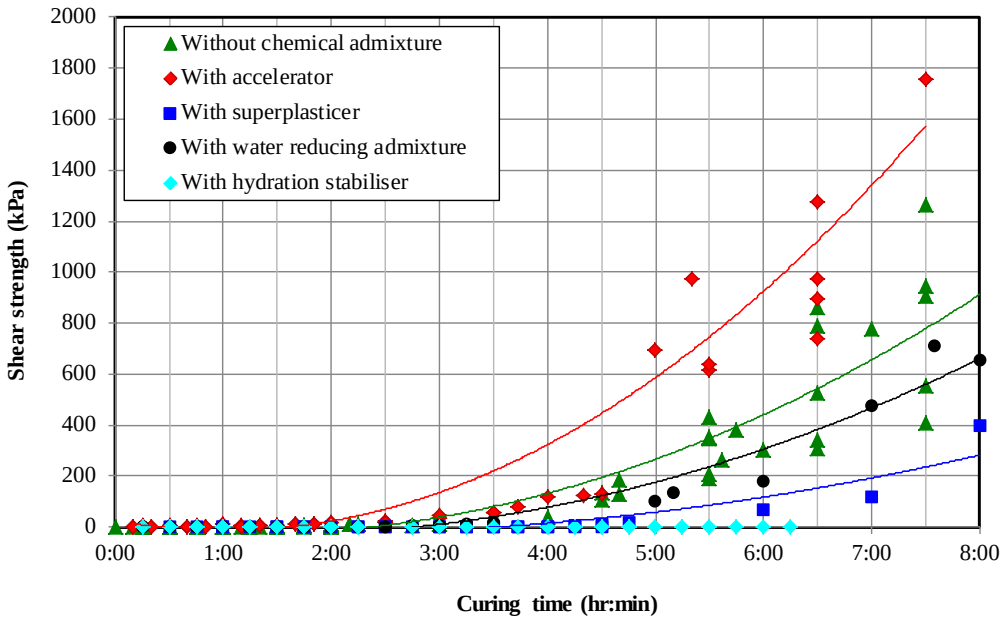

Figure 3.43. Shear strength developments of shotcrete paste with and without the influences of chemical admixture during the first (8) hours of hydration.

3.8.3 Typical stress – strain curves and mode of failure of shotcrete paste with an accelerator

Generally, most of the shotcrete in underground mining application use accelerator for early strength development. Therefore, only the typical deviator stress (σ_1-σ_3) and axial strain behaviour and mode of failure of shotcrete paste samples mixed with accelerator are described in this section. Figures 3.44 to 3.47 show a typical deviator stress (σ_1-σ_3) and axial strain curves for the triaxial test at 3, 4, 5 and 6 hours curing respectively. The photograph of the samples after triaxial test at 3, 4, 5 and 6 hours curing are shown in Figure 3.48 to 3.51, respectively. Based on the deviator stress (σ_1-σ_3) and axial strain behaviour, and the physical observation of the samples after triaxial test as shown in the photographs, the following conclusions can be made:

- At 3 hour curing, the specimens failed in shear and compression mode and continue deformed axially with increasing stress or strain hardening behaviour.

- At 4 and 5 hours curing, the specimens failed in shear and compression at low confinement (100 kPa) and shear mode at higher confinement (200 & 300 kPa). After failure the specimens continue to deform with an almost constant stress or yielding behaviour.

- At 6 hours curing, the specimens fail in shear and brittle mode. After failure, the specimens continue to deform with shearing and dilation.

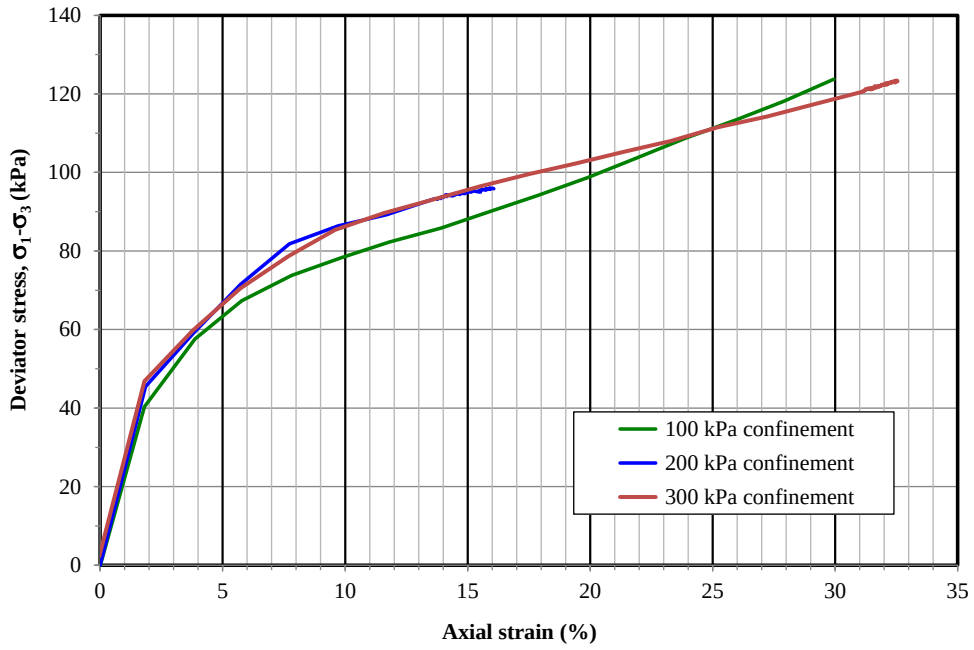

Figure 3.44. Deviator stress versus axial strain curves from triaxial test on shotcrete paste with accelerator samples at 3 hours curing.

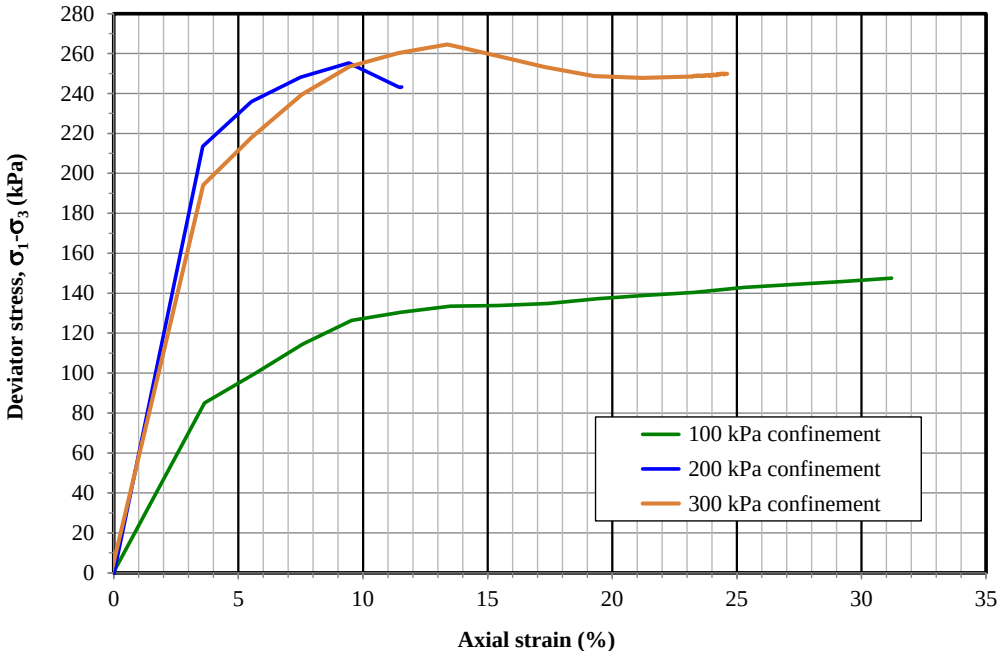

Figure 3.45. Deviator stress versus axial strain curves from triaxial test on shotcrete paste with accelerator samples at 4 hours curing.

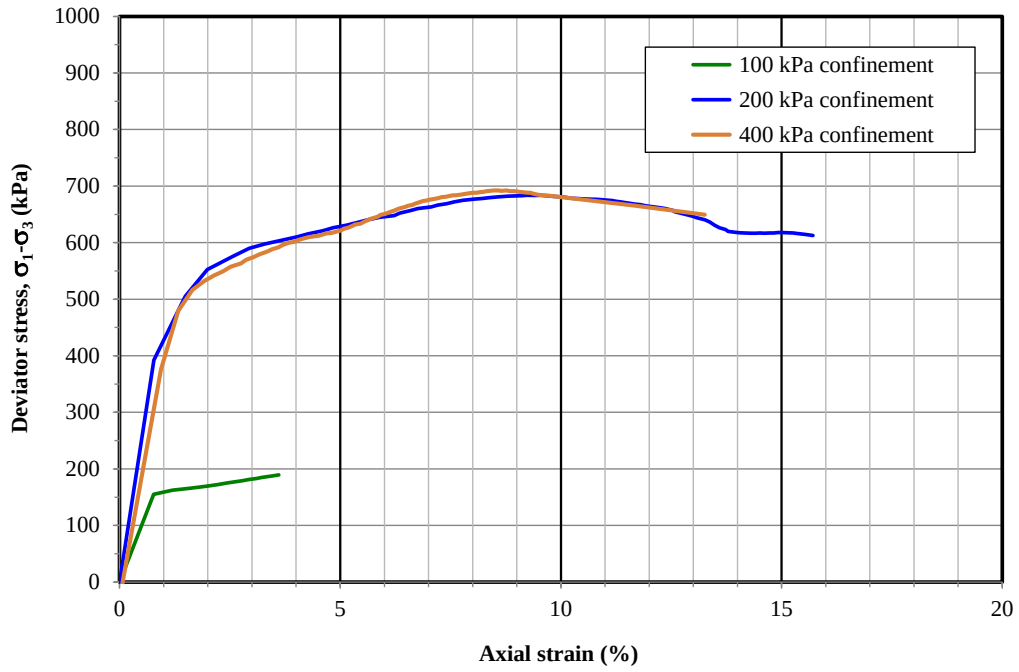

Figure 3.46. Deviator stress versus axial strain curves from triaxial test on shotcrete paste with accelerator samples at 5 hours curing.

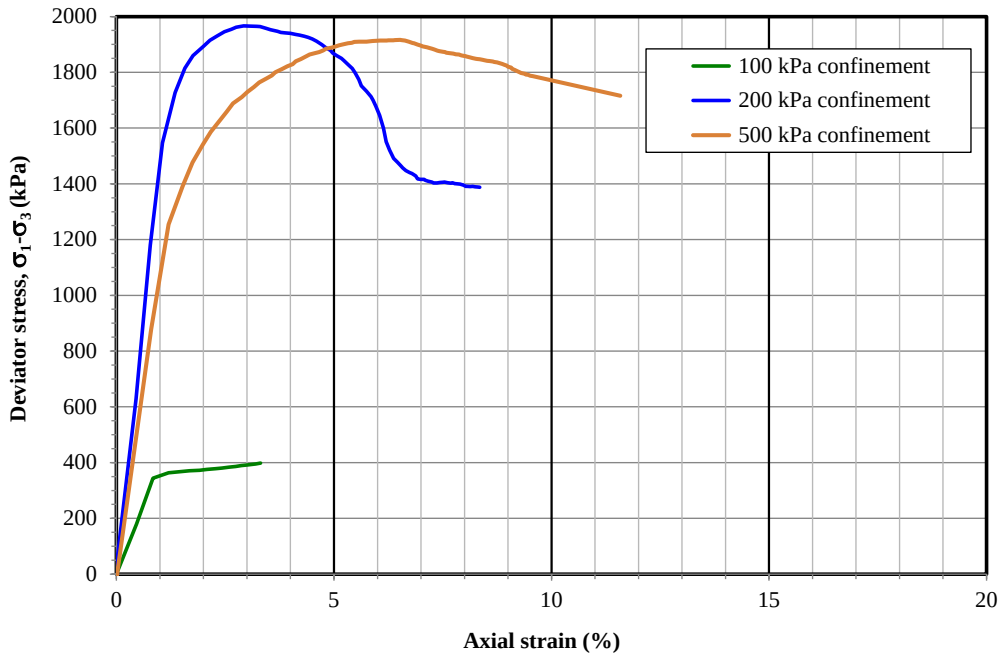

Figure 3.47. Deviator stress versus axial strain curves from triaxial test on shotcrete paste with accelerator samples at 6 hours curing.

Figure 3.48. Shotcrete paste with accelerator specimens after 3 hours curing triaxial test.

Figure 3.49. Shotcrete paste with accelerator specimens after 4 hours curing triaxial test.

Figure 3.50. Shotcrete paste with accelerator specimens after 5 hours curing triaxial test.

Figure 3.51. Shotcrete paste with accelerator specimens after 6 hours curing triaxial test.

3.8.4 Shear strength of shotcrete paste with the influences of accelerator, synthetic fibres, sand and aggregates (Shear strength of synthetic fibre reinforced concrete with accelerator)

Figures 3.52 shows the triaxial test result conducted on a shotcrete paste samples mixed with accelerator and synthetic fibres. The detailed test data are presented in Appendix – B. Tables 3.12 shows the summary of shear strength test results. Figures 3.53 and 3.54 show shear strength development of shotcrete paste with accelerator and synthetic fibres, and with only accelerator for 4 and 8 hours, respectively. Table 3.12, Figure 3.53 and 3.54 suggested that, shear strength of shotcrete paste mixed with synthetic fibres and accelerator was slightly higher than that of shotcrete paste mixed with accelerator only. The shear strength ranges from 0.5 to 17 kPa and 12 to 145 kPa between 0 to 1 hour and 1.1 to 3.25 hours, respectively.

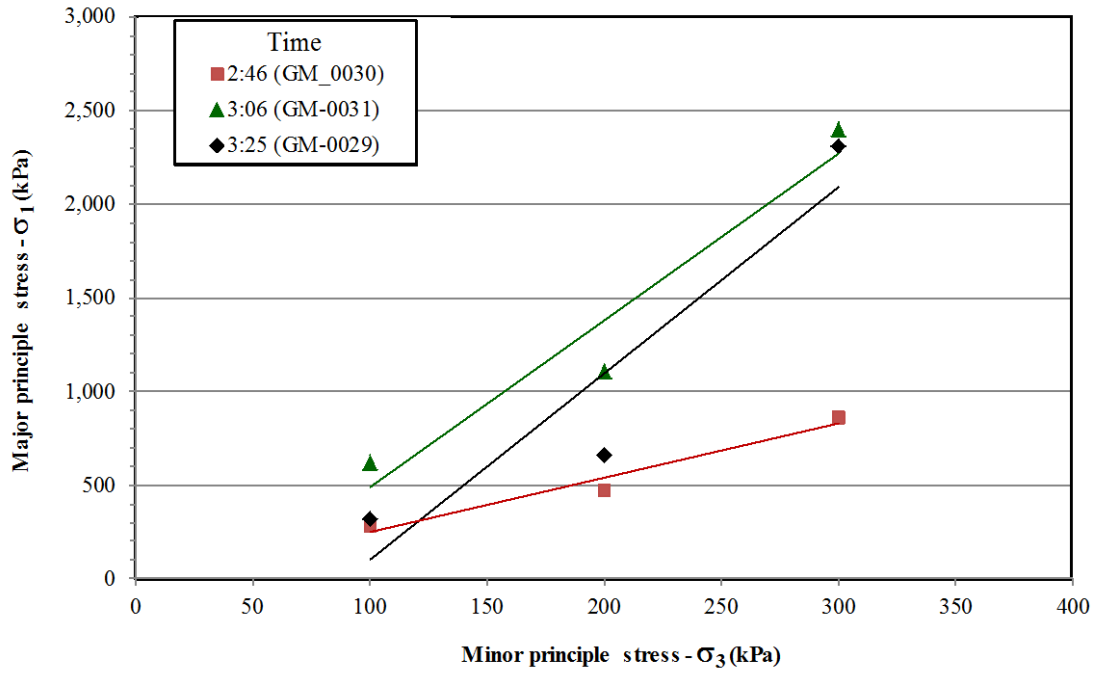

Figure 3.52. Triaxial test results for shotcrete paste batch No. GM_0029 to 0031.

Table 3.12. Shear strength of shotcrete paste with accelerator and synthetic fibres.

Curing (hr:min)	Shear strength (kPa)		
	GM_0029	GM_0030	GM_0031
0:02	-	8.58	-
0:05	-	6.72	-
0:06	-	-	3.19
0:09	14.75	-	-
0:11	-	14.96	-
0:15	17.14	7.28	-
0:16	-	-	11.91
0:20	-	0.46	-
0:30	-	-	6.03
0:40	-	14.62	-
0:45	-	-	7.55
0:50	-	8.84	-
1:00	-	15.34	13.43
1:00	-	-	15.57
1:10	-	12.18	-
1:20	-	-	17.67
2:46	-	14.00	-
3:06	-	-	67.00
3:25	145.00	-	-

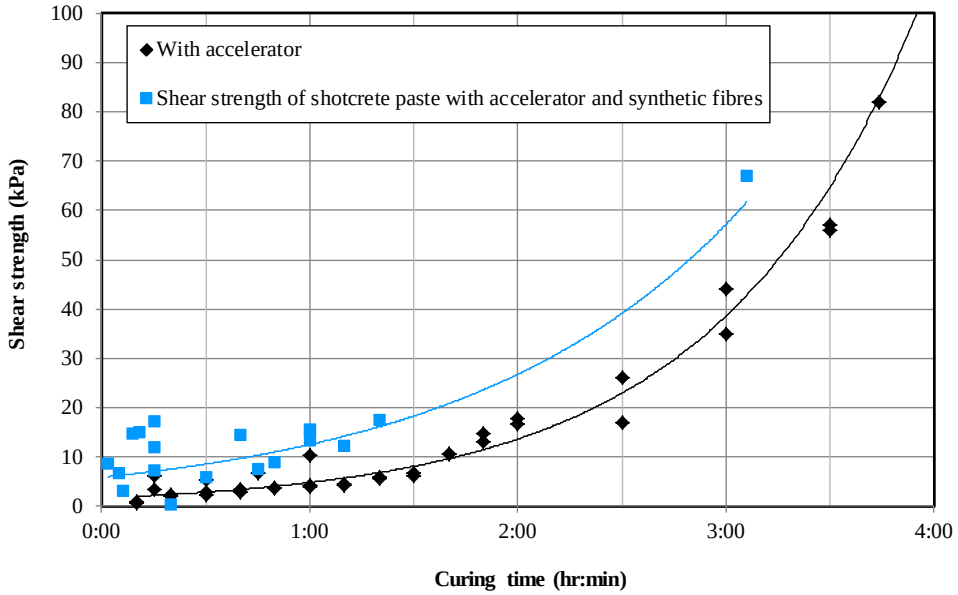

Figure 3.53. Shear strength developments of shotcrete paste, influences of accelerator and synthetic fibres during the first (4) hours of hydration.

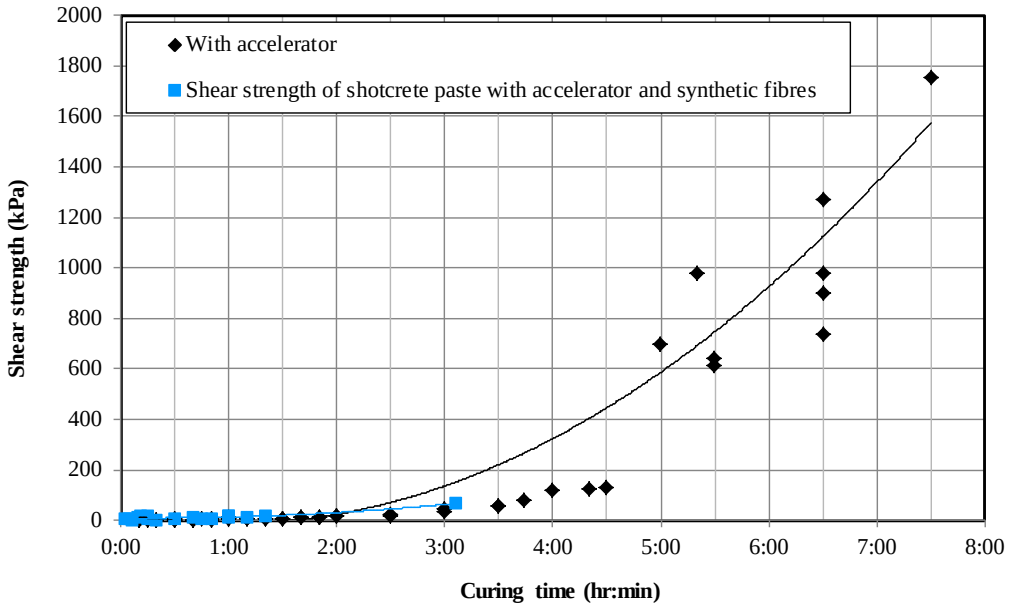

Figure 3. 54. Shear strength developments of shotcrete paste, influences of accelerator and synthetic fibres during the first (8) hours of hydration.

Figures 3.55 shows the triaxial test result conducted on the shotcrete paste samples mixed with accelerator and synthetic fibres, sand, aggregate. In other words, the mix can be called “synthetic fibre reinforced concrete with accelerator. The detailed test data are presented in Appendix – B. Tables 3.13 shows the summary of shear strength test results. Figures 3.56 and 3.57 show shear strength development of shotcrete paste with accelerator and synthetic fibres, with accelerator only and accelerator, synthetic fibres, sand and aggregate for 4 and 8 hours, respectively. Table 3.13, Figures 3.56 and 3.57 suggested that, shear strength of shotcrete paste mixed with synthetic fibres, sand, aggregates and accelerator (Synthetic fibre reinforced concrete with accelerator) was slightly higher than that of shotcrete paste mixed with synthetic fibres accelerator. It ranges from 10.6 to 13.7 kPa and 69 to 83 kPa between 0 to 20 minutes and 3.5 to 4.1 hours, respectively.

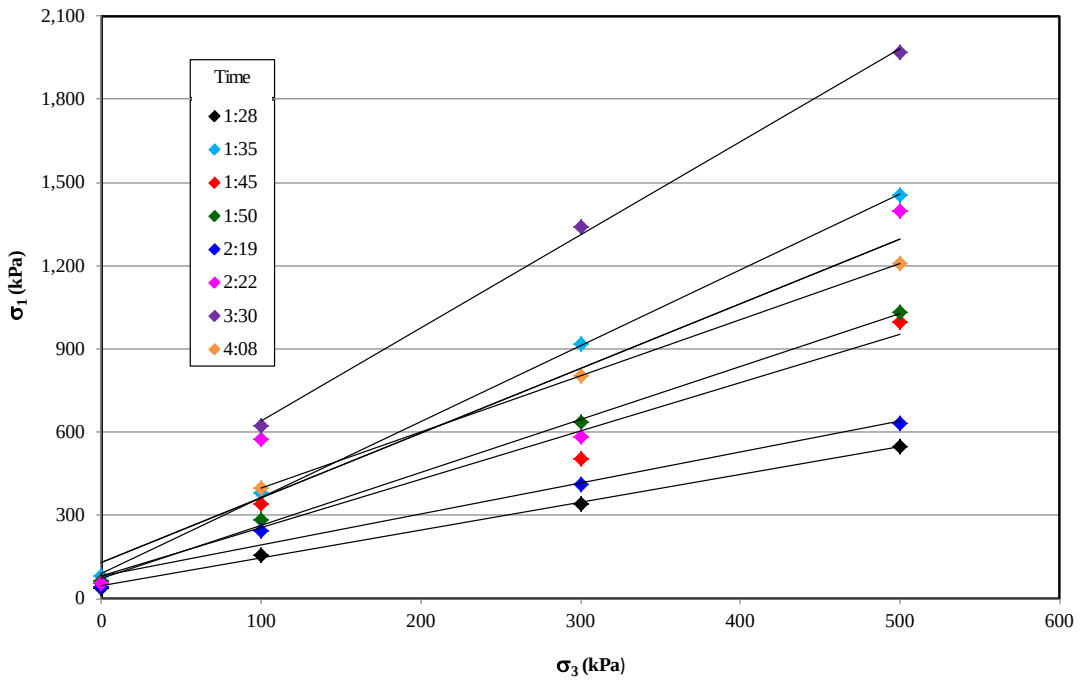

Figure 3.55. Triaxial test results for shotcrete paste batch No. GM_0034 to GM_0045.

Table 3.13. Shear strength of shotcrete paste with accelerator and synthetic fibres, sand and aggregates (Shear strength of synthetic fibre reinforced concrete with accelerator).

Curing (hr:min)	Shear strength (kPa)							
	GM_0034	GM_0038	GM_0039	GM_0041	GM_0042	GM_0043	GM_0044	GM_0045
0:02	10.60	-	-	-	-	-	-	-
0:20	13.70	-	-	-	-	-	-	-
1:19	-	-	-	-	-	-	39	-
1:22	-	-	-	-	-	-	-	43
1:25	-	-	-	-	31	-	-	-
1:28			-			23	-	-
1:50	-	-	-	27.00	-	-	-	-
2:04	-	-	28.00	-	-	-	-	-
3:30	-	83.00	-	-	-	-	-	-
4:08	69.00	-	-	-	-	-	-	-

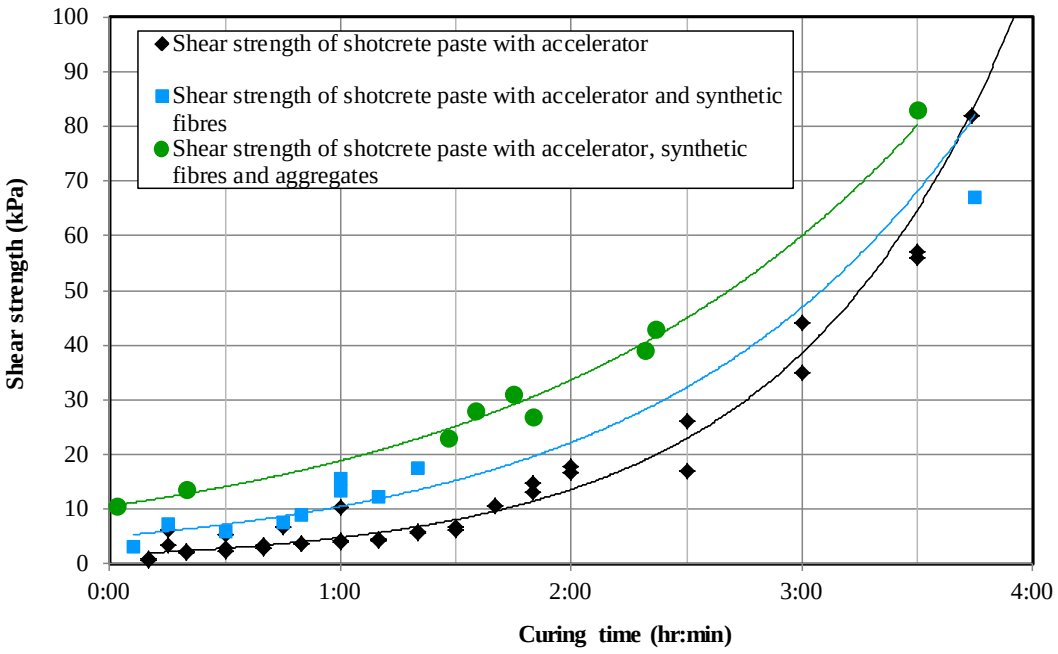

Figure 3.56. Shear strength developments of shotcrete paste. Influences of accelerator and synthetic fibres, sand and aggregates (Synthetic fibre reinforced concrete with accelerator) during the first (4) hours of hydration.

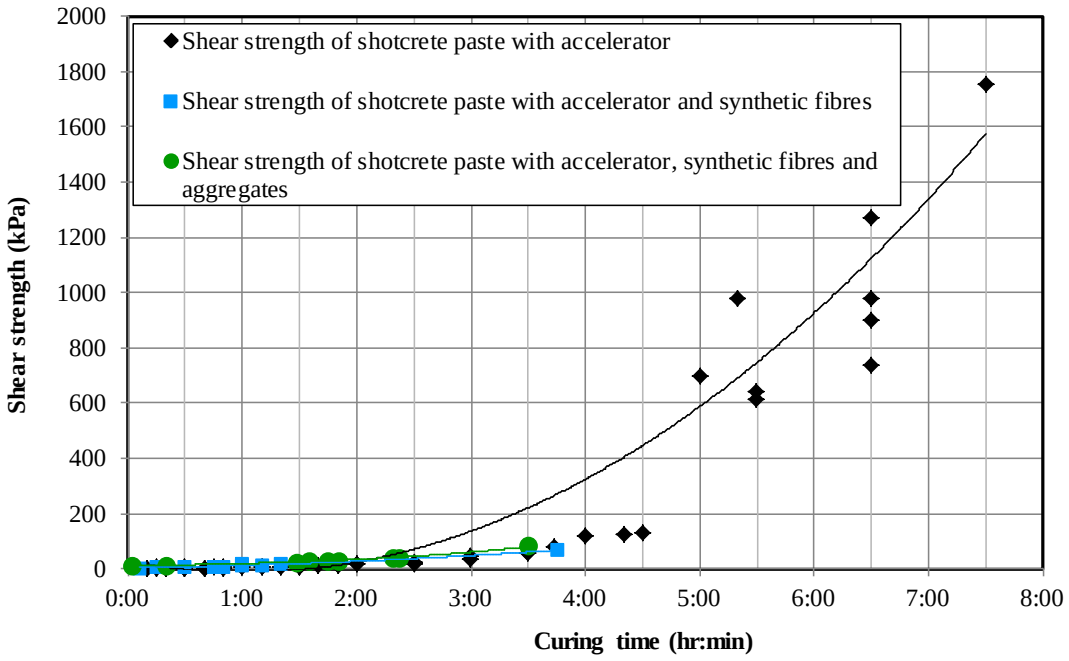

Figure 3.57. Shear strength developments of shotcrete paste. Influences of accelerator and synthetic fibres, sand and aggregates (Synthetic fibre reinforced concrete with accelerator) during the first (8) hours of hydration.

3.9 Influence of synthetic fibre in early age shotcrete paste

A pull-out shear strength test was conducted to investigate the effect of synthetic fibre in early age shotcrete paste. Table 3.14 shows the mechanical properties of Shogun Barchip synthetic fibre used for pull-out shear strength test.

Table 3.14. Mechanical properties of synthetic fibre (Shogun Barchip).

Length (mm)	Width (mm)	Thickness (mm)	Tensile strength (MPa)	Axial force capacity (N)	Bond strength required to break the fibre with 24 mm embedment (MPa)
48	0.65	1.22	550	436.15	22.92

The testing procedure was,

- A “C” shape steel pile with 50 mm diameter was cut into half to simulate a crack, Figure 3.58 a.

- A layer of shotcrete paste was casted inside a steel pipe and a single synthetic fibre was installed as shown in Figure 3.58 b. The midpoint of a fibre was placed at the point of a simulated crack.

- Another layer of shotcrete paste was casted to cover the fibre, Figure 3.58 c.

- A pull-out shear strength test was conducted using Avery Universal testing machine, Figure 3.59.

Figure 3.60 shows a completely pulled-out (24 mm) fibre after pull-out shear strength test.

(a)

(b)

(c)

Figure 3.58. Installation of fibre for pull-out shear test.

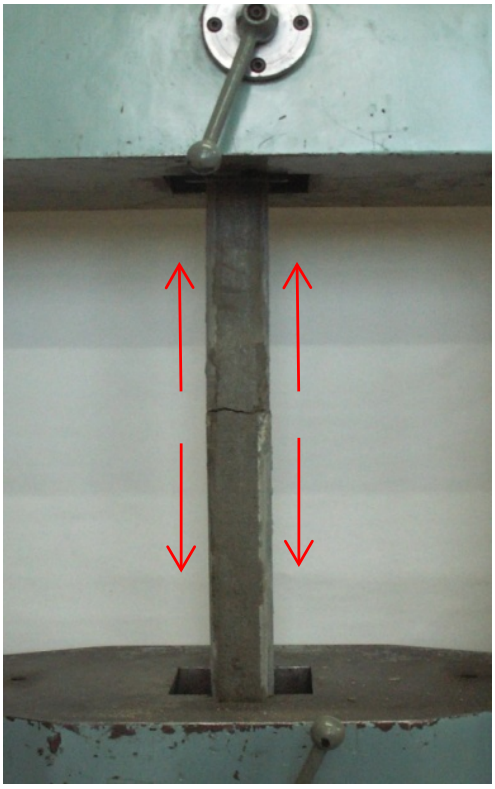

Figure 3.59. Pull-out shear strength test with Avery universal testing machine.

Figure 3.60. Fibre pull-out after test.

A summary of pull-out shear strength test results in presented in Table 3.15 shows that the pull-out shear strength of shotcrete paste at age 3 to 4 hours and 6.5 to 8 hours ranges from 0.3 to 0.6 MPa and 0.9 MPa, respectively.

Since, a minimum bond strength required to break a synthetic fibre is 23 MPa in shotcrete matrix, the load transfer of fibre is insignificant in the early age strength of shotcrete. Therefore early age strength of shotcrete is mainly controlled by the shear strength of shotcrete matrix only, not the strength of the fibres.

Table 3.15. Pull-out shear strength test result.

Curing time (hours:minute)	**Embedment length (mm)**	**Width (mm)**	**Thickness (mm)**	**Pull-out load (N)**	**Pull-out shear strength (MPa)**
3:30	24	0.65	1.22	23	0.3
4:30	24	0.65	1.22	50	0.6
6:30	24	0.65	1.22	80	0.9
8:00	24	0.65	1.22	80	0.9

3.10 Conclusions and discussions

The mechanical and physical properties of shotcrete at early age are mainly those associated with the cementitious matrix. Consequently, the research results from this chapter were mainly focused on testing a shotcrete paste comprising the cementitious matrix and the influences of chemical additives, synthetic fibres and aggregates.

The test programs for this research consisted of 3 stages, such as, stage 1, stage 2 and stage 3. Stage 1 experiments were conducted as an initial study to identify the requirements and to set up the frame work of the research in order to complete the objectives as described in Chapter 1, Section 1.2. During the research stage 1, the mechanical properties of shotcrete paste, such as, UCS and shear strength tests were conducted using the WASM 50 ton Avery 50 universal test machine and the Haake VT550 rheorometer, respectively. The physical properties of shotcrete paste, such as heat of hydration (temperature) and electrical resistance were measured with IntelliRock II™ temperature measurement system and electrical multimeter, respectively. The research stage 2 was conducted based on the research out come from stage 1. In the research stage 2, the shear strength was conducted with a Haake VT550 rheorometer and a Wykeham Farrance traixial test system (WF4010). The electrical resistance was measured with a new device (Prototype v1 which will be described in Chapter 4) developed in this research. In the research stage 3, the method for determination of shear strength was the same as for research stage 2. The electrical resistance was measured with different versions of newly developed prototype.

The stage 1 initial experiments suggested that, the minimum shear strength of shotcrete paste with w/c ratio 0.44 is 33 Pa. After 3 hours curing the paste become very stiff and the yield stress cannot be measured with the VT550 viscomenter. At 4 hours curing the paste becomes hardened and the UCS is 0.87 MPa. The estimate for minimum shear strength of the paste is 33 Pa and the maximum is about 0.44 MPa (at 4 hours without accelerator).

The correlation of temperature development in underground shotcrete wall and calculated degree of hydration with curing time did not provide a good indication of re-entry time.

Research stages 2 and 3 suggested that, the shear strength is influenced by different chemical admixtures, synthetic fibres and aggregates. Generally, the shear strength increased exponentially during the first 4 and 8 hours of curing in all shotcrete paste mixes except for the shotcrete paste mixed with a hydration stabiliser. The shear strength of shotcrete paste mixed with accelerator was significantly higher than that of shotcrete paste mixed without chemical admixture. The shear strength of shotcrete paste mixed with water reducing admixture was slightly lower than that of shotcrete paste mixed without chemical admixture. The shear strength of shotcrete paste mixed with superplasticer was significantly lower than that of shotcrete paste mixed without chemical admixture. The shear strength of shotcrete paste mixed with hydration stabiliser was extremely lower than that of shotcrete paste mixed without chemical admixture.

The typical stress and strain curves suggested that, at 3 hour curing, the specimens failed in shear and compression mode and continue to deform axially with increasing stress or strain hardening behaviour. At 4 and 5 hours curing, the specimens failed in shear and compression at low confinement (100 kPa) and in shear mode at higher confinement (200 & 300 kPa). After failure the specimens continue to deform with almost constant stress or yielding behaviour. At 6 hours curing, the specimens failed in shear and brittle mode. After failure, the specimens continue to deform with shearing and dilation.

Shear strength of shotcrete paste mixed with accelerator and synthetic fibres was slightly higher than that of shotcrete paste mixed with only accelerator. Similarly, shear strength of shotcrete paste mixed with accelerator, synthetic fibre and aggregates was slightly higher than that of shotcrete paste mixed with accelerator and synthetic fibres.

A summary of pull-out shear strength test results in presented in Table 3.15 shows that the pull-out shear strength of shotcrete paste at age 3 to 4 hours and 6.5 to 8 hours ranges from 0.3 to 0.6 MPa and 0.9 MPa, respectively.

A minimum bond strength required to break a synthetic fibre is 23 MPa in shotcrete matrix. A pull-out shear strength test results suggested that, the load transfer of fibre is insignificant in the early age strength of shotcrete. Therefore early age strength of shotcrete is mainly control by the shear strength of shotcrete matrix only, not the strength of the fibres.

CHAPTER 4

DEVELOPMENT OF EARLY AGE STRENGTH EVALUATION APPARATUS

4.1 Introduction

One of the objectives of this research is to determine approximately, by some form of simple, robust, unambiguous field test when re-entry conditions of the shotcrete have been met in situ. Based on compressive literature review described in Chapter 2, and results from the initial research stage 1 (Chapter 3, 3.8), it was concluded the electrical method is the best method to correlated with the physical and mechanical properties of cement-based materials.

The apparatus to measure the in-situ electrical resistance of shotcrete was developed in this research. The prototypes probes were experimented in the laboratory for different mixes, sample geometry, voltage input, electrodes, electrodes layout and geometry, and penetration depth before being tested in the field for in situ shotcrete use in underground mine.

4.1.1 Four electrodes linear array – electrical resistors in series

The experiment started with four electrodes linear array. Electrically, the materials between the electrodes are considered as resistors and they are in a series circuit. A layout and electrical circuit of resistance measurement with 4 electrodes- linear array is shown in Figures 4.1 and 4.2, respectively. The shotcrete mix designs were as presented in Table 3.1. During electrical resistance measurement, all the samples were cured in a temperature and humidity control chamber, which was set up at 30 °C and 90 % humidity to simulate the typical underground mining conditions in Western Australia.

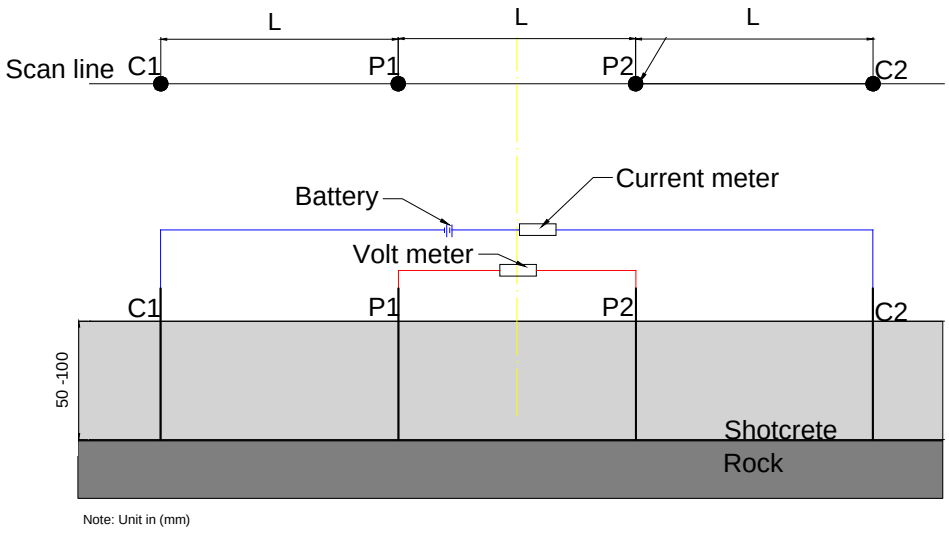

Figure 4.1. Layout of resistance measurement with 4 electrodes- linear array.

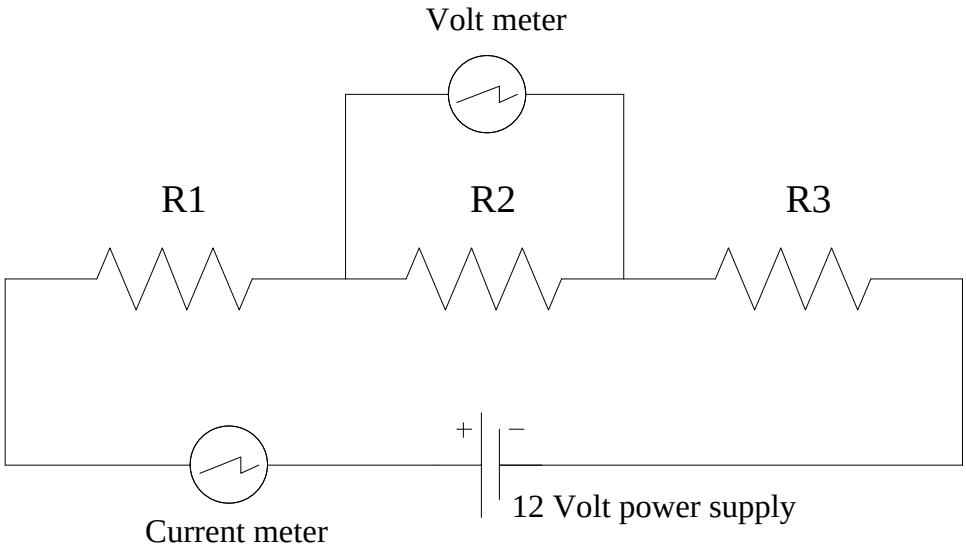

Figure 4.2. Electrical circuit of 4 electrodes- linear array.

Figure 4.3 shows the electrical resistance of cement paste without accelerator casted in different mould dimensions and conditions. Generally, the electrical resistance of cement paste without accelerator gradually increased with curing time and the range of resistance decreased with the larger sample size. From (0) to (8) hours curing time, the electrical resistance of cement paste without accelerator casted in (39 x 222 x 32) mm (width x length x height) plastic box, (100 x 400 x 100) mm wooden box

and (350 width x 400 length x 100 height) mm wooden box with rock (granite/sandstone) base ranged from 60 to 160, 20 to 55 and 7 to 30 Ohm, respectively. A wooden box with a rock base was used to simulate the actual curing condition in an underground place, where the shotcrete is sprayed onto a rock wall.

Figure 4.4 shows a comparison of electrical resistance of cement paste mix with and without accelerator. The electrical resistance of cement paste without accelerator casted in a wooden box with a granite base gradually increased after mixing until 4 hours of curing and does not change significantly from 4 to 5 hours curing. The electrical resistance significantly increased after 5 hours curing. The electrical resistance of cement paste with accelerator casted in a wooden box with a granite base gradually decreased after mixing until 1 hours of curing and does not change significantly from 1 to 2 hours curing. The electrical resistance significantly increased after 3 hours curing. The electrical resistance of cement paste with and without accelerator casted in a wooden box with a sandstone base showed a similar trend with that of casted in a wooden box with a granite base but with more scatter data. The scatter data was due to the porous nature of the sandstone, which absorbs water from the cement paste mix during hydration process. Similarly, Figure 4.5 shows the trends of electrical resistance for cement-sand mortar mix with and without accelerator. The range of electrical resistance increased in cement-sand mortar due to the lesser conductivity of sand in the mortar.

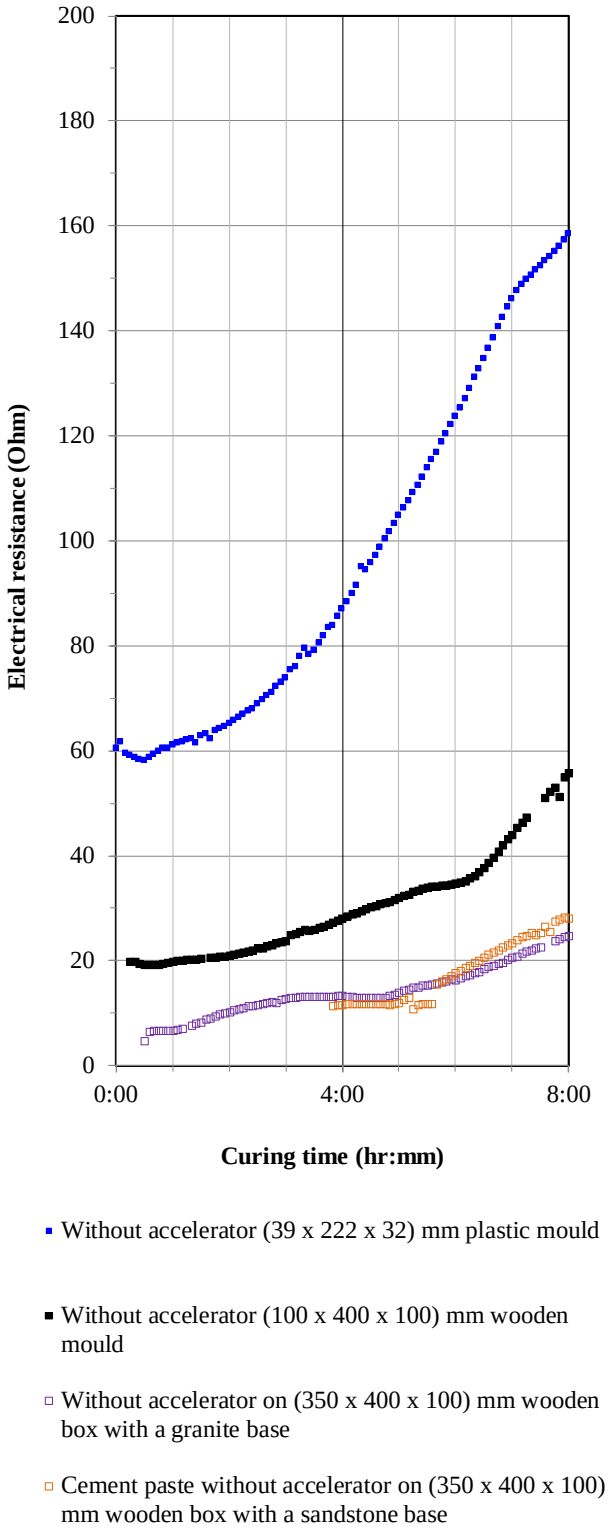

Figure 4.3. Electrical resistance cement paste without accelerator measured with 4 electrodes – linear array.

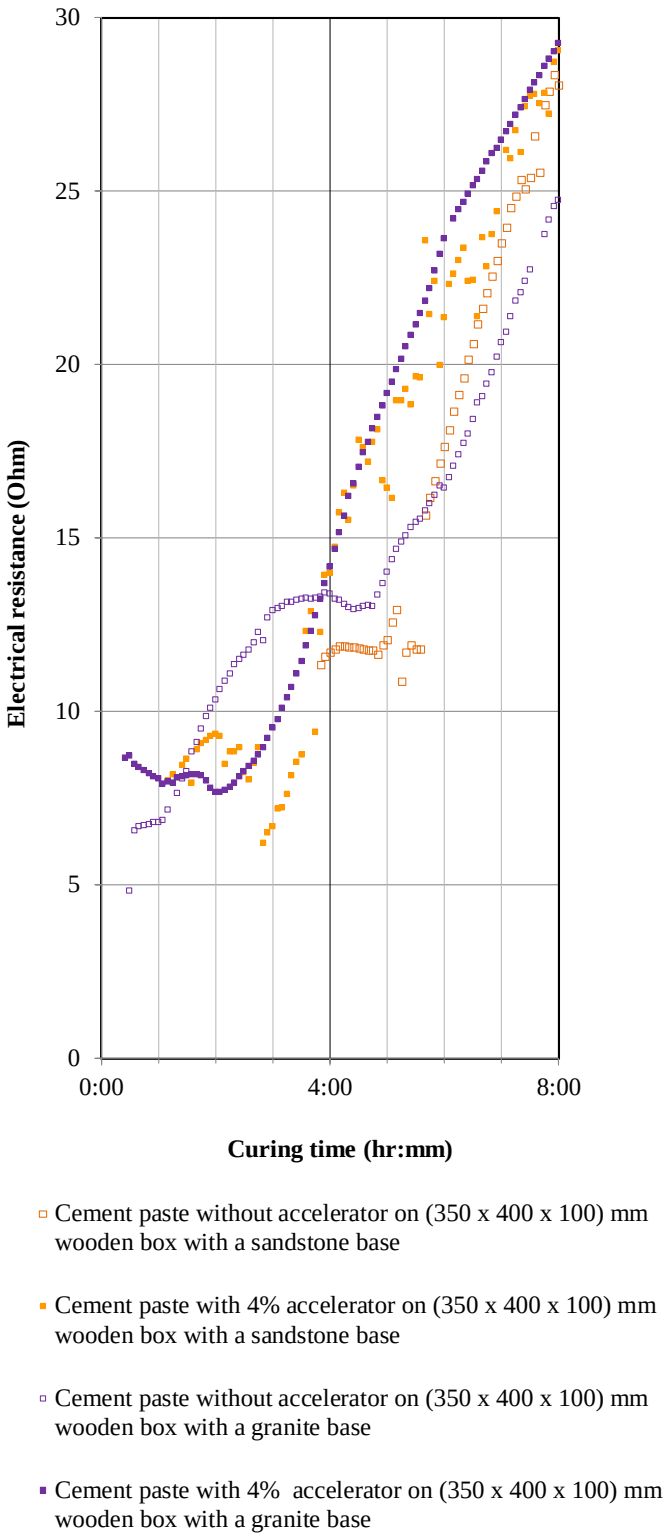

Figure 4.4. Electrical resistance cement paste with and without accelerator measured with 4 electrodes – linear array.

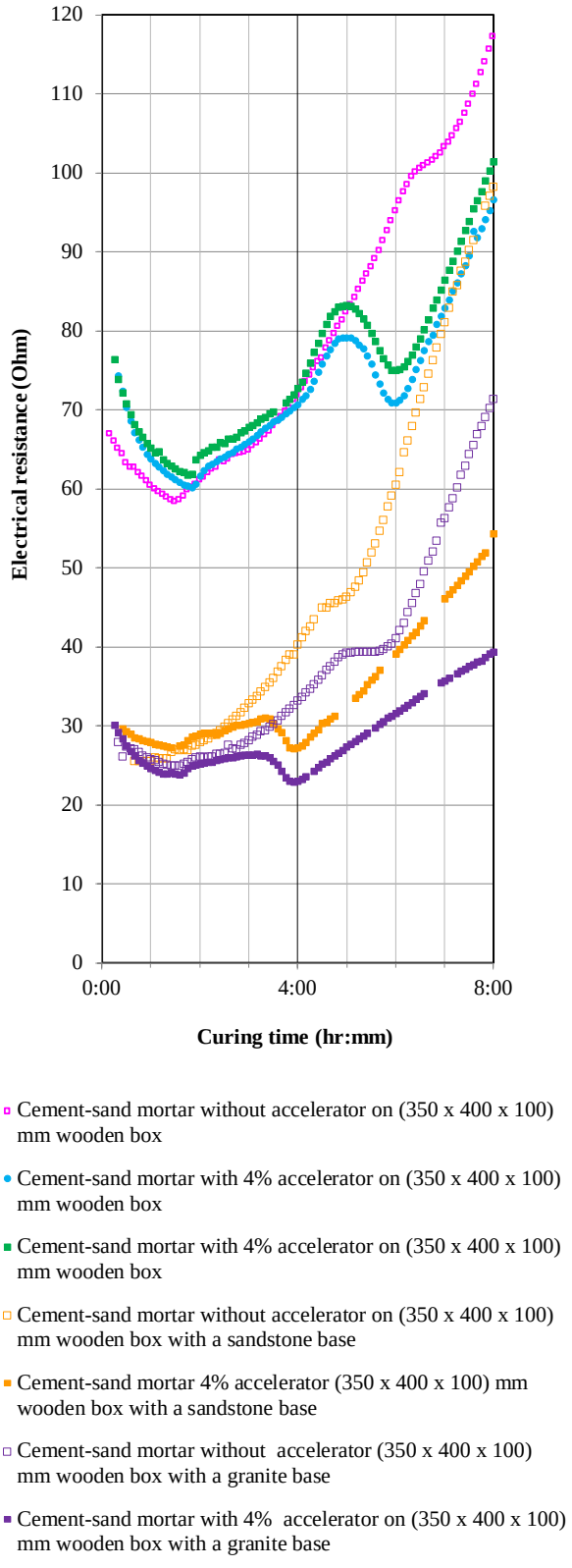

Figure 4.5. Electrical resistance cement-sand mortar with and without accelerator.

The conclusions based on the results from the stage 1 experiments with four electrodes linear array using different mould sizes and designs are:

- All the results shown in Figures 4.3 to 4.5 suggest that, the electrical resistance development with time has a unit profile of “Decrease – Increase – Decrease – Continuously Increase” through the curing time.

- The chemical reactions and hydration process, such as pre-inducting, induction, acceleratory and post-acceleratory process highly influenced the electrical resistance throughout the curing time. Therefore, measurement of electrical resistance development with time can identify the exact time when a change in the hydration process occurs.

- The electrical resistance ranges from about 10 to 120 Ohm within 8 hours of curing time. The rate and magnitude of electrical resistance with time were different with the mix design and sample size and mould type used.

- The electrical resistance of shotcrete paste with accelerator is about 20 % lower than that of shotcrete paste without accelerator between 1 to 4 hours curing time.

- The electrical resistance of sand-cement mortar is about 24 % to 68 % higher than that of shotcrete paste.

- Comparing the results shown in Figure 4.3 and 4.5, the larger the samples size, the lower the electrical resistance that was measured for the shotcrete paste with or without chemical accelerator.

- The electrical resistance development with time for shotcrete paste casted in a wooden mould with a sandstone base showed more scatter than that of shotcrete paste casted in a wooden mould having a granite base.

After conducting the experiments with different samples size and mould, it was decided to use (350 x 400 x 400 x 100) mm wooden mould with a granite base throughout this research.

4.1.2 Four electrodes circular array – electrical resistors in parallel

A new electrical resistance measurement probe with four electrodes in circular array was invented during research stage 2 to improve the resolution and accuracy of the resistance measurement. Figure 4.6 shows a prototype electrical resistance probe (v1) invented during the research stage 2. Figure 4.7 shows the electronic circuit of electrical resistance measurement probe and data logging unit. In the circular array the materials which considered the resistors are in a parallel circuit as show in Figure 4.7. The invention of electrical resistance probe was patented in Australia as well as internationally. The details patent document is presented in Appendix - C.

Figure 4.8 and 4.9 shows electrical resistance measurement probe and data logging unit in the laboratory. Generally, the electric current and voltage were measured and recorded continuously every 30 seconds for 8 to 24 hours curing time using a Datatataker DT80 data logger. The electrical resistance was calculated according to Ohm's law.

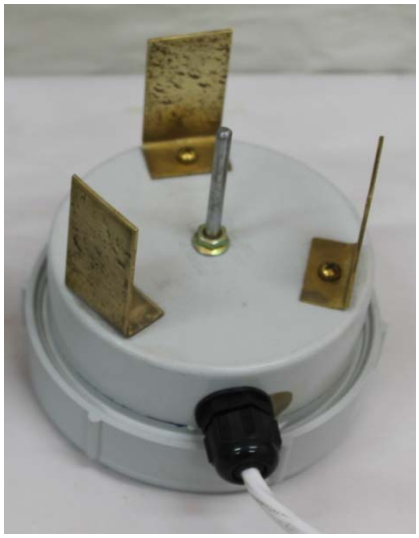

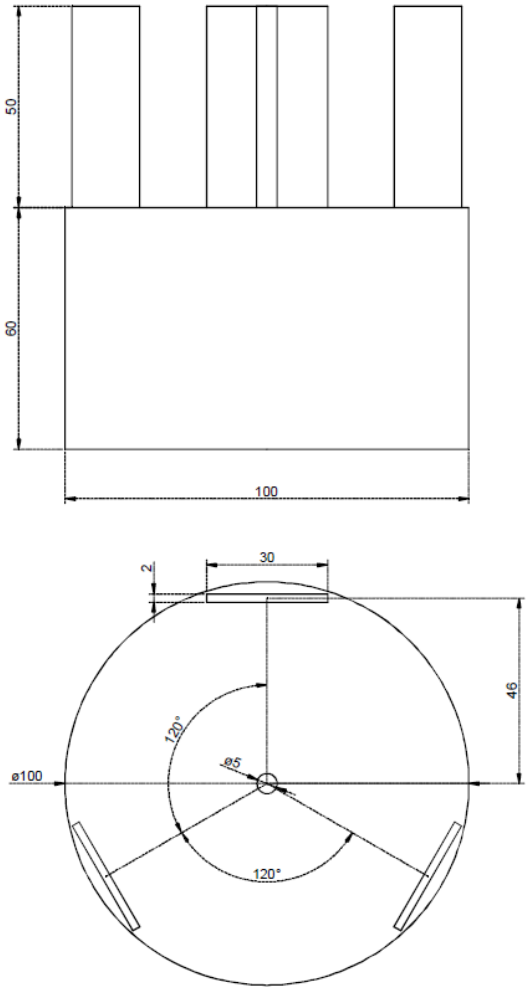

Prototype – V1
Negative electrodes made from 2 mm thick brass sheet
Positive electrode made from steel bolt
Housing made from PVC pipe
All fasteners are brass
Wire connected to terminals using brass coupling

Figure 4.6. The electrical resistance measurement probe prototype - V1 .

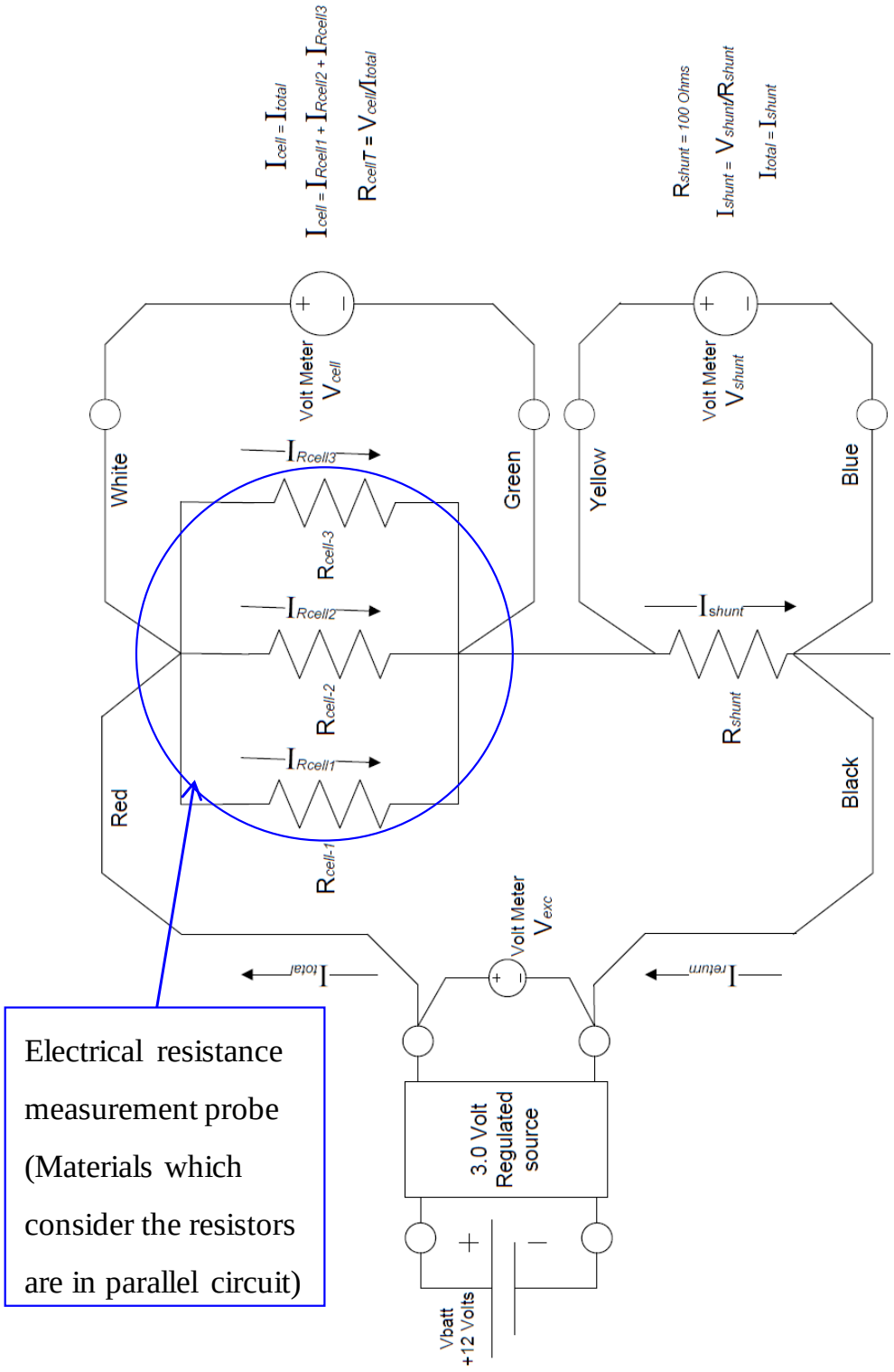

Figure 4.7. The electronic circuit for the new resistance measurement probe and data logging unit.

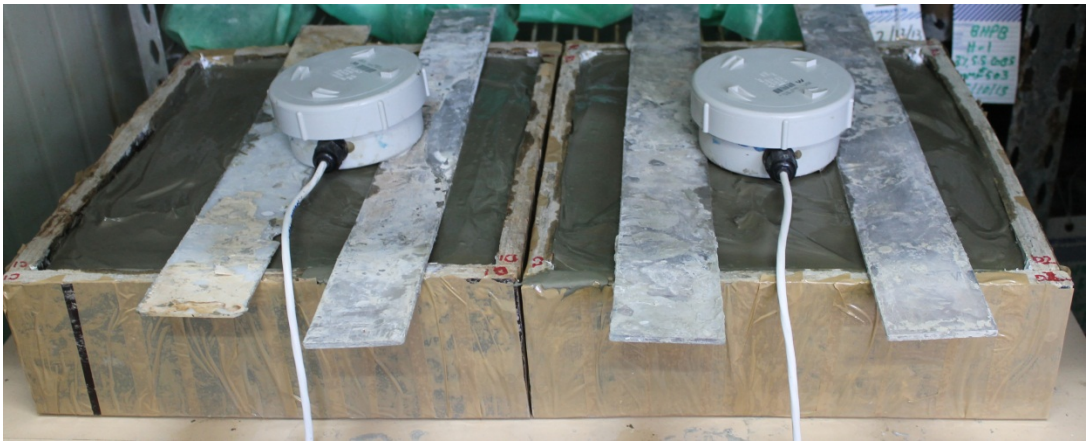

Figure 4.8. The electrical resistance measurement probe installed in a shotcrete paste sample.

Figure 4.9. The electrical resistance measurement system in the laboratory set-up.

4.2 Influences of chemical admixture, synthetic fibres and aggregate on shotcrete paste on electrical resistance measured probe with version V1 during Research Stage 2

4.2.1 Electrical resistance of shotcrete paste without chemical admixture

The electrical resistances of cement paste without accelerator measured with four electrodes - circular array are presented in Figure 4.10. It shows up to 8 hours of curing. The initial resistance, at about 10 minutes after mixing is about 80 Ohm. This initial time is also known as pre-induction period as described in Chapter 2, Figure 2.1. After 10 to 30 minutes, the resistance gradually increases from 200 to 300 Ohm until 2 to 3 hours curing, which indicates the induction period with slow chemical reaction taking place between the cement particles and water. After 2 to 3 hours curing, the resistance starts to decrease significantly, which indicates the end of the induction period and the start of a second stage reaction. At the start of second stage, the main reaction begins rapidly and transformed some part of mixing the water into a chemical solution with highly concentrated Calcium Hydroxide (CH). Figure 4.11 shows the electrical resistance development up to 24 hours curing. After 4 to 5:30 hours curing, the resistance starts to increase continuously. The continuous increase in resistance is an indication of the formation of hydration products that reduce the amount of free water available for conduction. The period is also known as acceleratory period where precipitation of Calcium Hydroxide (CH) and Calcium silicate hydrated (CSH) occurs.

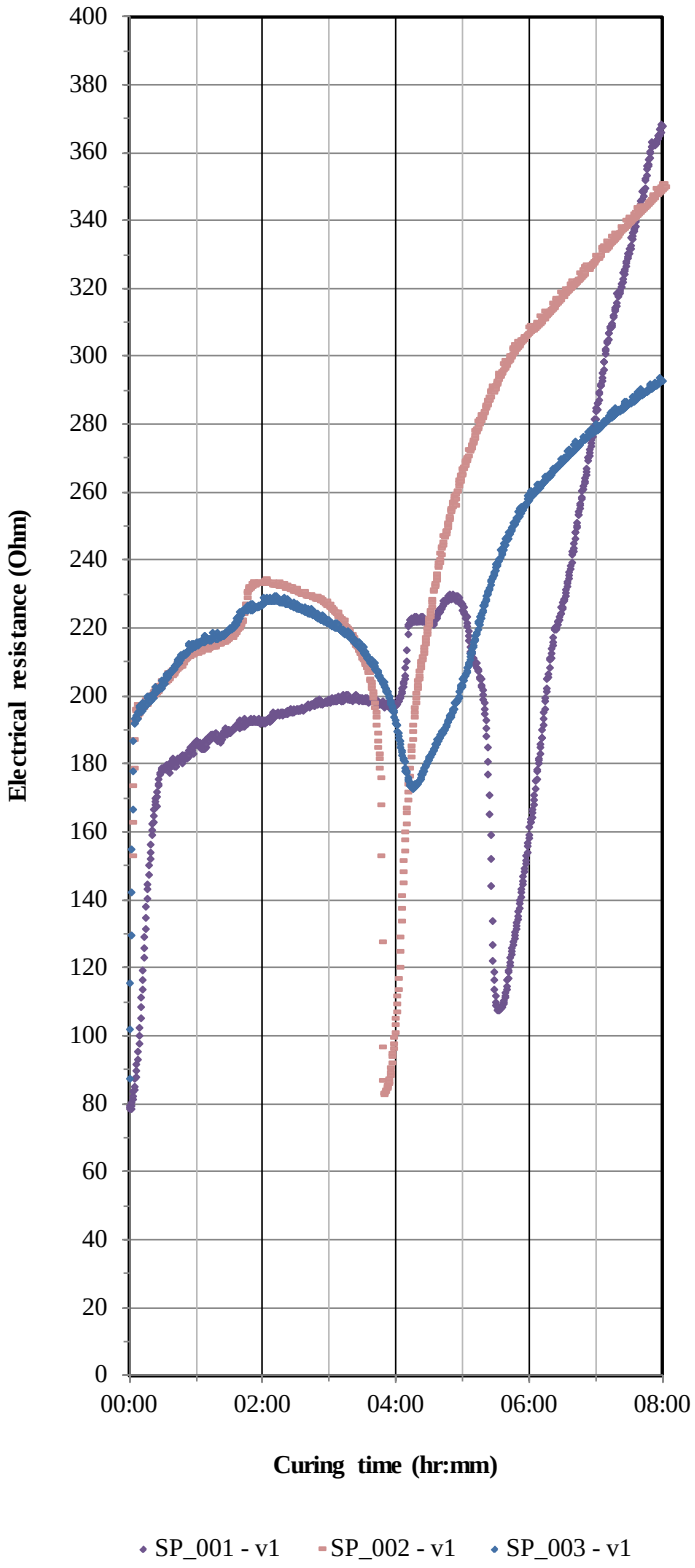

Figure 4.10. Electrical resistance development with time in cement paste without chemical admixture (8 hours).

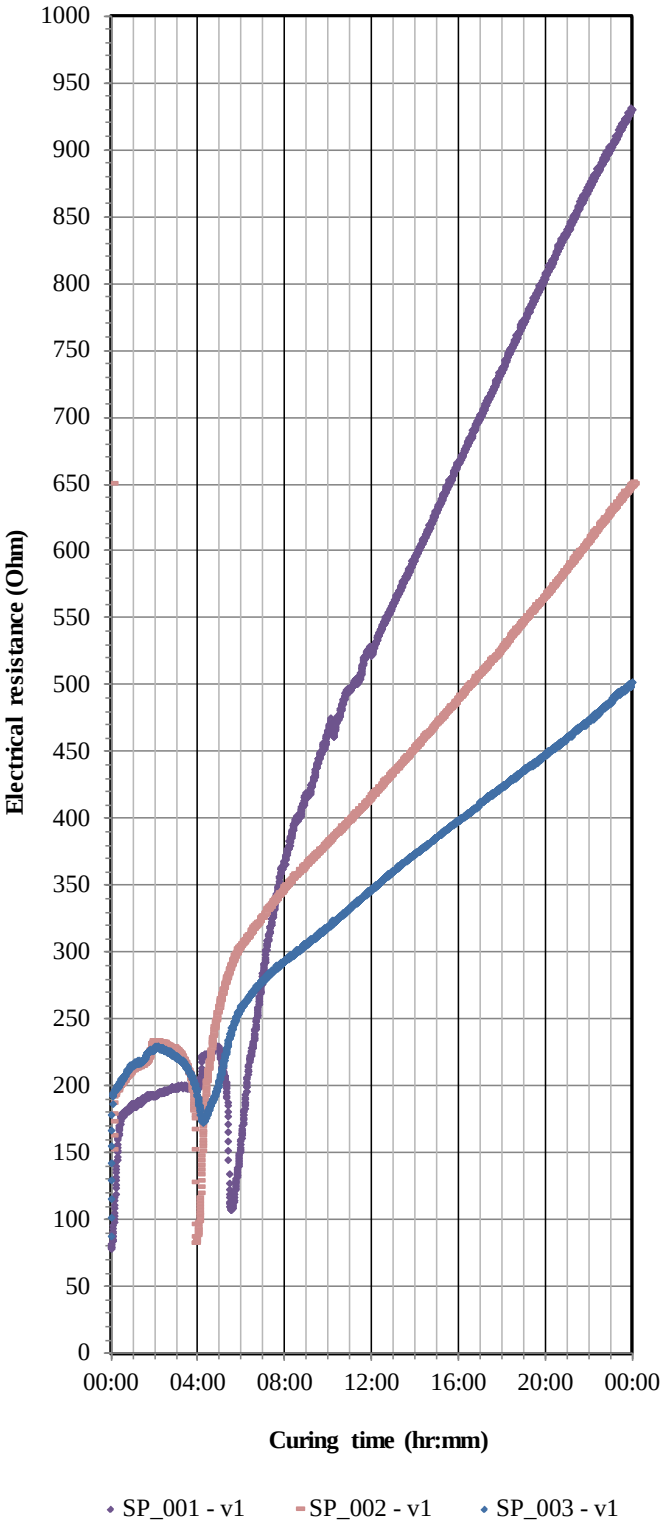

Figure 4.11. Electrical resistance development with time in cement paste without accelerator (24 hours).

4.2.2 Electrical resistance of shotcrete paste with accelerator

The electrical resistance of cement paste with accelerator measured with four electrodes - circular array is presented in Figure 4.12. It shows up to 8 hours of curing. Additions of accelerator significantly change the course of the chemical reactions and affect the profile of electrical resistance development with time. The pre-induction and induction period take places very quickly during the first 10 minutes of following mixing time. The resistance at about 10 minutes after mixing ranges from 60 to 90 Ohm. It slightly decreases until about 30 minutes and does not change significantly until 1.5 hours to 2.5 hours of curing. During this period the resistance ranges from 55 – 65 Ohm. This low and moderately constant resistance indicates the high ionic concentrations (such as, Na^+, K^+, Ca^{2+}, SO_4^{2-} and OH^-, etc.) in the mix, which reduce the mobility of electrical charges. After 2 to 3 hours curing, the first acceleratory period begins and the resistance starts to increase sharply. It shows the accelerated reactions of C_3S with the formation of hydration products. The accelerated reactions continue up to 4 to 5 hours of curing. According to Burge (2001), Aluminium Sulphate in the "Accelerator" reacts with calcium hydroxide ($Ca(OH)_2$), which is one part of hydration products and produce additional ettringite and aluminium hydroxide. This fills the capillary pores within 4 hours of hydration. Figure 4.13 shows the same graphs but up to 24 hours curing time. The graphs show that after 4 to 5 hours the electrical resistance gradually decreased again until about 5 to 8 hours of curing. This indicates another stage of chemical reactions which requires more detailed studies (chemical and electron microscopy but not undertaken as part of this research). After 5 to 8 hours of curing the electrical resistance continuous increased with the formations of more hydration products and increasing strength.

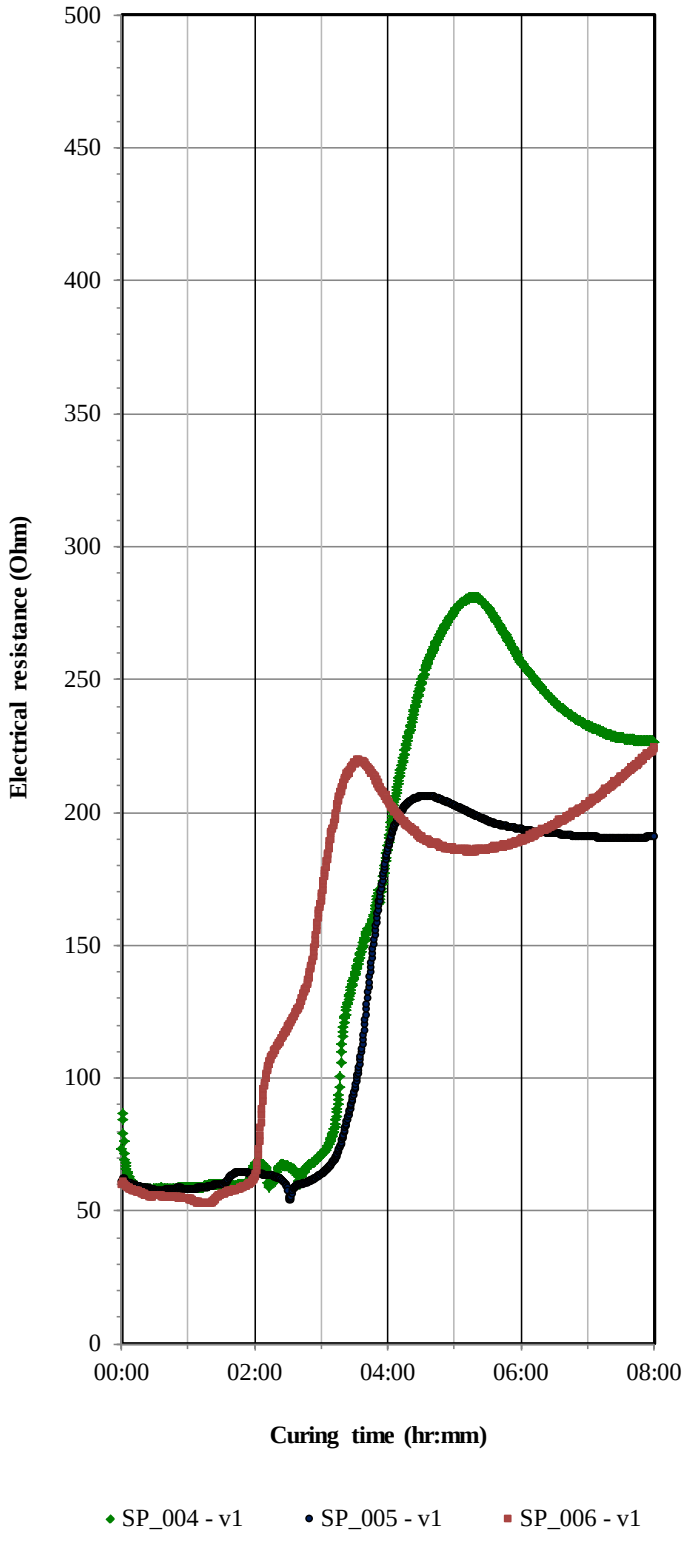

Figure 4.12. Electrical resistance development with time in cement paste with accelerator (8 hours).

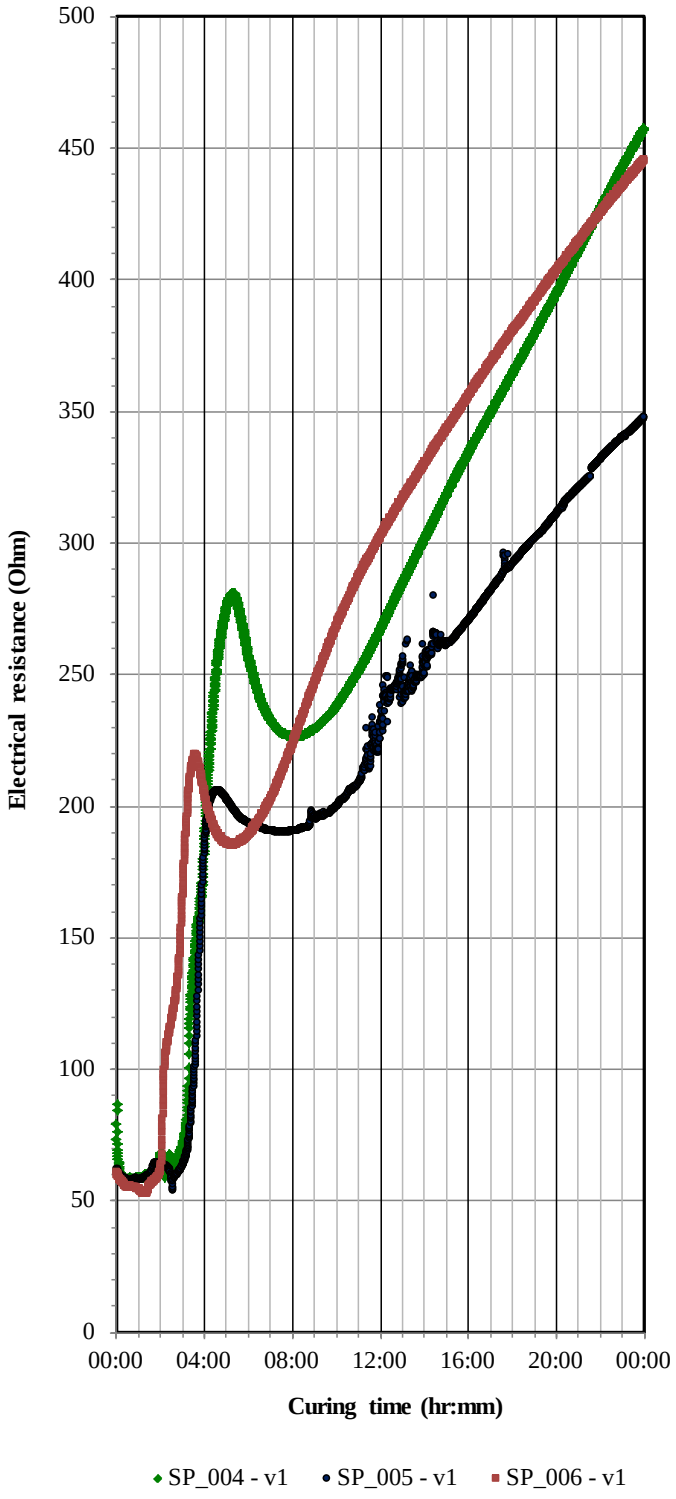

Figure 4.13. Electrical resistance development with time in cement paste with accelerator (24 hours).

4.2.3 Electrical resistance of shotcrete paste with superplasticiser

The electrical resistances of cement paste with superplasticiser measured with four electrodes - circular array are presented in Figure 4.14. It shows up to 8 hours of curing. The initial resistance is about 200 to 230 Ohm at about 10 minutes after mixing which indicate a pre-induction period as described in Chapter 2, Figure 2.1. After 10 to minutes, the resistance remains almost the same until 4.5 hours curing, which indicates that an induction period with slow chemical reaction take places between cement particles and water. After 4.5 hours curing, the resistance starts to decrease significantly, which indicates the end of the induction period and the start of a second stage reactions similar to the cement paste mixed without chemical additive. Figure 4.15 shows electrical resistance development up to 24 hours curing. After about 7 hours curing, the resistance starts to increase continuously. The continuous increase in resistance is an indication of the formation of hydration products that reduce the amount of free water available for conduction.

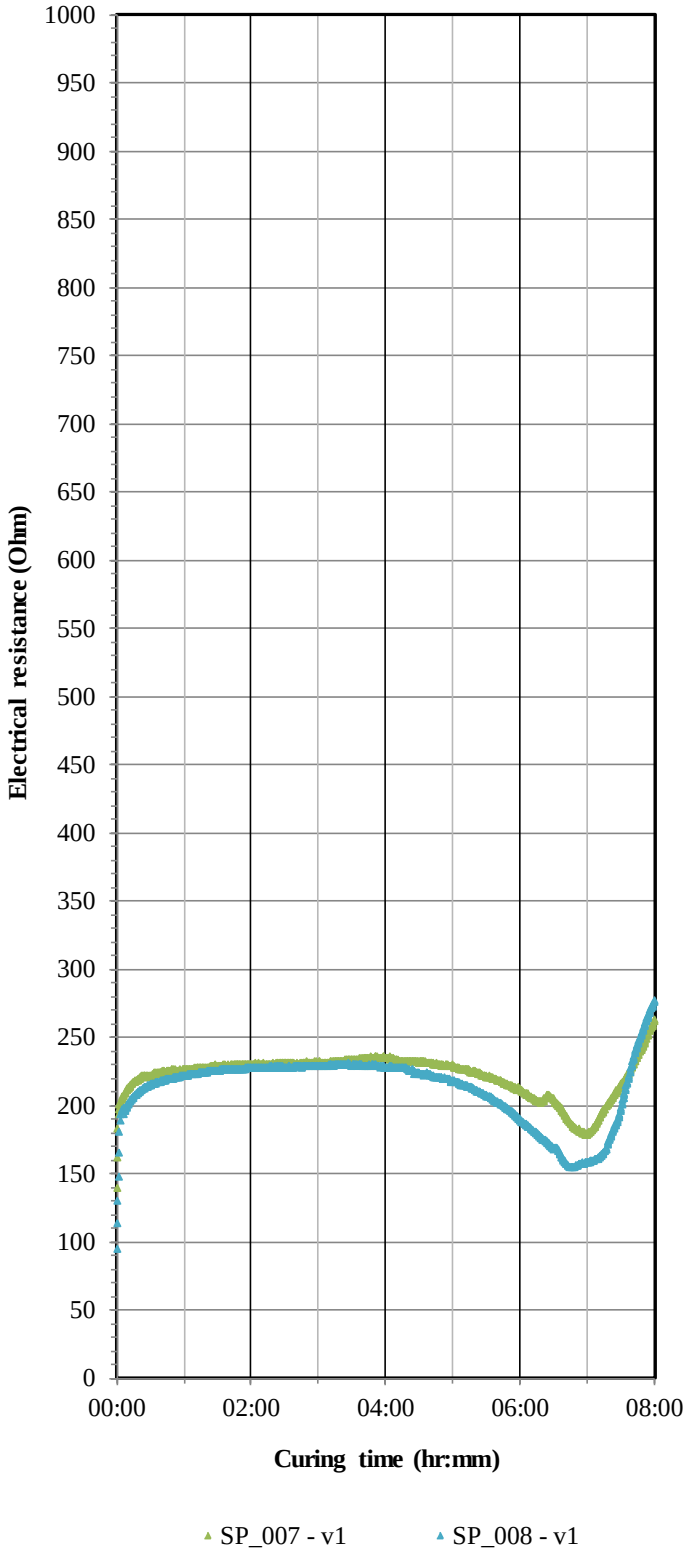

Figure 4.14. Electrical resistance developments with time in cement paste with Superplasticiser (8 hours).

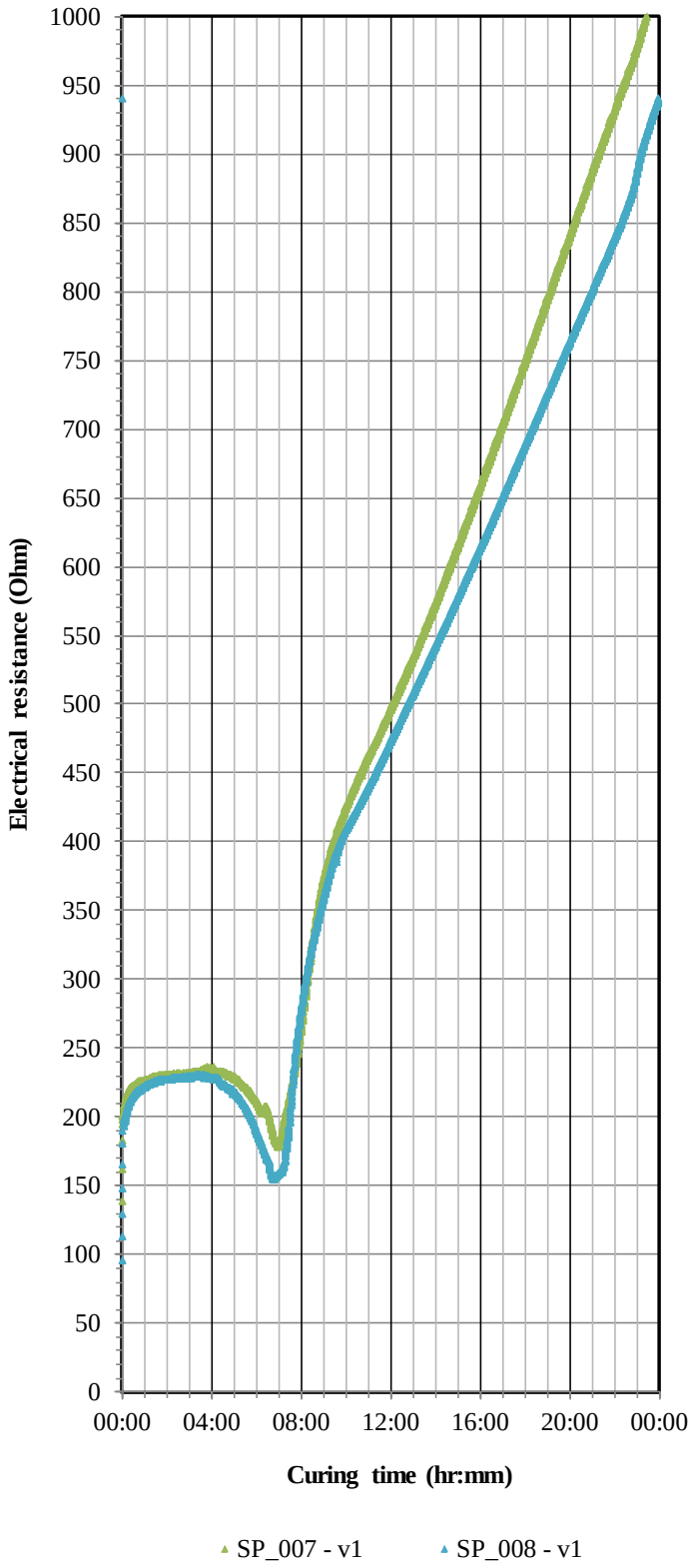

Figure 4.15. Electrical resistance developments with time in cement paste with Superplasticiser (24 hours).

4.2.4 Electrical resistance of shotcrete paste with water reducing admixture

The electrical resistance of cement paste with water reducing admixture measured with four electrodes - circular array is presented in Figure 4.16. It shows up to 8 hours of curing. The initial resistance is about 200 Ohm and gradually increases to about 240 Ohm until 2 hours curing, which indicate a longer pre-induction period than cement paste mixed without chemical admixture. After 2 hours the resistance remains almost the same until 4.5 to 5.5 hours curing and slightly variant between 4.5 to 5.5 and 7 hours curing with resistance ranges from 240 and 260 Ohm. This also indicates a longer induction period with a slow chemical reaction. The second stage reactions start at about 7 hours curing. Figure 4.17 shows electrical resistance development up to 24 hours curing. After about 7 hours curing, the resistance starts to increase continuously due to the formation of hydration products that reduces the amount of free water available for conduction.

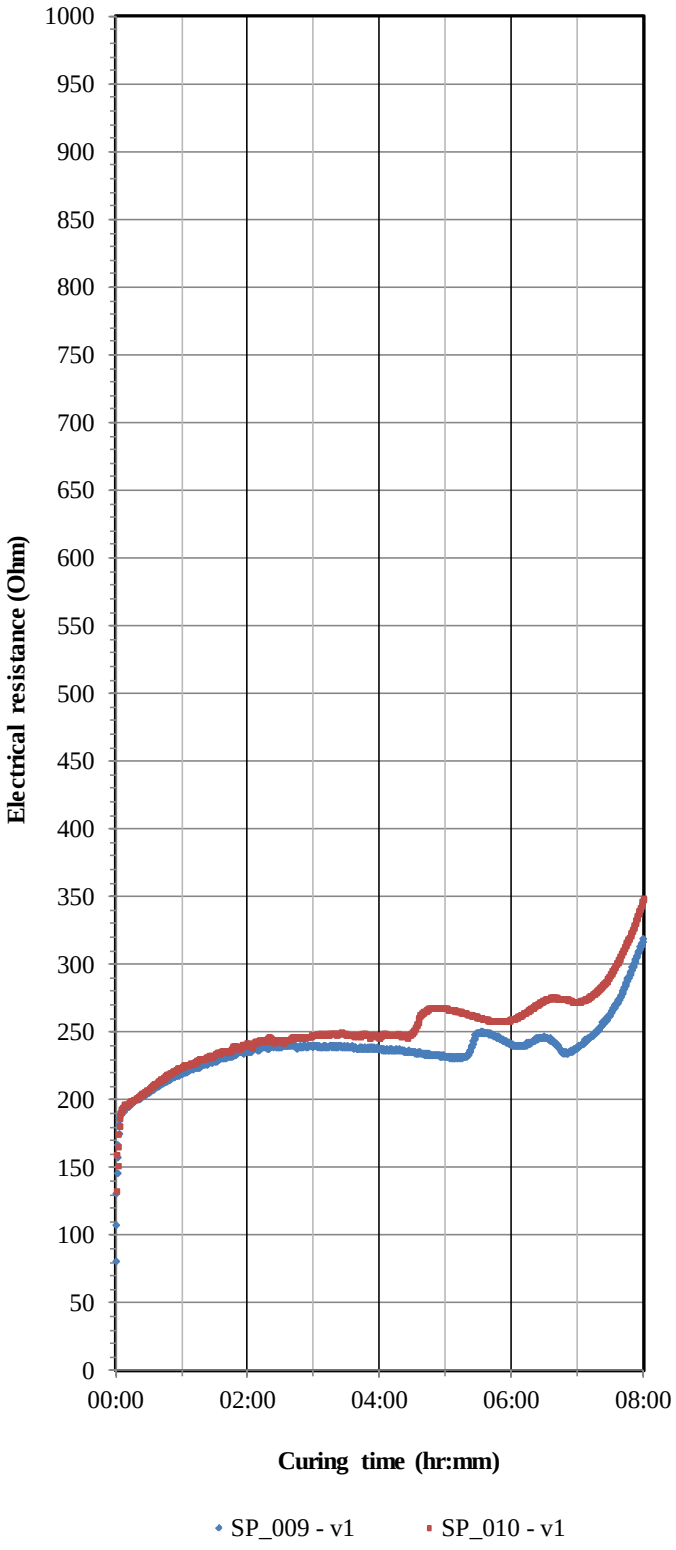

Figure 4.16. Electrical resistance developments with time in cement paste with water reducing admixture (8 hours).

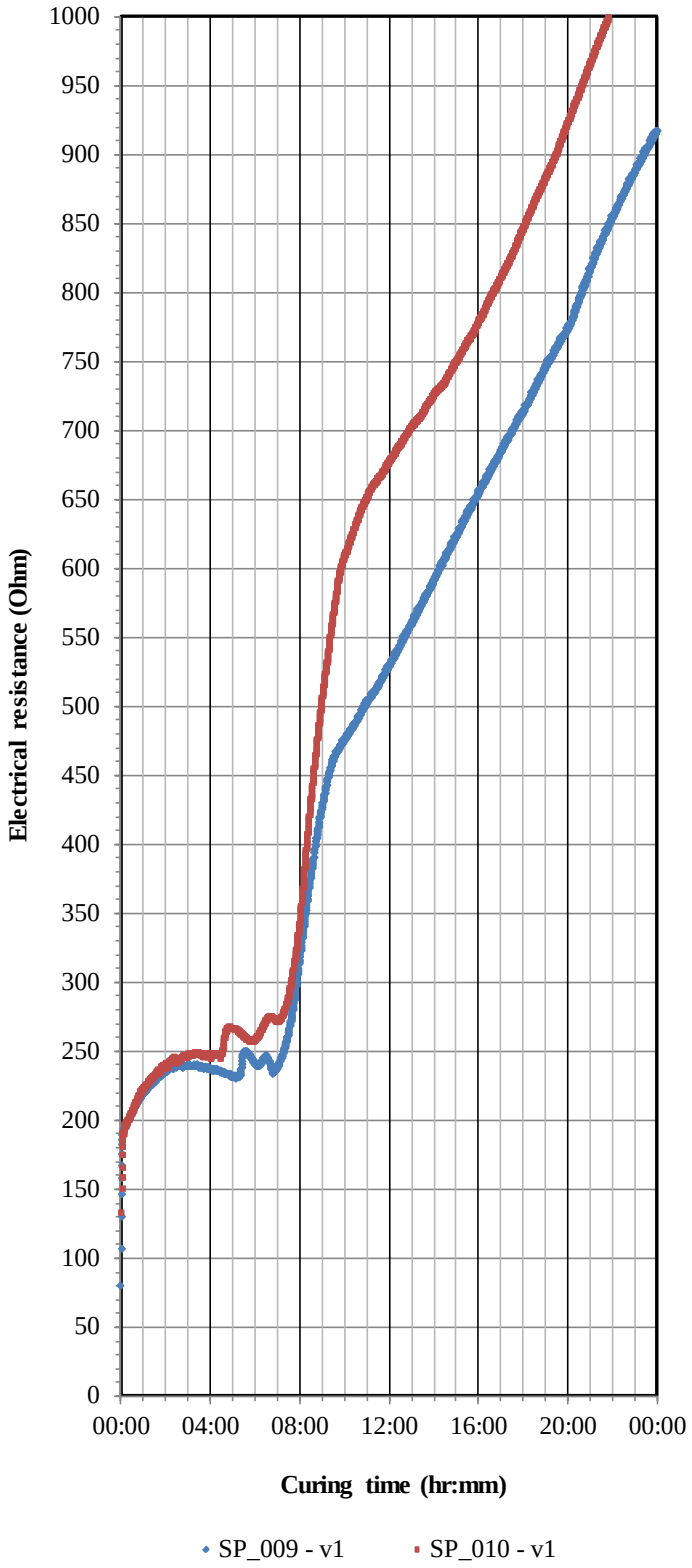

Figure 4.17. Electrical resistance developments with time in cement paste with water reducing admixture (24 hours).

4.3 Influences of different probe designs on shotcrete paste on electrical resistance - Research Stage 3

During Research Stage 3, another 4 prototype probes with different electrodes geometry and size were made to investigate their influences on the shotcrete paste (without chemical admixture and with different chemical admixture) electrical resistance. Figures 4.18 to 4.21 show the details of new prototype probes V1.1, V1.2, V2, V2.1. The details of Research Stage 3 program is presented in Appendix C. The following sections compare and explain the measurement results.

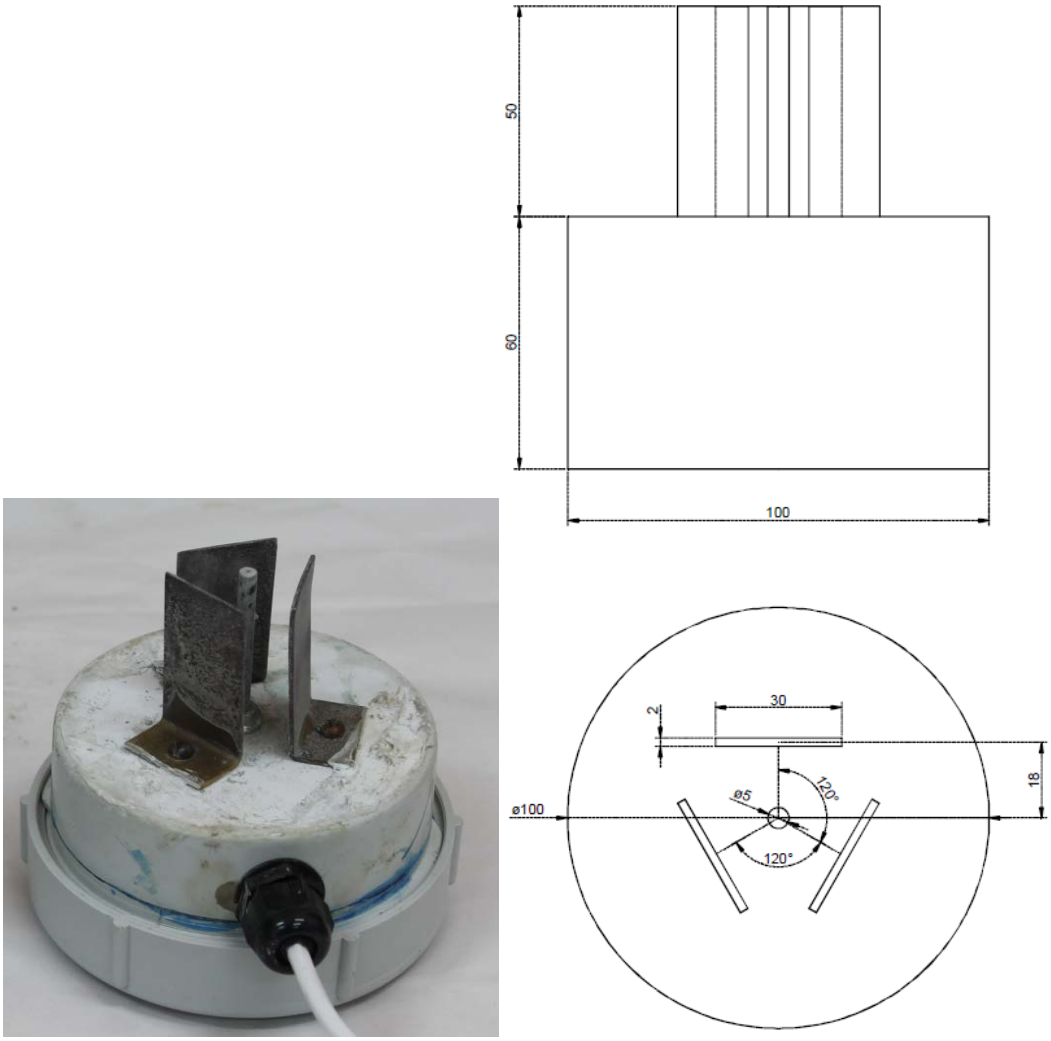

Prototype – v1.1
Negative electrodes made from 2 mm thick brass sheet
Positive electrode made from steel bolt
Housing made from PVC pipe
All fasteners are brass
Wire connected to terminals using brass coupling

Figure 4.18. The electrical resistance measurement probe prototype - V1.1.

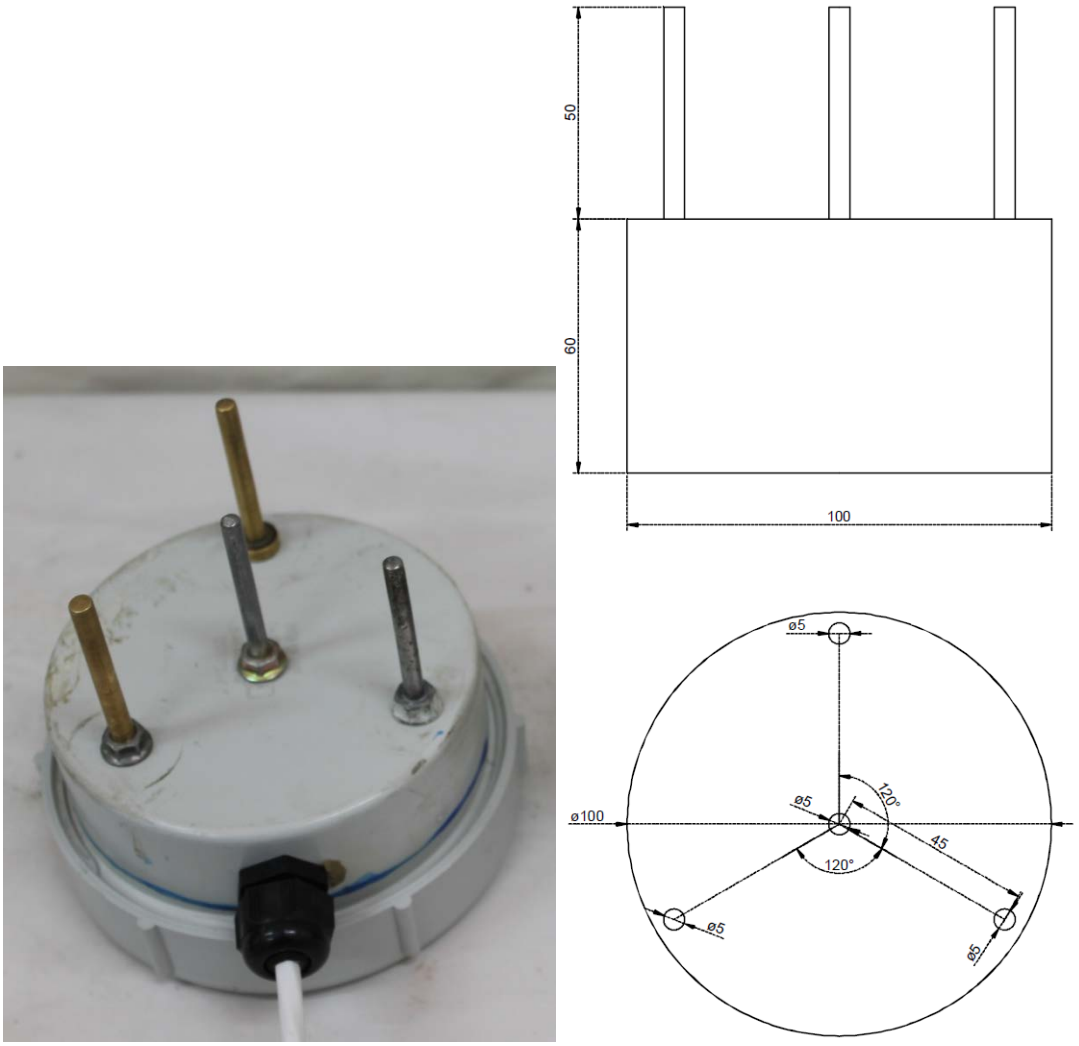

Prototype – v1.2
Negative electrodes made from steel bolt (12 O'clock), the rest are nickel plated
Positive electrodes made from steel bolt
Housing made from PVC pipe
All fasteners are brass
Wire connected to terminals using brass coupling

Figure 4.19. The electrical resistance measurement probe prototype - V1.2.

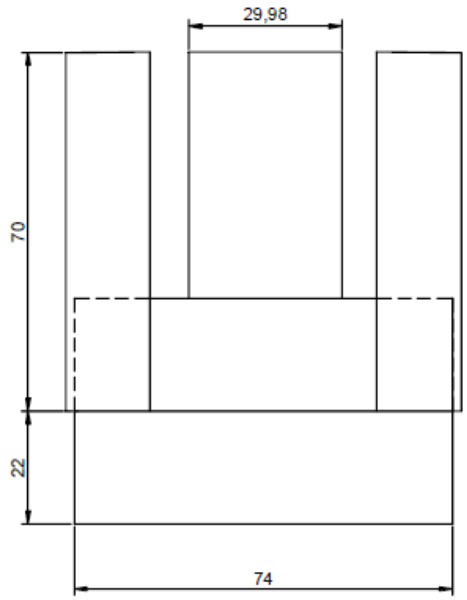

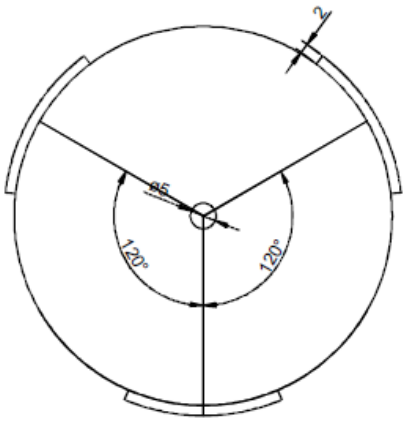

Prototype – v2
Positive electrodes made from copper pipe (AS143)
Negative electrodes made from M6 x 70 mm high tensile chrome plated bolt
Housing made from 65 mm Vinidex PVC end cap
Locknuts are zinc plated, screws and washers are brass
Wire connected to terminals using eye lugs

Figure 4.20. The electrical resistance measurement probe prototype - v2 .

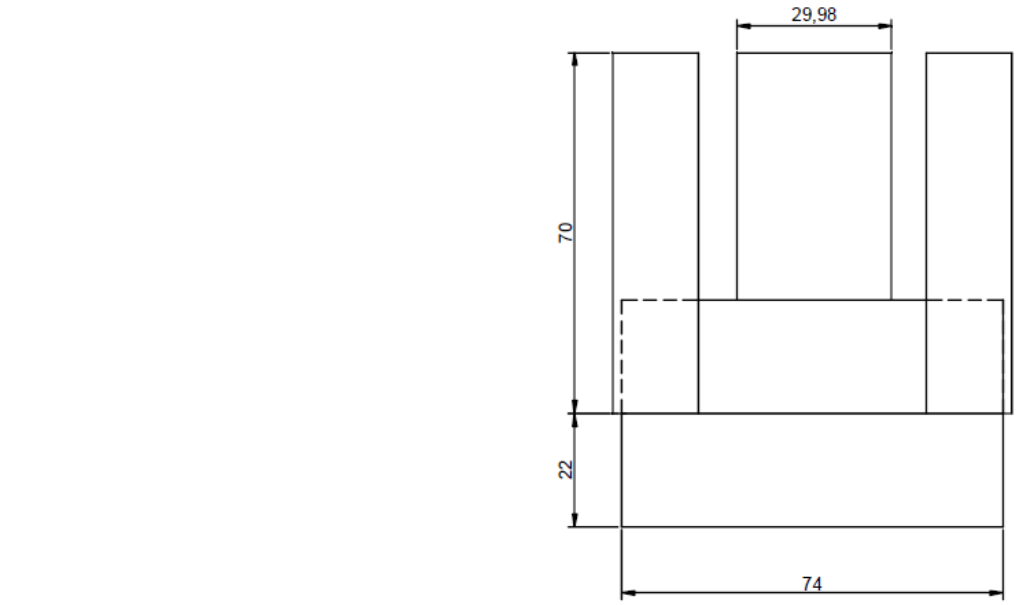

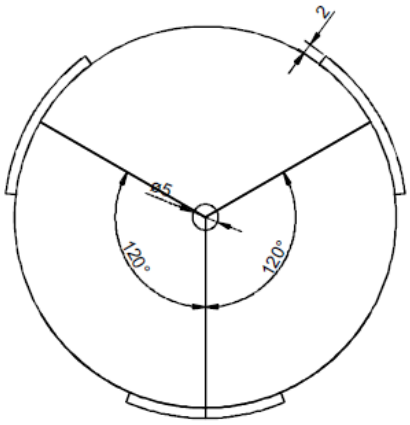

Prototype – v2.1
Positive electrodes made from 1.5 mm thick brass sheet
Negative electrodes made from M6 x 70 mm high tensile chrome plated bolt
Housing made from 65 mm Vinidex PVC end cap
Locknuts are zinc plated, screws and washers are brass
Wire connected to terminals using eye lugs

Figure 4.21. The electrical resistance measurement probe prototype - v2.1.

4.3.1 Influences of electrodes distance

Figures 4.22 shows prototype probe V1 and Prototype probe V1.1. Figures 4.23 and 4.24 show a measurement results conducted with probe V1 and V1.1 for the shotcrete paste mix without chemical admixture. The purpose of this comparison was to determine how the distance between the positive and negative electrodes has an effect on the resistance readings. The distance between positive and negative electrodes in prototype V1 is 46 mm and 18 mm in prototype V1.1 respectively. The measurement results show that, generally the shorter distance between the positive and negative electrodes, the better the sensitivity of measured resistance. At about 4 hours curing, the measured change in resistance for prototype V1.1 is more prominent than prototype V1. (The sudden drop in measured resistance between curing time 16 and 20 hours in the test GM_0001 V1.1 is due to moving of the sample box).

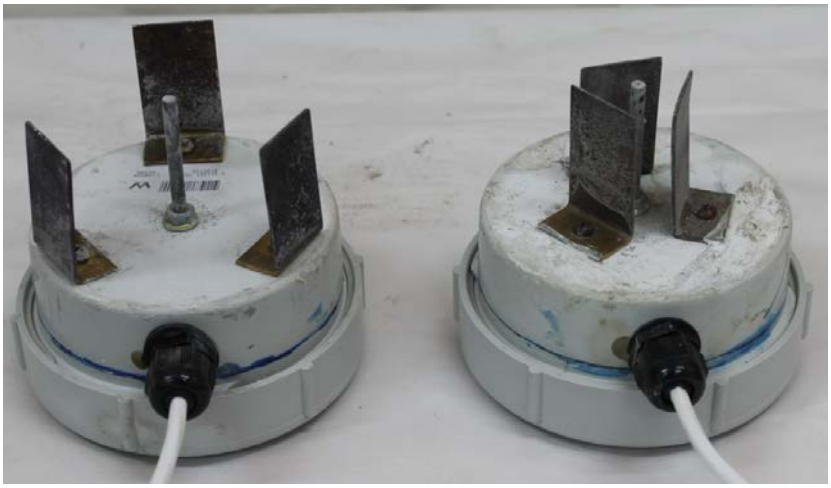

Figure 4. 22. Prototype V1 (left) and Prototype V1.1 (right).

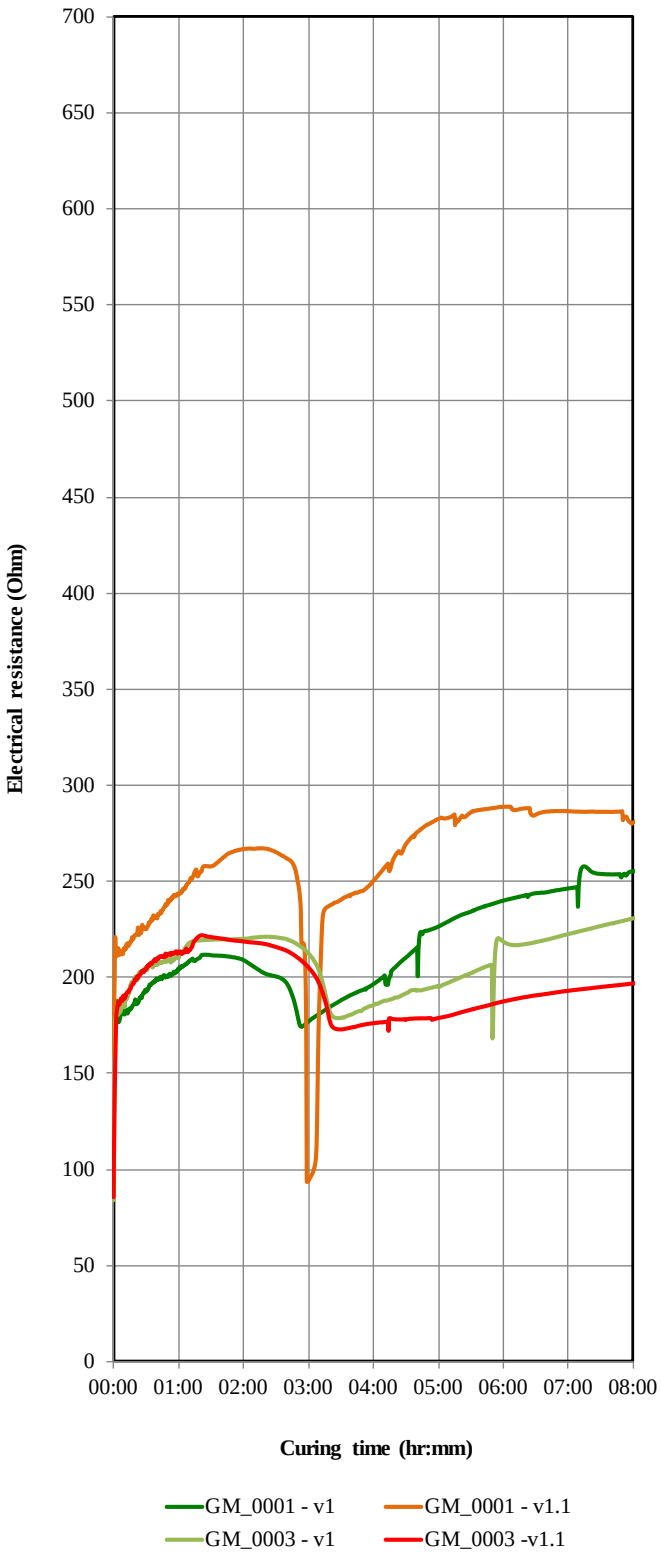

Figure 4.23. Electrical resistance developments with time in shotcrete paste without chemical admixture (8 hours).

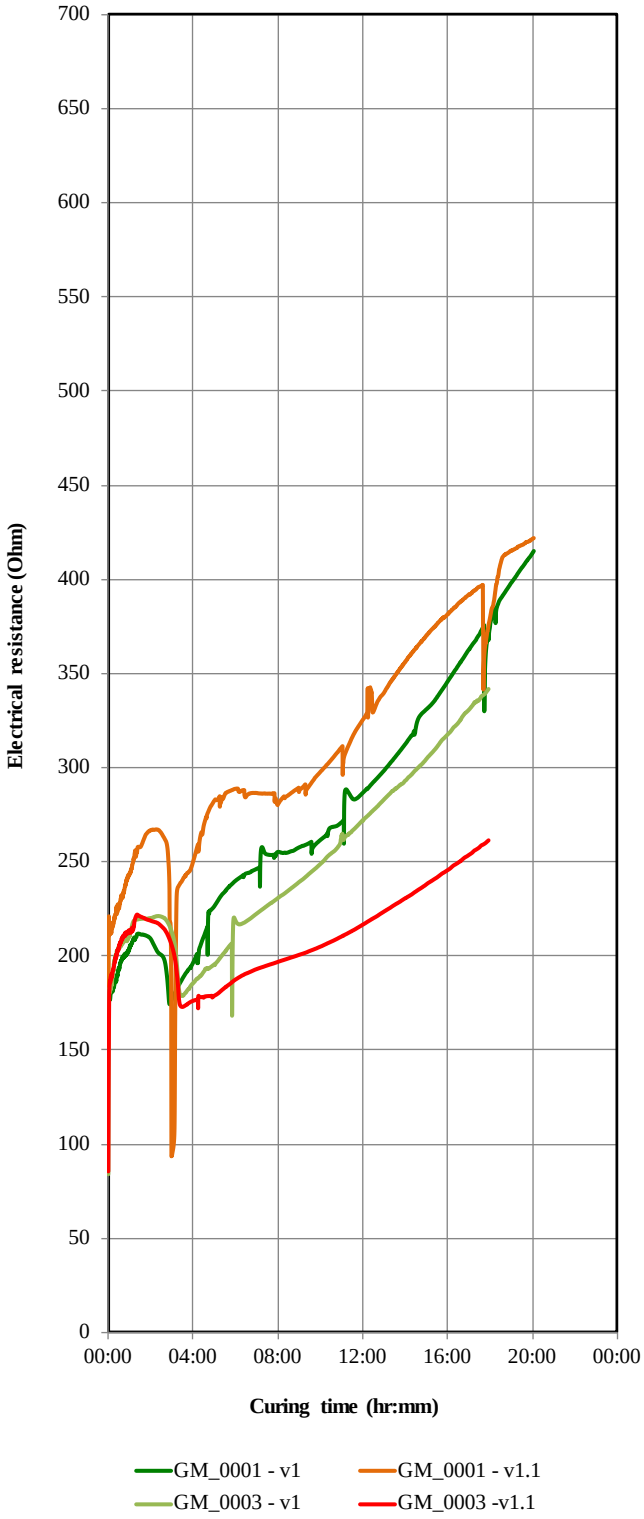

Figure 4.24. Electrical resistance developments with time in shotcrete paste without chemical admixture (24 hours).

4.3.2 Influences of geometry and surface area of electrodes

Figures 4.25 shows prototype probe V1.2 and Prototype probe V1. Figures 4.26 and 4.27 show the measurement results conducted with probe V1 and V1.2 for the shotcrete paste mix without chemical admixture. The purpose of this comparison was to determine how the geometry and surface area of the electrodes has an effect on the resistance readings. The positive electrode of prototype V1 was made up of 5 mm steel bolt and the negative electrodes were made up of 2 mm thick brass sheet. All electrodes in prototype V1.2 were made up of 5 mm diameter steel bolts. The measurement results show that, the bigger the surface area of the probe, the better the sensitivity to the resistance measured. At about the 4 curing time, the measured change in resistance for prototype V1.2 is less prominent than prototype V1.

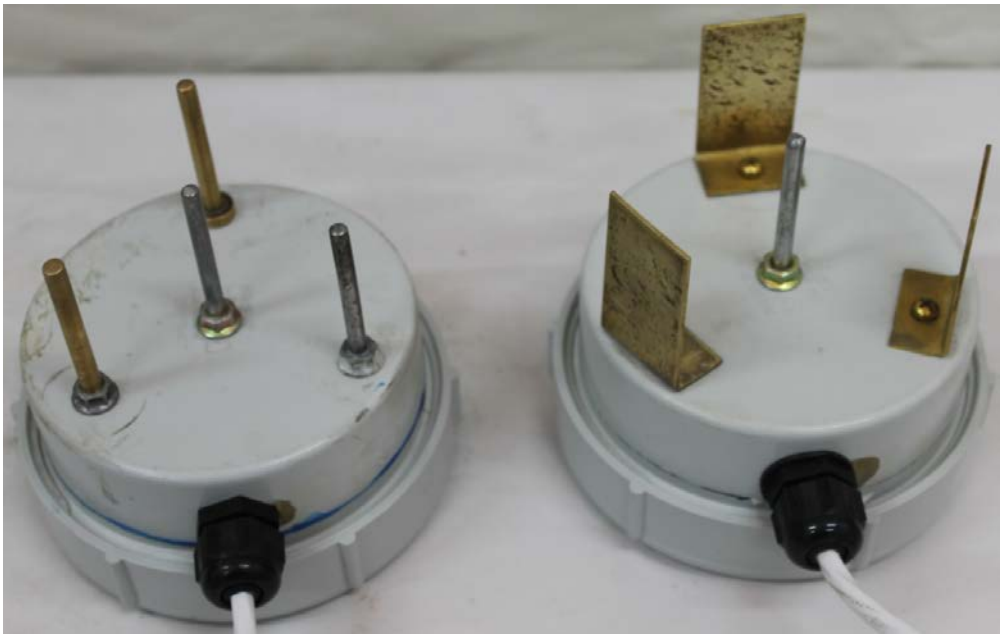

Figure 4. 25. Prototype V1.2 (left) and Prototype V1 (right).

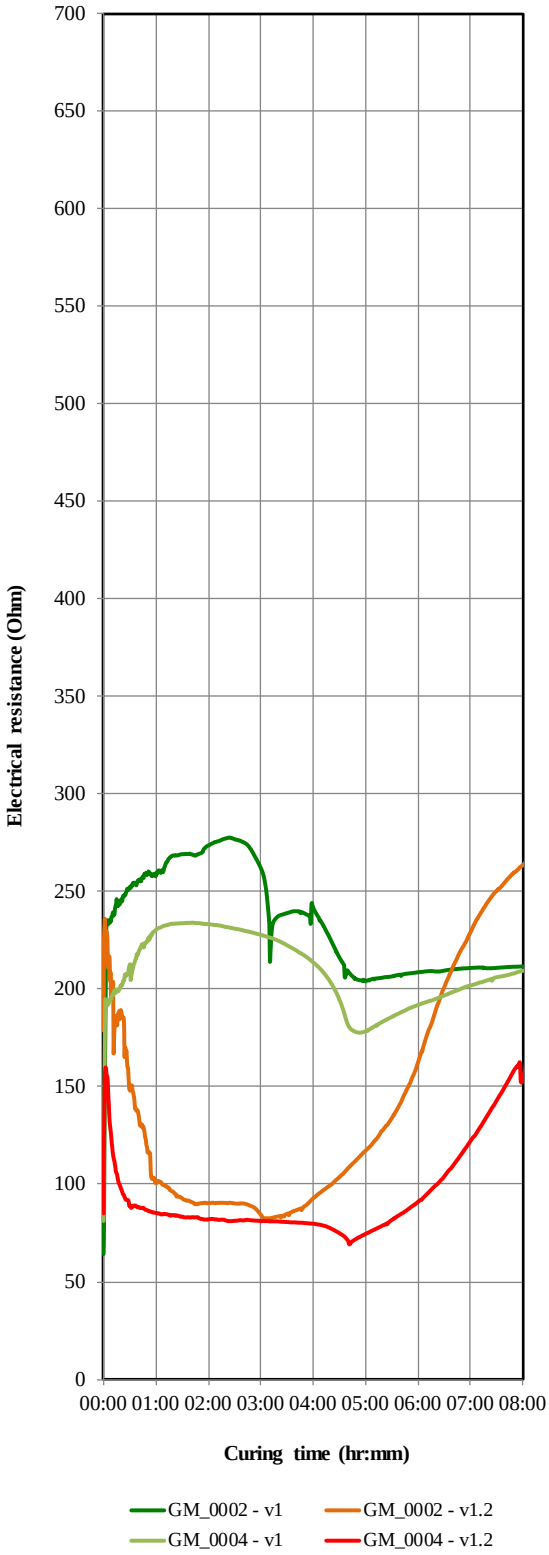

Figure 4.26. Electrical resistance developments with time in shotcrete paste without chemical admixture (8 hours).

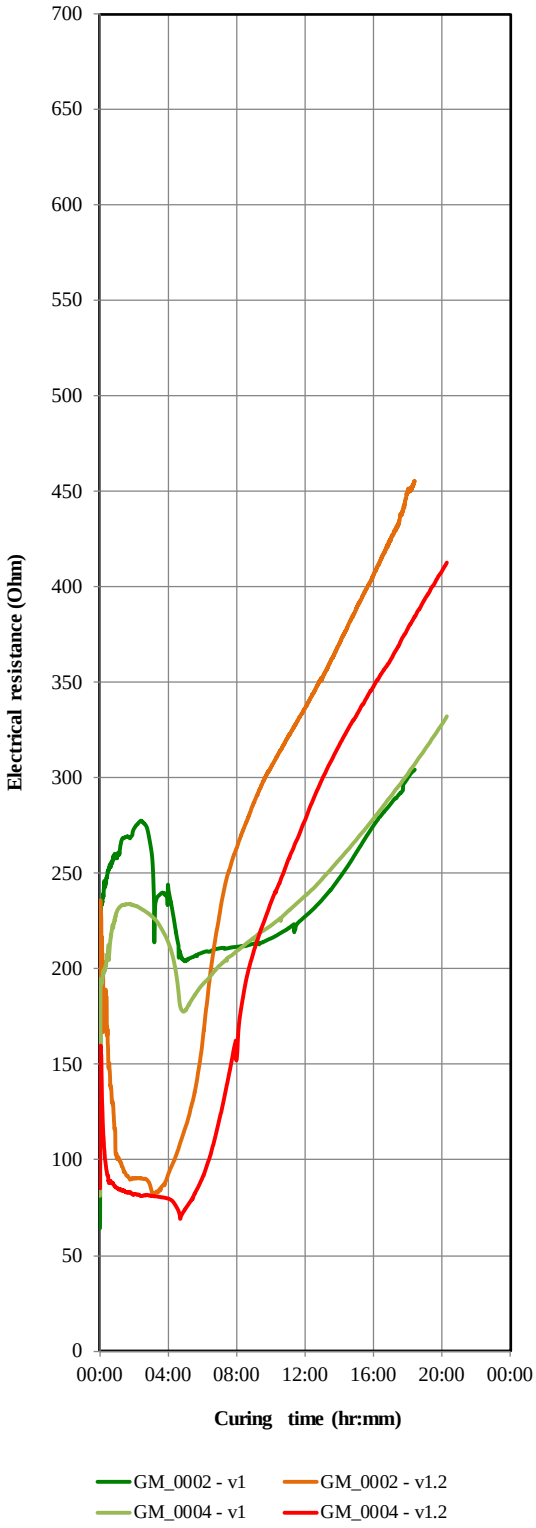

Figure 4.27. Electrical resistance developments with time in shotcrete paste without chemical admixture (24 hours).

4.3.3 Influences of the overall size of the probe

Figure 4.28 show a comparison for prototype probe V1 and V2. The purpose of this comparison was to determine how the overall size for the probe and the materials used for the electrodes has an effect on the resistance readings. The overall size of prototype probe V1 is 100 mm diameter and the distance between the positive and negative electrodes is 46 mm. The overall size of prototype probe V2 is 74 mm diameter and the distance between the positive and negative electrodes is 37 mm. Both of the positive electrodes probe V1 and V2 were made up of 5 mm steel bolt. The negative electrodes of probe V1 were made up of 2 mm thick brass sheet and that of V2 were made up of 2 mm thick copper sheet. Figures 4.29 and 4.30 show a measurement results conducted with prototype probe V1 and V2 for the shotcrete paste mix without chemical admixture. The measurement results show that, the trend of electrical resistance measurements were similar for both probe V1 and V2 up to 4.5 hours curing. After 4 and half hours curing the electrical resistance measured with V1 sharply increased with curing time. After 4 and half hours the electrical resistance measured with V2 gradually increased with curing time. This is due to the electrical conductivity of copper used in probe V2 is higher than that of brass used in V1.

Figure 4. 28. Prototype V2 (left) and Prototype V1 (right).

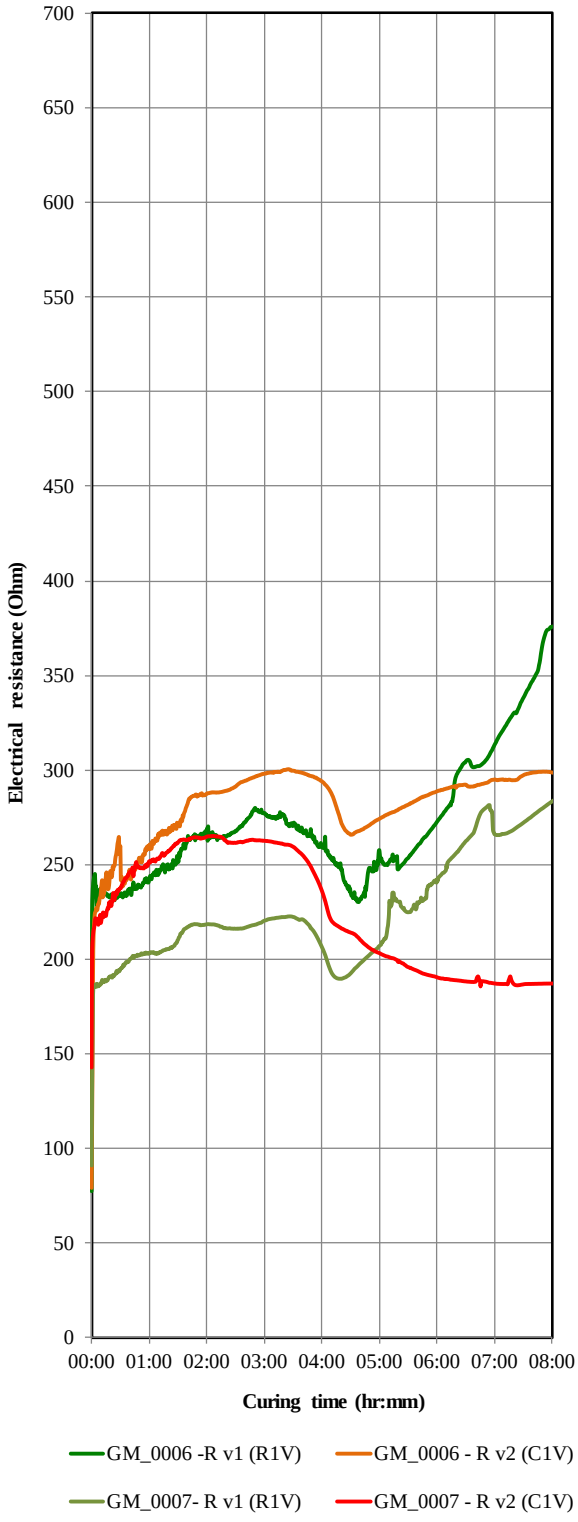

Figure 4.29. Electrical resistance developments with time in shotcrete paste without chemical admixture (8 hours).

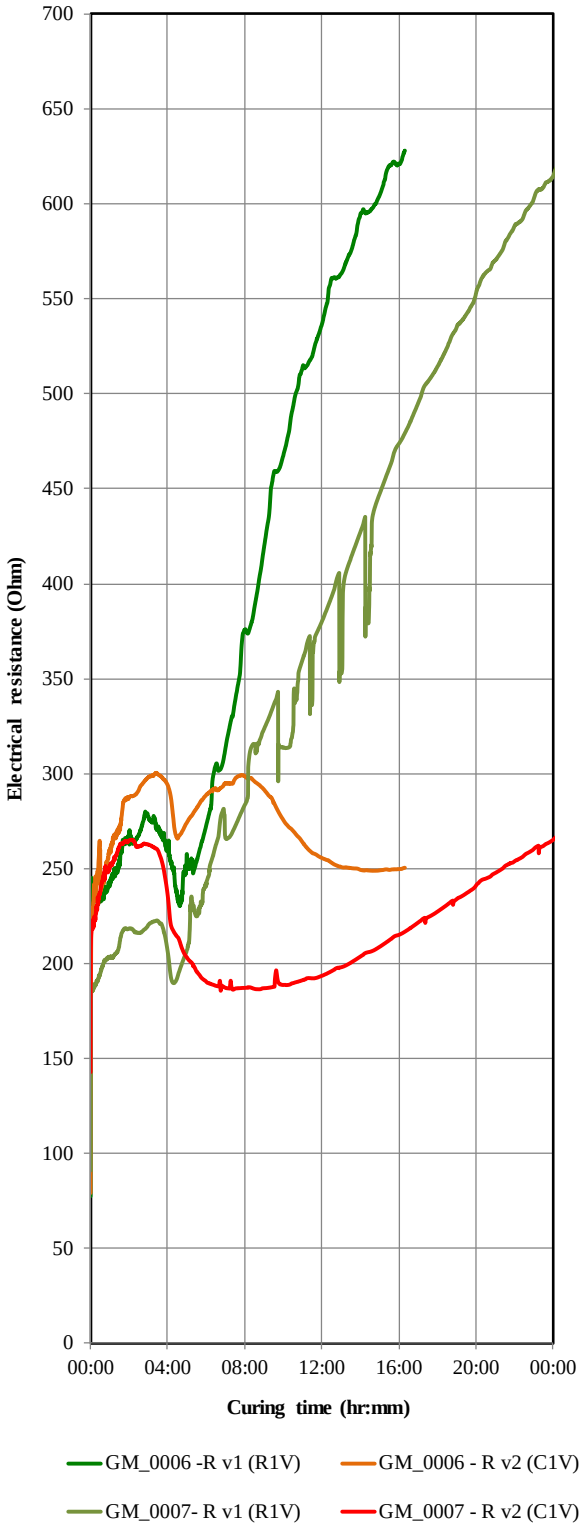

Figure 4.30. Electrical resistance developments with time in shotcrete paste without chemical admixture (24 hours).

4.3.4 Influences of the type of material use for electrodes

Figure 4.31 shows a comparison for prototype probe V2 and V2.1. Figures 4.32 and 4.33 show the measurement results conducted with prototype probe V2 and V2.1 for the shotcrete paste mix without chemical admixture. The purpose of this comparison was to confirm the influence of the materials used for the electrodes on the resistance readings. The overall size of prototype probe V2 and V2.1 are the same. Both of the positive electrodes of probe V2 and V2.1 were made up of 5 mm steel bolt. The negative electrodes of probe V2 were made up of 2 mm thick copper sheet and that of V2.1 were made up of 2 mm thick brass sheet. The measurement results show that, the electrical resistance measured with probe V2 shows a lower value than that measured with probe V2.1. This confirmed the using a high electrical conductivity material such as copper gives a lower electrical resistivity profile.

Figure 4.31. Prototype V2 (left) and Prototype V.2.1 (right).

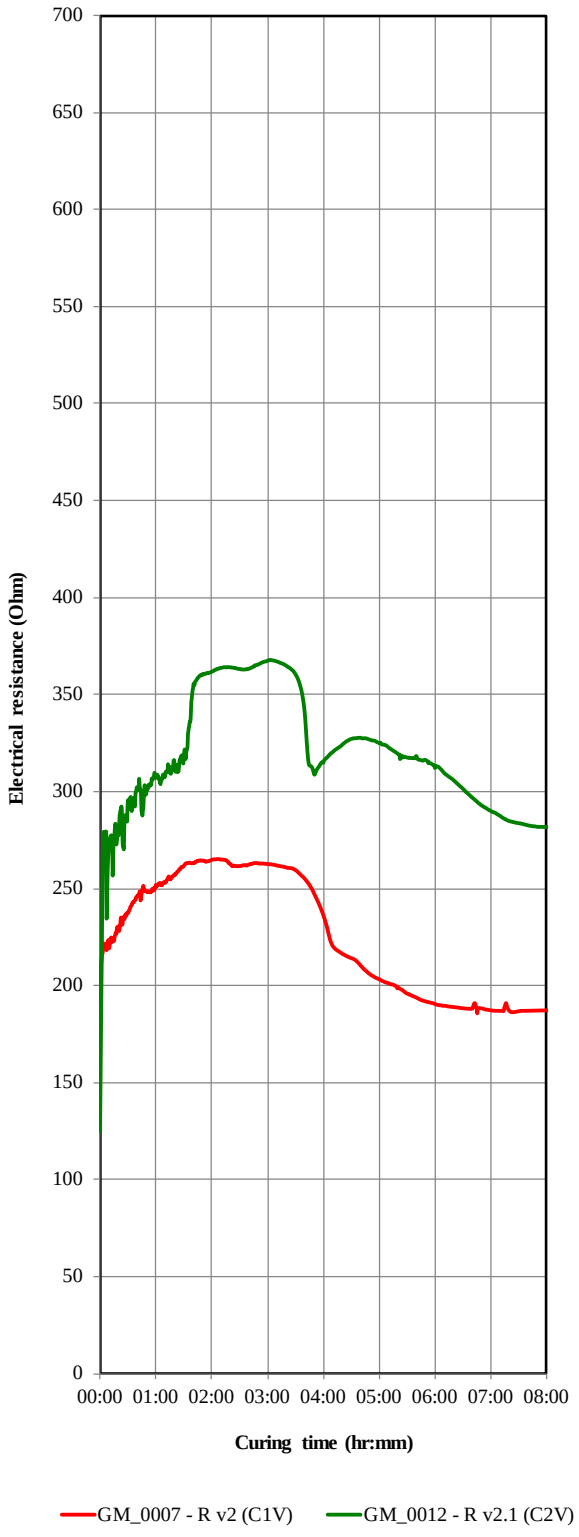

Figure 4.32. Electrical resistance developments with time in shotcrete paste without chemical admixture (8 hours).

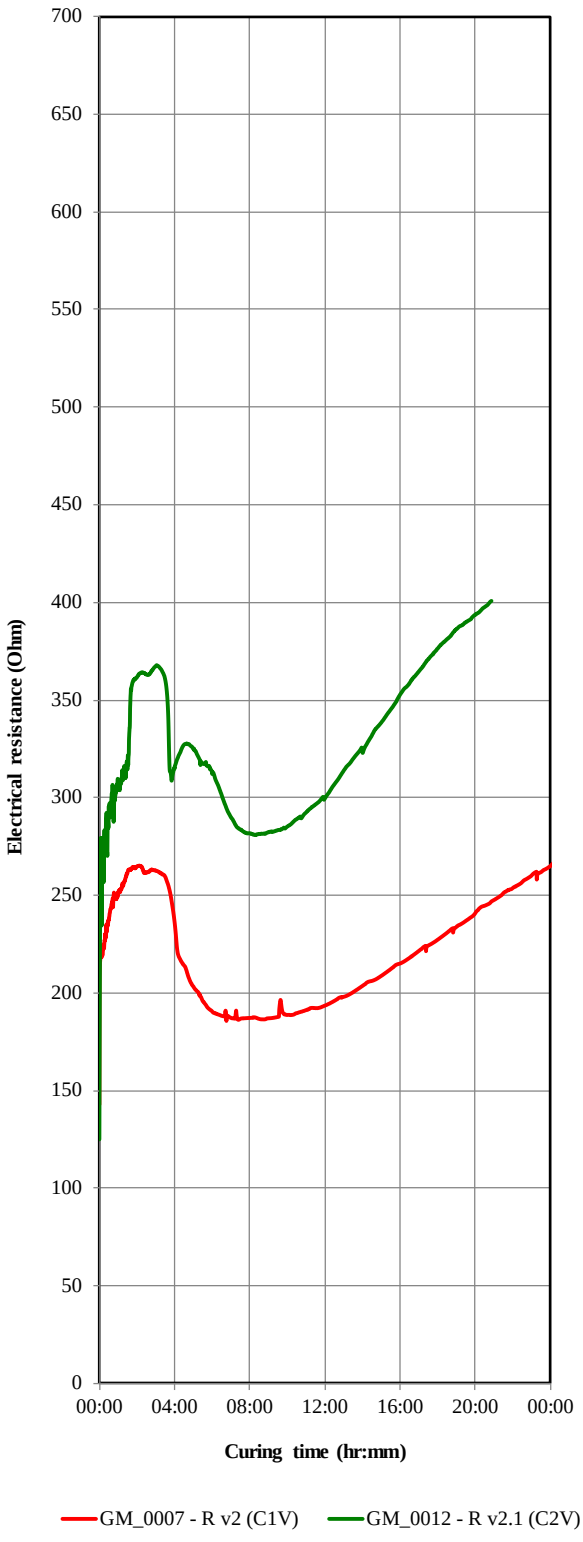

Figure 4.33. Electrical resistance developments with time in shotcrete paste without chemical admixture (24 hours).

4.3.5 Additional electrical resistance measurement with prototype V2.1

After conducting a series of test as described in sections 4.1.1 to 4.3.4, it was concluded that, the prototype probe (V2.1) was the best design for the measurement of electrical resistance to correlate to shear strength. Therefore, additional measurements were conducted with prototype probe V2.1 to measure electrical resistance of shotcrete paste mix with and without chemical admixtures. A typical electrical resistance of shotcrete paste with and without the influences of chemical admixture, measured with prototype probe V2.1 is show in Figure 4.34 for 8 hours curing and in Figure 4.35 for 24 hours curing. The details test results are presented in Appendix D.

The typical test results show that, the initial electrical resistance of shotcrete paste without chemical admixtures was about 200 Ohm and gradually increased to about 225 Ohm until 2 hours curing. The electrical resistance gradually decreased to about 170 Ohm until about 4 hours curing. After 4 hours curing, it continuously increased to 500 Ohm within the next 24 hours. An overall profile of the electrical resistance of shotcrete paste with superplasticiser, water reducing admixture, and hydration stabiliser are similar to that of electrical resistance without chemical admixture. The electrical resistance of shotcrete paste with accelerator is significantly different to the others. The initial resistance was about 60 Ohm and gradually decreased to about 50 Ohm only until about 2 hours curing. After about 2 hours curing, it sharply increased to about 170 Ohm until 4 hours curing. After 4 hours, it continuously increased to 270 Ohm within the next 24 hours.

The differences were mainly due to the different temperature within the shotcrete paste evolved from the chemical reaction during cement hydration. This temperature is also known as heat of hydration. The influence of temperature due to heat of hydration on the electrical resistance is described in the next Section 4.4.

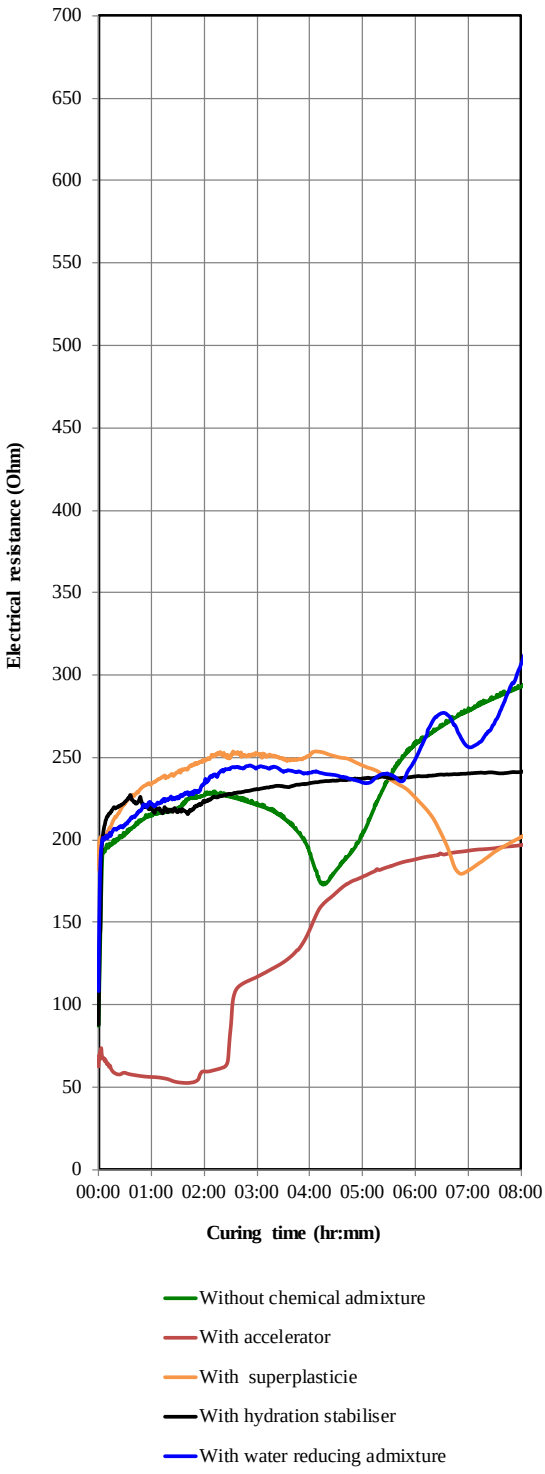

Figure 4.34. A typical electrical resistance developments with time measured with prototype probe V2.1 in shotcrete paste without and with different types chemical admixture (8 hours).

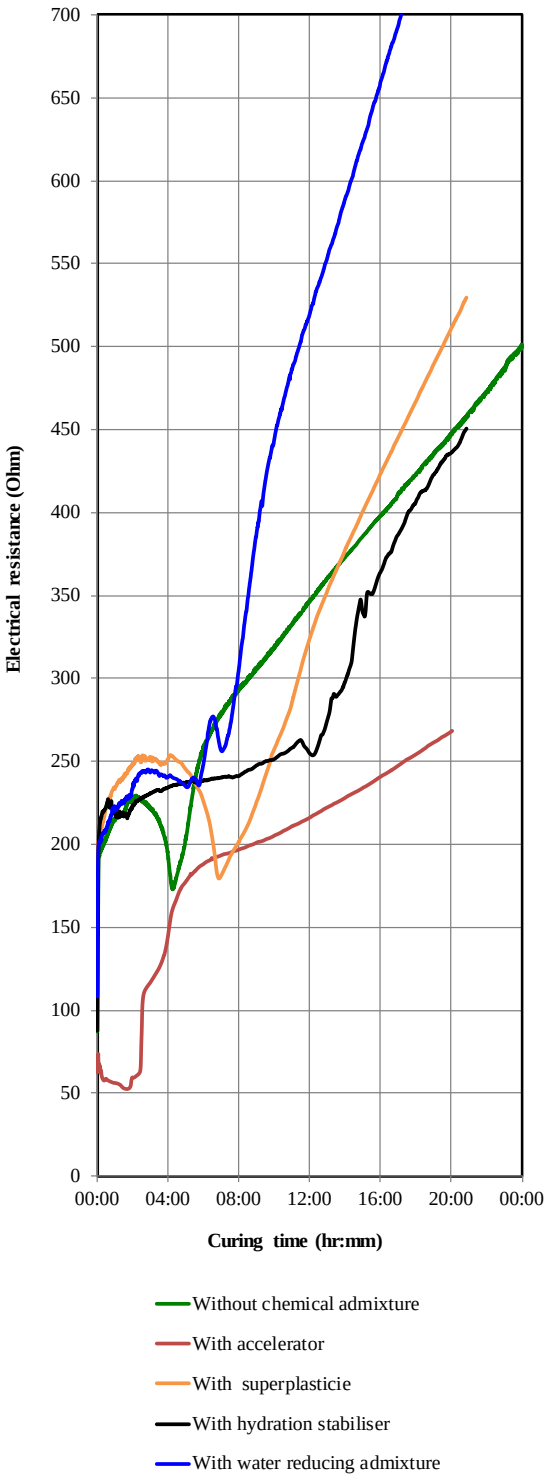

Figure 4.35. A typical electrical resistance developments with time measured with prototype probe V2.1 in shotcrete paste without and with different types chemical admixture (24 hours).

4.4 Influences of temperature due to heat of hydration on the electrical resistance of shotcrete paste

The fundamental chemistry of cement hydration and hydration mechanism are described in Sections 2.3.1.1.1 and 2.3.1.2. It is well established that, heat evolves during cement hydration due to the exothermic chemical reactions between cement and water. Based on that fundamental chemistry, different types of chemical admixtures have been invented in order to alter the hydration process as desired. The chemistry of the most common chemical admixtures used for underground shotcrete application is described in Section 2.3.5.

During Research Stage 3, the temperature development due to the heat of hydration was measured simultaneously with a thermocouple while measuring electrical resistance. The typical results of temperature and electrical resistance development with time for the shotcrete paste without chemical admixture, with water reducing admixture, with superplasticiser, with hydration stabiliser and with accelerator are presented in Figures 4.36 to 4.40. A comparison of all typical results of temperature and electrical resistance development with time is shown in Figure 4.41.

The test results show that, at the first or pre-induction stage (Figure 2.1, Taylor et. al, 1984) and second stage or induction stage (slow reactions) of hydration (Figure 2.1, Taylor et. al, 1984), the electrical resistance gradually increase with a gradually increasing temperature up to the point where the temperature start to increase sharply.

From that point the electrical resistance gradually decrease with continuously increasing temperature up to the peak. This section is the hydration acceleratory stage as show in Figure, 2.1. At this stage the temperature continuously increase due to excessive exothermic chemical reactions. When the temperature increases, the atoms in the shotcrete paste vibrate violently and create more free electrons to become carriers of electric current. Therefore, the electrical conductivity increase

and electrical resistance decrease. The magnitude and rate of temperature and electrical resistance increasing and decreasing is different form each mix, especially for the mix with accelerator. The higher the heat of hydration evolved from the hydration process, the lower the electrical resistance as it can be seen in the hydration process of the shotcrete paste with accelerator. The electrical resistance of shotcrete paste form the start of induction period to end of the acceleratory period is mainly affect by the chemical reactions and concentration of ions. The results in this research support the early study conducted by Calleja (1952) as described in Section 2.4.2.3.

After, the temperature development reached to the peak, it decrease gradually while the electrical resistance start to increase continuously. This is due to the increased degree of hydration. Figure 4.42 shows temperature and calculated degree of hydration (calculated with the procedure described in Section 3.3) development with time for shotcrete paste without and with different chemical admixtures.

The end of acceleratory period (The time at the peak temperature and the time at the point where electrical resistance start to increase continuously.) indicated by temperature and electrical resistance was different. It shows that the changes in electrical current flow happen first and the heat of hydration due to exothermic chemical reactions evolved after a certain amount of delay time. It shows heat from the chemical reactions evolved after the formation of hydration products. Therefore, the strength development can be under-estimated with the development of heat of hydration. The delay times varies with different types of shotcrete paste. Table 4.1 shows different delay time between temperature and electrical resistance developments.

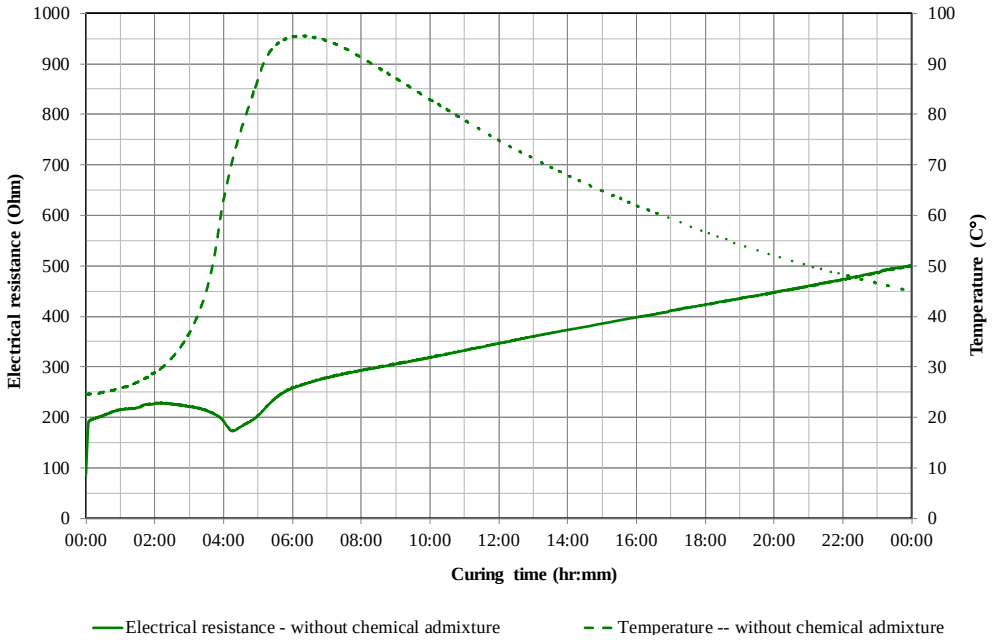

Figure 4.36. A typical result of electrical resistance (solid line) and temperature (dashed line) development with time for shotcrete without chemical admixture.

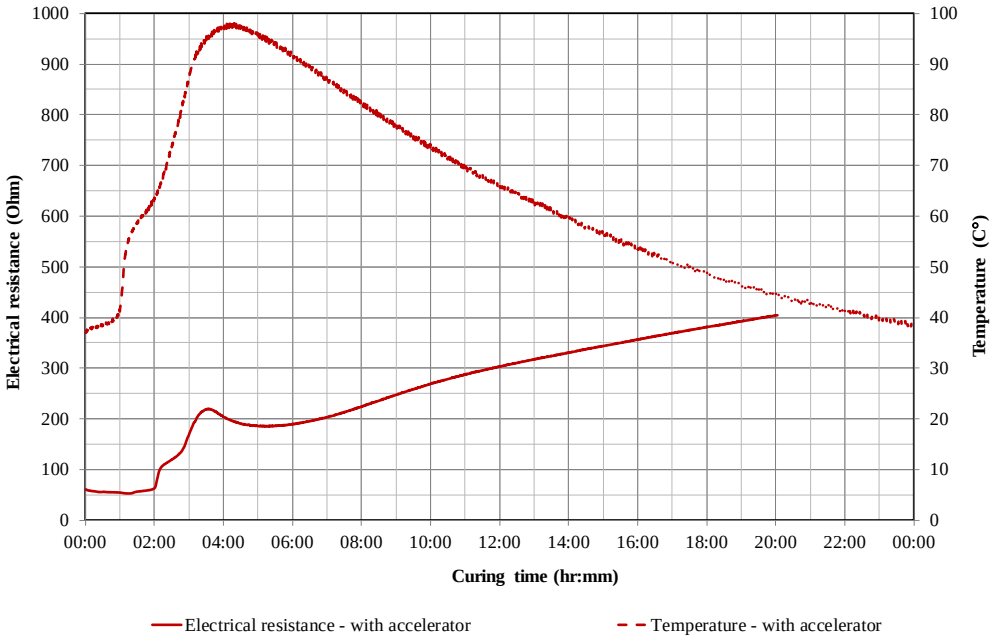

Figure 4.37. A typical result of electrical resistance (solid line) and temperature (dashed line) development with time for shotcrete with accelerator.

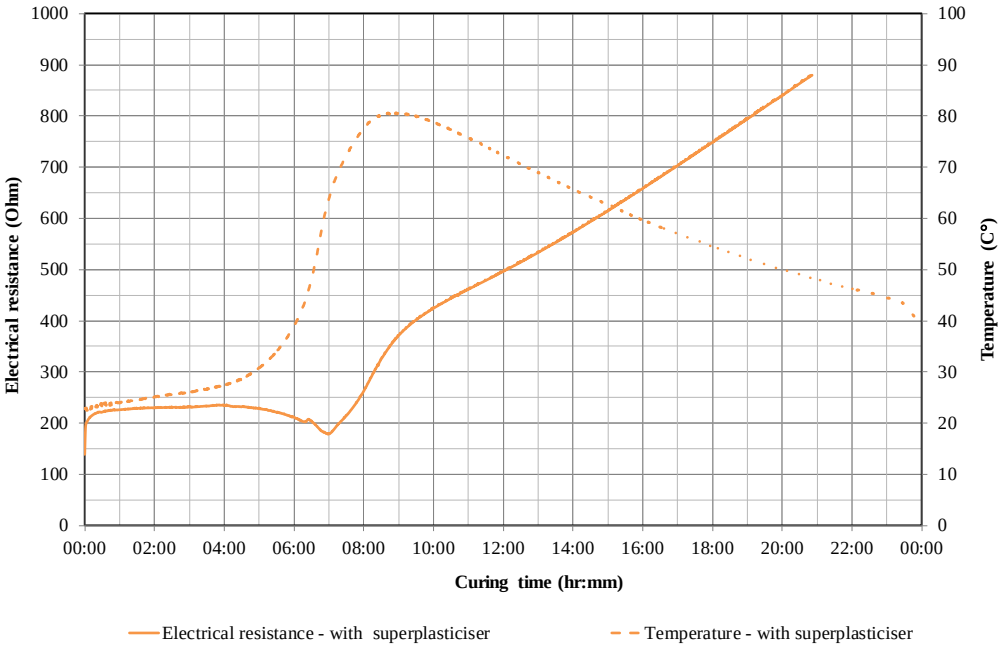

Figure 4.38. A typical result of electrical resistance (solid line) and temperature (dashed line) development with time for shotcrete with superplasticiser.

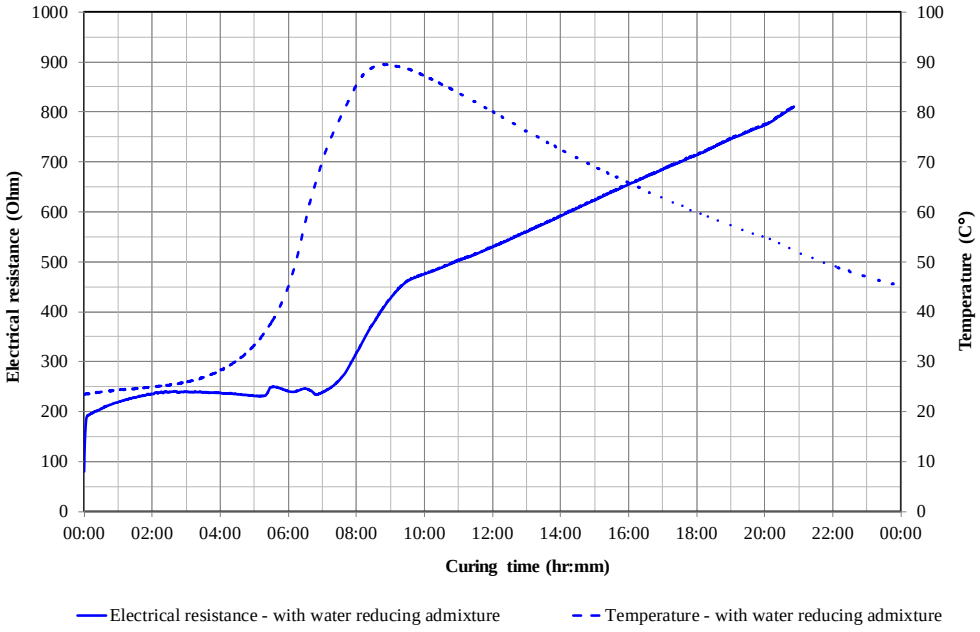

Figure 4.39. A typical result of electrical resistance (solid line) and temperature (dashed line) development with time for shotcrete with water reducing admixture.

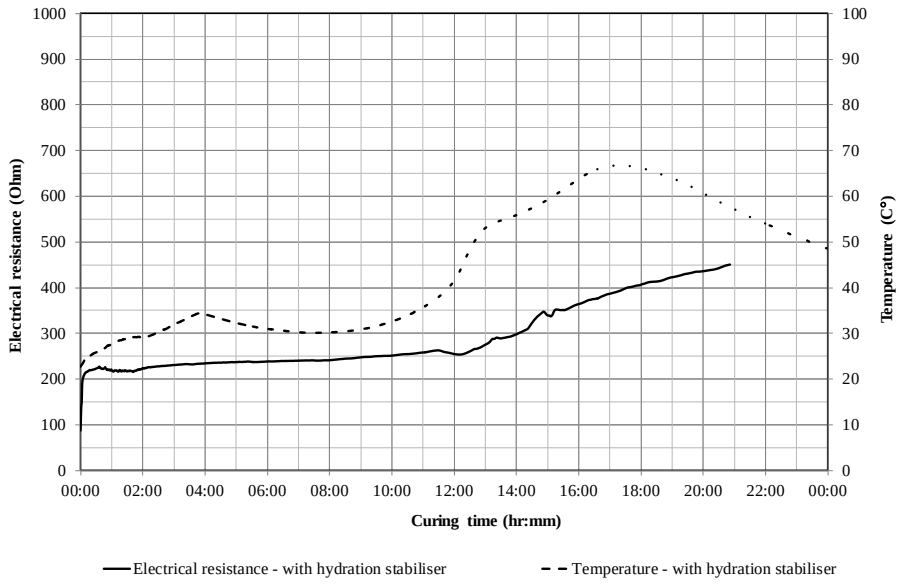

Figure 4.40. A typical result of electrical resistance (dashed line) and temperature (solid line) development with time for shotcrete with hydration stabiliser.

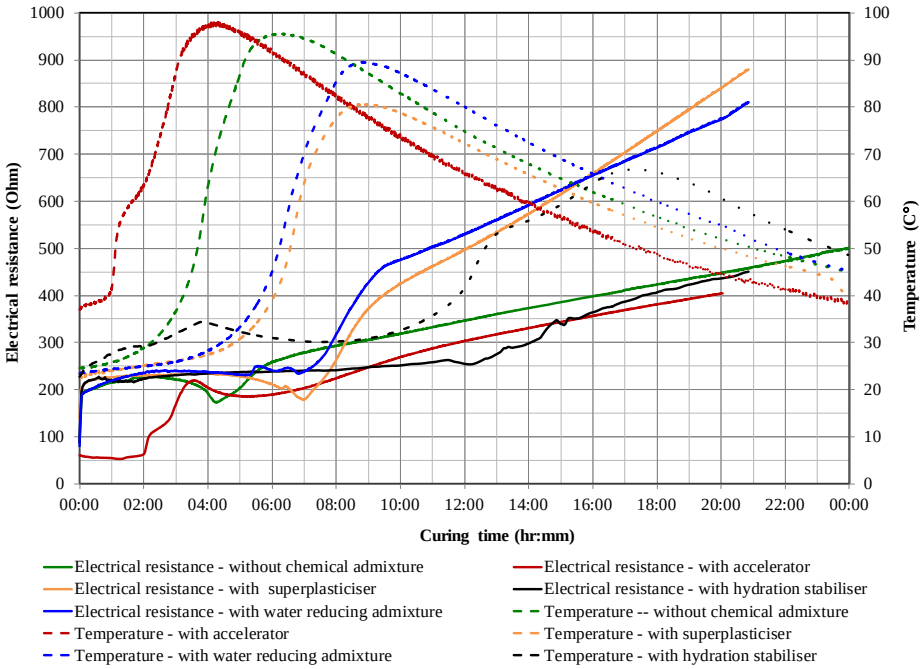

Figure 4.41. A comparison of typical result of electrical resistance (solid lines) and temperature (dashed lines) development with time for shotcrete without and with different chemical admixtures.

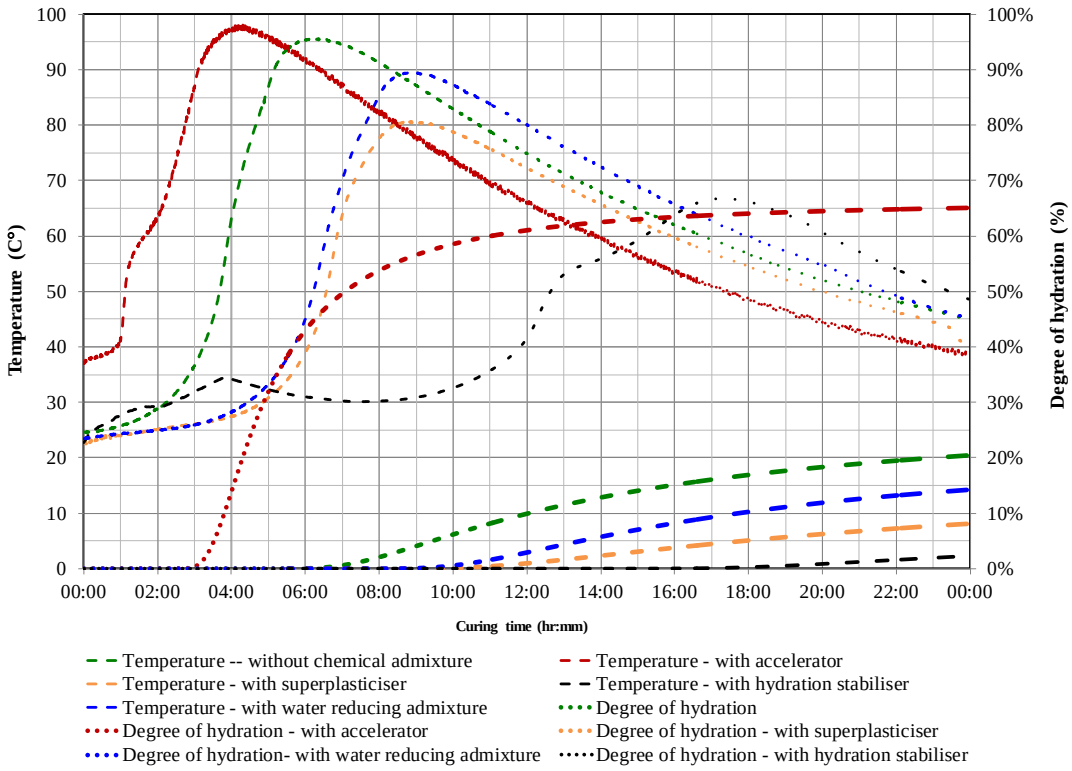

Figure 4.42. A typical temperature (dashed lines) and calculated degree of hydration (dotted lines) development with time for the shotcrete paste without and with different chemical admixtures.

Table 4. 1. Different delay time between temperature and electrical resistance developments.

Mix ID.	Shotcrete paste	Time at peak tempearture (hr:mm)	Time at electrical resistance continuously increase (hr:mm)	Delay time (hr:mm)
1	Without chemcial admixture	6:00	4:10	1:50
2	With water reducing admixtures	8:50	6:50	2:00
3	With superplasticiser	9:00	7:00	2:00
4	With hydration stabiliser	17:00	12:00	5:00
5	With accelerator	4:10	2:00	2:10

4.5 Development of prototype wireless probe - Research Stage 4

All the electrical resistance data described in Research Stages 1 to 3 were undertaken with the prototype probes (V1, V1.1, V1.1, V2 & V2.1) with copper wire cable connected to a data logger. Using copper wire cable for a direct communication link between the probe and the data logger would increase the total cost of the In Cycle Shotcrete (ICS) situation for an underground excavation. Therefore, a new prototype probe V2.1W, which is a wireless version of prototype probe V2.1, was invented during the Research Stage 4. The wireless probe eliminates the use of copper wire which makes the probe easy for installation and subsequently reducing the total cost for ICS. It also has the potential to radically change how the future instrumentation and monitoring system can be deployed in an underground mining environment. Figure 4.43 shows picture and drawing of prototype probe V2.1W. The following sections describe the measurement results using wireless probe V2.1W.

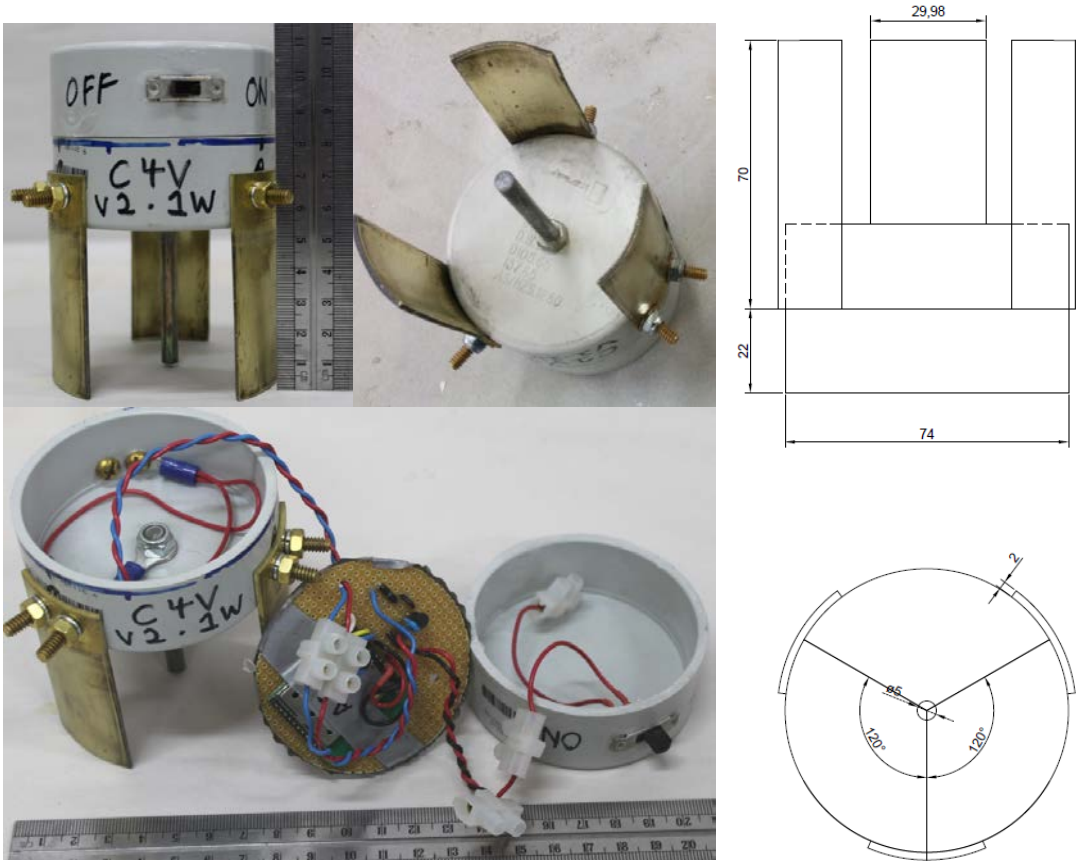

Prototype – v2.1W
Positive electrodes made from 2 mm thick brass sheet
Negative electrodes made from M6 x 70 mm high tensile chrome plated bolt
Housing made from 65 mm Vinidex PVC end cap
Locknuts are zinc plated, screws and washers are brass
Wire connected to terminals using eye lugs

Figure 4.43. The electrical resistance measurement probe with wireless data collecting system - V2.1W.

4.5.1 Influence of accelerator and synthetic fibres and aggregates on electrical resistance of shotcrete measured with wireless probe V2.1W

Figures 4.44 shows an electrical resistance measurement on shotcrete paste with accelerator and synthetic fibres using the wireless probe V2.1W. Figure 4.45 shows the electrical resistance developments with time for shotcrete paste with accelerator and synthetic fibres for 8 hours curing. It shows that the electrical resistance of shotcrete paste with accelerator and synthetic fibres ranges from 60 to 70 Ohm during the first 3 hours, which is much less than the electrical shotcrete paste mixed only with accelerator for a given curing time. Given the electrical resistance of synthetic fibre is greater than 20 Mega Ohm, the results show that, addition of the synthetic fibres created a pore water drainage path which increase the electrical conductivity and therefore decrease electrical resistance at the early age of cement hydration.

Figure 4.44. Electrical resistance measurement with wireless probe V2.1W.

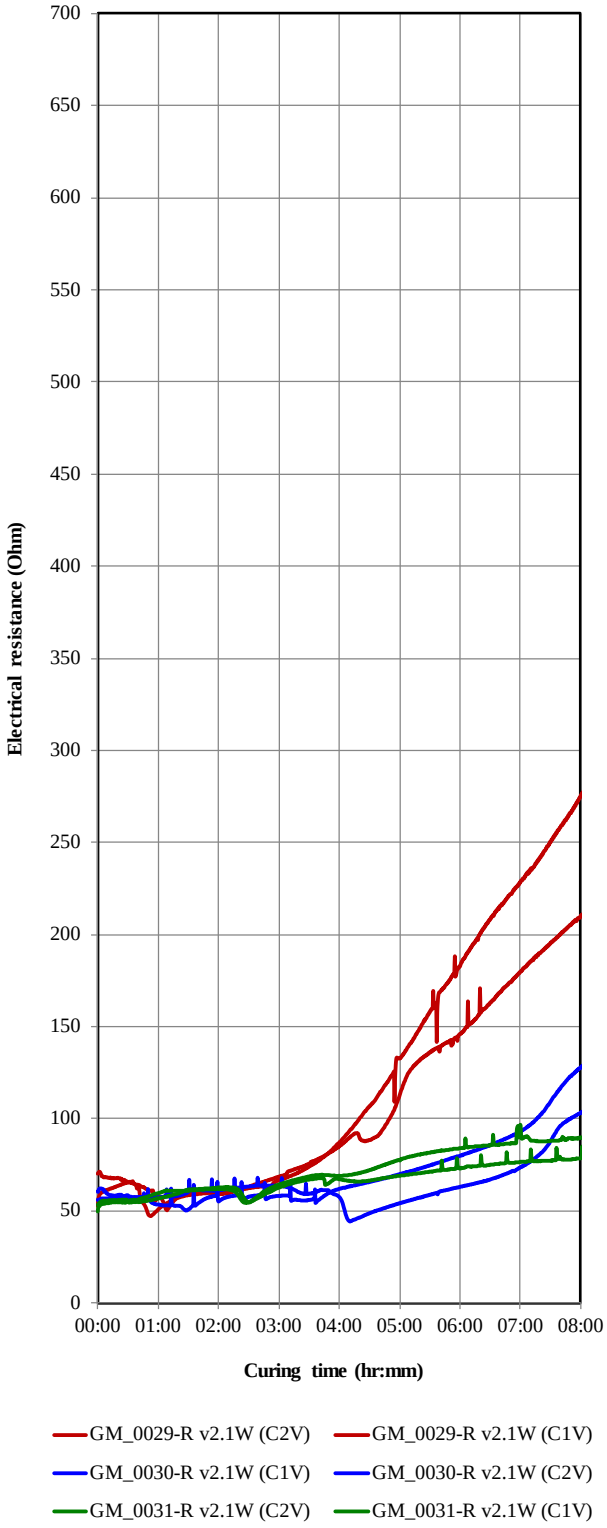

Figure 4.45. Electrical resistance developments with time in shotcrete paste with accelerator and synthetic fibres (8 hours).

Figure 4.46 shows electrical resistance developments with time for shotcrete paste with accelerator, synthetic fibres and aggregates for 8 hours curing. The results show that addition of aggregates significantly increases the overall range of electrical resistance.

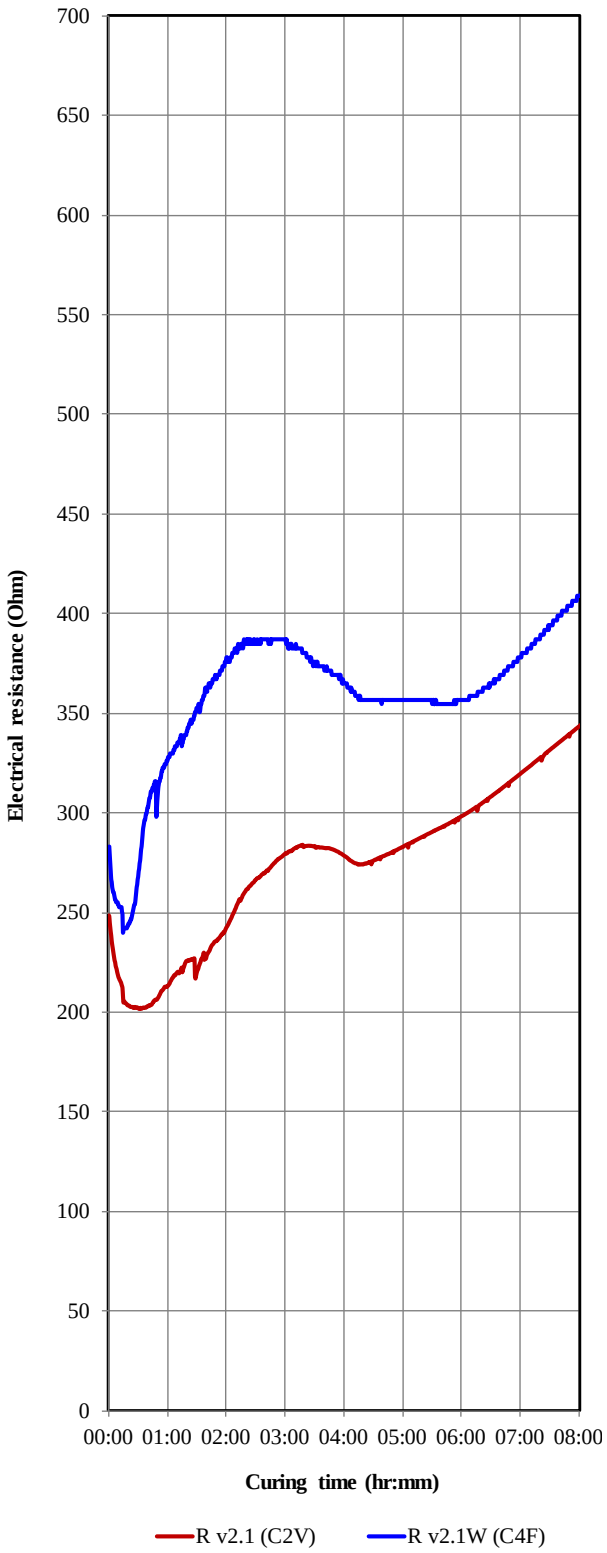

Figure 4.46. Electrical resistance developments with time in shotcrete paste with accelerator, synthetic fibres and aggregates (8 hours).

4.6 In situ electrical resistance of shotcrete at early age – Research stage 5

Sections 4.1 to 4.5 described the research stages for the developing the electrical resistance measurement probe and the influences of chemical admixtures, synthetic fibres and aggregates on the shotcrete paste electrical resistance. After conducting a series of measurements with the prototype probes in the laboratory, the most suitable probe V2.1/V2.1W was used to measure in situ electrical resistance of shotcrete at early age in an underground excavation.

4.6.1 Trial in situ electrical resistance measurement at Sunrise Dam Mine site – February, 2014

A trial measurement for the electrical resistance was conducted on an in situ shotcrete panel sprayed on an underground mine. During the trial measurement, the original prototype probe flat ends was modified to have spikes ends for easier installation in to the in situ shotcrete layer. Figure 4.47 shows the modified probes version V2.2 (wire) and V2.22W (wireless), as well as the wireless data collecting system. Figure 4.48 shows a picture of installed probes and data logging system. The electrical resistance developments with time for shotcrete panel sprayed on underground mine wall is shown in Figure 4.49. The trial measurement results show that, the initial electrical resistance of in situ shotcrete ranges from about 170 to 400 Ohm and it gradually increased to 250 to 500 Ohm within 2 hours curing. The profile of each test results was different for different installation point. It shows the inhomogeneous nature in the sprayed shotcrete.

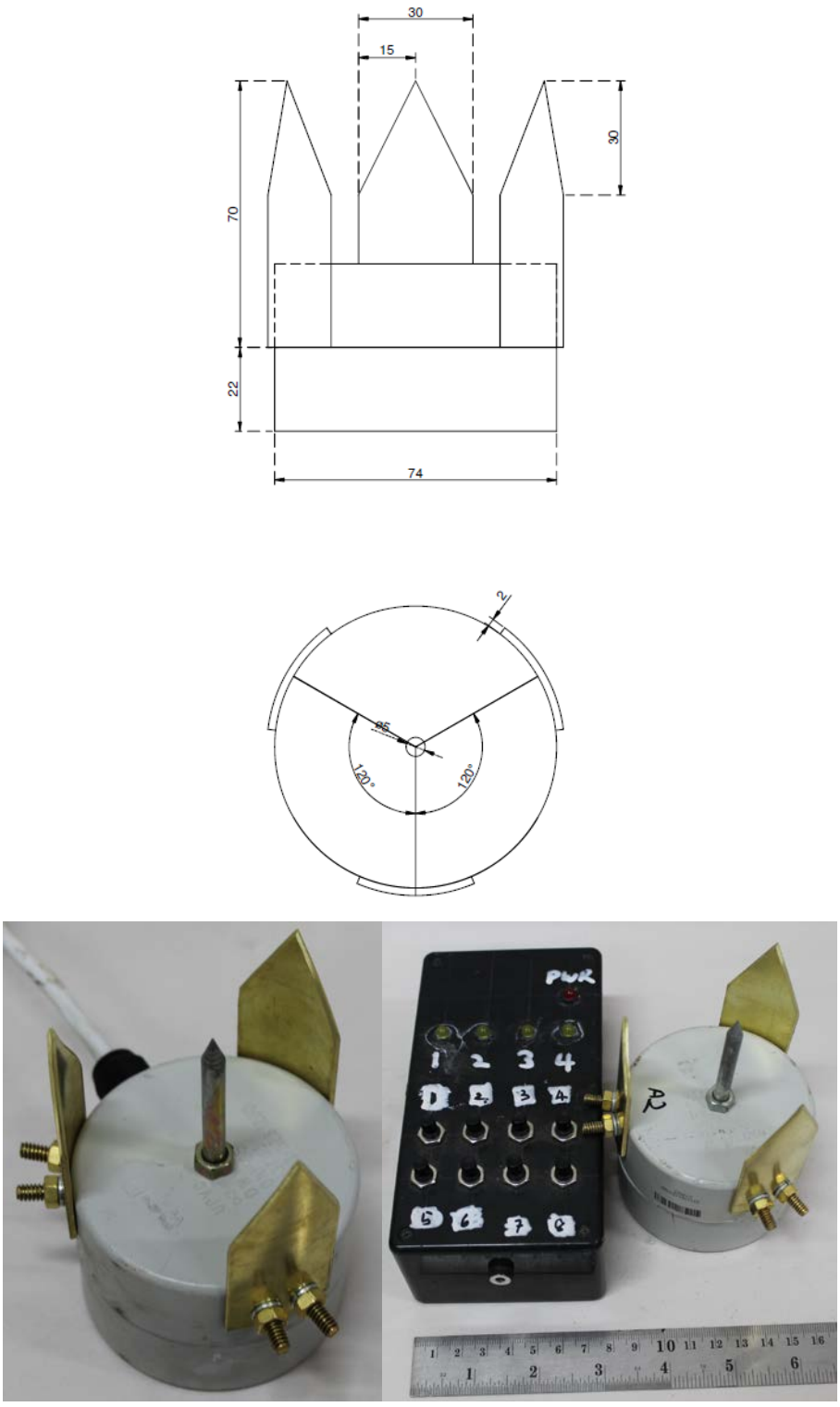

Figure 4.47. Electrical resistance measurement probe version V2.2 (Wire) and V2.2W (Wireless), and wireless data collecting unit for in situ measurement.

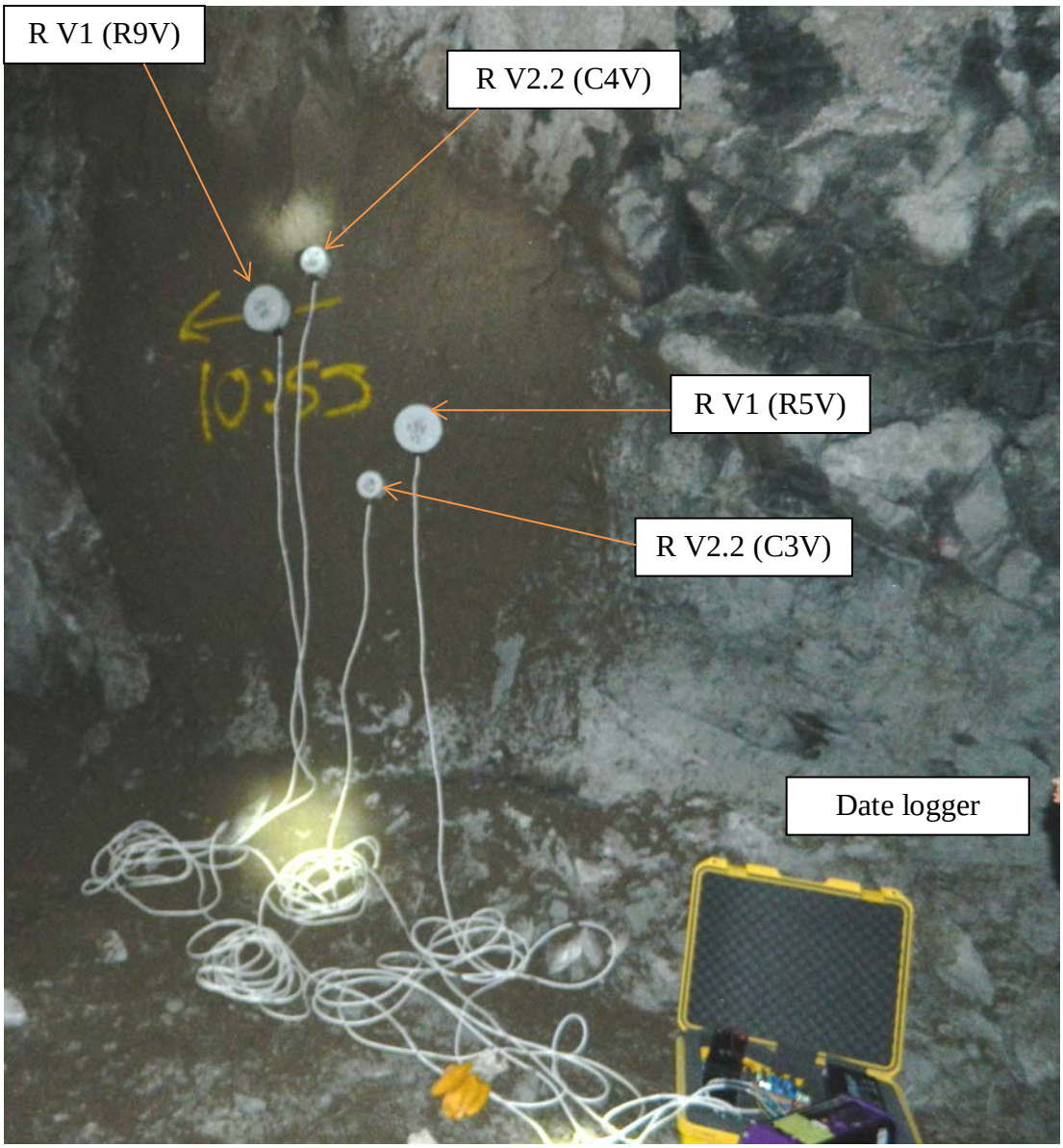

Figure 4.48. In situ electrical resistance measurement on shotcrete panel sprayed on underground mine wall.

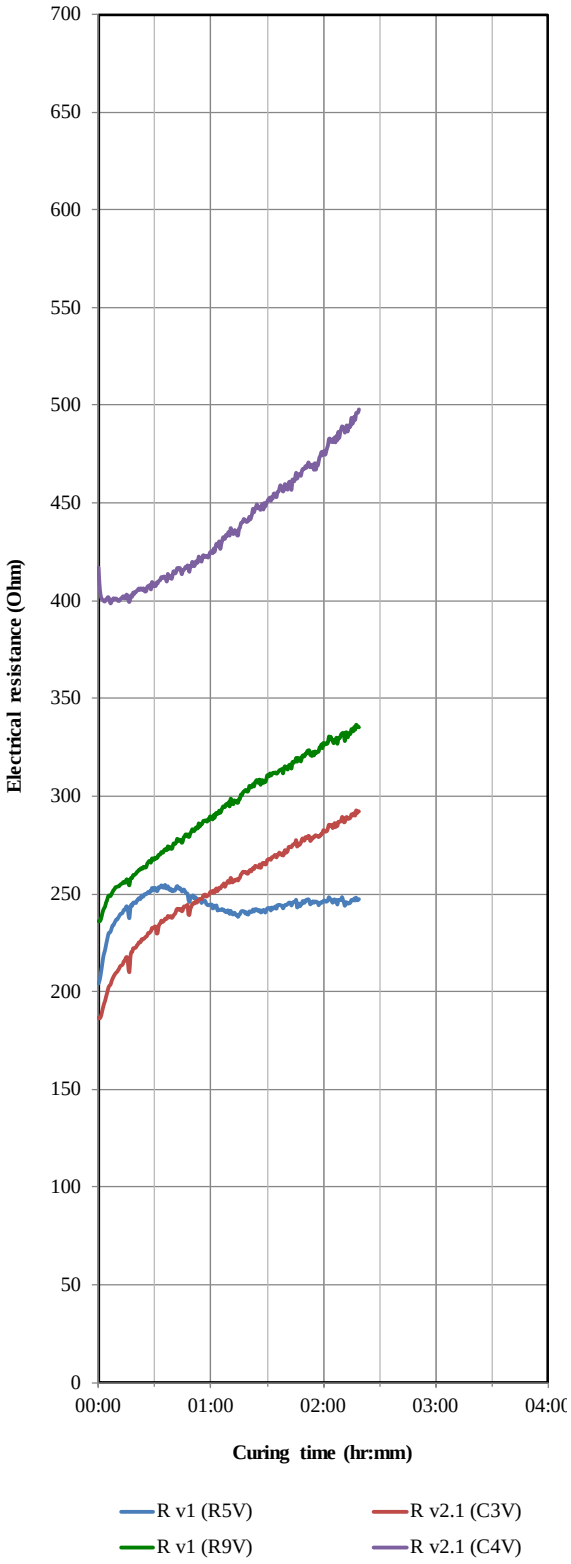

Figure 4.49. Electrical resistance developments with time for shotcrete panel sprayed on an underground mine wall (4 hours).

4.6.2 In situ shotcrete electrical resistance measurement at Sunrise Dam mine site – April 2014

After the initial trial measurement, the electrical resistance of in situ shotcrete used for the actual ground support in an underground mine development was measured for the first time using prototype probe V2.2. This version uses copper wire connected to the data logger for data collection. The probes were installed 15 minutes after shotcrete spraying. Data were logged after 15 minutes of probe installation. A sketch and photo showing location of the probes are presented in Figures 4.50 and 4.51. The electrical resistance developments with time for in situ shotcrete within the first 4 hours is shown in Figure 4.52. The results show that, the electrical resistance profile for an in situ shotcrete were different with different installation. This is due to the inhomogeneous properties of in situ shotcrete. The initial electrical resistance measured with probe ID number CV5, C6V, C7V and C8V were about 125, 170, 210 and to 320 Ohm, respectively and sharply increased to about 210, 300, 300 and 420 Ohm, respectively, within 15 minutes. After 15 minutes the electrical resistance gradually increased to about 295, 375, 375, 450 Ohm, respectively, until 3 hours. After 3 hours the electrical resistance gradually decrease within 4 hours of data collecting period. Figure 4.53 shows a comparison of electrical resistance for in situ shotcrete in the field and electrical resistance of synthetic fibre reinforced concrete measured in the laboratory. It shows that, the results measured in the field and in the laboratory were very similar.

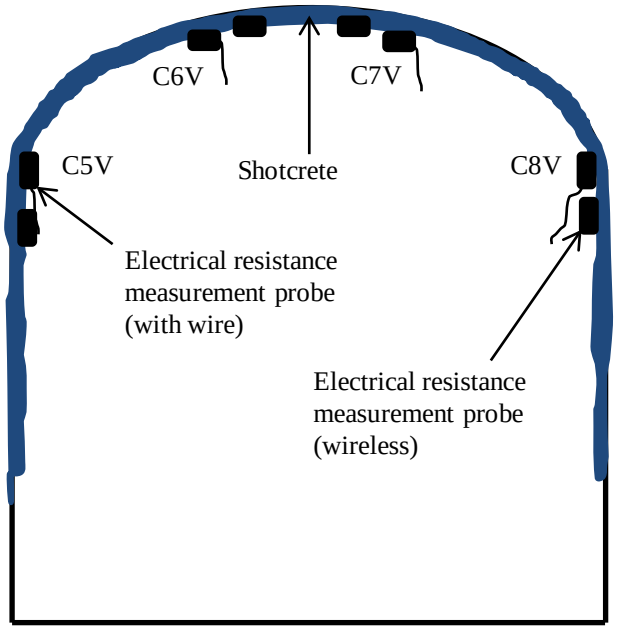

Note: Wireless probes were not fully activated

Figure 4.50. Locations of electrical resistance measurement probes.

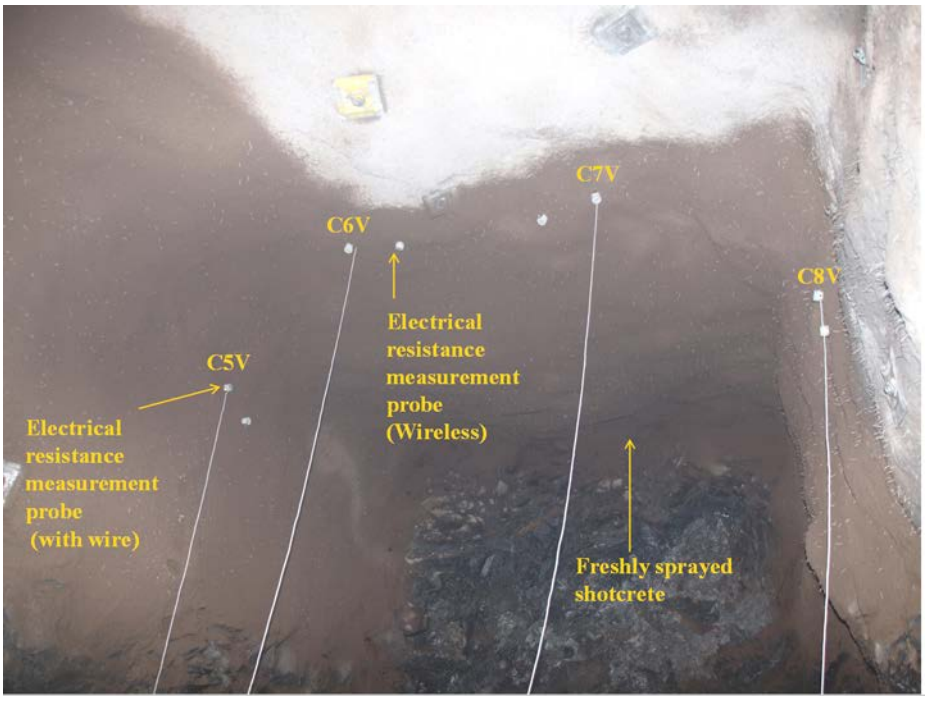

Figure 4.51. Picture showing location of electrical resistance measurement probes.

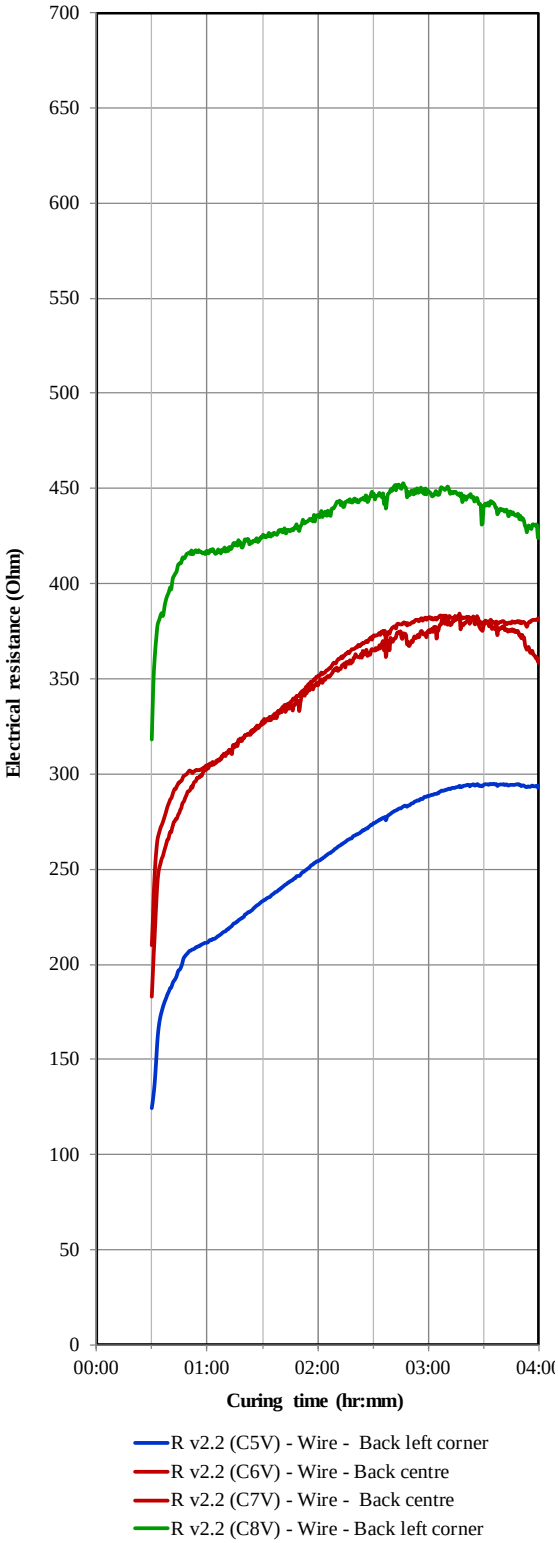

Figure 4.52. Electrical resistance developments with time for in situ shotcrete (4 hours).

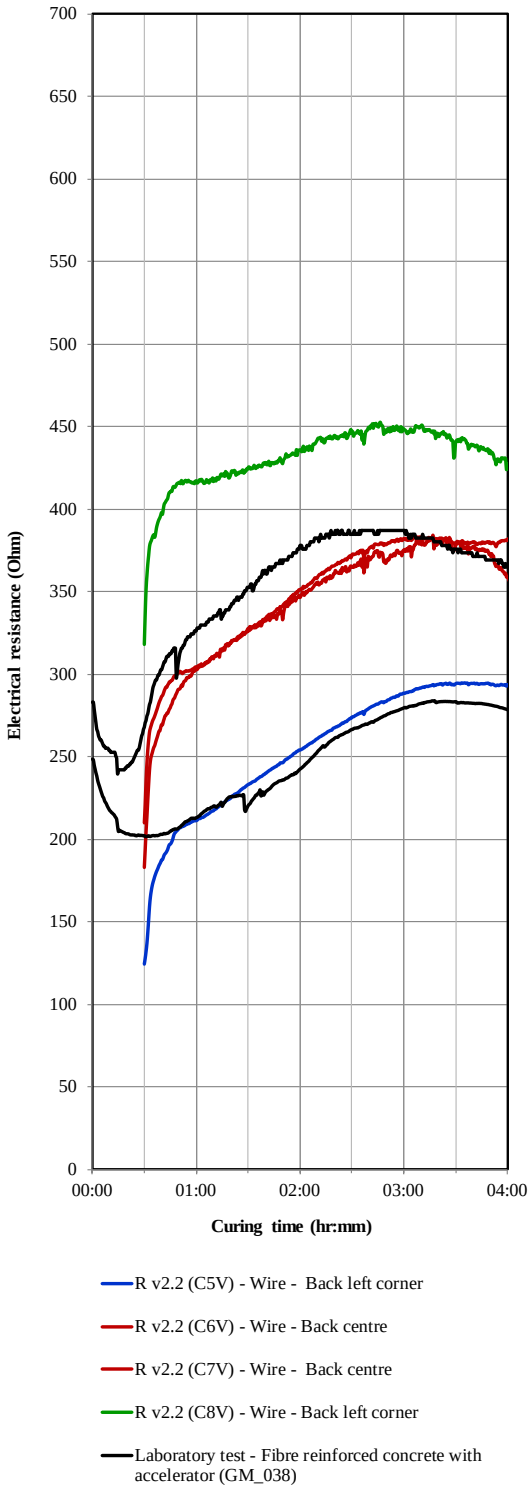

Figure 4.53. A comparison of electrical resistance developments with time for in situ shotcrete and laboratory test results for fibre reinforced concrete with accelerator. (4 hours).

4.6.3 In situ shotcrete electrical resistance measurement at Sunrise Dam mine site – May 2014

The electrical resistance of in situ shotcrete used for the actual ground support in an underground mine development was measured for the second time at Sunrise Dam mine site. At this time, both prototype probe V2.2, which uses copper wire connected to the data logger for data collection and prototype probe V2.2W, which uses wireless system data collection were installed.

In addition, the prototype wireless probes with LED light indicator were also installed at the same time. The development of the function of prototype wireless probes with LED light indicator will be described in the next Chapter 5, Section 5.6.

The probes were installed after 15 minutes of completing shotcrete spraying and data were start logging after 25 minutes of probe installation. A sketch and photo showing location of the probes are presented in Figures 4.54 and 4.55. Figure 4.56 shows the power supply and data logger for wire and wireless electrical resistance measurement probes. Figure 4.57 shows the measurement results from the second time and Figure 4.58 shows a comparison of results from the first time and second time measurement for a different probe locations such as left corner, centre and right corner of the tunnel back (top). The results presented in Figures 4.57 and 4.58 suggested that all the electrical resistance show a similar profile. The different values were due to the inhomogeneous nature of shotcrete at different location.

Figure 4.59 shows the same results but comparing the results measured with wire probes (V2.2) and wireless probes (V2.2W). It shows that both wire probes and wireless probe gave similar results. No data were lost during wireless data transmission.

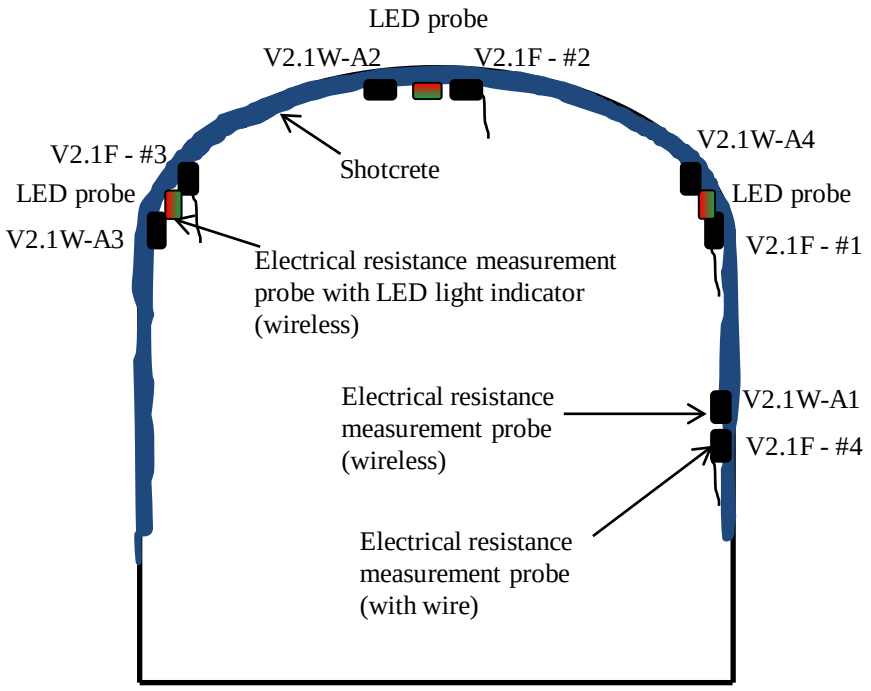

Figure 4.54. Locations of electrical resistance measurement probes.

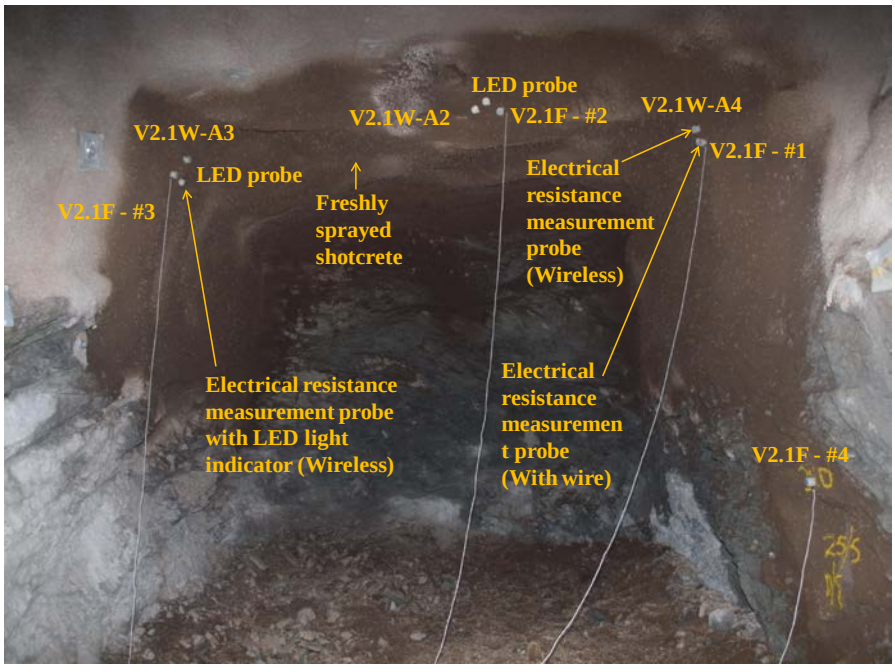

Figure 4.55. Picture showing location of electrical resistance measurement probes.

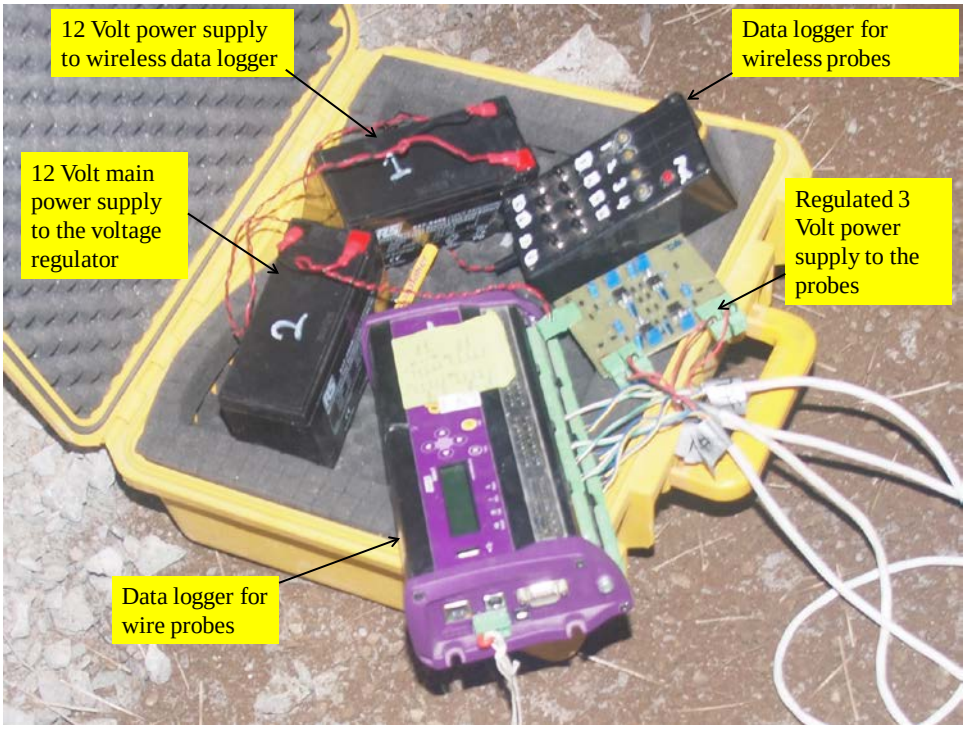

Figure 4.56. Power supply and data logger for wire and wireless electrical resistance measurement probes.

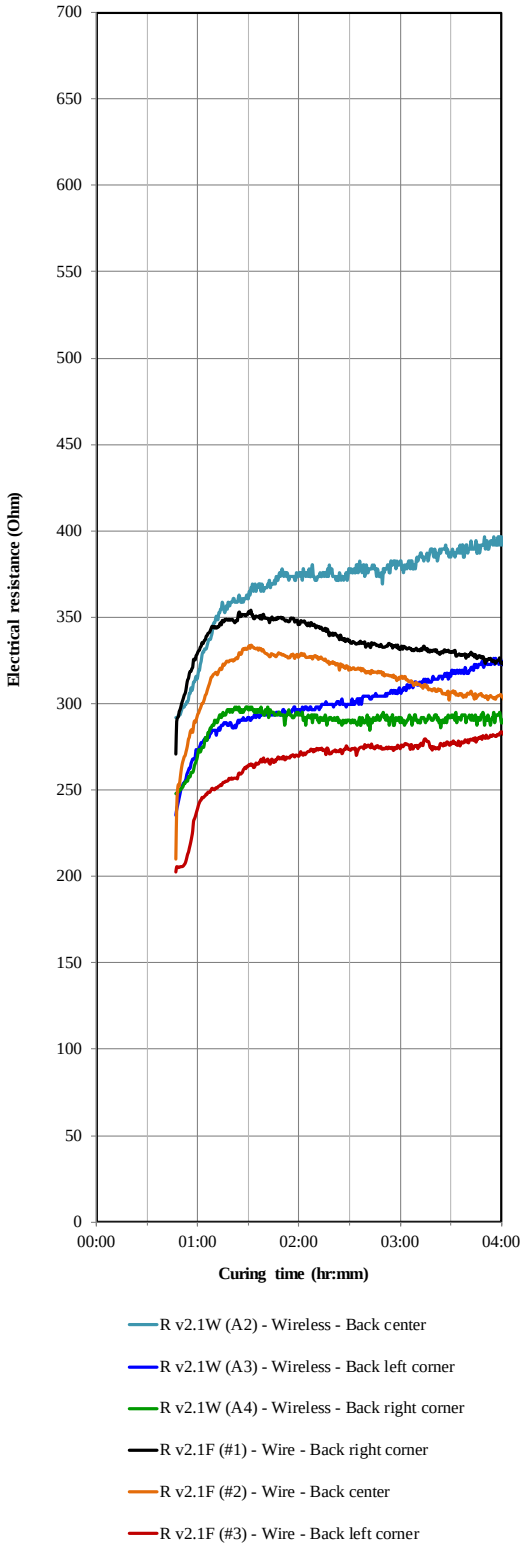

Figure 4.57. Electrical resistance developments with time for in situ shotcrete (4 hours).

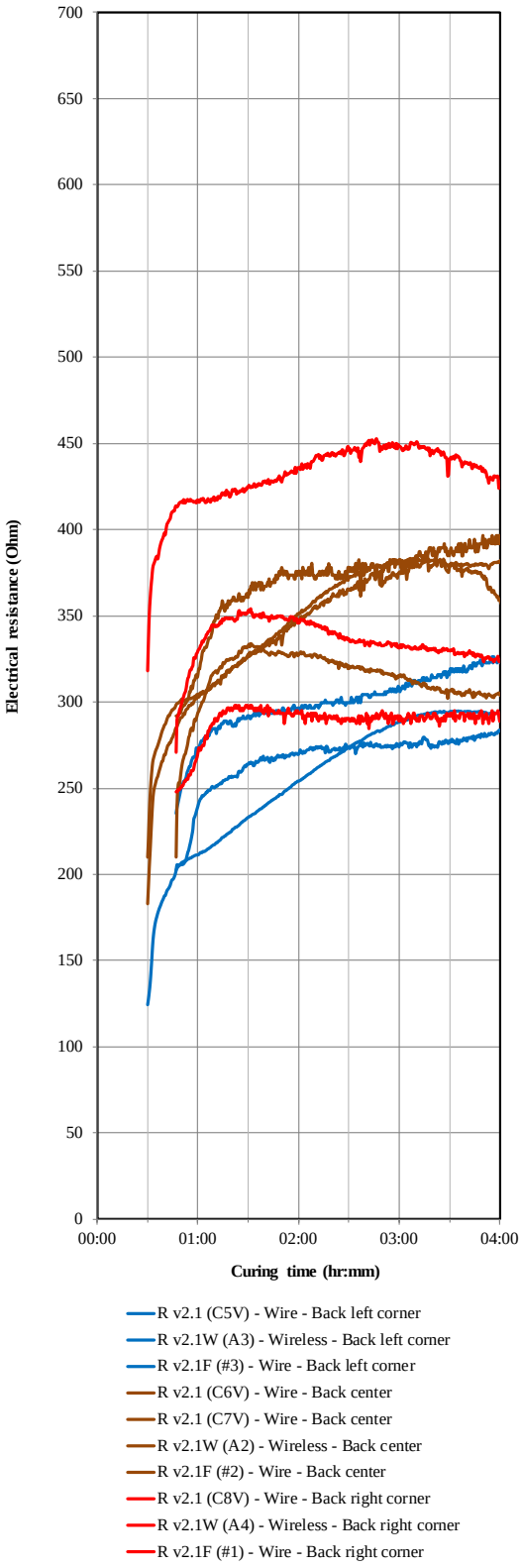

Figure 4.58. Electrical resistance developments with time for in situ shotcrete: A comparison for different locations (4 hours).

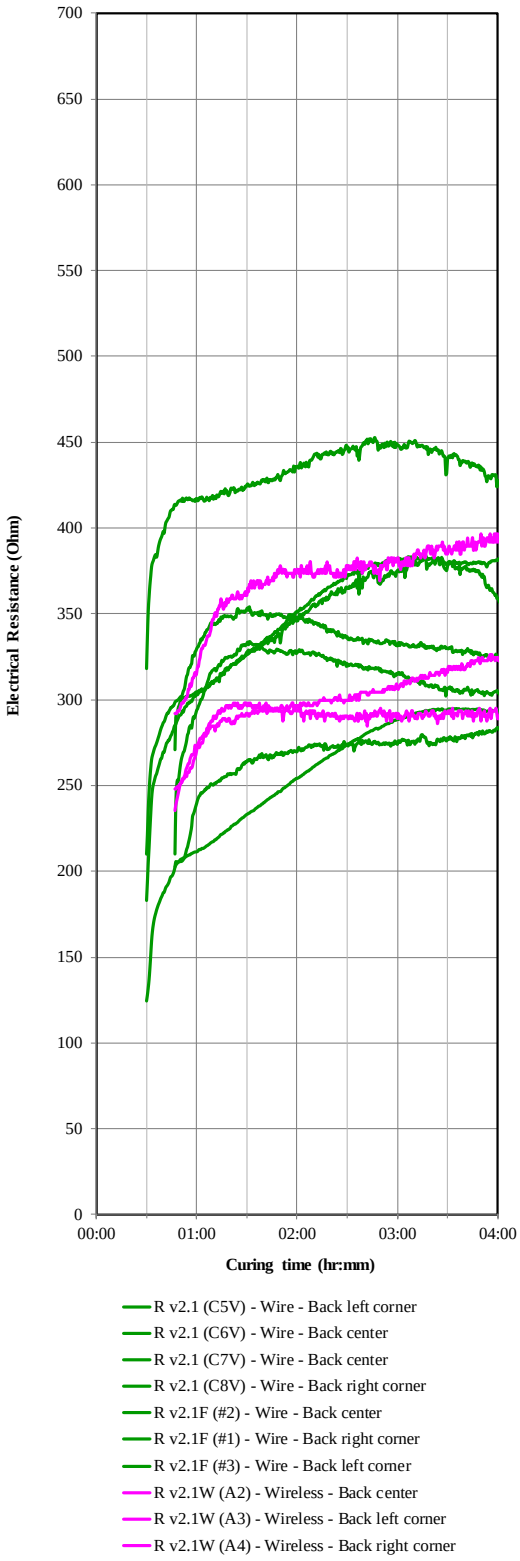

Figure 4.59. Electrical resistance developments with time for in situ shotcrete: A comparison between wire and wireless probe (4 hours).

4.7 Conclusions and discussions

One of the objectives of this research was to determine approximately, by some form of simple, robust, unambiguous field test when re-entry conditions of the shotcrete have been met in situ. Based on a comprehensive literature review described in Chapter 2, and results from the initial research (Chapter 3, 3.8), it was concluded the electrical method is the best method to correlate with the physical and mechanical properties of cement-based materials. During the research stage 1 to 4 a series of shear strength test for different mixes of shotcrete paste were conducted and the shear strength test results were presented in Chapter 3. At the same time, different designs of electrical resistance measurement prototype probes were invented during this research. The prototypes probes were experimented in the laboratory for different mixes, sample geometry, voltage input, electrodes, electrodes layout and geometry, and penetration depth before being tested in the field for in situ shotcrete use in underground mine. The electrical resistance of different shotcrete paste were measured simultaneously while conducting shear strength test. This chapter mainly presented the development of prototype electrical resistance probes and the measurement results with those prototype probes. The conclusions based on the test results from each research stage are as follow.

4.7.1 Research stage 1

All the tests during Research Stage 2 were conducted with 12 Volt supply voltage. The experiments started with “four electrodes liner array”. Electrically, the materials between the electrodes are considered as resistors and they are in a series circuit. The tests were conducted for shotcrete paste and cement-sand mortar without chemical admixture and as well as with chemical admixture (accelerator). The samples were casted in different mould such as, plastic mould, wooden mould and wooden mould with rock (granite and sandstone) base.

All the results show that, the electrical resistance development with time has a unit profile of “Decrease – Increase – Decrease – Continuously Increase” through the curing time. The chemical reactions and hydration process, such as pre-inducting, induction, acceleratory and post-acceleratory process are highly influenced by the electrical resistance through the curing time. Therefore, measurement of electrical resistance development with time can identify the exact time when there is a change in the hydration process.

The electrical resistance ranged from about 10 to 120 Ohm within 8 hours of curing time. The rate and magnitude of electrical resistance with time were different with the mix design and sample size and mould type. Generally, the electrical resistance of shotcrete paste with accelerator is lower than that of shotcrete paste without accelerator. The electrical resistance of sand-cement mortar is higher than that of a shotcrete paste. The larger the samples size the lower the electrical resistance that was measured for the shotcrete paste with or without chemical accelerator. The electrical resistance development with time for shotcrete paste casted in a wooden mould with a sandstone base was more scattered than that measured for a shotcrete paste casted in wooden mould with granite base. After conducting the experiments with different samples size and mould, it was decided to use (350 x 400 x 400 x 100) mm wooden mould with granite base throughout this research.

4.7.2 Research Stage 2

A new electrical resistance measurement probe with four electrodes in a circular array was invented during Research Stage 2 to improve the resolution and accuracy of the resistance measurement. In the circular array the materials which considered the resistors are in a parallel circuit. The invention of electrical resistance probe was patented in Australia as well as Internationally.

During the Research Stage 2, the influences of chemical admixtures, synthetic fibres and aggregates on shotcrete paste on the electrical resistance development with time were measured with prototype probe version V1.

The conclusions based on the results from the Stage 2 experiments with prototype probe version V1 are:

- All the electrical resistance measurement conducted during Research Stage 2 used 3 Volt power supply.

- Although the supply voltage was lower than the experiments used in the Research Stage 1, the measured electrical resistance of the shotcrete paste was higher than that of the shotcrete paste for a given mix design. This is the advantage of using the four electrodes - circular array prototype (Version V1) invented in this research.

- The time at a changing chemical reaction or transition of hydration process can be identified exactly with the high resolution electrical resistance profile development with time.

- Addition of chemical admixtures such as accelerator, superplasticiser, water reducing admixture significantly change the profile of electrical resistance development with time.

4.7.3 Research Stage 3

The objective of the Research Stage 3 was to investigate the influences of electrodes geometry, distance (distance between positives and negative electrode) and material type used in the prototype probe with circular array.

The conclusions based on the results from the Stage 3 experiments are:

- Influences of electrodes distance - The shorter distance between the positives and negative electrode, the better the sensitivity of the measured resistance.

- Influences of geometry and surface area of electrodes - The bigger the surface area of the probe, the better the sensitivity to resistance measured.

- Influences of the overall size the probe - The measurement results show that, the trend of electrical resistance measurements were similar for both prototype probe V1 which has 100 mm diameter overall probe size and prototype probe V2, which has 46 mm diameter overall probe size.

- Influences of the type of material use for electrodes - The electrical resistance measured with probe V2, which has copper positive electrodes shows a lower value than that measured with probe V2.1, which has brass positive electrodes. This confirmed the using a high electrical conductivity material such as copper gives a lower electrical resistivity profile.

- Prototype probe version V2.1 was the best design for the measurement of electrical resistance to correlate with shear strength. The overall size of the prototype probe V2.1 was 74 mm. The positive and negative electrodes were made with 1.5 mm thick brass sheet and 6 mm diameter high tensile chrome plated steel bolt, respectively.

- All the additional electrical resistance profile measured with prototype probe version V2.1 were similar to the electrical resistance profile measured with prototype probe version V1 for a given shotcrete paste and curing time. Though, the results measured with V2.1 were more consistence than that of V1.

- During Research Stage 3, the temperature development due to the heat of hydration was measured simultaneously with a thermocouple while measuring electrical resistance.

- The heat of hydration due to exothermic chemical reactions highly influences the electrical resistance of a shotcrete paste. The higher the heat of hydration evolved from the hydration process, the lower the electrical resistance.

- The changes in electrical current flow happen first and the heat of hydration due to exothermic chemical reactions evolved after a certain amount of delay time. The delay times varies with different types of shotcrete paste.

- The strength development can be under-estimated with the development of heat of hydration.

4.7.4 Research Stage 4

A prototype probe V2.1W, which is a wireless version of prototype probe V2.1, was invented during the Research Stage 4. The influences of accelerator and synthetic fibres, and accelerator synthetic fibres and aggregates (Fibre reinforced concrete) on electrical resistance of shotcrete paste were investigated using prototype wireless probe V2.1W.

The electrical resistance of shotcrete paste with accelerator and synthetic fibres is much less than the electrical shotcrete paste mixed only with accelerator for a given curing time.

The addition of aggregates significantly increases the overall range of electrical resistance.

4.7.5 Research Stage 5

After conducting a series of measurements with the prototype probes in the laboratory, the most suitable probe V2.1/V2.1W was used to measure in situ electrical resistance of shotcrete at early age in the underground mine.

A trial measurement for the electrical resistance was conducted on an in situ shotcrete panel sprayed on the underground mine. During the trial measurement, the original prototype probe flat ends was modified to spikes ends for easier installation into the shotcrete sprayed in an underground mine. The trial measurement results showed that, the initial electrical resistance of in situ shotcrete ranged from about 170 to 400 Ohm and it gradually increased to 250 to 500 Ohm within 2 hours curing. The profile of each test results was different with different installation point. It showed the inhomogeneous nature in the sprayed shotcrete.

After the initial trial measurement, the electrical resistance of in situ shotcrete used for the actual ground support in an underground mine development was measured for the first time using prototype probe V2.2, which uses copper wire connected to the data logger for data collection. Similar to the results from the trial test, the electrical resistance profile of in situ shotcrete were different with different installation place due to the inhomogeneous properties of in situ shotcrete. A comparison of electrical resistance of in situ shotcrete and electrical resistance of synthetic fibre reinforced concrete measured in the laboratory were very similar.

The results from the second time electrical resistance measurement for in situ shotcrete were conducted with both wire probes (V2.2) and wireless probes (V2.2W). The results were similar and no data were lost during wireless data transmission.

4.7.6 Summary for Research Stage 1 to 5

A simple, robust, unambiguous field test instrument was successfully invented in this research to determine when re-entry conditions of the shotcrete have been met in situ. In addition, the instrument invented in this research can measure the electrical resistance development with time for any types of cement base materials, which electrical resistance changes with curing time and the results can correlate with the strength development. However, it important to firmly install the instrument into the shotcrete layer as soon as possible after sprayed.

CHAPTER 5

CORRELATION OF SHEAR STRENGTH AND ELECTRICAL RESISTANCE

5.1 Introduction

This chapter describes the correlation and concept of measuring electrical resistance to infer the development of shear strength with time to determine a safe re-entry time in an underground excavation. The development of shear strength of shotcrete paste at early age presented in Chapter 3 and electrical resistance development with time presented in Chapter 4 are correlated in this Chapter. The correlation is then implemented into developing the theory and tool for calculation a safe re-entry time after shotcrete application in underground excavation.

5.2 Determination of safe re-entry time based on a correlation of electrical resistance with shear strength development with time

A rational estimation of safe re-entry time, for In Cycle Shotcrete (ICS), the electrical resistance measuring probe may be developed as follows:

- Shotcrete that has been sprayed within a standard mould, set up within the excavation. The electrical resistance may be continuously measured and recorded electronically with time using a data-logger.

  and/or

- Shotcrete that has been sprayed onto an overhanging (e.g. roof) or non-overhanging (e.g. wall) surface and a resistance measure taken. Multiple electrical resistance measures may be taken at multiple positions or the probe may be left in position and logged electronically with time.

5.2 Concept and correlation of electrical resistance to infer the development of shear strength to determine safe re-entry time

As described in Chapter 2, shotcrete is a cementitious material, comprising cement, supplementary cementitious materials, fine and coarse aggregates, chemical admixtures, water and in some cases, reinforcing fibres. This heterogeneous mixture of solids and fluids is combined into a mixing device that 'shears' the mix for a given duration. The mix is then pumped to a pneumatic nozzle that sprays it onto a surface to form a heterogeneous layer of solids and fluids that harden into a dense concrete layer. The mechanical properties of the cementitious matrix (i.e. all components other than coarse aggregates and reinforcement fibres) hydrate from a fluid to a paste which then hardens into a solid. The physical, chemical, thermal and mechanical properties of each of the matrix constituents affects the properties of the gelling and hardening shotcrete. The properties of the gelling shotcrete are those associated with the cementitious matrix and therefore it is predominantly the change in the cementitious matrix that will indicate the early mechanical response of shotcrete.

Chapter 3 presented the shear strength of shotcrete paste at early age and Chapter 4 presented the electrical resistance development with time. Figure 5.1 shows a correlation of these three parameters during the first four hours of hydration. Time after spraying is set as the abscissa (Hours), the left ordinate scales the measured electrical resistance (Ohm) and the right ordinate scales the shear strength (kPa).

During the first one hour of hydration the electrical resistance of the in situ shotcrete increased about 50%. After one hour it increased/decreased about 1 % to 5 % within the next 3 hours. Importantly, this non-linear rate of change and the significant magnitude of change define 'electrical resistance' as an imminently suitable shear strength indicator to measure in terms of both accuracy and sensitivity. It is important to recognise that shotcrete paste shows exponential strength gain over the initial hours of hydration of the cementitious components. It is graphs like this, obtained for different shotcrete mixes that can be used in conjunction with

engineering support calculations to determine a safe re-entry time under a freshly sprayed shotcrete layer.

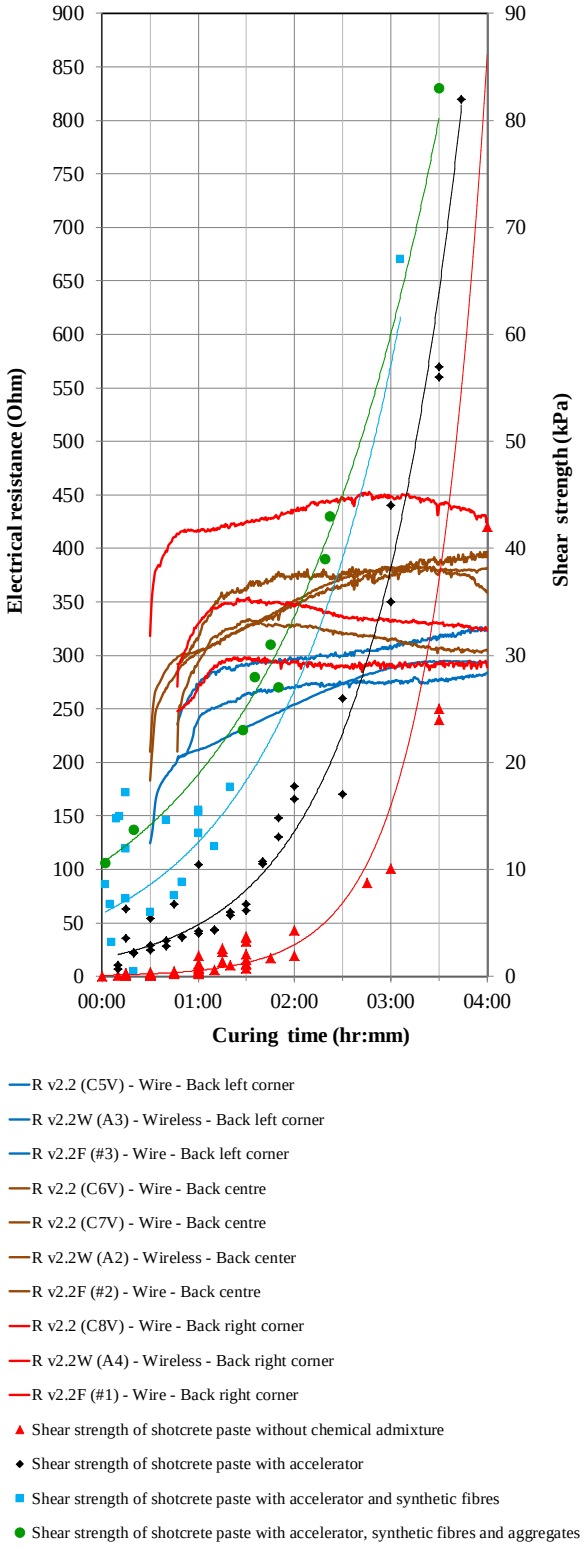

Figure 5.1. Correlation of in situ electrical resistance of Sunrise Dam Mine shotcrete and shear strength development with time.

5.4 Calculation of safe re-entry time for In Cycle Shotcrete

There are two structural requirements of the freshly sprayed shotcrete layer:

1. It must support its own mass within minutes of being applied to the surface.
2. It must support the super-incumbent mass of an estimated unstable volume of rock.

In the first instance, the shotcrete supports its own mass by development of a bond strength (comprising adhesion and mechanical interlock) between itself and the substrate and by development of intrinsic shear strength. Consider a one metre square block of rock with shotcrete layer having a thickness 't_s' (unit weight of 'γ' in kN/m^3), which could be formed within a typical 1.2 x 1.2 meter rockbolt patten used in the mining industry as shown in Figure 5.2.

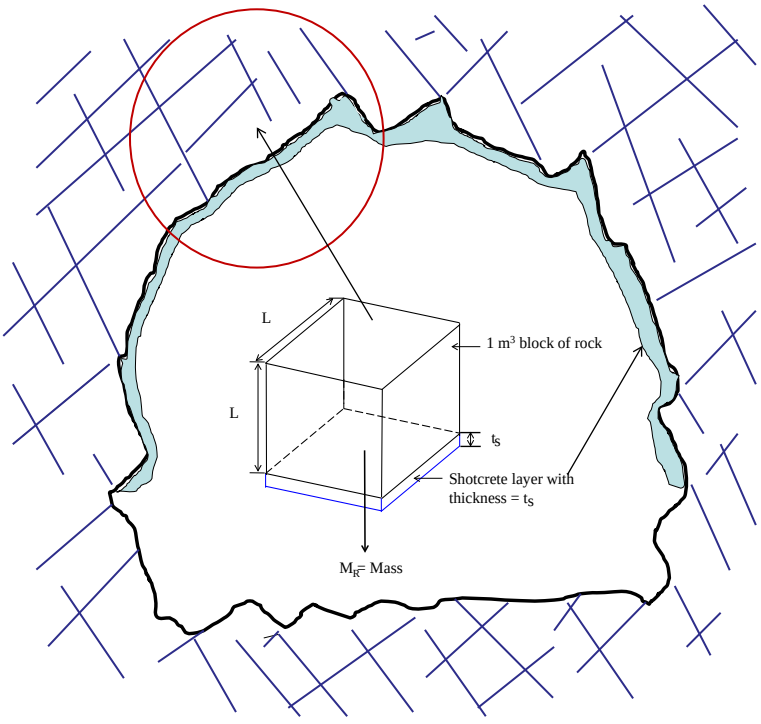

Figure 5.2. A 1 m^3 block of rock with shotcrete layer with thickness (t_s).

In the case of zero shear strength, the minimum bond strength required for the shotcrete layer with thickness 't_s' is equal to the vertical stress due to its own weight. This can be calculate by following equation,

$$\sigma_{vs} = \gamma \times t_s \quad (5.1)$$

Where,

σ_{vs} = Vertical stress (kPa)

γ = Unit weight (kN/m^3)

t_s = Thickness of shotcrete layer (mm)

A typical unit weight of synthetic fibre reinforced shotcrete is 23 kN/m^3. Therefore, a the minimum bond strength required for the shotcrete layer with thickness 't_s' is about (γt_s/1000) kPa (or about 0.023t_s kPa).

In the case of zero bond strength, the minimum shear strength strength required for shotcrete to support its own weight is calculated by the following.

$$\tau_s = \frac{F}{A} \quad (5.2)$$

Where,

τ_s = Shear strength of shotcrete (kPa)

F = Force (kN)

A = Cross sectional area (m^2)

In general, the equation for the Force due to gravity is,

$$F = m_s g \quad (5.3)$$

Where;

m_s = Mass of shotcrete (kg)

g = Gravitational force (kN/kg)

Therefore, equation (5.2) can be written,

$$\tau_s = \frac{m_s \times g}{4 \times \sqrt{2} \times t_s} \quad (5.4)$$

The formula for "mass of a shotcrete (m_s) " is,

$$m_s = V_s \times \rho_s \quad (5.5)$$

Where,

V_s = Volume of shotcrete (m^3)

ρ_s = Density of shotcrete (kg/m^3)

t_s = Thickness of shotcrete layer (m)

Substitute equation (5.5) into equation (5.4), the shear strength can be calculated with equation (5.6),

$$\tau_s = \frac{V_s \times \rho_s \times g}{4 \times \sqrt{2} \times t_s} \quad (5.6)$$

The volume of shotcrete (V_s) for a (1 m^3) block of rock with a shotcrete layer thickness "t_s" is,

$$V_s = 1 \times 1 \times t_s \quad (5.7)$$

Substitute equation (5.7) into equation (5.6),

$$\tau_s = \frac{1^2 \times t_s \times \rho \times g}{4 \times \sqrt{2} \times t_s} \quad (5.8)$$

By eliminating "t_s" in equation (5.8), Shear strength of shotcrete is given by,

$$\tau_s = \frac{\rho_s \times g}{4\sqrt{2}} \quad (5.9)$$

Unit weight of shotcrete (γ_s) is given by,

$$\gamma_s = \rho_s \times g \quad (5.10)$$

Substitute equation (5.10) into equation (5.9) the shear strength of shotcrete is given by,

$$\tau_s = \frac{\gamma_s}{4\sqrt{2}} \quad (5.11)$$

A typical unit weight of synthetic fibre reinforced shotcrete is 23 kN/m^3.

$$\tau_s = \frac{23}{4\sqrt{2}} \quad (5.12)$$

$$\tau_s = 4 \text{ kPa} \quad (5.13)$$

Therefore, the minimum shear strength strength required for shotcrete to support its own weight is typically about 4 kPa.

In almost all cases, where bond and shear strength development initiate simultaneously after spraying, both laboratory investigations and in situ experience have shown that the required strength levels for shotcrete to support itself are easily achieved.

In the second instance, the shotcrete must be capable of supporting the mass of loose rock blocks that may become unstable and represent a risk to personnel that enter the excavation. The volume of loose rock that may become unstable is naturally minimised during blasting by waves that vibrate the excavation surfaces and by subsequent hydro-scaling procedures that clean the excavation surfaces.

The specific arrangement of excavation span, stress and structural geology associated with each excavation will be different and the specification of a single or standard unstable volume of rock is not possible. However, an example calculation shows that within a few hours of spraying, shotcrete is quite capable of supporting a significant volume of unstable rock and that this volume or mass of rock may be calculated as a function of layer thickness and time after spraying.

Consider, the case of the minimum shear strength required to be developed within the shotcrete to support a regular tetrahedral block of rock with 1.0 m side lengths as shown in Figure 5.3. If this block existed in the roof of an underground excavation, its face triangle (i.e. the expression of its shape visible in the roof when viewed from beneath) would be an equilateral triangle with side-lengths of 1 meter. Figure 5.4 shows the thickness of shotcrete along shear plane.

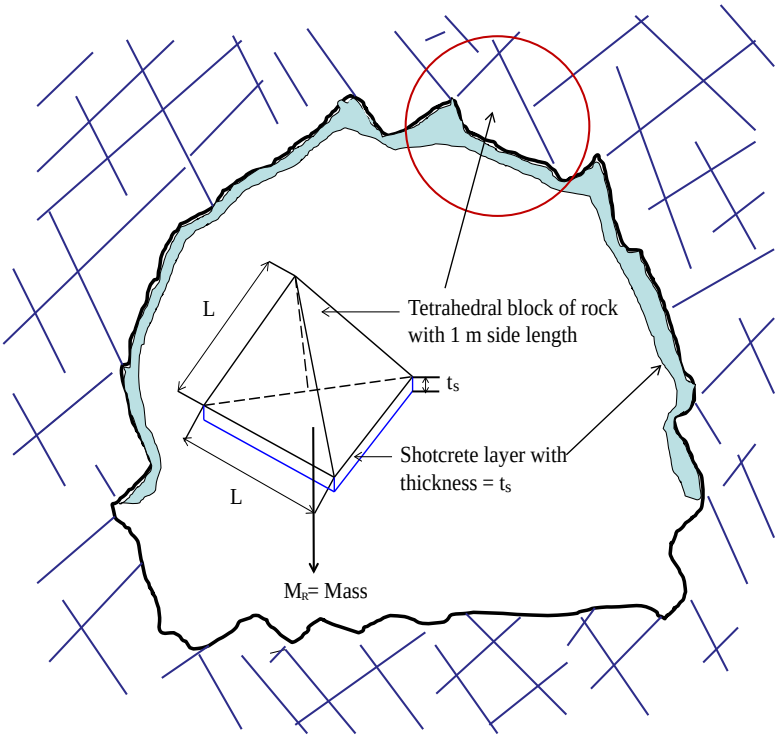

Figure 5.3. A tetrahedral block of rock with shotcrete layer with thickness (t_s).

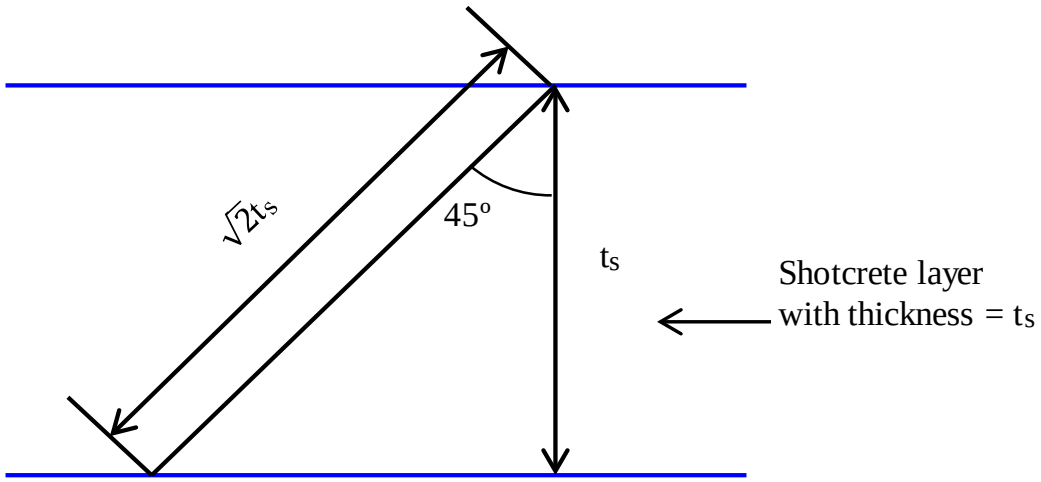

Figure 5.4. Thickness of shotcrete along a shear plane.

The minimum shear strength required for shotcrete to support 1 m^3 block and regular tetrahedral block of rock with 1 m side length can be calculated by the following equation.

$$\tau_s = \frac{M_R \times g}{4 \times \sqrt{2} \times t_s} \quad (5.\ 14)$$

Where,

τ_s = Shear strength of shotcrete (kPa)

M_R = Mass for rock block (kg)

g = Gravitational force (kN/kg)

t_s = Thickness of shotcrete layer (m)

This example calculation is illustrated in Table 5.1 for a minimum shear strength required for shotcrete with different thickness to support 1 meter cube block of rock and in Table 5.2 for a minimum shear strength required for shotcrete with different thickness to support a regular tetrahedral block of rock with 1 meter side lengths. The time required for a shotcrete to achieve the corresponding minimum shear strength was calculated from the correlation of best fit shear strength development and curing time curves shown in Figure 5.5.

Table 5.1. Minimum shear strength required for shotcrete with different thickness to support 1 meter cube block of rock.

Shotcrete thickness (mm)	Minimum required shear strength of shotcrete to support 1 meter cube block of rock (Mass=2.7 tonne) (KPa)	Curing time for shotcrete paste without additive and admixture (hr:mm)	Time for shotcrete paste with accelerator (hr:mm)	Time for shotcrete paste with accelerator and synthetic fibres (hr:mm)	Time for shotcrete paste with accelerator, synthetic fibres and aggregates (hr:mm)
50	93.6	3:39	3:34	3:35	3:44
60	78.0	3:33	3:24	3:22	3:26
70	66.8	3:28	3:17	3:11	3:10
80	58.5	3:24	3:10	3:02	2:56
90	52.0	3:21	3:04	2:53	2:44
100	46.8	3:17	2:58	2:46	2:33

Table 5.2. Minimum shear strength required for shotcrete with different thickness to support a regular tetrahedral block of rock with 1 meter side lengths.

Shotcrete thickness (mm)	Minimum required shear strength of shotcrete to support a regular tetrahedral block of rock (Side Lengths = 1 metre , Mass = 0.4 tonne) (KPa)	Curing time for shotcrete paste without additive and admixture (hr:mm)	Curing time for hotcrete paste with accelerator (hr:mm)	Curing time for shotcrete paste with accelerator and synthetic fibres (hr:mm)	Curing time for shotcrete paste with accelerator, synthetic fibres and aggregates (hr:mm)
10	67.5	3:29	3:17	3:12	3:11
20	33.8	3:07	2:42	2:23	2:00
30	22.5	2:55	2:21	1:54	1:18
40	16.9	2:46	2:06	1:34	0:49
50	13.5	2:39	1:55	1:18	0:26
60	11.3	2:34	1:46	1:05	0:07
70	9.6	2:29	1:38	0:54	-
80	8.4	2:25	1:31	0:44	-
90	7.5	2:21	1:25	0:36	-
100	6.8	2:18	1:19	0:29	-

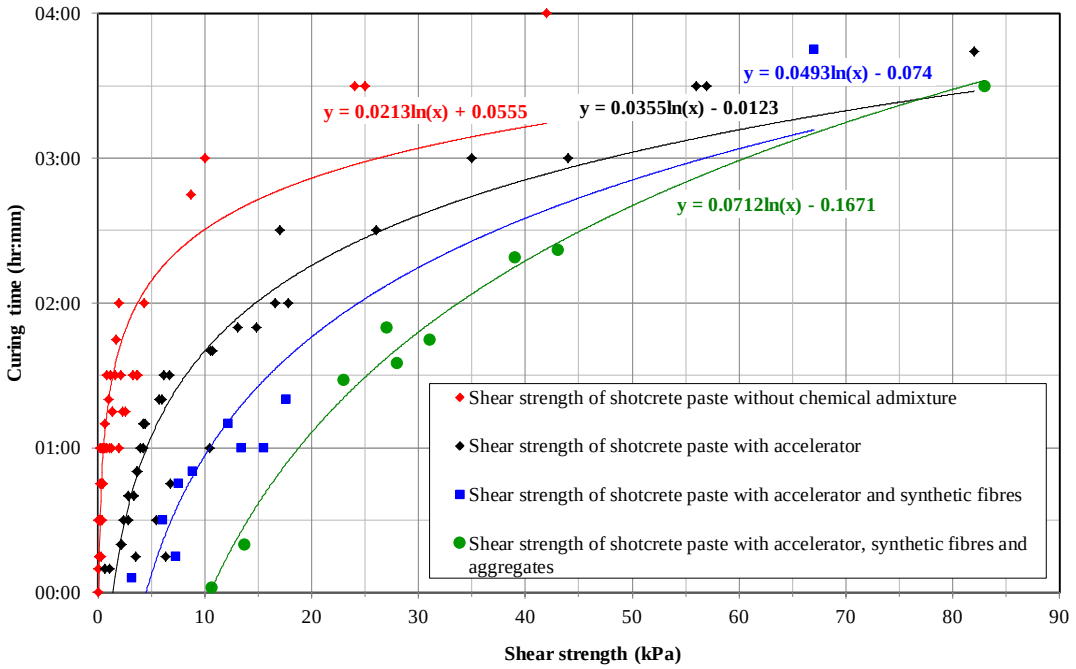

Figure 5.5. Correlation of best fit shear strength development and curing time curves.

Figure 5.6 shows the shear strength required to be developed for different thickness layers of shotcrete to support 1 meter cube block of rock. It is computed for a rock with an average unit weight 27 kN/m^3 (this is a common assumption for most rock types) which results in a total mass of the block of 2700 kg (2.7 tonne). The graphs show that an average shotcrete layer of about 50 mm thickness needs to develop a shear strength of about 93 kPa in addition to supporting its own mass. That level of shear strength will develop at about 3:45 (hr:mm) after spraying, for a shotcrete mix with accelerator, synthetic fibres and aggregates.

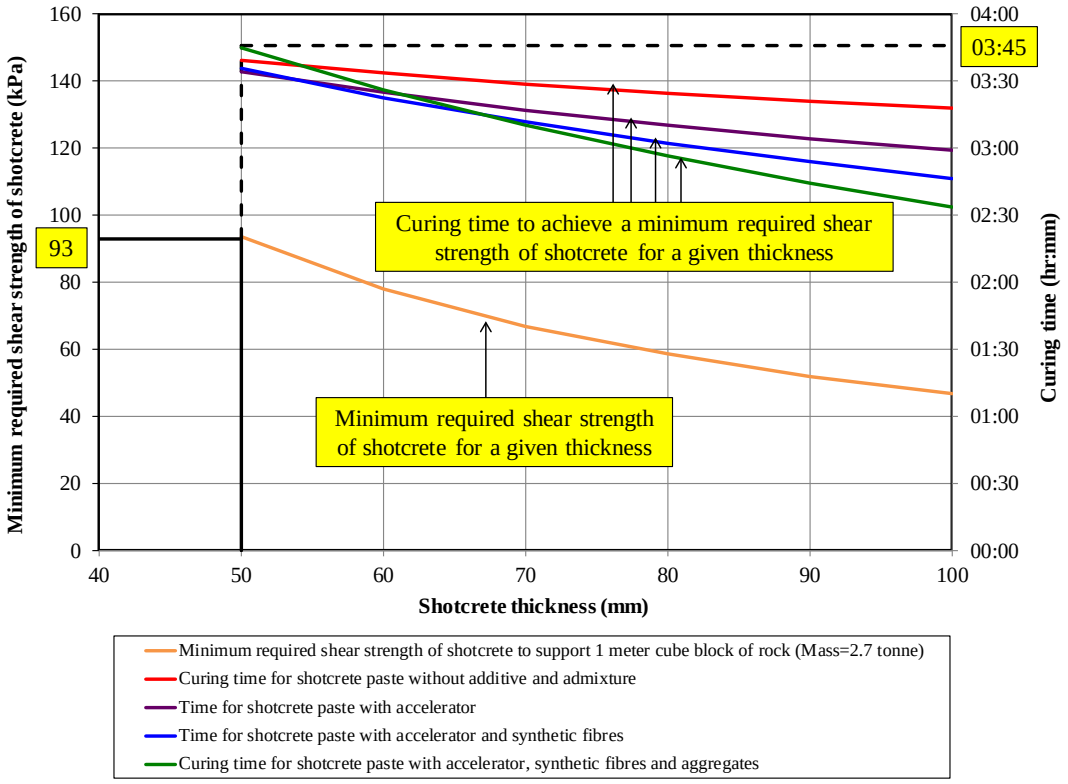

Figure 5.6. A graph of minimum shear strength required to develop in a shotcrete in order to support 1 meter cube block of rock.

Figure 5.7 shows the shear strength required to be developed for different thickness layers of shotcrete to support a regular tetrahedral block of rock with 1 m side lengths. It is also computed for a rock with an average unit weight 27 kN/m^3 (this is a common assumption for most rock types) which results in a total mass of the block of 400 kg (0.4 tonne). The graphs show that an average shotcrete layer of about 50 mm thickness needs to develop a shear strength of about 13.5 kPa in addition to supporting its own mass. That level of shear strength will develop at about 40 minutes after spraying, for a shotcrete mix with accelerator, synthetic fibres and aggregates. It is clear that more wait-time is required for thinner layers of shotcrete.

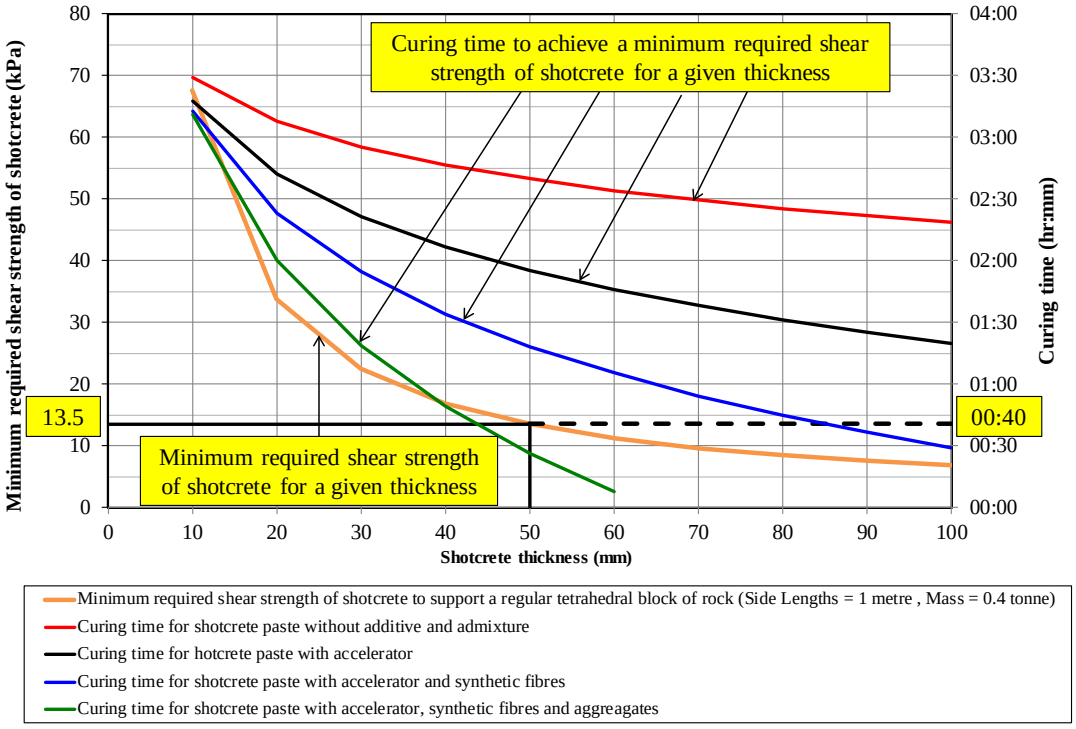

Figure 5.7. A graph of minimum shear strength required to develop in a shotcrete in order to support a regular tetrahedral block of rock with 1 meter side lengths.

5.5 Development of prototype wireless probe with LED light indicator

Based on the correlation of in situ electrical resistance and shear strength development with time described in Section 5.2 and the calculation of safe re-entry time for In Cycle Shotcrete (ICS) presented in Section 5.4, another prototype probe with LED light indicator was invented during this research. A photo of electrical resistance measurement probe with LED light indicator is shown in Figure 5.8. The flow chart algorithm to determine the LED to indicate red or green light is shown in Figure 5.9.

Figure 5.8. Electrical resistance measurement probe with LED light indicator.

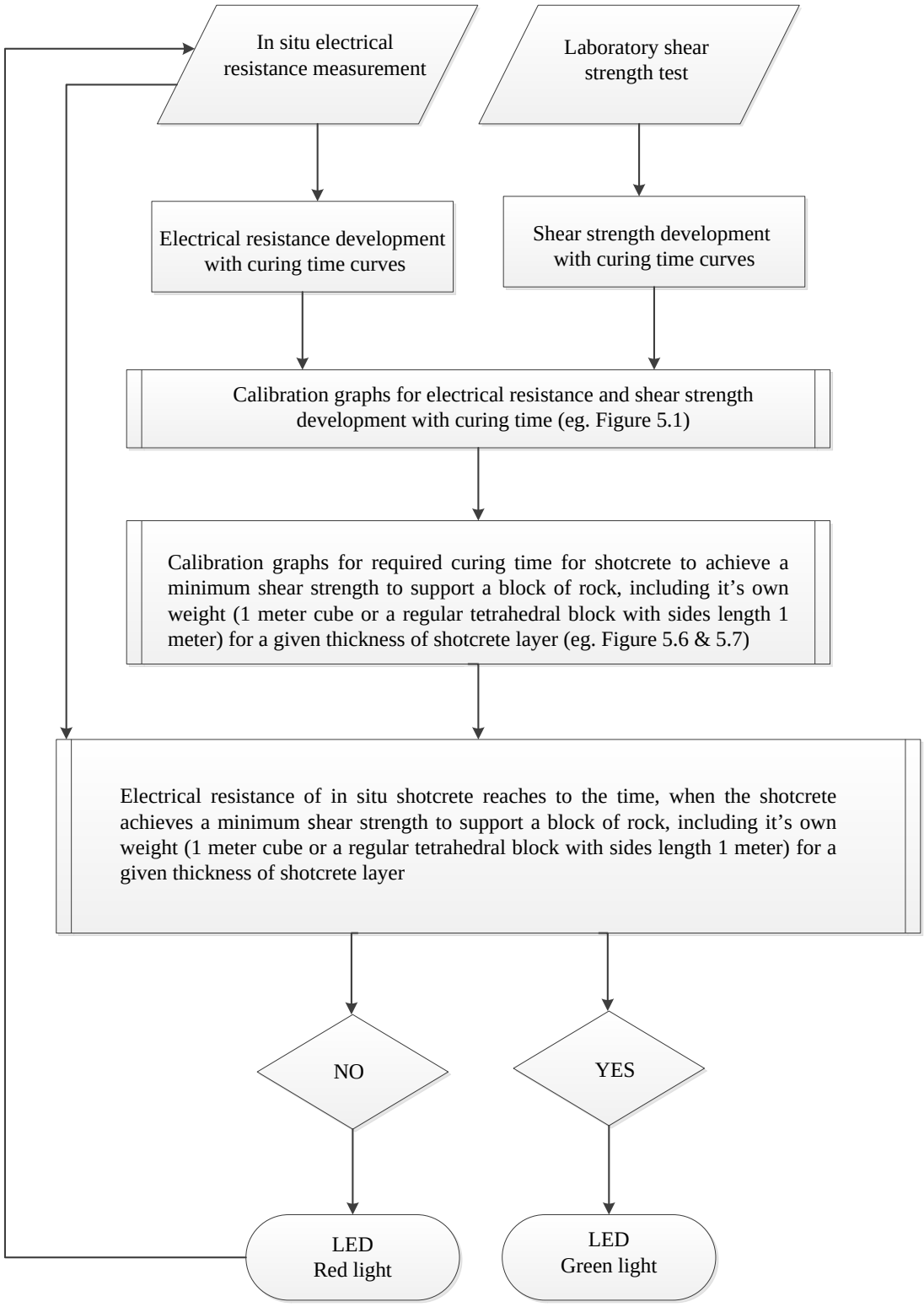

Figure 5.9. Flow chart algorithm to determine the LED to indicate red or green light.

Considering an unstable block a regular tetrahedral block with 1 meter sides length (0.4 tonne) or 1 meter cube (2.7 tonne) of rock, which could be formed with a typical (1.2 x 1.2) meter bolt patten used in the mining industry:

- The LED light indicates “Red” when the shear strength of shotcrete less than the minimum required strength to support its own weight and an unstable 0.4 or 2.7 tonne block of rock.

- The LED light turn to “Green” when the shear strength of shotcrete reaches the minimum required strength to support its own weight and an unstable 0.4 or 2.7 tonne block of rock.

5.6 Conclusions and discussions

This chapter describes the correlation and concept of measuring electrical resistance to infer the development of shear strength with time to determine a safe re-entry time in an underground excavation.

During the first hour of hydration the electrical resistance of the in situ shotcrete increased about 50%. Following this initial period it increased/decreased about 1 % to 5 % within the next 3 hours. At the same time the shotcrete paste shows exponential strength gain over the initial hours of hydration of the cementitious components. This non-linear rate of change and the significant magnitude of change define ‘electrical resistance’ as an imminently suitable shear strength indicator to measure in terms of both accuracy and sensitivity.

The shear strength required to be developed for a 50 mm thick layer of shotcrete to support 1 meter cube block of rock is about 100 kPa, in addition to supporting its own mass. That level of shear strength will develop at about 3 hours after spraying, for the shotcrete mix with 4 % accelerator and synthetic fibres and about

3:45 (hr:mm) after spraying, for the shotcrete mix without accelerator and synthetic fibres.

The shear strength required to be developed for a 50 mm thick layer of shotcrete to support a regular tetrahedral block of rock with 1.0 m side lengths is about 13.5 kPa, in addition to supporting its own mass. That level of shear strength will develop at about 40 minutes after spraying, for the shotcrete mix with 4 % accelerator and synthetic fibres and about 2.25 hours after spraying, for a mix without accelerator and synthetic fibres.

A wireless prototype probe with LED light indicator was invented during this research. The LED has been programmed to turn the light to indicate “Red” when the shear strength of the shotcrete is less than the minimum required strength to support its own weight and an unstable 0.4 or 2.7 tonne block of rock. The LED light turns to “Green” when the shear strength of the shotcrete reaches the minimum required strength to support its own weight and that of an unstable 0.4 or 2.7 tonne block of rock.

CHAPTER 6

MECHANICAL PROPERTIES OF HARDENED SHOTCRETE

6.1 Introduction

Chapter 5 described and correlated the electrical resistance and shear strength of shotcrete paste at early age of 0 to 8 hours, which can determined the safe re-entry time. After 8 hours the cement hydration process continues and thus the strength of shotcrete also increases with an increasing time. Generally, the ultimate strength of shotcrete is defined when 90 % of cement hydration is completed at 28 days of curing. The strength development throughout the complete hydration process also can be monitored with the instrument invented during this research. The electrical resistance after 24 hours is estimated to be continuously increased with the increasing degree of cement hydration. Therefore the electrical resistance of shotcrete after 24 hours was not measured in this research. However, the mechanical properties of hardened shotcrete, that is, after 24 hours curing were studied during this research to understand a full scale of strength (UCS, shear & tensile strength) development. The study included both the peak and post-peak (elastic and plastic) regions under uniaxial and triaxial loading, to predict the shear strength in terms of cohesion, friction and dilation angle and, to examine how these parameters vary with curing time.

6.2 A complete stress-strain relation

In the elastic region the strains are linearly related to the stress as assumed in Hooke's Law (Hooke, 1705). In the elastic region strains are uniquely determined by stresses and can be computed directly using Hooke's law without any regard to how the stress state was attained. Mathematically, elastic strain and stress can be simply written as:

$$\varepsilon^{e} = \frac{\sigma}{E} \tag{6. 1}$$

Where, ε^{e} is elastic strain, σ is stress and E is Young's modulus.

In the plastic region, the strains are not uniquely determined by the stresses but depend on the whole history of loading or how the stress state was reached. An essential part of plasticity theory is to define when the material starts to deform or yield. A failure criterion is used to describe by a point at which fracture or yield occurs. The criterion under which yield occurs is called a yield criterion. The most widely used yield criterion is the Coulomb yield criterion (Coulomb, 1776),

$$\tau = c + \sigma_n \tan\emptyset \tag{6. 2}$$

Where, τ and σ_n represent shear stress and normal stress, respectively. Compressive stress components are treated as positive, as is usual in geomechanics. The parameters c and ϕ are assumed to be constants called the cohesion and the angle of internal friction. In reality, c and ϕ change with stress level. Once the yield criterion is satisfied, the material will flow obeying the flow rule. The flow rule is termed associated if the plastic strains are associated directly with the yield surface and if not it is termed non-associated. The non-associated flow rule states that the plastic strain rate is proportional to the derivatives of the plastic potential with respect to the corresponding stress. This can be described by the following equation.

$$\delta\varepsilon^p = \lambda \frac{\partial g}{\partial g} \tag{6. 3}$$

where, $\delta\varepsilon^p$ is plastic strain increment, λ is Lagrange or plastic multiplier and 'g' is a plastic potential. The definition of plastic potential function 'g' suggested by Radenkovic (1961) is,

$$g = \tau + \sigma \sin\psi + \text{constant} \tag{6. 4}$$

where, ψ is the dilation angle. Hansen (1958) suggested, a dilation angle is defined as the ratio of plastic volume change over plastic shear strain. The direction of

deformation which lies at a dilation angle above the shearing surface is shown in Figure 6.1.

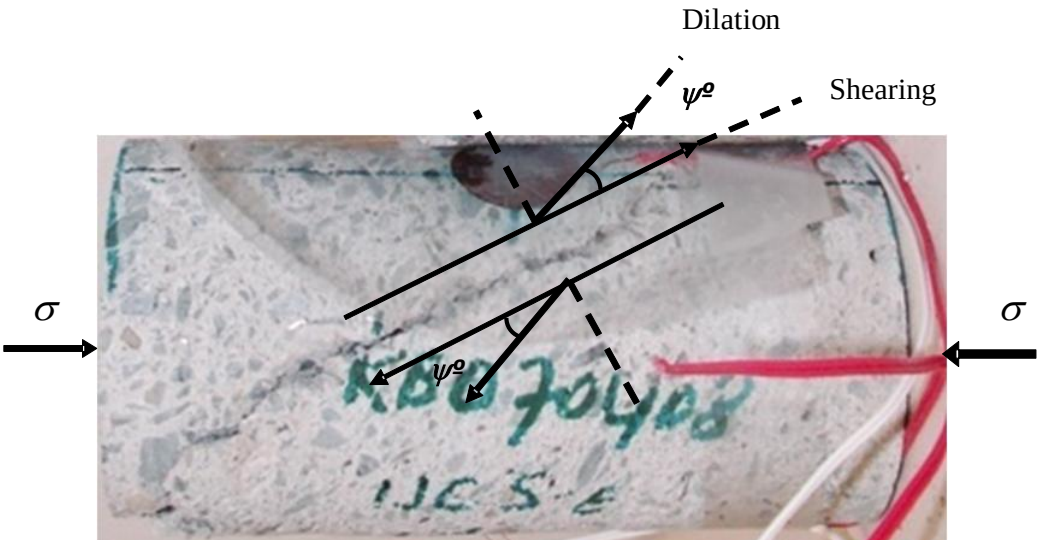

Figure 6.1. Shearing and dilation.

For the Mohr-Coulomb yield criterion, Equation (6.4) can be written in terms of principal stresses for triaxial test conditions where, σ2=σ3,

$$g = \frac{1}{2}(\sigma_1 - \sigma_3) + \frac{1}{2}(\sigma_1 + \sigma_3)\sin\psi + \text{constant} \qquad (6.5)$$

The principal plastic strain rates are obtained by differentiating equation (6.5) with respect to the principal stresses as given in equation (6.3):

$$\begin{bmatrix} \delta\varepsilon_1^p \\ \delta\varepsilon_2^p \\ \delta\varepsilon_3^p \end{bmatrix} = \lambda \begin{bmatrix} \frac{1}{2}(1+\sin\psi) \\ \frac{1}{2}(-1+\sin\psi) \\ \frac{1}{2}(-1+\sin\psi) \end{bmatrix} \qquad (6.6)$$

where, $\delta\varepsilon_1^p$, $\delta\varepsilon_2^p$ and $\delta\varepsilon_3^p$ are major, intermediate and minor plastic strain increment. It follows that,

$$\delta\varepsilon_v^p = \lambda \sin\psi \quad (6.7)$$

$$\delta\varepsilon_1^p = \frac{1}{2}\lambda(1 + \sin\psi) \quad (6.8)$$

where, the volumetric strain increment $\delta\varepsilon_v^p$, is the sum of $\delta\varepsilon_1^p$, $\delta\varepsilon_2^p$ and $\delta\varepsilon_3^p$.

By eliminating λ from equations (7) and (8), sin ψ is given by,

$$\sin\psi = \frac{\delta\varepsilon_v^p}{2\delta\varepsilon_1^p + \delta\varepsilon_v^p} \quad (6.9)$$

This equation for sin ψ can be expressed as,

$$\sin\psi = \frac{1}{(2\delta\varepsilon_1^p/\delta\varepsilon_v^p)+1} \quad (6.10)$$

The ratio $2\delta\varepsilon_1^p/\delta\varepsilon_v^p$ is equivalent to the slope of the volumetric – axial strain curve. Therefore, the inverse of the slope can be substituted into Equation (6.10) to obtain the dilation angle ψ.

A plastic strain ε^p found by subtracting the elastic strain from the total strain, may written as:

$$\varepsilon^p = \varepsilon^t - \varepsilon^e \quad (6.21)$$

6.3 Mix design and curing method

The wet mix shotcrete used in these investigations is similar to that used at the one of underground gold mines in the Eastern Gold Fields region, Kalgoorlie, Western Australia. Shotcrete panels were sprayed on site and delivered to the WASM geomechanics laboratory on the same day. The specimen were cored from the panels and stored in a curing chamber, which was set at 30ºC and 90% humidity. The tests were conducted on three batches of samples after at four different curing periods

(1, 3, 7 and 28 days). All of the shotcrete batches have the same mix design which given in Table 6.1.

Table 6.1. Steel fibre reinforced shotcrete mix design.

Material	**Quantity for 1 m^3**
Cement (General Purpose)	440 kg
Coarse aggregate (Max. 7 mm)	220 kg
Crusher dust	1300 kg
Sand	1640 kg
Water	150 Lt
Steel fibres (Dramix)	30 kg
Liquid Meyco (MS 685)	11 Lt
Delvo Stabiliser	5 Lt
Rheobuild 1000	8 Lt
Pozzolith 322NI	1.3 Lt
Accelerator	4% of cement

6.4 Test method

Both uniaxial and triaxial compressive test were conducted according to the test method suggested by International Society of Rock Mechanics (ISRM 1981, 1999 & Fairhurst & Hudson, 1983). These tests were performed using an Instron, servo controlled hydraulic testing machine. The loading rate of the machine was set at 0.12 mm/min. The strains were measured with two biaxial foil strain gages with 10 mm gage length that were installed diametrically at specimen mid-height. The triaxial compression test is a useful test method to obtain complete stress-strain response of the SFRS sample and to derive the shear strength parameters and dilation angles.

Three different confining pressures 1, 2 and 3 MPa were applied to three specimens. Figure 6.2 shows Instron, servo controlled hydraulic testing machine for triaxial and UCS test set up.

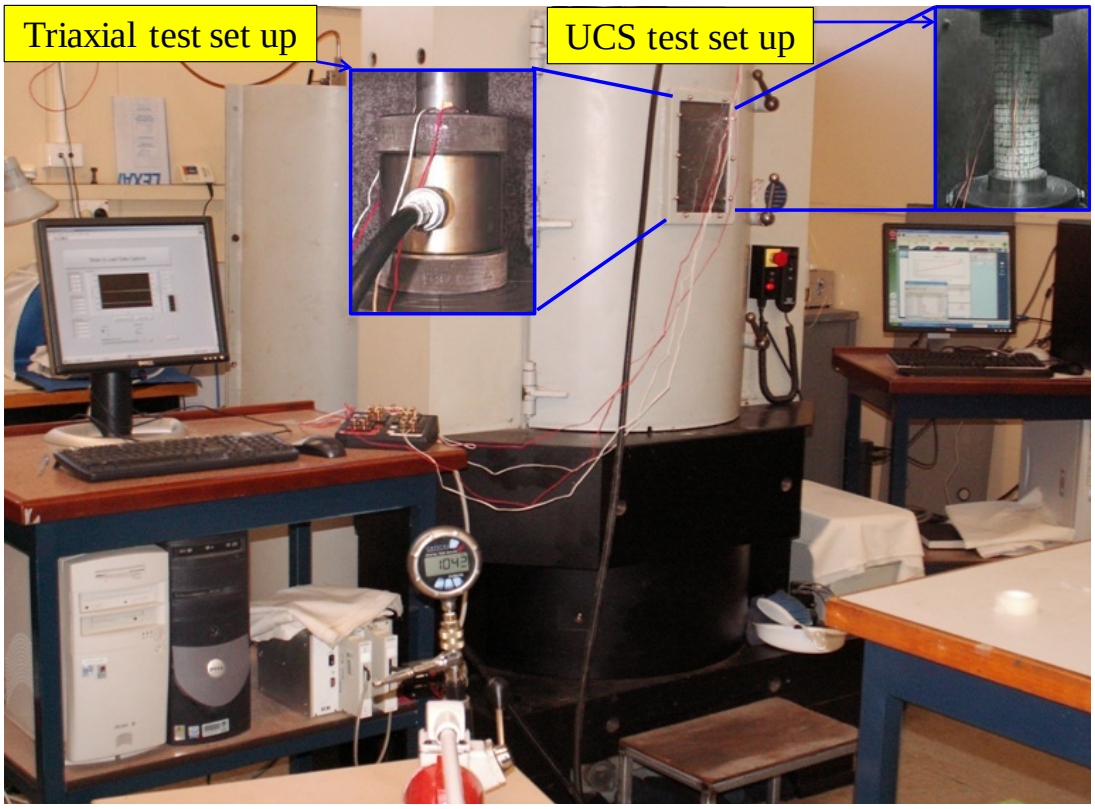

Figure 6.2. Instron servo controlled hydraulic testing machine for triaxial and UCS test set up.

The uniaxial tensile strength (UTS) test or Brazilian test was obtained according to the test method suggested by ISRM (1978). The test was performed with Avery universal testing machine as shown in Figure 6.3. Load and displacement were monitored and stored at resolutions of 0.01kN and 0.02mm, respectively.

Figure 6.3. Avery universal testing machine set up for uniaxial tensile strength test.

6.5 Results and discussion

6.5.1 Uniaxial compressive strength test results

The test results are summarised in Table 6.2. Figure 6.4 shows a typical shotcrete samples before and after UCS test. The stress versus strain curves from UCS test is shown in Figure 6.5. The test results show that UCS increases with curing time and that Young's modulus and Poisson's ratio do not change significantly. The yield point of the curves increased with increasing UCS. After yield, non-linear strain hardening can be observed until it reaches peak. After peak, localized damage develops and strain softening and/or the "snap-back" begins. The "snap-back" implies that the materials failed in brittle mode. Globally, the SFRS continued to deform in shear associated by dilation with the load taken by the steel fibres. The effective steel fibres are those which span the failure surface and are firmly anchored on both sides. The post peak behaviour of SFRS is highly dependent on the numbers and orientation of the effective fibres. The influence of effective is described in Chapter 2, Section 2.2.4.

Table 6.2. Summary of UCS test with complete stress-strain measurement.

Batch No.	Curing (Days)	Unit weight (kN/m^3)	UCS σ_c (MPa)	Elastic properties					
				Young's modulus			Poisson's ratio		
				Et_{50} (GPa)	Es (GPa)	Ea (GPa)	νt_{50}	νs	νa
1	1	20.71	16.2	-	-	-	-	-	-
2	1	20.71	18.1	14	15	14	0.36	0.31	0.42
3	1	23.44	18.3	11	16	11	0.20	0.28	0.19
1	3	23.44	23.4	-	-	-	-	-	-
2	3	22.75	18.3	12	15	12	0.28	0.29	0.28
3	3	23.39	22.9	9	13	8	0.16	0.21	0.16
1	7	23.54	28.5	-	-	-	-	-	-
2	7	23.48	23.2	16	21	16	0.23	0.34	0.22
3	7	23.57	25.7	14	17	14	0.17	0.29	0.17
1	28	23.44	32.8	15	21	14	0.21	0.31	0.21
2	28	23.68	27.2	18	28	17	0.30	0.29	0.29
3	28	23.05	31.5	11	16	10	0.17	0.22	0.15

Et50 = Tangent Young's modulus

Es = Secant Young's modulus

Ea = Average Young's modulus

νt50 = Tangent Poisson's ratio

νs = Secant Poisson's ratio

νa = Average Poisson's ratio

Figure 6.4. A typical shotcrete sample before and after Uniaxial Compressive Strength test.

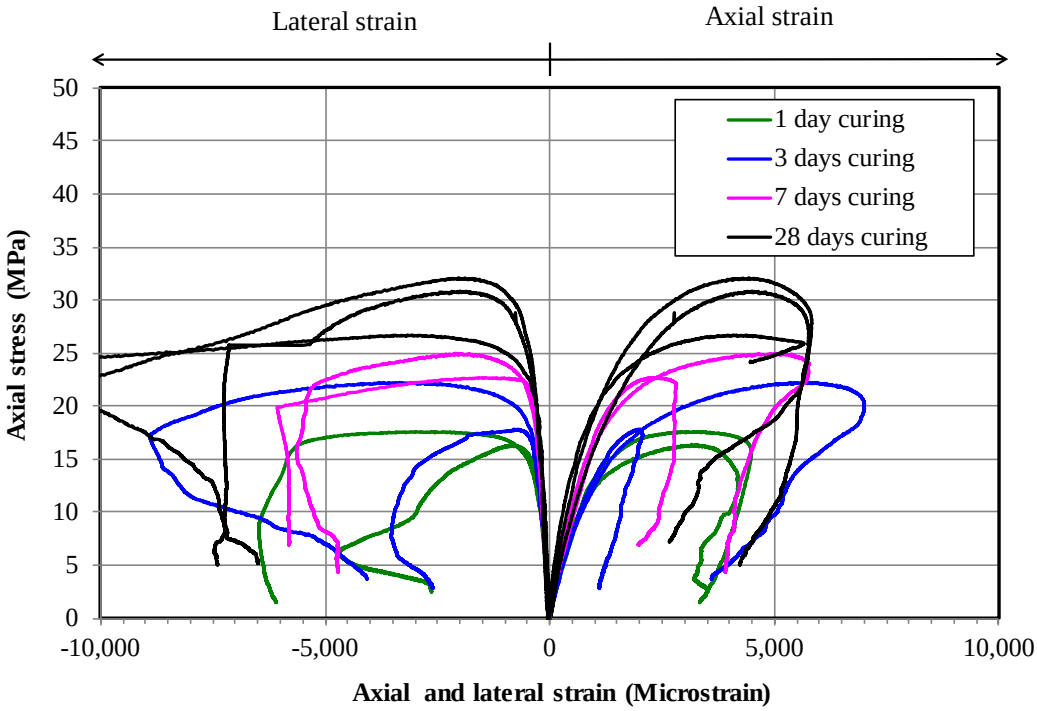

Figure 6.5. Stress versus strain curves from Uniaxial Compressive Strength test.

6.5.2 Uniaxial tensile strength (Brazilian) test results

Similar to the UCS tests, the tensile strength also increases with curing age. The summary of Uniaxial tensile strength (Brazilian) test results is given in Table 6.3. A typical shotcrete samples before and after Uniaxial tensile strength is shown in Figure 6.6. Figure 6.7 shows the load-displacement curves for indirect tensile strength tests. The results suggested that, after first crack the load is taken by the effective fibres and the ultimate tensile strength depends on the numbers and orientation of the effective fibres. Figure 6.8 shows a correlation between the UCS and peak tensile strength. The correlation suggests that the peak tensile strength of SFRS is about 15% of UCS.

Table 6.3. Summary Uniaxial tensile strength test.

Batch No.	Curing (days)	Peak tensile strength (MPa)
3	1	2.4
3	1	2.5
2	3	3.4
3	3	2.8
3	3	4.3
3	3	3.5
2	7	4.4
2	7	4.0
3	7	3.6
3	7	2.8
3	7	3.2
1	28	5.5
1	28	4.0
2	28	4.9
3	28	5.4
3	28	5.1
3	28	4.8

Figure 6.6. A typical shotcrete sample before and after Uniaxial tensile strength test.

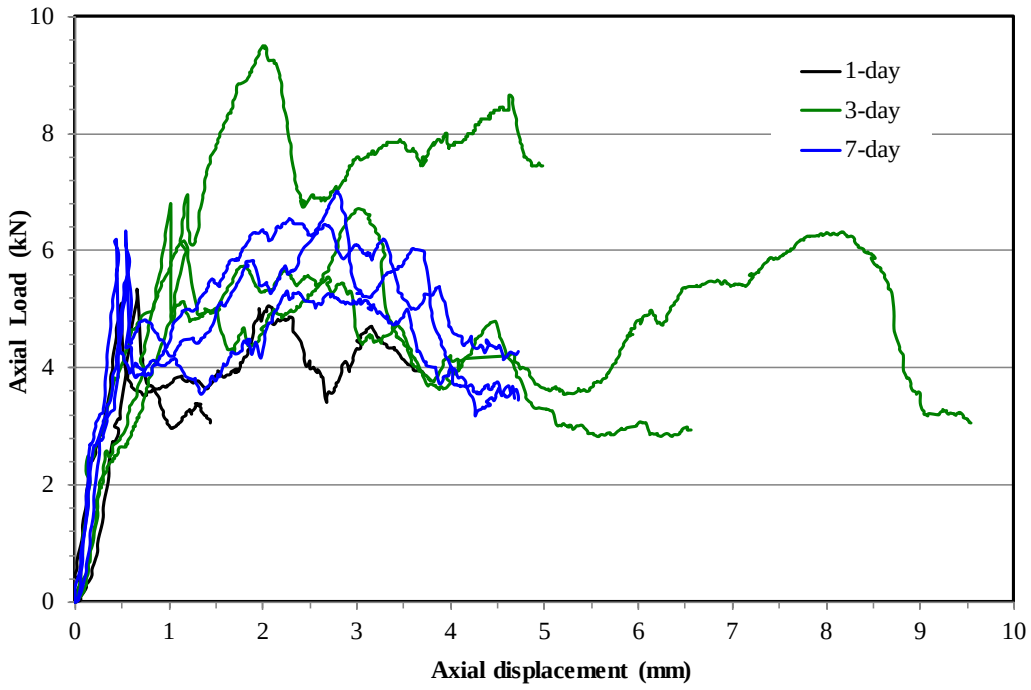

Figure 6.7. Load – displacement curves from Uniaxial tensile strength test.

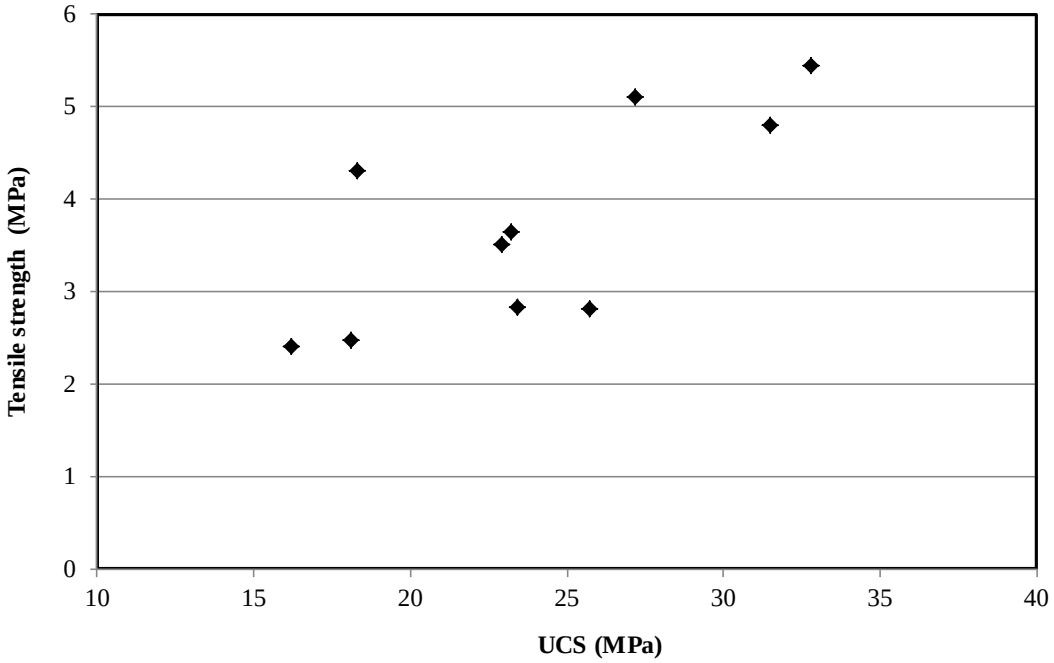

Figure 6.8. Correlation of peak tensile strength and UCS.

6.5.4 Triaxial test results

A summary of test results is given in Table 6.4. The detailed test results are presented in Appendix E. The shear strength parameters presented in Table 6.4 are calculated based on Coulomb's failure theory as described Chapter 3, Section 3.5. A typical shotcrete samples before and after triaxial test is shown in Figure 6.9. Alternatively, the peak and residual strength envelopes plotted on the "p–q" plane are also shown in Figures 6.10 and 6.11, respectively. Generally, the shear strength increased with curing time. The friction and dilation angles do not change significantly with curing time. The residual strength is influenced by confining pressure. The main cause of increase in strength is an increase in cohesion, with the slopes of the lines associated with friction angle being very similar.

Table 6.4. Summary of triaxial tests result.

Batch No.	Curing (Days)	Shear strength				Dilation angle, ψ°
		Peak		Residual		
		c (MPa)	ϕ°	c (MPa)	ϕ°	
1	1	4	38	-	-	-
2	1	4	45	2	45	8
3	1	5	36	5	32	13
1	3	5	40	3	42	-
2	3	4	40	3	41	10
3	3	6	38	-	-	12
1	7	8	35	5	35	-
2	7	5	40	4	41	10
3	7	6	40	5	38	10
1	28	8	38	7	18	12
2	28	11	18	-	-	12
3	28	8	38	-	-	10

Figure 6.9. Typical shotcrete samples before and after triaxial test.

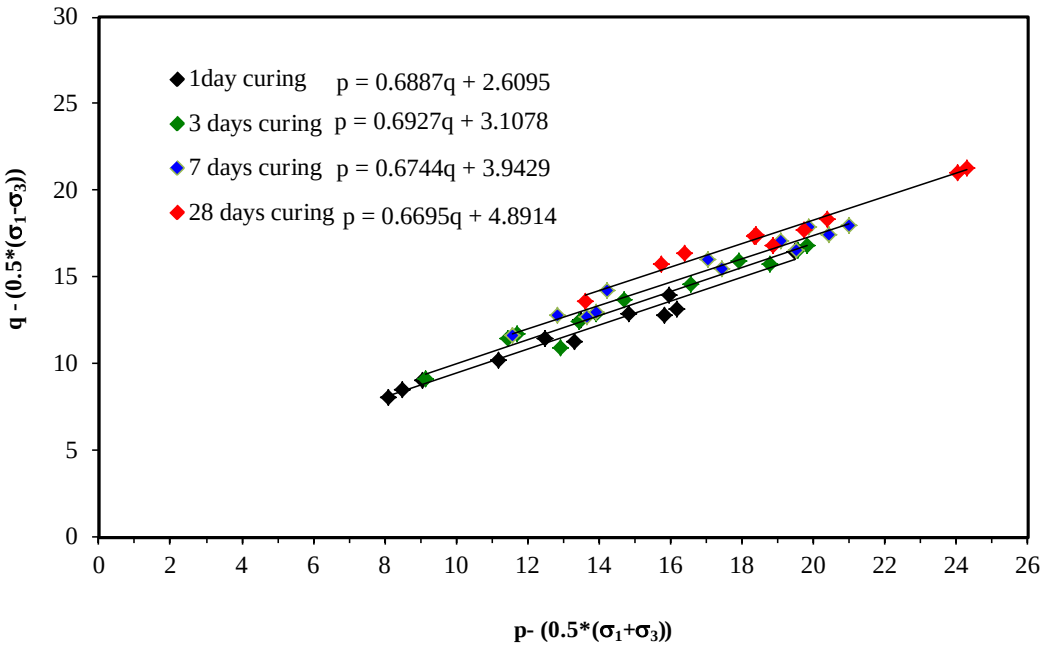

Figure 6.10. Peak shear strength envelopes plotted on p-q plane.

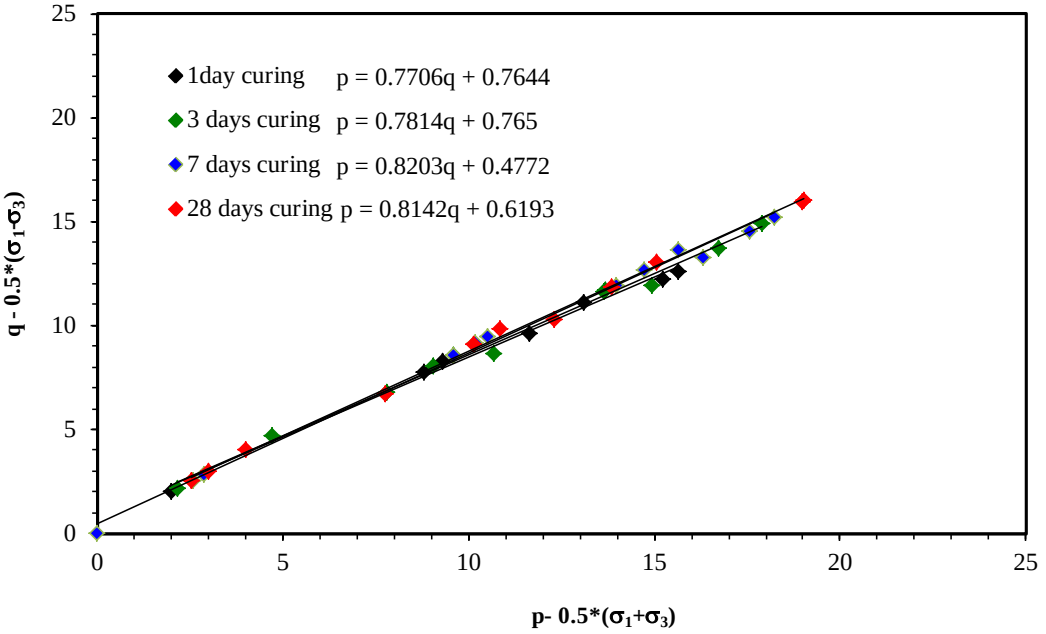

Figure 6.11. Residual shear strength envelopes plotted on p-q plane.

6.5.3 Stress – strain behaviours and dilation angle

The stress-strain curves shown in Figures 6.12 to 6.14 (including Figure 6.5) can be used to calculate the plastic strain rate at peak and residual using the total strain equation 6.11. The plastic strain increased with increased confining pressure. The peak stress does not change significantly from 1 day to 7 days curing but significantly increased at 28 days. The dilation angles are calculated from the axial and volumetric stain curves as described in Section 6.2. Figures 6.15 to 6.18 show axial and volumetric strain curves from Uniaxial Compressive Strength test and, triaxial test at 1, 2 and 3 MPa confinement, respectively. A correlation of friction and dilation angle is shown in Figure 6.19. This suggests that, higher dilation occurred in samples with lower friction angle. Also, the amount of dilation decreases with increasing confining pressure.

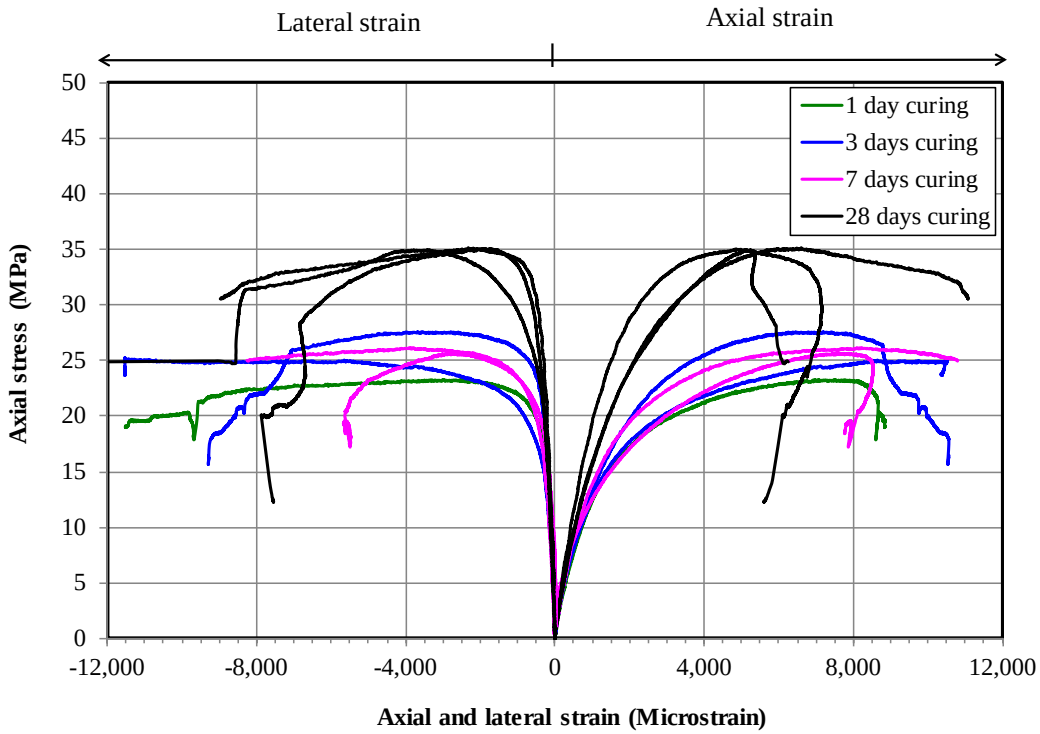

Figure 6.12. Stress versus strain curves from triaxial test at 1 MPa confinement.

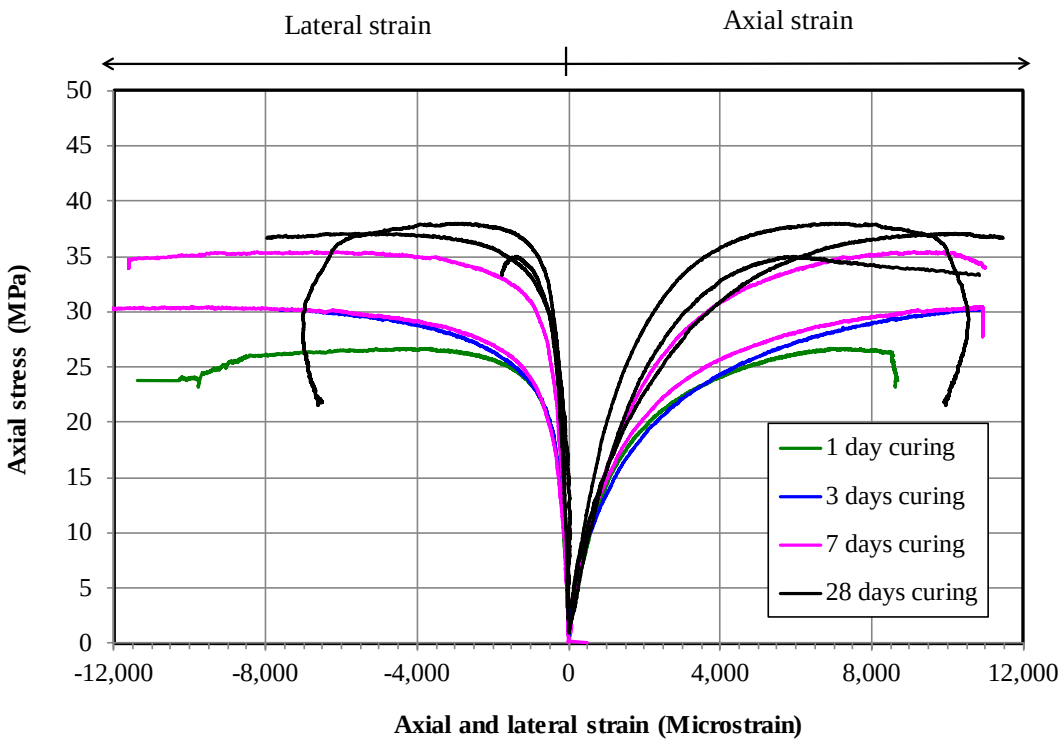

Figure 6.13. Stress versus strain curves from triaxial test at 2 MPa confinement.

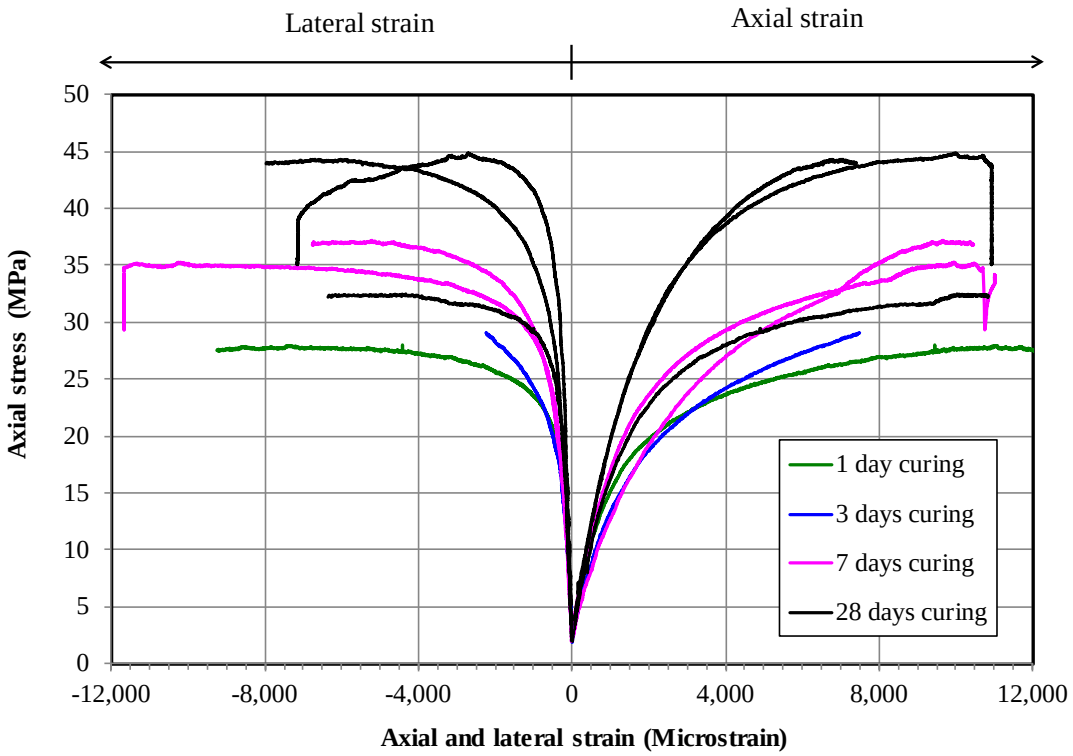

Figure 6.14. Stress versus strain curves from triaxial test at 3 MPa confinement.

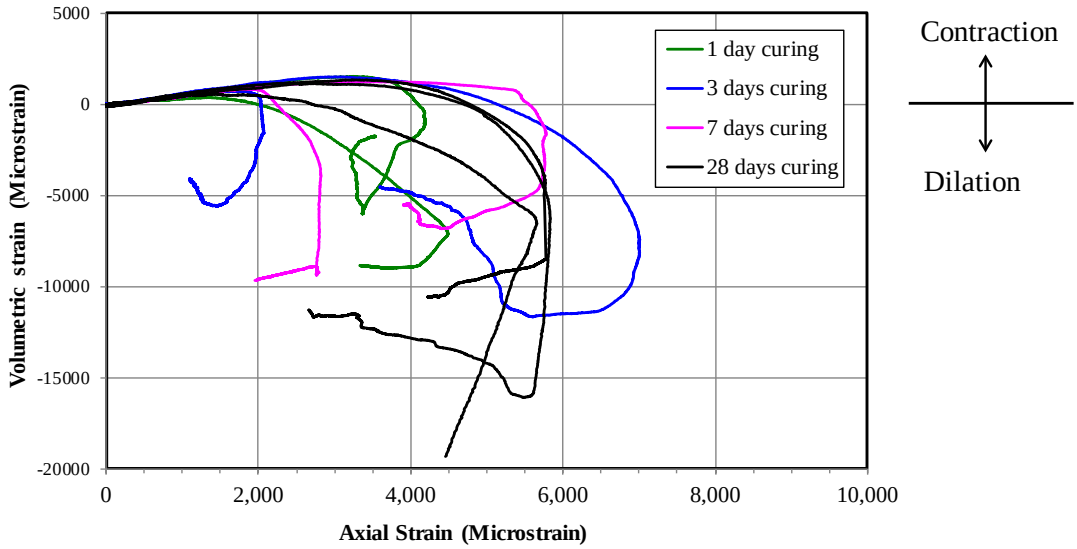

Figure 6.15. Volumetric versus axial strain curves from Uniaxial Compressive Strength test.

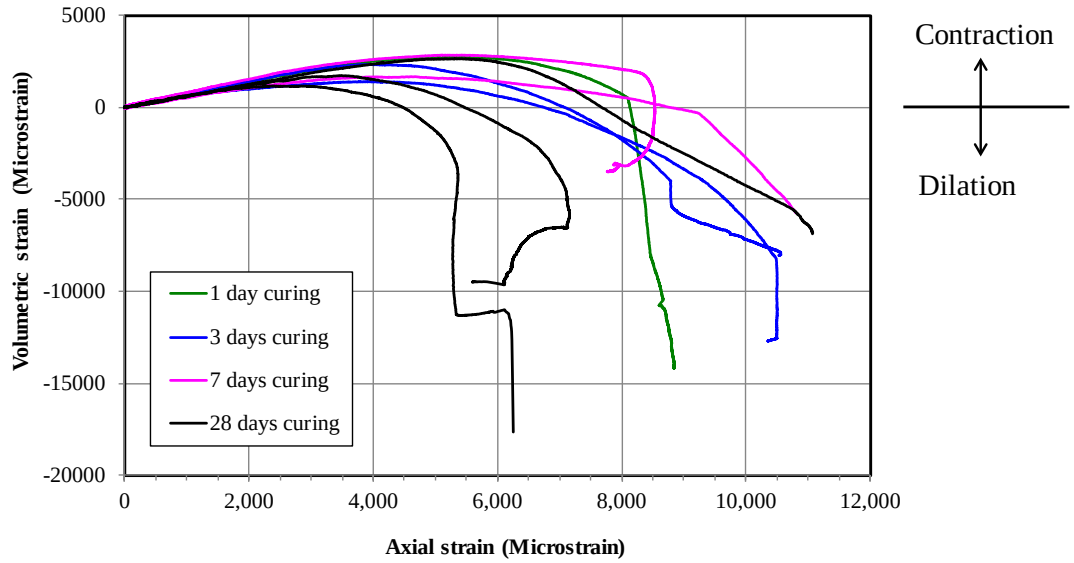

Figure 6.16 Volumetric versus axial strain curves from triaxial test at 1 MPa confinement.

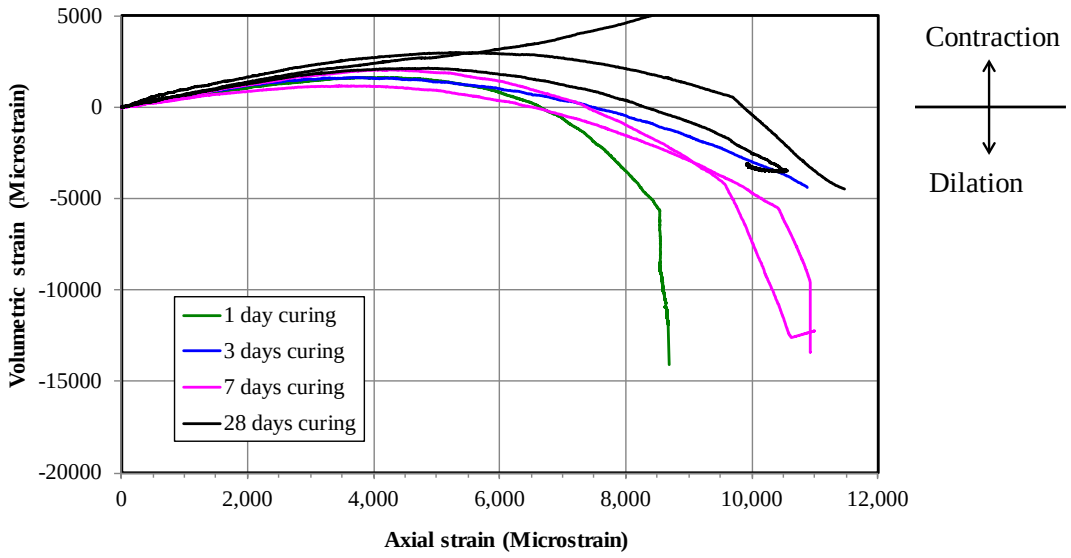

Figure 6.17. Volumetric versus axial strain curves from triaxial test at 2 MPa confinement.

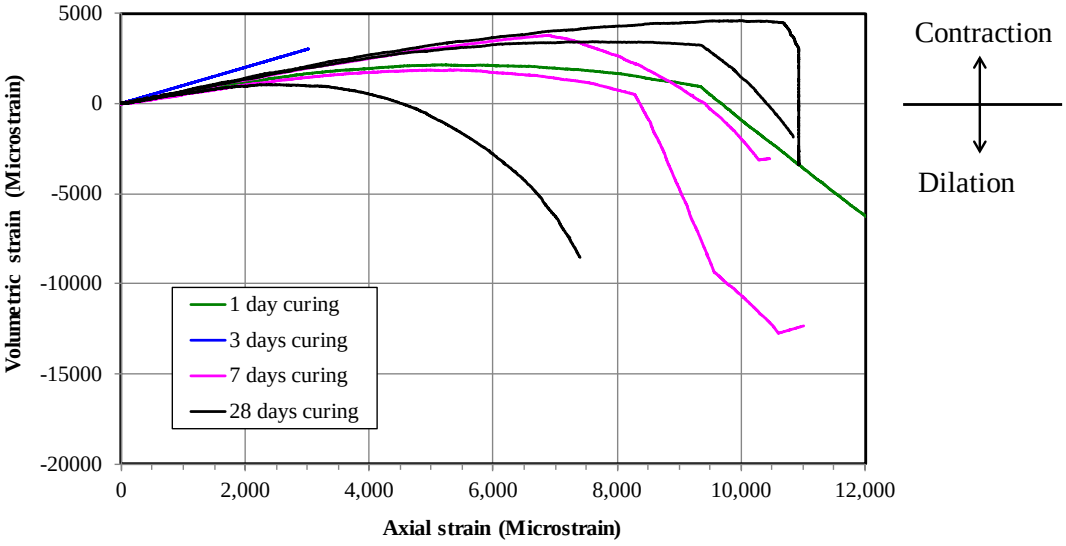

Figure 6.18. Volumetric versus axial strain curves from triaxial test at 3 MPa confinement.

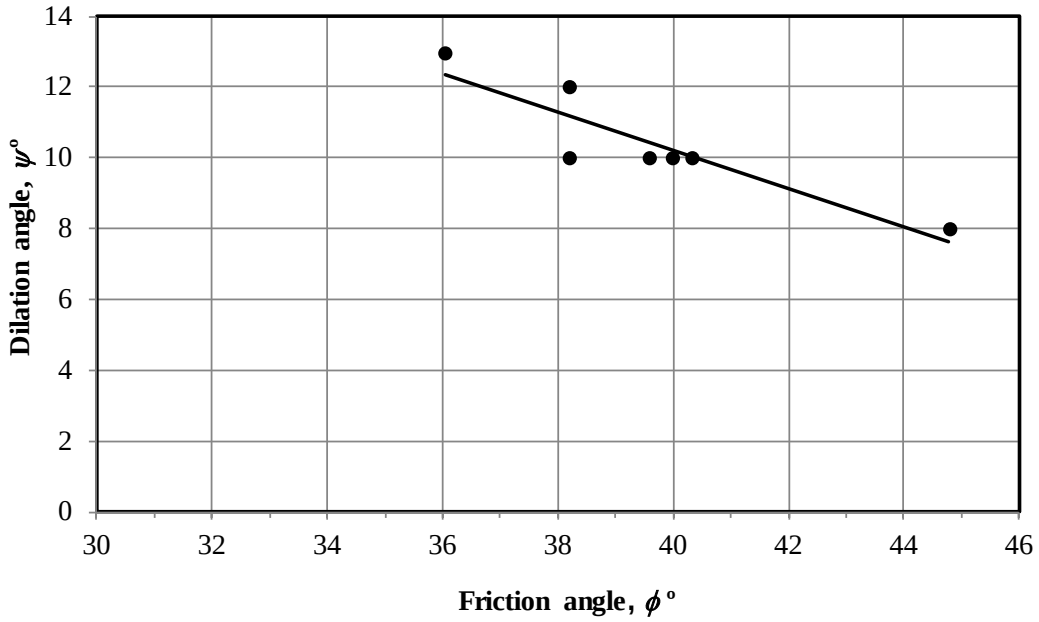

Figure 6. 19. Correlation between friction angle and dilation angle.

6.6 Conclusions and discussions

The mechanical properties of hardened shotcrete, that is, after 24 hours curing were studied during this research to understand a full scale of strength development. The study includes both the peak and post-peak (elastic and plastic) regions under uniaxial and triaxial loading in order, to predict the shear strength in terms of cohesion, friction and dilation angle and also, to examine how these parameters vary with curing time. Based on the test results, the following conclusions can be drawn:

- The average UCS at 1, 3, 7 and 28 days curing were 18, 22, 26 and 31 MPa respectively.
- The average tensile strength at 1, 3, 7 and 28 days curing were 2, 4, 4 and 5 MPa respectively.
- The tensile strength is about 15% of UCS.
- The average Young's modulus at 1, 3, 7 and 28 days curing were 13, 10, 15 and 14 GPa respectively.

- The average Poisson's ratio at 1, 3, 7 and 28 days curing were 0.3, 0.2. 0.2 and 0.2 respectively.
- The average peak cohesion at 1, 3, 7 and 28 days curing were 4, 5, 6 and 9 MPa respectively.
- The average peak friction angle at 1, 3, 7 and 28 days curing were 40, 39, 38 and 31 degree respectively.
- The average residual cohesion at 1, 3, 7 and 28 days curing were 4, 3, 5 and 7 MPa respectively.
- The average residual friction angle at 1, 3, 7 and 28 days curing were 39, 42, 38 and 18 degree respectively.
- The residual strength is influence by the confining pressure as the specimen responses in continuously strain hardening after post peak. Dilation angle ranges from 8 to 13 degree and does not change significantly with curing time. It decreases with increasing fraction angle. The amount of dilation decrease with increasing confining pressure.
- A complete stress-strain response can be subdivided in to linear elastic and non-linear plastic region. The non-liner plastic regions include strain hardening up to the post peak (continue at high confining pressure), snap-back or/and strain softening after post peak.
- The snap-back curves occurs when the SFRS locally response in the brittle mode to the uniaxial loading.
- The post peak behaviour is influence by the confining pressure, the number and orientation of effective fibres.

CHAPTER 7

CONCLUSIONS

7.1 Summary

This research objectives were, (1) to accurately define the 'strength' developed in the shotcrete with time for worst, average and best conditions for the shotcrete mix and it's in situ curing environment, (2) to adequately define the minimum strength required of the shotcrete to support itself and how much time is required for that strength to develop after application, (3) To adequately define the minimum strength required of the shotcrete to support the excavation and (4) to determine approximately, by some form of simple, robust, unambiguous field test when re-entry conditions of the shotcrete have been met in situ. This research has successfully achieved all the objectives.

7.2 Original contributions developed by this research

This research has made many scientific contributions to the fields of both civil and mining industries related to the mechanics of materials such as, concrete, shotcrete and rock. The overview of original contribution by this research is presented in Figure 7.1

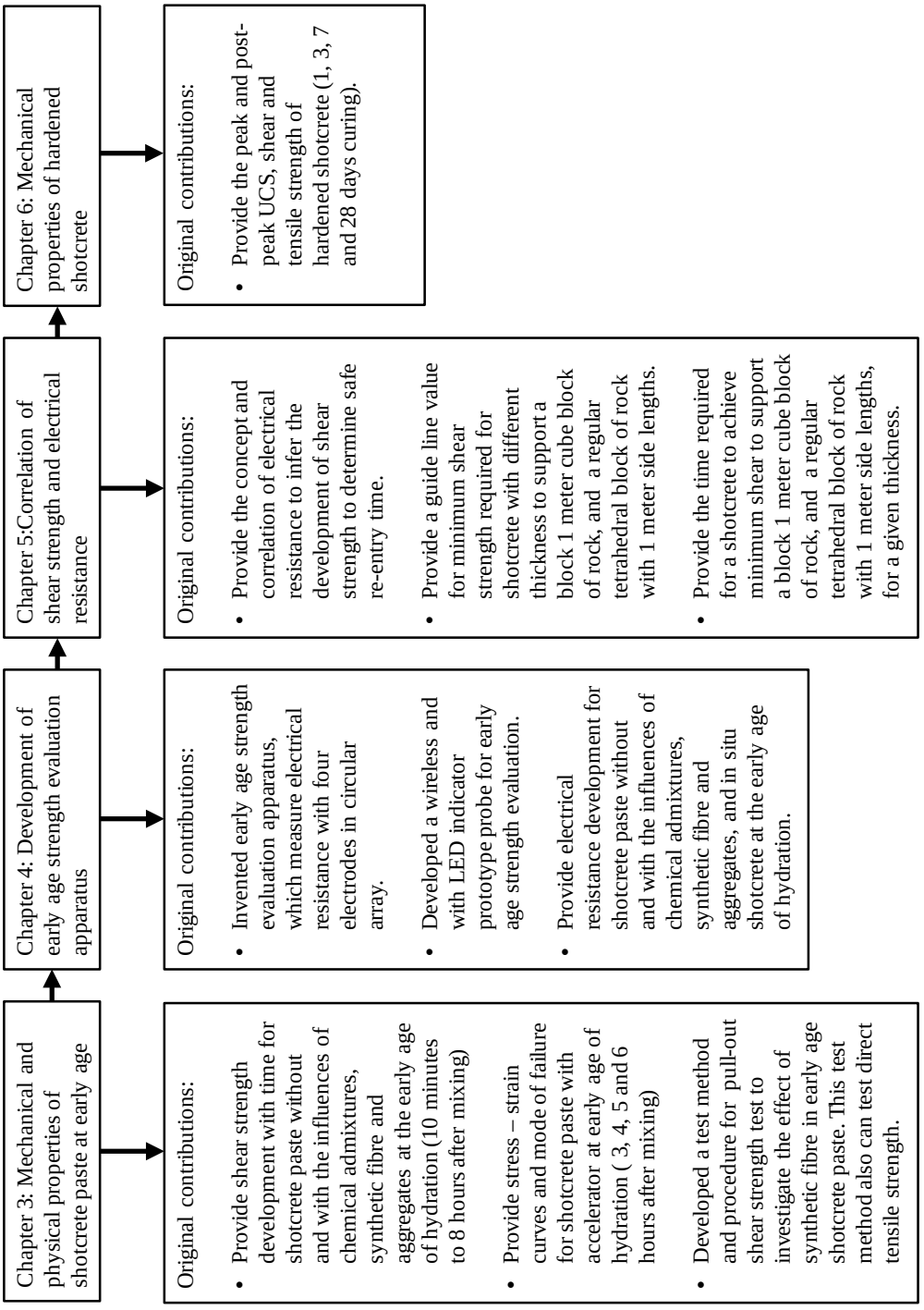

Figure 7. 1. Overview of the original contribution by this research.

7.3 Main conclusions

7.3.1 Chapter 2

The literature review presented in Chapter 2 addresses the current State-of-the-Art shotcrete mix design, the constituent materials properties and their influences on the strength development, the early strength and existing test methods.

The early strength of the shotcrete generally refers to the strength development from the time of spraying (0) to (4) hours curing. It is usually determined by indirect methods and correlated to the strength development with time. The measured properties include; penetration resistance, pull out force, temperature, electrical conductivity and resistivity and ultrasonic wave velocity. The measurement method can be broadly categorised as destructive and non-destructive determination. Although compression, tension, shear, torsion or flexure strength are possible to be correlated to the indirectly measured parameters, the current literature show uniaxial compressive strength (UCS) is the most commonly property used.

This research was focused on the fundamentals of shear strength development of shotcrete with time at early age, especially 0 to 4 hours. Therefore, a continuous literature search related to “the shear strength development of shotcrete with time at early age” was conducted from the beginning to the end of this research, which was from July, 2006 to October, 2014. With the best knowledge of the researcher, no specific literature on “the shear strength development of shotcrete with time at early age” was published during this period.

7.3.2 Chapter 3

The mechanical and physical properties of shotcrete at early age are mainly those associated with the cementitious matrix. Consequently, the research results from this

chapter were mainly focused on testing a shotcrete paste comprising the cementitious matrix and the influences of chemical additives, synthetic fibre and aggregates.

The typical stress and strain curves suggested that, at 3 hours curing time, the specimens failed in shear and compression mode and continue to deform axially with increasing stress or strain hardening behaviour. At 4 and 5 hours curing, the specimens failed in shear and compression at low confinement (100 kPa) and in shear mode at higher confinement (200 & 300 kPa). After failure the specimens continue to deform with almost constant stress or yielding behaviour. At 6 hours curing, the specimens failed in shear and brittle mode. After failure, the specimens continue to deform with shearing and dilation.

Shear strength of shotcrete paste mixed with accelerator and synthetic fibres was slightly higher than that of shotcrete paste mixed with only accelerator. Similarly, shear strength of shotcrete paste mixed with accelerator, synthetic fibre and aggregates was slightly higher than that of shotcrete paste mixed with accelerator and synthetic fibres.

A summary of pull-out shear strength test results in presented in Table 3.20 shows that the pull-out shear strength of shotcrete paste at age 3 to 4 hours and 6.5 to 8 hours ranges from 0.3 to 0.6 MPa and 0.9 MPa, respectively.

A minimum bond strength required to break a synthetic fibre is 23 MPa in shotcrete matrix. A pull-out shear strength test results suggested that, the load transfer of fibre is insignificant in the early age strength of shotcrete. Therefore early age strength of shotcrete is mainly control by the shear strength of shotcrete matrix only, not the strength of the fibres.

7.3.3 Chapter 4

One of the objectives of this research was to determine approximately, by some form of simple, robust, unambiguous field test when re-entry conditions of the shotcrete have been met in situ.

Based on a comprehensive literature review described in Chapter 2, and results from the initial research (Chapter 3, 3.8), it was concluded the electrical method is the best method to correlate with the physical and mechanical properties of cement-based materials. During the research stage 1 to 4 a series of shear strength test for different mixes of shotcrete paste were conducted and the shear strength test results were presented in Chapter 3. At the same time, different designs of electrical resistance measurement prototype probes were invented during this research.

The prototypes probes were experimented in the laboratory for different mixes, sample geometry, voltage input, electrodes, electrodes layout and geometry, and penetration depth before being tested in the field for in situ shotcrete use in underground mine. The electrical resistance of different shotcrete paste were measured simultaneously while conducting shear strength test. This chapter mainly presented the development of prototype electrical resistance probes and the measurement results with those prototype probes.

The research has shown that a simple, robust, unambiguous field test instrument was successfully invented in this research to determine when re-entry conditions of the shotcrete have been met in situ. The electrical resistance probe has been patented in Australia as well as Internationally.

The invented instrument can also measure the electrical resistance development with time for any types of cement base materials, in which the electrical resistance changes with curing time and the results can correlate with the strength development.

7.3.4 Chapter 5

Chapter 5 describes the correlation and concept of measuring electrical resistance to infer the development of shear strength with time to determine a safe re-entry time in an underground excavation.

A wireless prototype probe with LED light indicator was invented during this research. The LED has been programmed to turn the light to indicate “Red” when the shear strength of the shotcrete is less than the minimum required strength to support its own weight and an unstable 0.4 or 2.7 tonne block of rock. The LED light turns to “Green” when the shear strength of the shotcrete reaches the minimum required strength to support its own weight and an unstable 0.4 or 2.7 tonne block of rock.

7.3.5 Chapter 6

The mechanical properties of hardened shotcrete, that is, after 24 hours curing were studied during this research to understand a full scale of strength development. The study includes both the peak and post-peak (elastic and plastic) regions under uniaxial and triaxial loading in order, to predict the shear strength in terms of cohesion, friction and dilation angle and also, to examine how these parameters vary with curing time. The test results provide the peak and post peak Uniaxial Compressive Strength (UCS), shear and tensile strength of hardened shotcrete at 1, 3, 7 and 28 days curing.

7.4 Limitation of this research

All the early mechanical properties of shotcrete paste were tested in the laboratory. These mechanical properties mainly focused on the shear strength testing, which is critical at early age of hydration, that is, 0 to 4 hours after sprayed.

The shear strength of shotcrete paste was correlated to the in situ electrical resistance of the shotcrete sprayed in underground mine, to indicate the safe re-entry time for In Cycle Shotcrete. The safe re-entry time is when the freshly sprayed shotcrete achieved the minimum shear strength to support to support a block 1 meter cube block of rock or a regular tetrahedral block of rock, for a given thickness.

One assumption was, the shotcrete must supports its own mass by development of a bond strength (comprising adhesion and mechanical interlock) between itself and the substrate and by development of intrinsic shear strength, within minutes of being applied to the surface.

After a safe re-entry time, the shotcrete will continue with hydration and finally become fully hardened shotcrete. When the shotcrete become fully hardened its strength and mode of failure will be different to that of 0 to 4 hours. The research did not cover the strength of the fully hardened shotcrete, for the underground rock support.

7.5 Future work and industry application

Based on the results from the initial experiments a high capacity vane shear testing equipment was designed and a manufacture was contracted to build the equipment. A schematic design of WASM high capacity vane shear testing equipment is shown in Figure 7.2. A high capacity vane shear testing equipment can be used to measure the shear strength of fresh shotcrete in the field to improve the calibration graphs for a re-entry time for any given underground mine.

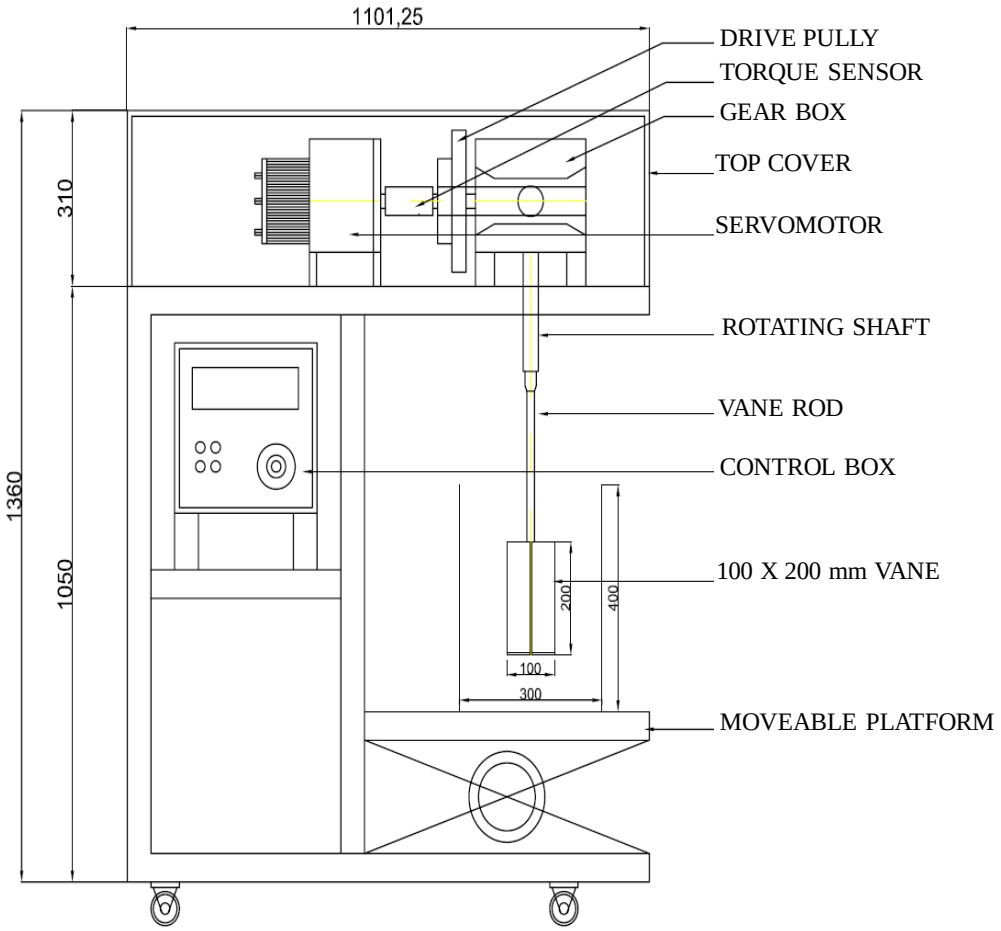

Figure 7.2. Schematic design of WASM high capacity vane shear testing equipment.

REFERENCES

Abdun-Nur., E., (1961), 'Fly ash in concrete – An evaluation', Bulletin No. 284, Highway Research Board, Washington D.C., 138 pp.

ACI 234R-06, (2006), 'Guide for use of silica fume in concrete', ACI committee 234, American Concrete Institute, Farmington Hills, MI.

ACI 506.5R-09, (2009), 'Guide for specifying underground shotcrete', ACI committee 506, American Concrete Institute, Farmington Hills, MI.

ACI 233R-03, (2003), 'Slag cement in concrete and mortar', ACI committee 233, American Concrete Institute, Farmington Hills, MI.

ACI 232.2R-03, (2003), 'Use of fly ash in Concrete', ACI committee 233, American Concrete Institute, Farmington Hills, MI.

ACI 544.1R-96, (1996), 'State-of-the-Art report on fibre reinforced concrete', American Concrete Institute, Farmington Hills, MI.

Adamson, A.W. and Gast, A.P., (1997), 'Physical chemistry of surfaces' 6th Edition, John Wiley & Sons, New York, 808 pp.

Aïtcin, P.C., Pinsonneault, P. and Roy, D.M., (1984), 'Physical and chemical characterization of condensed silica fume', Ceramic Bulletin, V.63, No.12, pp. 1487-1491.

Angelskaar, T., (2003), 'Cement accelerator and method', International PCT Patent No WO 03/045872 A1, MBT Holding AG.

Angelskaar T., (2004), 'Admixture', International PCT Patent No WO 2004/106258 A2, Construction Research & Technology GmbH.

Armelin, H.S., Banthia, N., (1998), 'On the rebound - Minimizing shotcrete rebound with fibres', Concrete International, Volume 20, Issue 9, pp. 74-79.

AS3972, (2010), 'General purpose and blended cements', Standard Australia, Sydney, NSW.

ASTM C1240-10a, (2010), 'Standard specification for silica fume used in cementitious mixtures', ASTM International, West Conshohocken, PA.

ASTM C618-08a, (2008), 'Standard specification for coal fly ash and raw or calcined natural pozzolan for use in concrete', ASTM International, West Conshohocken, PA.

ASTM C989-10, (2010), 'Standard specification for slag cement for use in concrete and mortars', ASTM International, West Conshohocken, PA.

ASTM C219 - 07a, (2007), 'Standard terminology relating to hydraulic cement', ASTM International, West Conshohocken, PA.

ASTM C39/C39 M-09a, (2009), 'Standard test method for compressive strength of cylindrical concrete specimens', ASTM International, West Conshohocken, PA.

ASTM C1602/C1602M-06, (2006), 'Standard Specification for mixing water used in the production of hydraulic cement concrete', ASTM International, West Conshohocken, PA.

ASTM C150/C 150M-09, (2009), 'Standard specification for Portland cement', ASTM International, West Conshohocken, PA.

ASTM C125-10a, (2010), 'Standard terminology relating to concrete and concrete aggregates', ASTM International, West Conshohocken, PA.

Bernard, E.S., (2008), 'Early-age load resistance of fibre reinforced shotcrete linings', Tunneling and Underground Space Technology, Volume 23, pp.451-460.

Beaupré, D., (1994), 'Rheology of high performance shotcrete', PhD thesis, Department of Civil Engineering, University of British Columbia, Vancouver, BC, Canada, 250 pp.

Bogue, R. H., (1929), 'Calculation of the compounds in Portland cement', Portland cement association fellowship, Bureau of standards, Washington D.C.

Bogue, R. H., (1947), 'The chemistry of Portland cement', Reinhold Publishing Corp., New York, 572 pp.

Burton, W.K., Cabrera, N. and Frank, F.C., (1951), 'The growth of crystals and the equilibrium structure of their surfaces', Phil. Trans. R. Soc. Lond. A 243 (866), pp. 299–358.

Bracher, G., (2005), 'Worldwide sprayed concrete: State-of-the-art report', International symposium on waterproofing for underground structures, Sao Paulo, Brazil.

Bullard, J.W., Jennings, H.M., Livingston, R.A., Nonat, A., Scherer, G.W., Schweitzer, J.S., Scrivener, K.L., Thomas, J.J., (2011), 'Mechanisms of cement

hydration', Cement and Concrete Research, Vol. 41, Issue 12, Elsevier B.V., pp. 1208-1223.

Bürge, T.A., (2001), 'Mode of action of alkali-free sprayed shotcrete accelerators', Proceeding of International Conference on Engineering Developments in Shotcrete, Bernard, E.S. (ed), Hobart, Tasmania, Balkema Publishers, The Netherlands, pp. 79-85.

Byfors, J., (1980), 'Plain concrete at early ages' Technical Rep. No. 3:80, Swedish Cement and Concrete Institute, Stockholm, Sweden.

CAA, (2006), 'Admixture Sheet – ATS 5: Concrete Air entraining admixtures', Cement Admixtures Association, West Midlands.

Calleja, J., (1952), 'New technique in the study of setting and hardening of hydraulic materials', Journal of ACI, Volume 23, No.7, pp. 525-536.

Clements, M., (2004), 'Comparison of methods for early age strength testing of shotcrete', Proceedings of the 2nd International Conference on Engineering Developments in Shotcrete, Cairns, Queensland, Australia, E.S. Bernard (Ed.), Taylor and Francis Group, London, pp. 81-87.

Collepardi, S., Coppola, L., Troli, R., and Collepardi, M., (1999), 'Mechanism of actions of different superplasticisers for high performance concrete, Proceedings of the 2nd CANMET/ACI Conference, Gramado, Brazil, SP 186, pp 503-524.

Coulomb, C.A., (1776), 'Essais sur une application des regles des maximis et minimis à quelques problems de statique relatifs à l'architecture'. Mem.Acad.

De Belie, N., Grosse, C.U., Kurz, J., and Reinhardt, H.W., (2005), 'Ultrasound monitoring of the influence of different accelerating admixtures and cement types for shotcrete on setting and hardening behaviour', Cement and Concrete Research, Volume 35, Issue 11, pp. 2087–2094.

Diamantidis, D., and Bernard E.S., (2004), 'Comparison of methods for early age strength testing of shotcrete, Proceedings of the 2nd International Conference on Engineering Developments in Shotcrete, Cairns, Queensland, Australia, Bernard, E.S. (Ed.), Taylor and Francis Group, London, pp. 109-126.

Diamond, S., (1976), 'Cement paste microstructure – an overview at several levels', Proceeding ofInternational Conference in Hydraulic Cement Paste, their Structure and Properties, Sheffield, Cement and Concrete Assoc., Slough, pp. 2-30.

Dove, P.M., Han, N., and Yoreo, J.J.D., (2005), 'Mechanisms of classical crystal growth theory explain quartz and silicate dissolution behavior', Proceedings of the National Academy of Sciences, U.S.A. 102 (43), pp. 15357–15362.

Dove, P.M. and Han, N., (2007), 'Kinetics of mineral dissolution and growth as reciprocal microscopic surface processes across chemical driving force', AIP Conference Proceedings Vol. 916, pp. 215–234.

BS EN 197-1, (2000), 'Cement – Part 1: Composition, specification and conformity criteria for common cements', British Standards Institution, London, 46 pp.

Edmeades, R.M. and Hewlett, P. C., (1988), 'Cement admixtures, Lea's Chemistry of Cement and Concrete, 4th. Edition, Hewlett, P.C. (Ed.), Elsevier Ltd, Oxford, pp. 841-905.

Elastoplastic, (2007), Bar Chip synthetic Reinforcing Fibre Product Data Sheet, www.elastoplastic.com.

Fairhurst, C. E.,& Hudson, J. A., (1999), Draft ISRM suggested method for the complete stress-strain curve for intact rock in uniaxial compression. Int J Rock Mech Min Sci. Volume 36, pp.279- 289.

Farrington S. A., and Christensen B. J, (2003), 'The Use of chemical admixtures to facilitate placement of concrete at freezing temperatures', Proceedings of 7th CANMET/ACI International Conference on Superplasticizers and Other Chemical Admixtures in Concrete, Malhotra, V.M (Ed.,), ACI International SP-217-5, USA, pp 71-85.

Fredlund, D.G. and Rahardjo, H., (1993), 'Soil mechanics for unsaturated soils', John Wiley & Sons Inc, New York, 517 pp.

Freiesleben-Hansen, P. and Pedersen, E. J., (1977), 'Maturity computer for Controlled curing and hardening of concrete', Nordisk Betong, No. 1, pp. 21-25.

Fukuhara M., Goto, S., Asaga, K., Diamon, M., Kondo, R. (1981), 'Mechanisms and kinetics of C4AF hydration with gypsum', Cement and Concrete Research, Volume 11, pp.407-414.

Gartner, E.M. and Gaidis, J.M., (1989), 'Hydration mechanisms I'., Materials Science of Concrete Volume 1,American Ceramic Society, Westerville, OH, pp. 95–125.

Gaidis, J.M. and Gartner, E.M., (1989), 'Hydration mechanisms II' Materials Science of Concrete Volume 2, American Ceramic Society, Westerville, OH, pp. 9–39.

Garshold, K. and Melbye, T., (1996), 'Practical experience with alkalifree, non-caustic liquid accelerators for sprayed concrete', Second International Symposium on Sprayed Concrete, Gol, Norway, pp. 257-268.

Gartner, E.M., Young,J.F., Damidot, D.A., Jawed, J., (2002), 'Hydration of Portland cement', Structure and Performance of Cements, 2ndEdition, Bensted, J. and Barnes, P., (Eds.), Spon Press, New York, pp. 57–113.

Gere, J.M., and Timoshenko, S.P., (1990), "Mechanic of material", Third edition, PWS-Kent Publishing Company, Boston, 809 pp.

Glasstone, S., Laidler, K.J., Eyring, H., (1941), 'The theory of rate processes', McGraw-Hill, New York, 611 pp.

Girmscheid, G. and Moser, S., (2001), 'Fully automated shotcrete robot for rock support', Computer-aided Civil and Infrastructure Engineering, vol. 16, pp. 200-215.

Hansen, C.E.B., (1958), Line ruptures regarded as narrow rupture zones - Basic equations based on kinematic considerations. In proceeding of conference on Earth Pressure Problem, Brussels.

Higginson, E.C., Wallace, G.B., Ore, E.L., (1963), 'Effect of maximum size of aggregate upon compressive strength of mass concrete', Symposium On Mass Concrete, ACI SP-6, Detroit, Michigan, pp. 219-56.

Hooke, R., (1705),The posthumous Works, Containing his Cutlerian Lectures, and other Discourses. Read at the Meeting of the Illustrious Royal Society.

Hogan, F.J. and Meusel, J.W., (1981), 'Evaluation for durability and strength development of a ground granulated blast furnace slag', Cement, Concrete and Aggregates, Volume 3, No.1, pp. 40-52.

Hyett, A.J., Bawden, W.F., Coulson, A.L., (1992), 'Physical and mechanical properties of normal Portland cement pertaining to fully grouted cable

bolts',Proceeding of international symposium on rock support, Sudbury, Canada. Rotterdam A.A. (Ed.), Balkema. pp. 341-348.

ISRM, (1981), Suggested methods for determining the uniaxial compressive strength and deformability of rock material.In: Brown ET editor. Rock characterization, testing and monitoring: ISRM suggested Methods. Oxford: Pergamon, pp. 137–40.

ISRM, (1983), Suggested methods for determining the strength of rock materials in triaxial compression: revised version. Int J Rock Mech Min Sci. Volume 20, pp. 285-290.

ISRM, (1978), Suggested methods for determining tensile strength of rock mateials.Int J Rock Mech Min Sci., Volume 15, pp.90-103.

Jawed, I., Skalny, J., Young, J.F., (1984), 'Hydration of cement', Structure and Performance of Cements, Applied Science Publisher, London, pp. 237-318.

Jennings, H.M., Dalgleish, B.J., Pratt, P.L., (1981), 'Morphological development of hydration tricalcium silicate as examined by electron microscopy techniques',Journal of the American Ceramic Society, Volume 64, No.10, pp. 567-572.

Jolin, M., (1999), 'Mechanisms of placement and stability of dry process shotcrete', PhD thesis, University of British Columbia, Vancouver, BC, Canada, 152 pp.

Jolin, M., Beaupre, D., and Mindess, S. (1999), 'Tests to characterize properties of fresh dry dixshotcrete',Cement and Concrete Research, Volume 29, pp. 753-760.

Kaschiev, D. and Van Rosmalen, G.M., (2003), 'Review: nucleation in solutions revisited', Crystal Research and Technology, Wiley-VCH Verlag GmbH & Co., Volume 38, pp. 555–574.

Keller, G.V. and Frischknecht, F.C, (1966), 'Electrical methods in geophysical prospecting', Pergamon, Oxford, 517 pp.

Khalaf, F.M. and Wilson J.G., (1999), 'Electrical properties of freshly mixed concrete', Journal of Materials in Civil Engineering, Volume 11, No. 3, pp. 242-248.

Knight, B., Rasping M. and Clegg, I., (2006), 'Wet-mix shotcrete as a material, process and ground control component of a 21st century underground mining operation', Proceedings of the 10th International Conference Shotcrete for Underground Support X, Whistler, BC, Canada, Morgan, D and Parker, H. (Eds.), American Society of Civil Engineers, pp. 298-306.

Kusterle, W. and Lukas, W., (1990), 'High-grade shotcrete for the single permanent shotcrete lining method', Proceeding of 3rdConference on Shotcrete Technology, Institut für Baustofflehre und Materialprüfung, Universität Innsbruck, Innsbruck-Igls , pp. 29–40.

Lane, R.O., (1983), 'Effects of fly ash on freshly mixed concrete', Concrete international, Volume 10, pp. 50-52.

Le Chatelier, H. (1882),'The constitution of hydraulic mortars', Comptes Rendus de, Volume 94,Translated by Mack, J.L. (1905), Mc.Graw-Hill, New York, 13 pp.

Lea, F. M. (1970), 'The chemistry of cement and concrete', 3rd Edition, Edward Arnold, London, 727 pp.

McCarter WJ, (1984), 'The electrical response characteristics of setting cement paste'Magazine of Concrete Research, Volume 36, pp.42 - 49.

Melbye, T.A., (1996), 'Sprayed concrete for rock support', 4th edition, MBT International Underground Construction Group, Zurich, 186 pp.

Mills, R. and Lobo, V.M.M., (1989), 'Self-diffusion in electrolyte solutions', Elsevier B.V., Amsterdam, 317 pp.

Morel, F.M.M. and Hering, J.H.,(1983), 'Principles and applications of aquatic chemistry', John Wiley & Sons, Inc., New York, 608 pp.

Molhotra, V.M., Ramachandran, V.S., Feldman, R.F., Aïtcin, P.C., (1987), 'Condensed silica fume in concrete', CRC press Inc., Boca Raton, 221 pp.

Morgan, D.R., (1988), 'Dry-mix silica fume shotcrete in western Canada', Concrete International, Volume 10, No.1, pp.24-32.

Myrdal, R., (2007), 'State of the art report, accelerating admixtures for concrete', SINTEFF Building and Infrastructure, Concrete Innovation Centre (COIN), Trondheim, 23 pp.

Nagi, M.A, Okamoto, P.A., Kozikowski, R.L., Hover, K., (2007), 'Evaluating air-entraining admixtures for highway Concrete', NCHRP report578, Transportation Research Board, Washington, 49 pp.

Neville, A.M., (1995), 'Properties of concrete', 4th Edition, Pearson Education Ltd., Essex, 844 pp.

O'Toole, D. and Pope, S., (2006), 'Design, testing and implementation of In-Cycle Shotcrete in the northern 3500 orebody', Proceedings of the 10th International

Conference on Shotcrete for Underground Support X, Whistler, BC, Canada., Morgan, D and Parker, H (Eds.), American Society of Civil Engineers, pp. 316-327.

Poole, J.L, Riding, K.A., Folliard, K.J., Juenger, M.C.G., and Schindler, A.K., (2007), "Methods for calculating activation energy for Portland cement", ACI Materials Journal, Volume. 104, No.1, pp. 303-311.

Popovics, S. (1992), 'Concrete materials: properties, specifications, and testing', Noyes Publications, New Jersey, 542 pp.

Powers, T.C., (1968), 'The properties of fresh concrete', John Wiley & Sons, Inc., New York, 664 pp.

Pinto, R.C.A., and Hover K.C., (1999), "Application of maturity approach to setting times", ACI Materials Journal, Vol. 96, NO. 6, pp. 686-691.

Radenkovic, D., (1961), Théorèmes limites pour un matériau de Coulomb á dilation non standardisée. C.R. Ac.Sc. 252, Paris, pp. 4103-04.

Ramachandran, V.S.,(1995), 'Concrete admixture handbook: Properties, science and technology', 2ndEdition, Ramachandran, V.S. (Ed.), National Research Council Canada, Noyes Publications, Ottawa, 1153 pp.

Regourd, M., (1980), 'Characterization of thermal activation of slag cements', Proceeding, 7thInternational Congress on the Chemistry of Cements, Septima, Paris, Volume 2, pp. 105-111.

Reny, S, Jolin, M., (2011), 'Improve your shotcrete: Use coarse aggregates', Shotcrete Magazine, American Shotcrete Association, Farmington Hills, MI. Volume 13. No. 1, pp. 26-28.

Rispin, M., B. Knight and Dimmock, T., (2003), 'Early re-entry into working faces in mines through modern shotcrete technology - Part II',Canadian Institute of Mining - Mines Operations Centre, Saskatoon, SK, Canada.

RILEM,(2002), 'The hydration of tricalcium aluminate and tetracalcium aluminoferrite in the presence of calcium sulphate, Mathematical Modelling of Hydration of Cement',RILEM Technical Committees 68-MMH Task Group 3 report, RILEM publication, Bagneux, France, pp-137-147.

Roy, D.M., and Idorn, G.M., (1982), 'Hydration, structure and properties of blast furnace slag cement, mortars and concrete', ACI journal, Volume 79, No.6, pp. 445-457.

Saw, H., Villaescusa, E., Windsor, C. R., & Thompson, A. G. (2009), "Non-linear, elastic - plastic response of steel fibre reinforced shotcrete to uniaxial and triaxial compression testing", International Conference on Shotcrete for Underground Support XI, Davos, Switzerland.

http://services.bepress.com/eci/shotcrete/

Schindler, A. K., (2002), 'Concrete hydration, temperature development, and setting at early-ages', Ph.D. dissertation, Univ. of Texas at Austin, Austin, Texas, 531 pp.

Schindler, A.K., (2004), 'Prediction of concrete setting', Proceedings of the RILEM Conference on Advances in Concrete through Science and Engineering, Evanston, Illinois, RILEM publication, Bagneux.

Schindler, A. K. (2004), "Effect of temperature on hydration of cementitious materials", ACI Materials Journal, Volume. 101, No. 1, pp. 72–81.

Sellevold, E.J., (1987), 'The function of condensed silica fume in high strength concrete', Proceeding of Symposium on utilisation of high strength concrete, Holand, I., Helland, S., Jakobsen, B. and Lenschow, R. (Eds.), Tapir Publishers, Trondheim, pp. 39-49.

Sellevold, E.J. and Nilsen, T., (1987), 'Condensed silica fume in concrete: A world review, Supplementary cementing materials for concrete', Malhotra, V.M. (Ed.), Canmet, Ottawa, Canada, pp. 165-243.

Shimizu, Y., (1928), 'An electrical method for measuring setting time of Portland cement paste', Mill Section of Concrete, Volume 32, No. 5,pp. 111-113.

Smolczyk, H.G., (1978), 'The effect of the chemistry of slag on the strength of blast furnace cements', Zement KalGips, Volume 31, No. 6, pp. 294-296.

Sommer M., (2000), 'Alkalifreier abbindeand erhärtungsbeschleuniger, European Patent No EP 1 167 317 A1,Sika AG.

Somorjai, G.A., (1994), 'Introduction to surface chemistry and catalysis', John Wiley & Sons Inc., New York, 667 pp.

Taylor, H.F.W, Barret, P., Brown, P.W., Double,D.D, Frohnsdorff, G., Johansen, V., Ménétrier-Sorrentino, D., Odler, I., Parrott, L.J., Pommersheim, J.M. , Regourd, M. and Young, J.F, (1954), 'The hydration of tricalcium silicate',Journal of Mechanics of Materials and Structures, Volume 17, pp. 457–468.

Taylor, H.F.W, (1997), 'Cement chemistry', 2nd Edition, Thomas Telford Services Ltd, London, 459 pp.

Thompson, A.G. and Windsor, C.R., (1998), 'Cement grouts in theory and reinforcement practice', Proceeding of 3rdNorth American Rock Mechanics Symposium, NARMS' 98, Cancun, Mexico, Paper No. AUS-330-2.

Valenti, S., (1996), 'Aluminium accelerator for cement', UK Patent No GB 2 307 475 A, Sandoz Ltd.

Van Beek, A., (2000), 'Dielectric properties of young concrete – Non destructive dilectric sensor for monitoring the strength development of young concrete', PhD Thesis, Delft University Press, Netherlands, 176 pp.

Van Breugel, K., (1997), 'Simulation of hydration and formation of structure in hardening cement based materials', Ph.D. Thesis, Delft University Press, Netherlands, 305 pp.

Windsor, C. R., (1996), 'Rock reinforcement systems', International Journal of Rock Mechanics and Mining Sciences & Geomechanics, Volume 34, Issue 6 , pp.919-951.

Windsor, C. R., (1999), "Structural design of shotcrete linings", Australian Shotcrete Conference and Exhibition, Sydney, IBC Conference, pp. 34.

Windsor, C.R., (2009), 'A Review of geotechnical practice at BHP Billiton Cannington Mine',CRC Mining – Western Australian School of Mines Confidential Report, pp. 30.

Wood, K., (1981), 'Twenty years of experiences with slag cement', Symposium on slag cement, University of Alabama, Birmingham.

Yildirim, H. and Sengul, O., (2011), 'Modulus of elasticity of substandard and normal concrete', Construction and Building Materials, Volume 25, pp. 1645-1652.

APPENDIX – A

LABORATORY TEST PROGRAM

Table A.1. Stage 2 test program.

ID	Objective	Mix design	Mould
SP_001-v1 to SP_003 v1	To measure electrical resistance of shotcrete cement without accelerator	Shotcrete paste, w/c 0.44	(400x300x100) mm Granite base, Wood walls
SP_004-v1 to SP_006 v1	To measure electrical resistance of shotcrete cement with accelerator	Shotcrete paste, w/c 0.44 with accelerator (4 % of cement)	(400x300x100) mm Granite base, Wood walls
SP_007-v1 to SP_008 v1	To measure electrical resistance of shotcrete cement with superplasticiser	Shotcrete paste, w/c 0.44 with superplasticiser (1.5 % of cement)	(400x300x100) mm Granite base, Wood walls
SP_009-v1 to SP_0010 v1	To measure electrical resistance of shotcrete cement with water reducing admixture	Shotcrete paste, w/c 0.44 and water reducing admixture (0.2 % of cement)	(400x300x100) mm Granite base, Wood walls

Table A.1. Laboratory test program for research stage 3.

ID	Objective	Mix design	Mould	Probe 1	Probe 2	Probe 3	Probe 4	Electrical Data	Vane shear test	Triaxial test
GM_0001	To determine if the displacement between the	Shotcrete paste, w/c 0.44	(400x300x100) mm Granite base, Wood walls	v1 R1V	v1.1 R4V	-	-	Yes	Yes	No
GM_0002	To determine if the size/type of electrode has	Shotcrete paste, w/c 0.44	(400x300x100) mm Granite base, Wood walls	v1.2 R6V	v1 R9V	-	-	Yes	Yes	No
GM_0003	Repeat test GM_0001	Shotcrete paste, w/c 0.44	(400x300x100) mm Granite base, Wood walls	v1.1 R4V	v1 R1V	-	-	Yes	Yes	No
GM_0004	Repeat test GM_0002	Shotcrete paste, w/c 0.44	(400x300x100) mm Granite base, Wood walls	v1 R9V	v1.2 R6V	-	-	Yes	Yes	No
GM_0005	To confirm if the new mould will not have an	Shotcrete paste, w/c 0.44	(230x230x55) mm Granite base, Silicon walls	v1 R1V	v1.1 R4V	-	-	Yes	Yes	No
GM_0006	To determine the difference in performance	Shotcrete paste, w/c 0.44	(400x300x100) mm Granite base, Wood walls	v2 C1V	v1 R1V	-	-	Yes	No	No
GM_0007	Repeat GM_0006	Shotcrete paste, w/c 0.44	(400x300x100) mm Granite base, Wood walls	v2 C1V	v1 R1V	-	-	Yes	No	No
GM_0008	Repeat GM_0006	Shotcrete paste, w/c 0.44	(230x230x55) mm Granite base, Silicon walls	v1 R9V	v2.1 C1V	-	-	Yes	No	No
GM_0009	To determine changes in measured resistance for	Shotcrete paste, w/c 0.44	(230x230x55) mm Granite base, Silicon walls	v1 R1V	v1 R9V	-	-	Yes	No	No
GM_0010	To the determine if an unclean electrodes	Shotcrete paste, w/c 0.44	(230x230x55) mm Granite base, Silicon walls	v1 R1V	v1 R9V	-	-	Yes	No	No
GM_0011	To determine measured electrical resistance and	Shotcrete paste, w/c 0.44	(400x300x100) mm Granite base, Wood walls	v2.1 C1V	v2.1 C3V	-	-	Yes	Yes	Yes
GM_0012	To determine measured electrical resistance and	Shotcrete paste, w/c 0.44	(400x300x100) mm Granite base, Wood walls	v2.1 C2V	-	-	-	Yes	Yes	Yes
GM_0013	To determine if position of the probe will affect its	Shotcrete paste, w/c 0.44	(400x300x100) mm Granite base, Wood walls	v2.1 C2V	-	-	-	Yes	No	No
GM_0014	To determine measured electrical resistance and	Shotcrete paste, w/c 0.44 accelerator (4% of cement)	(400x300x100) mm Granite base, Wood Walls	v2.1 C1V	-	-	-	Yes	Yes	Yes
GM_0015	To determine measured electrical resistance and	Shotcrete paste, w/c 0.44 accelerator (4% of cement)	(400x300x100) mm Granite base, Wood Walls	v2.1 C2V	v2.1 C3V	-	-	Yes	Yes	Yes

Table A.2. Laboratory test program for research stage 3.

ID	Objective	Mix design	Mould	Probe 1	Probe 2	Probe 3	Probe 4	Electrical Data	Vane shear test	Triaxial test
GM_0016	To determine measured electrical resistance and shear strength for cement	Shotcrete paste, w/c 0.44 with superplasticiser (1.5 % of cement)	(400x300x100) mm Granite base, Wood Walls	v2.1 C1V		-	-	Yes	No	No
GM_0017	To determine measured electrical resistance and shear strength for cement	Shotcrete paste, w/c 0.44 with superplasticiser (1.5 % of cement)	(400x300x100) mm Granite base, Wood Walls	v2.1 C2V	v2.1 C3V	-	-	Yes	No	No
GM_0018	To determine measured electrical resistance and shear strength for cement	Shotcrete paste, w/c 0.44 with hydration stabiliser (0.5 % of cement)	(400x300x100) mm Granite base, Wood Walls	v2.1 C1V		-	-	Yes	Yes	No
GM_0019	To determine measured electrical resistance and shear strength for cement	Shotcrete paste, w/c 0.44 with hydration stabiliser (0.5 % of cement)	(400x300x100) mm Granite base, Wood Walls	v2.1 C2V	v2.1 C3V	-	-	Yes	Yes	No
GM_0020	To determine measured electrical resistance and shear strength for cement paste with accelerator, superplasticiser, hydration stabiliser and water reducing admixture	Shotcrete paste, w/c 0.44 accelerator (4% of cement), superplasticiser (1.5 % of cement), hydration stabiliser (0.5 % of cement) and water reducing admixture (0.2 % of cement)	(400x300x100) mm Granite base, Wood Walls	v2.1 C1V		-	-	Yes	Yes	No
GM_0021	To determine measured electrical resistance and shear strength for cement paste with accelerator, superplasticiser, hydration stabiliser and water reducing admixture	Shotcrete paste, w/c 0.44 accelerator (4% of cement), superplasticiser (1.5 % of cement), hydration stabiliser (0.5 % of cement) and water reducing admixture (0.2 % of cement)	(400x300x100) mm Granite base, Wood Walls	v2.1 C2V	v2.1 C3V	-	-	Yes	Yes	Yes

Table A.3. Laboratory test program for research stage 3.

ID	Objective	Mix design	Mould	Probe 1	Probe 2	Probe 3	Probe 4	Electrical Data	Vane shear test	Triaxial test
GM_0022	To determine measured electrical resistance with water reducint admixture	Shotcrete paste, w/c ratio 0.44 with water reducing admixture (0.2 % of cement)	(400x300x100) mm Granite base, Wood Walls	v2.1 C4V		-	-	Yes	Yes	Yes
GM_0023	To compare measured electrical resistance with	Shotcrete paste, w/c ratio 0.44	(230x230x55) mm Granite base, Silicon Walls	v2.1 C4V	v2.1W C2V	-	-	Yes	No	No
GM_0024	To compare measured electrical resistance with	Shotcrete paste, w/c ratio 0.44	(230x230x55) mm Granite Base, Silicon Walls	v2.1 C4V	v2.1W C2V	-	-	Yes	No	No
GM_0025	To determine measured electrical resistance and shear strength for shotcrete paste with water reducing	Shotcrete paste, w/c ratio 0.44 with water reducing admixture (0.2 % of cement)	(400x300x100) mm Granite base, Wood Walls	v2.1 C5V	v2.1 C6V	-	-	Yes	Yes	Yes
GM_0026	To determine measured electrical resistance and shear strength for shotcrete	Shotcrete paste, w/c 0.44 with superplasticiser (1.5 % of cement)	(400x300x100) mm Granite base, Wood Walls	v2.1 C5V	v2.1 C6V	-	-	Yes	Yes	No
GM_0027	To determine measured electrical resistance and shear strength for shotcrete	Shotcrete paste, w/c 0.44 with superplasticiser (1.5 % of cement)	(400x300x100) mm Granite base, Wood Walls	v2.1 C5V	v2.1 C6V	-	-	Yes	Yes	No
GM_0028	To determine measured resistance of cement-paste	20kg cement, 8.75kg water	(230x230x55) mm Granite Base, Silicon Walls	v2.1W C1V	v2.1W C2V	-	-	Yes	No	No

Table A.4. Laboratory test program for research stage 4.

ID	Objective	Mix design	Mould	Probe 1	Probe 2	Probe 3	Probe 4	Electrical Data	Vane shear test	Triaxial test
GM_0029	To determine measured resistance of Cement + Fibre + Accelerator +	40kg cement, 17.5kg water, 0.12 kg fibre, 1.6kg accelerator	(400x300x100) mm Granite Base, Wood Walls	v2.1W C1V	v2.1W C2V	-	-	Yes	Yes	Yes
GM_0030	To determine measured resistance of Cement + Fibre + Accelerator +	40kg cement, 17.5kg water, 0.12 kg fibre, 1.6kg accelerator	400x300x100mm Granite Base, Wood Walls	v2.1W C1V	v2.1W C2V	-	-	Yes	Yes	Yes
GM_0031	To determine measured resistance of Cement + Fibre + Accelerator +	40kg cement, 17.5kg water, 0.12 kg fibre, 1.6kg accelerator	(400x300x100) mm Granite Base, Wood Walls	v2.1W C1V	v2.1W C2V	-	-	Yes	Yes	Yes
GM_0032	To determine if moisture entering probe is causing	10kg cement, 4.375kg water	(230x230x55) mm Granite Base, Silicon Walls	v2.1W C1V	v2.1W C2V	-	-	Yes	No	No
GM_0033	To determine if presence of more than 1 probe is	10kg cement, 4.375kg water	(230x230x55) mm Granite Base, Silicon Walls	v2.1W C1V		-	-	Yes	No	No
GM_0034	To determine measured resistance of Cement + Fibre + Accelerator + water + 7-10 + Dust + Sand mix with wireless	9.6 kg cement, 4.2kg water, 0.12kg fibre, 9.12kg 10-7 aggregate, 14.4kg dust, 18.72kg sand, 0.384kg accelerator	(400x300x100) mm Granite Base, Wood Walls	v2.1W C1V	v2.1W C2V	-	-	Yes	Yes	Yes
GM_0035	To determine if taking resistance measurements in	10kg cement, 4.375kg water	230x230x55mm Granite Base, Silicon Walls	v2.1W C1V	v2.1W C2V	-	-	Yes	No	No
GM_0036	To determine if spikes in resistance measurements	10kg cement, 4.375kg water	(230x230x55) mm Granite Base, Silicon Walls	v2.1W C3V	v2.1W C4V	-	-	Yes	No	No
GM_0037	To determine if the use of different battery	10kg cement, 4.375kg water	(230x230x55) mm Granite Base, Silicon Walls	v2.1W C1V	v2.1W C2V	-	-	Yes	No	No
GM_0038	To determine measured resistance of Cement + Fibre + Accelerator + water + 7-10 + Dust + Sand mix with wireless	9.6 kg cement, 4.2kg water, 0.12kg fibre, 9.12kg 10-7 aggregate, 14.4kg dust, 18.72kg sand, 0.384kg accelerator	(400x300x100) mm Granite Base, Wood Walls	v2.1W C1V	v2.1W C4F	v2.1 C2V	-	Yes	No	Yes,sample 3 membrane ruptured

Table A.5. Laboratory test program for research stage 4.

ID	Objective	Mix design	Mould	Probe 1	Probe 2	Probe 3	Probe 4	Electrical Data	Vane shear test	Triaxial test
GM_0039	To determine measured resistance of Cement + Fibre + Accelerator + water + 7-10 + Dust + Sand mix with wireless	9.6 kg cement, 4.2kg water, 0.12kg fibre, 9.12kg 10-7 aggregate, 14.4kg dust, 18.72kg sand, 0.384kg accelerator	(400x300x100) mm Granite Base, Wood Walls	V2.1W (A1)	V2.1W (A2)	V2.1W (A3)	V2.1W (A4)	Yes	No	Yes
GM_0040	Determine early shear strength of Cement + Fibre + Accelerator + water + 7-10 + Dust + Sand mix	3.2kg cement, 1.4kg water, 0.04kg fibre, 3.04kg 10-7, 4.8kg dust, 6.24kg sand, 0.128kg accelerator	-	-	-	-	-	No	No	Yes
GM_0041	Determine early shear strength of Cement + Fibre + Accelerator + water + 7-10 + Dust + Sand mix	3.2kg cement, 1.4kg water, 0.04kg fibre, 3.04kg 10-7, 4.8kg dust, 6.24kg sand, 0.128kg accelerator	-	-	-	-	-	No	No	Yes
GM_0042	Shear strength for shotcerete mix	3.2kg cement, 1.4kg water, 0.04kg fibre, 3.04kg 10-7, 4.8kg dust, 6.24kg sand, 0.128kg accelerator	-	-	-	-	-	No	No	Yes
GM_0043	Shear strength for shotcerete mix	3.2kg cement, 1.4kg water, 0.04kg fibre, 3.04kg 10-7, 4.8kg dust, 6.24kg sand, 0.128kg accelerator	-	-	-	-	-	No	No	Yes
GM_0044	Shear strength for shotcerete mix	3.2kg cement, 1.4kg water, 0.04kg fibre, 3.04kg 10-7, 4.8kg dust, 6.24kg sand, 0.128kg accelerator	-	-	-	-	-	No	No	Yes
GM_0045	Shear strength for shotcerete mix	3.2kg cement, 1.4kg water, 0.04kg fibre, 3.04kg 10-7, 4.8kg dust, 6.24kg sand, 0.128kg accelerator	-	-	-	-	-	No	No	Yes

APPENDIX – B

SHEAR STRENGTH TEST RESULTS

Table B.1. UCS and triaxial test results for shotcrete paste batch No. SS_001 (Without chemical admixture)

Batch No.	Sample No	Acerage Curing (hours:min)	Diameter-1 (mm)	Diameter-2 (mm)	Average Diameter (mm)	Length (mm)	Weight (g)	Load (KN)	Unit weight (KN/m^3)	Axiail stress (kPa)	σ_3 (kPa)	σ_1 (kPa)	Cohesion - c (kPa)	Friction angle ϕ°
SS_001	UCS1	4:30	51.4	51.05	51.225	117.25	472.2	0.75	19.54	363.92	0	363.92	105	26
	1		50.96	51.69	51.33	117.00	475.40	0.93	19.64	449.51	100	449.61		
	2		51.6	50.81	51.21	117.27	472.20	1.32	19.55	641.00	200	641.20		
	3		51.32	51.72	51.52	117.20	470.40	1.71	19.25	820.26	300	820.56		
	UCS1	5:30	51.46	50.93	51.20	113.20	452.70	2.64	19.43	1,282.50	0	1,282.50	354	30
	1		51.48	50.87	51.18	113.86	459.10	2.94	19.60	1,429.36	100	1,429.46		
	2		51.37	51.48	51.43	113.05	455.80	3.45	19.41	1,661.04	300	1,661.29		
	3		50.56	50.57	50.57	112.87	436.80	4.26	19.27	2,121.38	400	2,121.78		
	UCS1	6:30	51.9	50.99	51.445	114.19	458.2	5.52	19.30	2,655.60	0	2,655.60	864	23
	1		51.4	51.27	51.34	114.11	458.60	5.85	19.42	2,826.43	100	2,826.53		
	2		51.35	51.23	51.29	112.16	457.10	5.58	19.73	2,700.71	300	2,700.96		
	3		51.2	50.79	51.00	114.05	444.70	6.69	19.09	3,275.52	400	3,275.92		
	UCS1	7:30	51.22	51.2	51.21	114.26	458.20	8.91	19.47	4,325.92	0	4,325.92	1265	29
	3		51.44	50.41	50.93	113.82	446.90	10.77	19.28	5,287.66	500	5,288.16		

Table B.2. UCS and triaxial test results for shotcrete paste batch No. SS_002 (Without chemical admixture)

Batch No.	Sample No	Acerage Curing (hours:min)	Diameter-1	Diameter-2	Average Diameter	Length	Weight	Load	Unit weight	Axiail stress	σ_3	σ_1	Cohesion - c (kPa)	Friction angle ϕ°
			(mm)	(mm)	(mm)	(mm)	(g)	(KN)	(KN/m^3)	(kPa)	(kPa)	(kPa)		
SS-002	UCS1	4:00	50.04	50.78	50.41	117.39	458.9		19.59	0.00	0	0.00	36	15
	1		49.71	50.65	50.18	117.65	460.00	0.33	19.77	166.86	100	266.86		
	2		51.45	50.73	51.09	117.74	470.80	0.45	19.51	219.51	200	419.51		
	3		50.13	49.8	49.97	117.56	456.10	0.72	19.79	367.21	400	767.21		
	UCS1	5:00	51.33	50.22	50.78	117.44	461.30	0.78	19.40	385.22	0	385.22	75	31
	1		51.79	50.22	51.01	117.70	471.40	0.87	19.60	425.80	100	525.80		
	2		50.92	49.93	50.43	118.02	459.10	1.23	19.48	615.92	250	865.92		
	3		51.78	50.85	51.32	118.18	475.70	2.64	19.46	1,276.51	400	1,676.51		
	UCS1	6:00	51.39	51.67	51.53	116.3	466.8	2.49	19.25	1,193.96	0	1,193.96	301	35
	1		51.37	51.39	51.38	117.60	466.30	3.00	19.12	1,446.92	100	1,546.92		
	2		50.24	51.4	50.82	117.97	460.30	3.54	19.24	1,745.19	250	1,995.19		
	3		50.53	51.14	50.84	116.92	459.30	4.71	19.35	2,320.62	400	2,720.62		
	UCS1	7:00	51.68	50.83	51.26	118.99	473.80	5.34	19.30	2,588.09	0	2,588.09	778	30
	1		51.27	49.97	50.62	116.73	444.70	6.39	18.93	3,175.17	200	3,375.17		
	2		51.44	51.62	51.53	117.34	470.10	7.71	19.21	3,696.95	400	4,096.95		
	3		51.26	51.58	51.42	117.06	468.40	7.80	19.27	3,756.13	600	4,356.13		

Table B.3. UCS and triaxial test results for shotcrete paste batch No. SS_003 (Without chemical admixture)

Batch No.	Sample No	Acerage Curing (hours:min)	Diameter-1 (mm)	Diameter-2 (mm)	Average Diameter (mm)	Length (mm)	Weight (g)	Load (KN)	Unit weight (KN/m^3)	Axiail stress (kPa)	σ_3 (kPa)	σ_1 (kPa)	Cohesion - c (kPa)	Friction angle ϕ°
SS_003	UCS1	3:30	50.89	50.65	50.77	112.55	514	0.51	22.56	251.92	0	251.92	58	33
	1		51.44	51.2	51.32	114.61	526.10	0.81	22.19	391.58	100	491.58		
	2		51.12	50.73	50.93	114.83	525.00	1.48	22.45	726.62	200	926.62		
	3		50.82	51.04	50.93	116.16	529.70	1.93	22.38	947.37	300	1,247.37		
	UCS1	4:30	50.99	51.34	51.165	115.83	529.7	0.72	22.24	350.18	0	350.18	88	39
	1		51.02	49.6	50.31	116.51	515.50	1.42	22.26	714.32	100	814.32		
	2		50.84	50.41	50.63	115.89	520.00	2.55	22.29	1,266.83	250	1,516.83		
	3		51.47	51.21	51.34	117.04	532.40	3.53	21.97	1,705.19	400	2,105.19		
	UCS1	5:30	50.9	51.6	51.25	116.61	529.7	1.6	22.02	775.61	0	775.61	189	40
	1		51.31	51..45	51.31	117.38	538.30	2.38	22.18	1,151.02	100	1,251.02		
	2		51.2	51.63	51.42	117.63	539.00	4.04	22.07	1,945.86	250	2,195.86		
	3		50.8	50.03	50.42	115.19	508.70	4.36	22.12	2,184.12	400	2,584.12		
	UCS1	6:30	51.57	51	51.29	117.63	537.50	2.80	22.12	1,355.46	0	1,355.46	309	41
	1		50.72	51.69	51.21	117.19	536.80	3.81	22.24	1,850.16	100	1,950.16		
	2		51.39	51.36	51.38	118.14	535.80	4.22	21.88	2,035.72	250	2,285.72		
	3		50.28	50.65	50.47	117.06	517.20	5.99	22.09	2,994.72	400	3,394.72		
	UCS1	7:30	51.13	50.72	50.93	118.10	525.80	4.39	21.86	2,155.32	0	2,155.32	407	46
	1		51.48	50.31	50.90	117.91	526.10	5.56	21.93	2,732.97	200	2,932.97		
	2		50.77	50.63	50.70	118.39	516.30	8.93	21.60	4,423.29	400	4,823.29		
	3		51.81	51.13	51.47	118.30	535.40	10.56	21.75	5,075.34	600	5,675.34		

Table B.4. UCS and triaxial test results for shotcrete paste batch No. SS_004 (Without chemical admixture)

Batch No.	Sample No	Acerage Curing (hours:min)	Diameter-1 (mm)	Diameter-2 (mm)	Average Diameter (mm)	Length (mm)	Weight (g)	Load (KN)	Unit weight (KN/m^3)	Axiail stress (kPa)	σ_3 (kPa)	σ_1 (kPa)	Cohesion - c (kPa)	Friction angle ϕ°
SS_004	UCS1	2:30	50.7	51.29	50.995	115.54	520.1	0.35	22.04	171.37	0	171.37	44	32
	1		49.9	49.47	49.69	116.90	505.70	0.65	22.31	335.25	100	435.25		
	2		50.92	50.3	50.61	116.55	522.70	1.43	22.29	710.84	200	910.84		
	3		49.5	49.9	49.70	116.92	509.70	1.59	22.47	819.59	300	1,119.59		
	UCS1	3:30	50.85	49.98	50.415	115.79	499.4	0.56	21.61	280.53	0	280.53	54	40
	1		50.77	50.96	50.87	115.62	508.70	1.07	21.65	526.57	100	626.57		
	2		50.67	50.94	50.81	117.45	519.50	2.39	21.82	1,178.95	250	1,428.95		
	3		50.76	51.46	51.11	116.26	519.00	3.52	21.76	1,715.70	400	2,115.70		
	UCS1	4:30	51.44	51.36	51.4	115.82	519.7	1.27	21.62	612.05	0	612.05	131	43
	1		50.96	50.01	50.49	117.03	508.30	2.01	21.70	1,004.11	100	1,104.11		
	2		51.4	51.29	51.35	116.60	524.30	3.62	21.72	1,748.32	250	1,998.32		
	3		51.39	51.46	51.43	16.23	524.60	4.81	155.62	2,315.83	400	2,715.83		
	UCS1	5:30	51.33	51.47	51.4	116.58	522.4	2.22	21.60	1,069.88	0	1,069.88	210	46
	1		51.25	51.41	51.33	117.05	518.30	3.76	21.40	1,817.00	150	1,967.00		
	2		51.44	51.02	51.23	116.92	522.30	5.20	21.67	2,522.69	300	2,822.69		
	3		50.98	51.6	51.29	116.58	514.60	7.58	21.36	3,668.71	500	4,168.71		
	UCS1	6:30	50.32	51.19	50.76	116.91	514.70	3.52	21.76	1,739.78	0	1,739.78	343	47
	1		51.87	51.35	51.61	116.39	524.90	5.22	21.56	2,495.24	150	2,645.24		
	2		51.08	51.42	51.25	116.94	523.20	7.56	21.69	3,664.74	300	3,964.74		
	3		51.45	51.74	51.60	116.34	522.70	9.30	21.49	4,448.13	500	4,948.13		
	UCS1	7:30	51.03	50.09	50.56	116.83	508.8	5.32	21.69	2,649.77	0	2,649.77	555	46
	1		50.83	50.22	50.53	117.19	508.50	6.99	21.64	3,486.38	150	3,636.38		
	2		50.97	49.99	50.48	117.72	510.80	8.99	21.68	4,491.91	300	4,791.91		
	3		50.86	51.29	51.08	116.91	514.50	10.52	21.48	5,134.62	500	5,634.62		
	UCS1	8:30	51.09	50.77	50.93	116.81	515.3	9.64	21.65	4,731.95	0	4,731.95	1057	42
	1		51.61	51.58	51.60	115.64	523.70	11.55	21.66	5,524.30	200	5,724.30		
	2		50.98	50.04	50.51	116.47	506.50	12.29	21.70	6,133.48	400	6,533.48		
	3		50.68	51.72	51.20	117.52	528.10	14.75	21.83	7,164.10	600	7,764.10		

Table B.5. UCS and triaxial test results for shotcrete paste batch No. SS_005 (Without chemical admixture)

Batch No.	Sample No	Acerage Curing (hours:min)	Diameter-1 (mm)	Diameter-2 (mm)	Average Diameter (mm)	Length (mm)	Weight (g)	Load (KN)	Unit weight (KN/m^3)	Axiail stress (kPa)	σ_3 (kPa)	σ_1 (kPa)	Cohesion - c (kPa)	Friction angle ϕ °
SS_005	UCS1	3:30	51.34	51.44	51.39	111.02	453.90	0.61	19.71	294.09	0	294.09	141	18
	2		51.67	50.34	51.01	111.23	452.50	1.04	19.91	509.00	100	609.00		
	3		51.21	50.86	51.04	112.16	448.20	1.57	19.53	767.49	200	967.49		
	4		51.45	51.21	51.33	111.08	453.30	1.03	19.72	497.74	300	797.74		
	UCS1	4:30	51.5	50.3	50.9	111.23	445.8	1.96	19.70	963.23	0	963.23	235	30
	2		51.34	50.13	50.74	111.3	443.50	1.70	19.71	840.90	100	940.90		
	3		51.64	51.15	51.40	111.24	451.60	2.34	19.57	1,127.93	200	1,327.93		
	4		51.17	50.29	50.73	110.74	439.20	3.11	19.62	1,538.65	300	1,838.65		
	UCS1	5:30	51.4	51.55	51.475	111.58	454.5	4.05	19.57	1,946.13	0	1,946.13	432	43
	2		51.16	50.13	50.65	111.33	438.60	4.86	19.56	2,412.53	100	2,512.53		
	3		50.42	51.24	50.83	111.23	446.10	6.14	19.76	3,025.78	200	3,225.78		
	4		50.39	51.23	50.81	112.15	449.20	6.45	19.75	3,181.05	300	3,481.05		
	UCS1	6:30	51.75	51.08	51.415	110.63	451.6	7.31	19.66	3,520.85	0	3,520.85	789	40
	2		50.99	50.94	50.97	111.09	443.90	7.68	19.59	3,764.67	150	3,914.67		
	3		51.22	51.47	51.35	111.01	450.40	8.53	19.60	4,119.67	250	4,369.67		
	4		50.46	51.22	50.84	112.01	446.20	9.80	19.62	4,827.53	350	5,177.53		
	UCS1	7:30	50.11	50.87	50.49	110.58	436.10	8.39	19.70	4,190.45	0	4,190.45	946	46
	2		51.04	50.44	50.74	110.99	438.20	12.77	19.53	6,315.38	150	6,465.38		
	3		51.42	51.44	51.43	110.96	450.30	11.85	19.53	5,704.20	250	5,954.20		
	4		51.2	51.63	51.42	111.82	453.40	13.49	19.53	6,497.43	400	6,897.43		

Table B.6. UCS and triaxial test results for shotcrete paste batch No. SS_006 (Without chemical admixture)

Batch No.	Sample No	Acerage Curing (hours:min)	Diameter-1	Diameter-2	Average Diameter	Length	Weight	Load	Unit weight	Axiail stress	σ_3	σ_1	Cohesion - c (kPa)	Friction angle ϕ°
			(mm)	(mm)	(mm)	(mm)	(g)	(KN)	(KN/m^3)	(kPa)	(kPa)	(kPa)		
SS_006	UCS1	3:30	49.61	50.87	50.24	111.35	437.60	0.47	19.82	237.09	0	237.09	69	28
	2		49.92	50.83	50.38	112.13	447.10	0.79	20.01	396.38	100	496.38		
	3		49.99	50.64	50.32	111.31	443.50	1.08	20.04	543.17	200	743.17		
	4		49.66	50.46	50.06	112.51	441.20	1.50	19.92	762.11	300	1,062.11		
	UCS1	4:30	51.36	51.38	51.37	111.27	453.1	1.53	19.65	738.21	0	738.21	138	39
	2		51.26	51.37	51.32	111.52	454.50	1.60	19.71	773.64	100	873.64		
	3		51.02	50.93	50.98	111.90	453.00	2.27	19.84	1,112.30	200	1,312.30		
	4		51.4	51.01	51.21	112.79	457.30	3.66	19.69	1,777.32	300	2,077.32		
	UCS1	5:30	51.1	50.6	50.85	112.55	450.4	2.94	19.71	1,447.69	0	1,447.69	349	44
	2		51.06	50.43	50.75	111.9	443.60	4.73	19.60	2,338.76	100	2,438.76		
	3		51.29	51.51	51.40	110.82	450.10	5.68	19.57	2,737.36	200	2,937.36		
	4		52.04	50.6	51.32	112.66	457.60	5.90	19.64	2,852.26	300	3,152.26		
	UCS1	6:30	51.34	50.86	51.1	111.6	446.3	6.08	19.50	2,964.64	0	2,964.64	525	47
	2		51.46	51.34	51.40	111.43	454.60	6.26	19.66	3,016.88	150	3,166.88		
	3		51.23	50.79	51.01	112.39	446.90	8.70	19.46	4,257.14	250	4,507.14		
	4		51.55	51.63	51.59	111.90	456.40	10.53	19.51	5,037.41	400	5,437.41		
	UCS1	7:30	51.96	50.99	51.48	112.16	455.20	8.56	19.50	4,113.30	0	4,113.30	906	43
	2		50.67	50.39	50.53	111.57	438.70	9.32	19.61	4,647.58	150	4,797.58		
	3		51.59	51.36	51.48	111.51	452.10	11.54	19.48	5,545.27	250	5,795.27		
	4		50.13	51.5	50.82	112.22	446.60	11.55	19.62	5,695.18	400	6,095.18		

Table B.7. UCS and triaxial test results for shotcrete paste batch No. SS_007 (With accelerator)

Batch No.	Sample No	Acerage Curing (hours:min)	Diameter-1 (mm)	Diameter-2 (mm)	Average Diameter (mm)	Length (mm)	Weight (g)	Load (KN)	Unit weight (KN/m^3)	Axiail stress (kPa)	σ_3 (kPa)	σ_1 (kPa)	Cohesion - c (kPa)	Friction angle ϕ°
SS_007	UCS1	3:00	49.21	49.59	49.4	112.50	422.60	0.27	19.60	140.87	0	140.87	35	34
	1		49.22	51.1	50.16	111.11	422.00	0.71	19.22	359.30	100	459.30		
	2		51.36	50.83	51.10	112.49	432.40	1.38	18.75	673.03	200	873.03		
	3		50.89	50.94	50.92	112.10	429.00	1.80	18.80	884.08	300	1,184.08		
	UCS1	4:00	51.87	50.76	51.315	112.89	431.3	0.82	18.47	396.49	0	396.49	71	46
	1		50.12	50.89	50.51	112.24	421.10	1.69	18.73	843.58	100	943.58		
	2		49.71	50.94	50.33	112.68	422.30	2.53	18.84	1,271.93	200	1,471.93		
	3		51.63	51.27	51.45	111.76	431.50	4.07	18.57	1,957.64	300	2,257.64		
	UCS1	5:00	51.21	51.6	51.405	111.76	429.2	7.47	18.50	3,599.32	0	3,599.32	1153	25
	1		50.74	51.22	50.98	111.98	421.90	8.05	18.46	3,943.72	150	4,093.72		
	2		51.45	50.26	50.86	112.85	422.10	8.22	18.41	4,046.82	300	4,346.82		
	3		50.59	51.2	50.90	112.28	418.20	7.82	18.31	3,843.85	400	4,243.85		
		6:00	50.33	51.58	50.955	108.56	407.9	13.36	18.43	6,551.53	0	6,551.53	1886	30
			50.64	51.54	51.09	108.97	409.80	15.91	18.34	7,760.83	600	8,360.83		

Table B.8. UCS and triaxial test results for shotcrete paste batch No. SS_008 (With accelerator)

Batch No.	Sample No	Acerage Curing (hours:min)	Diameter-1 (mm)	Diameter-2 (mm)	Average Diameter (mm)	Length (mm)	Weight (g)	Load (KN)	Unit weight (KN/m^3)	Axiail stress (kPa)	σ_3 (kPa)	σ_1 (kPa)	Cohesion - c (kPa)	Friction angle ϕ°
SS_008	UCS1	2:30	50.8	50.77	50.785	110.85	425.80	0.17	18.96	83.92	0	83.92	26	21
	2		50.66	50.98	50.82	111.52	419.20	0.41	18.53	202.13	100	302.13		
	3		49.89	50.59	50.24	111.80	428.10	0.51	19.32	257.26	200	457.26		
	4		50.83	50.46	50.65	111.30	422.40	0.90	18.84	446.76	300	746.76		
	UCS1	3:30	51.64	51.16	51.4	112.4	433.1	0.52	18.57	250.60	0	250.60	57	41
	2		50.92	51.85	51.39	112.2	436.1	1.14	18.74	549.72	100	649.72		
	3		50.8	51.68	51.24	113.22	438.10	2.36	18.76	1,144.47	200	1,344.47		
	4		50.39	51.24	50.82	110.75	421.10	2.66	18.75	1,311.62	300	1,611.62		
	UCS1	4:30	51.72	51.42	51.57	113.01	435.9	3.29	18.47	1,575.11	0	1,575.11	376	39
	2		50.15	50.82	50.49	111.78	408.60	3.57	18.26	1,783.42	100	1,883.42		
	3		51.79	51.19	51.49	112.35	432.70	5.23	18.50	2,511.69	200	2,711.69		
	4		51.11	51.36	51.24	112.33	422.17	5.07	18.23	2,459.14	300	2,759.14		
	UCS1	5:30	50.4	50.82	50.61	112.36	408.2	3.82	18.06	1,898.89	0	1,898.89	416	41
	2		50.34	51.22	50.78	117.7	411.00	4.94	17.24	2,439.22	150	2,589.22		
	3		51.44	51.35	51.40	111.45	413.50	5.03	17.88	2,424.58	250	2,674.58		
	4		51.14	50.7	50.92	111.72	141.30	7.13	6.21	3,501.24	400	3,901.24		
	1	6:30	49.83	50.87	50.35	111.56	405.70	10.17	18.26	5,107.77	0	5,107.77	1273	36
	2		50.5	51.39	50.95	113.15	417.80	11.81	18.11	5,793.71	400	6,193.71		
	4		51.28	49.82	50.55	113.34	414.40	13.91	18.22	6,930.98	600	7,530.98		

Table B.9. UCS and triaxial test results for shotcrete paste batch No. SS_009 (With accelerator)

Batch No.	Sample No	Acerage Curing (hours:min)	Diameter-1 (mm)	Diameter-2 (mm)	Average Diameter (mm)	Length (mm)	Weight (g)	Load (KN)	Unit weight (KN/m^3)	Axiail stress (kPa)	σ_3 (kPa)	σ_1 (kPa)	Cohesion - c (kPa)	Friction angle ϕ°
SS_009	UCS1	2:30	50.71	50.61	50.66	111.89	490.90	0.27	21.77	133.95	0	133.95	48	25
	2		50.6	50.95	50.78	111.10	491.80	0.90	21.86	444.48	100	544.48		
	3		50.86	50.81	50.84	112.38	497.90	0.45	21.83	221.72	200	421.72		
	4		50.13	50.45	50.29	111.90	474.80	1.40	21.36	704.81	300	1,004.81		
	UCS1	3:30	50.51	51.21	50.86	111.07	476.5	0.6	21.12	295.33	0	295.33	59	36
	2		49.94	50.21	50.08	112.26	476.0	0.75	21.53	380.83	100	480.83		
	3		50.1	50.9	50.50	112.46	469.90	1.68	20.86	838.76	200	1,038.76		
	4		51.65	51.16	51.41	111.02	488.40	2.23	21.20	1,074.49	300	1,374.49		
	UCS1	4:30	51.79	50.99	51.39	111.46	493.8	1.32	21.36	636.40	0	636.40	131	41
	2		51.46	51.47	51.47	110.87	489.20	1.82	21.21	874.90	100	974.90		
	3		51.02	49.98	50.50	111.78	477.80	2.52	21.34	1,258.14	200	1,458.14		
	4		51.47	51.53	51.50	112.19	494.70	3.65	21.17	1,752.22	300	2,052.22		
	UCS1	5:30	50.62	51.21	50.915	12.46	485.9	2.37	191.53	1,164.04	0	1,164.04	240	48
	1		51.54	51.21	51.38	110.98	486.80	4.15	21.16	2,001.95	100	2,101.95		
	2		51.46	50.41	50.94	112.03	479.60	4.82	21.01	2,365.51	200	2,565.51		
	3		50.44	50.65	50.55	111.50	470.90	5.99	21.05	2,985.25	300	3,285.25		
	UCS1	6:30	51.26	51.6	51.43	111.88	492	7.33	21.17	3,528.43	0	3,528.43	898	37
	1		51.57	50.71	51.14	112.49	489.70	8.58	21.19	4,177.11	150	4,327.11		
	2		51.01	51.25	51.13	112.20	485.10	9.30	21.06	4,529.40	250	4,779.40		
	3		51.13	50.63	50.88	111.97	478.00	9.66	21.00	4,751.08	400	5,151.08		
	1	7:30	51.32	50.69	51.005	110.51	479.9	12.13	21.25	5,936.70	0	5,936.70	1756	29
	2		51.35	50.67	51.01	11.58	482.80	13.65	204.01	6,679.31	400	7,079.31		

Table B.10. UCS and triaxial test results for shotcrete paste batch No. SS_010 (With accelerator)

Batch No.	Sample No	Acerage Curing (hours:min)	Diameter-1 (mm)	Diameter-2 (mm)	Average Diameter (mm)	Length (mm)	Weight (g)	Load (KN)	Unit weight (KN/m^3)	Axiail stress (kPa)	σ_3 (kPa)	σ_1 (kPa)	Cohesion - c (kPa)	Friction angle ϕ°
SS_010	1	2:30	51.25	51.56	51.41	104.12	408.30	0.15	18.89	72.28	100	172.28	17	8
	2		51.25	51.56	51.41	104.12	408.30	0.21	18.89	100.27	200	300.27		
	3		51.25	51.56	51.41	104.12	408.30	0.29	18.89	137.32	300	437.32		
	1	3:30	51.09	50.97	51.03	103.04	401.00	0.30	19.03	146.19	100	246.19	56	6
	2		51.09	50:97	51.09	103.04	401.00	0.36	18.98	176.53	250	426.53		
	3		51.09	50:97	51.09	103.04	401.00	0.43	18.98	211.07	400	611.07		
	1	4:20	50.81	50.47	50.64	105.41	401.80	0.68	18.93	339.81	100	439.81	123	10
	2		50.81	50.47	50.64	105.41	401.80	0.82	18.93	404.90	250	654.90		
	3		50.81	50.47	50.64	105.41	401.80	0.95	18.93	470.83	400	870.83		
	1	5:20	50.65	51.12	50.89	103.48	395.80	4.97	18.81	2,444.66	100	2,544.66	976	12
	2		50.65	51.12	50.89	103.48	395.80	5.13	18.81	2,520.19	250	2,770.19		
	3													
	1	6:30	51.05	50.46	50.76	103.49	393.00	8.20	18.77	4,052.90	100	4,152.90	737	47
	2		50.5	50.38	50.44	105.26	394.20	11.43	18.74	5,720.13	250	5,970.13		
	3		50.95	51.41	51.18	104.66	401.80	11.77	18.66	5,718.99	400	6,118.99		

Table B.11. UCS and triaxial test results for shotcrete paste batch No. SS_011 (With accelerator)

Batch No.	Sample No	Acerage Curing (hours:min)	Diameter-1	Diameter-2	Average Diameter	Length	Weight	Load	Unit weight	Axiail stress	σ_3	σ_1	Cohesion - c (kPa)	Friction angle ϕ°
			(mm)	(mm)	(mm)	(mm)	(g)	(KN)	(KN/m^3)	(kPa)	(kPa)	(kPa)		
SS_011	1	4:00	50.42	50.23	50.33	110.53	417.10	2.15	18.97	1,079.18	100	1,179.18	31	58
	2		50.98	51.47	51.23	103.62	400.20	5.99	18.74	2,905.79	200	3,105.79		
	3		51.61	50.97	51.29	103.89	402.40	9.57	18.75	4,629.45	400	5,029.45		
	1	6:30	51.34	50.4	50.87	105.30	401.20	14.06	18.75	6,915.75	200	7,115.75	976	52
	2		51.45	50.31	50.88	103.59	406.80	16.77	19.31	8,246.42	300	8,546.42		
	3		50.89	50.91	50.90	103.47	393.80	18.84	18.70	9,260.28	500	9,760.28		

Table B.12. UCS and triaxial test results for shotcrete paste batch No. SS_012 (With accelerator)

Batch No.	Sample No	Acerage Curing (hours:min)	Diameter-1	Diameter-2	Average Diameter	Length	Weight	Load	Unit weight	Axiail stress	σ_3	σ_1	Cohesion - c (kPa)	Friction angle ϕ°
			(mm)	(mm)	(mm)	(mm)	(g)	(KN)	(KN/m^3)	(kPa)	(kPa)	(kPa)		
SS_012	UCS1	3:00	51.22	50.25	50.74	103.04	397.80	0.20	19.10	98.93	0	98.93	44	1
	1		51.06	50.75	50.91	97.56	382.70	0.18	19.27	85.99	100	185.99		
	2		49.84	50.63	50.24	99.26	375.10	0.19	19.07	95.86	200	295.86		
	3		50.67	50.22	50.45	99.98	387.00	0.22	19.37	112.43	300	412.43		
	1	4:00	51.14	50.75	50.95	99.31	387.50	0.29	19.14	141.92	100	241.92	117	3
	2		50.76	51.79	51.28	99.39	388.20	0.58	18.92	282.77	200	482.77		
	3		50.03	50.55	50.29	99.78	385.10	0.62	19.43	314.20	300	614.20		
	1	5:00	50.98	51.7	51.34	100.89	393.10	2.03	18.82	980.60	0	980.60	295	17
	2		51.62	51.4	51.51	99.38	391.10	1.58	18.88	759.02	200	959.02		
	3		51.16	50.67	50.92	100.28	386.80	1.55	18.94	759.28	400	1,159.28		

Table B.13. UCS and triaxial test results for shotcrete paste batch No. SS_013 (With superplasticier)

Batch No.	Sample No	Acerage Curing (hours:min)	Diameter-1 (mm)	Diameter-2 (mm)	Average Diameter (mm)	Length (mm)	Weight (g)	Load (KN)	Unit weight (KN/m^3)	Axiail stress (kPa)	σ_3 (kPa)	σ_1 (kPa)	Cohesion - c (kPa)	Friction angle ϕ°
SS_013	UCS1	6:00	50.03	50.83	50.43	100.60	382.40	0.39	19.03	195.25	0	195.25	70	19
	1		51.77	51.28	51.53	99.31	387.20	0.84	18.70	404.49	100	504.49		
	2		51.58	51.71	51.65	99.15	377.40	0.50	18.17	239.11	200	439.11		
	3		51.41	50.74	51.08	99.26	386.50	1.32	19.01	644.51	400	1,044.51		
	UCS1	7:00	51.36	51.27	51.315	103.52	407.6	1.01	19.04	488.36	0	488.36	118	38
	1		51.32	50.92	51.12	99.43	385.4	1.75	18.89	852.79	100	952.79		
	2		51.21	50.62	50.92	99.64	384.40	1.97	18.95	969.10	200	1,169.10		
	3		51.07	51.61	51.34	99.34	383.00	3.10	18.62	1,495.98	300	1,795.98		
	UCS1	8:00	50.14	51.41	50.775	102.11	397.3	2.94	19.22	1,451.97	0	1,451.97	396	35
	1		51.65	51.25	51.45	99.14	384.40	4.14	18.65	1,990.45	100	2,090.45		
	2		51.41	50.29	50.85	99.34	377.10	3.93	18.69	1,936.26	200	2,136.26		
	3		51.46	51.66	51.56	99.84	388.50	5.50	18.64	2,635.43	400	3,035.43		

Table B.14. UCS and triaxial test results for shotcrete paste batch No. SS_014 (With water reducing admixture)

Batch No.	Sample No	Acerage Curing (hours:min)	Diameter-1 (mm)	Diameter-2 (mm)	Average Diameter (mm)	Length (mm)	Weight (g)	Load (KN)	Unit weight (KN/m^3)	Axiail stress (kPa)	σ_3 (kPa)	σ_1 (kPa)	Cohesion - c (kPa)	Friction angle ϕ°
SS_014	UCS1	5:00	51.48	51.29	51.385	101.58	410.10	0.73	19.47	352.01	0	352.01	101	18
	1		50.38	50.78	50.58	100.51	388.90	0.59	19.26	291.89	100	391.89		
	2		51.13	51.39	51.26	99.79	399.60	0.85	19.40	411.25	200	611.25		
	3		51.01	51.19	51.10	99.97	400.50	1.37	19.53	666.07	400	1,066.07		
	UCS1	6:00	51.31	50.6	50.955	101.59	396	1.64	19.12	804.23	0	804.23	181	34
	1		51.27	51.7	51.49	99.2	396.2	1.69	19.18	811.82	100	911.82		
	2		50.62	51.22	50.92	99.44	394.90	2.20	19.50	1,080.82	200	1,280.82		
	3		50.99	50.59	50.79	99.80	393.00	3.17	19.44	1,563.45	300	1,863.45		
	UCS1	7:00	51.11	51.8	51.455	101.52	402.9	3.26	19.09	1,567.73	0	1,567.73	475	33
	1		50.86	50.69	50.78	99.01	390.10	3.93	19.46	1,941.14	100	2,041.14		
	2		50.69	50.77	50.73	99.51	391.50	5.29	19.46	2,616.75	200	2,816.75		
	3		50.44	50.68	50.56	99.37	387.00	5.00	19.40	2,492.27	400	2,892.27		
	UCS1	8:00	51.03	50.9	50.965	101.49	397.5	6.43	19.20	3,151.93	0	3,151.93	653	43
	1		50.7	50.64	50.67	99.12	381.40	6.19	19.08	3,069.72	100	3,169.72		
	2		51.15	51.36	51.26	99.69	400.90	8.74	19.49	4,235.88	200	4,435.88		
	3		50.02	51.54	50.78	100.04	393.50	9.52	19.42	4,702.76	400	5,102.76		

Table B.16. UCS and triaxial test results for shotcrete paste batch No. GM_0012 (Without chemical admixture)

Batch No.	Sample No	Acerage Curing (hours:min)	Diameter-1	Diameter-2	Average Diameter	Length	Weight	Load	Unit weight	Axiail stress	σ_3	σ_1	Cohesion - c (kPa)	Friction angle ϕ°
			(mm)	(mm)	(mm)	(mm)	(g)	(KN)	(KN/m^3)	(kPa)	(kPa)	(kPa)		
GM_0012	1	3:37	50.53	50.95	50.74	99.67	389.90	1.27	19.35	627.98	100	727.98	80	36
	2		51.67	51.31	51.49	100.18	402.20	1.77	19.28	851.52	200	1,051.52		
	3		51.81	51.38	51.60	100.05	405.20	2.53	19.37	1,209.36	300	1,509.36		
	1	4:40	51.48	51.17	51.33	99.53	396.3	2.66	19.25	1,287.13	100	1,387.13	188	45
	2		50.71	50.89	50.80	99.26	394.00	4.03	19.58	1,986.60	200	2,186.60		
	3		50.69	50.75	50.72	99.25	382.60	5.58	19.08	2,759.38	400	3,159.38		
	1	5:45	50.83	51.44	51.14	99.51	391.20	6.14	19.14	2,989.99	100	3,089.99	381	53
	2		51.21	51.51	51.36	99.25	395.50	10.12	19.23	4,884.73	300	5,184.73		
	3		50.25	51.05	50.65	99.22	384.30	12.47	19.22	6,189.45	500	6,689.45		

Table B.15. UCS and triaxial test results for shotcrete paste batch No. GM_0011 (Without chemical admixture)

Batch No.	Sample No	Acerage Curing (hours:min)	Diameter-1	Diameter-2	Average Diameter	Length	Weight	Load	Unit weight	Axiail stress	σ_3	σ_1	Cohesion - c (kPa)	Friction angle ϕ°
			(mm)	(mm)	(mm)	(mm)	(g)	(KN)	(KN/m^3)	(kPa)	(kPa)	(kPa)		
GM_0011	1	4:15	51.15	50.51	50.83	100.40	397.40	0.52	19.51	254.14	100	354.14	10	30
	2		51.49	51.3	51.40	99.64	406.90	0.84	19.68	405.29	200	605.29		
	3		50.88	51.02	50.95	99.19	405.20	1.35	20.04	660.53	300	960.53		
	1	5:37	50.27	50.82	50.55	99.64	390.4	2.29	19.53	1,140.87	100	1,240.87	263	32
	2		51.22	51.02	51.12	99.39	395.40	3.01	19.38	1,466.79	200	1,666.79		
	3		51.45	51.19	51.32	99.96	407.80	3.30	19.72	1,592.96	300	1,892.96		

Table B.17. UCS and triaxial test results for shotcrete paste batch No. GM_0014 (With accelerator)

Batch No.	Sample No	Acerage Curing (hours:min)	Diameter-1 (mm)	Diameter-2 (mm)	Average Diameter (mm)	Length (mm)	Weight (g)	Load (KN)	Unit weight (KN/m^3)	Axiail stress (kPa)	σ_3 (kPa)	σ_1 (kPa)	Cohesion - c (kPa)	Friction angle ϕ°
GM_0014	1	2:41	51.38	51.42	51.40	99.81	383.00	4.25	18.49	2,047.33	100	2,147.33	496	30
	2		51.58	50.38	50.98	98.99	372.00	3.84	18.41	1,883.24	200	2,083.24		
	3		50.99	51.18	51.09	99.60	375.30	5.02	18.38	2,450.63	300	2,750.63		
	1	3:44	51	51.11	51.06	100.01	372.5	3.76	18.19	1,834.24	100	1,934.24	582	23
	2		51.03	51.42	51.23	99.90	375.90	4.20	18.26	2,036.31	200	2,236.31		
	3		51.18	50.77	50.98	100.34	371.40	4.54	18.14	2,224.35	400	2,624.35		
	1	4:35	0.186806	51.35	25.77	100.51	379.70	5.13	72.44	9,837.14	100	9,937.14	2149	0
	2		0.202083	50.95	25.58	92.55	344.10	5.07	72.37	9,877.25	400	10,277.25		

Table B.18. UCS and triaxial test results for shotcrete paste batch No. GM_0015 (With accelerator)

Batch No.	Sample No	Acerage Curing (hours:min)	Diameter-1 (mm)	Diameter-2 (mm)	Average Diameter (mm)	Length (mm)	Weight (g)	Load (KN)	Unit weight (KN/m^3)	Axiail stress (kPa)	σ_3 (kPa)	σ_1 (kPa)	Cohesion - c (kPa)	Friction angle ϕ°
GM_0015	1	4:00	51.96	51.24	51.60	99.26	387.10	6.94	18.65	3,320.34	100	3,420.34	668	41
	2		50.91	51.6	51.26	99.99	388.40	7.53	18.83	3,649.93	200	3,849.93		
	3		51.97	51.55	51.76	99.60	390.00	8.58	18.61	4,078.25	300	4,378.25		

Table B.19. UCS and triaxial test results for shotcrete paste batch No. GM_0022 (With water reducting admixture)

Batch No.	Sample No	Acerage Curing (hours:min)	Diameter-1 (mm)	Diameter-2 (mm)	Average Diameter (mm)	Length (mm)	Weight (g)	Load (KN)	Unit weight (KN/m^3)	Axiail stress (kPa)	σ_3 (kPa)	σ_1 (kPa)	Cohesion - c (kPa)	Friction angle ϕ°
GM_0022	1	6:37	51.75	51.83	51.79	100.31	402.60	1.30	19.05	617.30	100	717.30	47	42
	2		51.09	51.35	51.22	100.73	388.80	2.16	18.73	1,046.16	200	1,246.16		
	3		51.34	51.14	51.24	100.17	384.30	2.97	18.60	1,440.43	300	1,740.43		

Table B.20. UCS and triaxial test results for shotcrete paste batch No. GM_0025 (With water reducting admixture)

Batch No.	Sample No	Acerage Curing (hours:min)	Diameter-1 (mm)	Diameter-2 (mm)	Average Diameter (mm)	Length (mm)	Weight (g)	Load (KN)	Unit weight (KN/m^3)	Axiail stress (kPa)	σ_3 (kPa)	σ_1 (kPa)	Cohesion - c (kPa)	Friction angle ϕ°
GM_0025	1	5:10	50.72	51.75	51.24	9.52	404.00	1.11	205.84	537.96	100	637.96	135	22
	2		51.15	51.2	51.18	99.58	396.20	1.23	19.34	598.24	200	798.24		
	3		51.51	51.69	51.60	99.17	403.40	1.62	19.45	776.45	300	1,076.45		
	1	7:35	51.05	51.2	51.13	100.92	398.0	4.71	19.21	2,293.84	100	2,393.84	711	25
	2		50.74	50.9	50.82	101.55	391.00	5.35	18.98	2,637.12	400	3,037.12		
	3		51.81	51.92	51.87	101.69	410.20	6.42	19.09	3,036.44	300	3,336.44		

Table B.21. Triaxial test results for shotcrete paste batch No. GM_0029 to GM_0031 (With accelerator and synthetic fibres)

Batch No.	Sample No	Acerage Curing (hours:min)	Diameter-1	Diameter-2	Average Diameter	Length	Weight	Load	Unit weight	Axial stress	σ_3	σ_1	Cohesion - c (kPa)	Friction angle ϕ°
			(mm)	(mm)	(mm)	(mm)	(g)	(KN)	(KN/m^3)	(kPa)	(kPa)	(kPa)		
GM_0029	1	3:25	108.10	105.40	106.75	195.00	3,157.60	1.99	18.09	222.89	100	322.89	141	55
	2		104.06	101.41	102.74	198.50	3,104.20	3.84	18.87	462.89	200	662.89		
	3		104.35	103.23	103.79	201.00	3,130.40	17.00	18.41	2,009.66	300	2,309.66		
GM_0030	1	2:46	102.98	104.37	103.68	198	3,171.2	1.50	18.97	178.05	100	278.05	14	29
	2		109.12	104.19	106.66	200.00	3,210.20	2.46	17.97	275.68	200	475.68		
	3		102.70	103.76	103.23	200.00	3,170.10	4.72	18.94	563.76	300	863.76		
GM_0031	1	3:06	102.29	104.43	103.36	202.00	3,209.60	4.39	18.94	522.63	100	622.63	67	53
	2		104.57	102.05	103.31	202.00	3,222.80	7.65	19.03	913.17	200	1,113.17		
	3		104.00	105.95	104.98	200.00	3,181.60	18.20	18.38	2,102.55	300	2,402.55		

Table B.22. Triaxial test results for shotcrete paste batch No. GM_0034 and GM_0038 (Shear strength of synthetic fibre reinforced concrete with accelerator)

Batch No.	Sample No	Acerage Curing (hours:min)	Diameter-1 (mm)	Diameter-2 (mm)	Average Diameter (mm)	Length (mm)	Weight (g)	Load (KN)	Unit weight (KN/m^3)	Axiail stress (kPa)	σ_3 (kPa)	σ_1 (kPa)	Cohesion - c (kPa)	Friction angle ϕ°
GM_0034	1	4:11	103.50	104.54	104.02	203.00	3,745.90	2.54	21.71	298.88	100	398.88	69	20
	2		106.17	104.44	105.31	200.00	3,646.20	4.39	20.93	504.19	300	804.19		
	3		102.35	104.29	103.32	202.00	3,711.50	5.94	21.91	708.25	500	1,208.25		
GM_0038	1	3:30	105.15	106.91	106.03	200	3,386.3	4.63	19.18	524.40	100	624.40	83	33
	2		104.11	101.43	102.77	203.00	3,262.80	8.61	19.38	1,038.07	300	1,338.07		
	3		105.71	100.75	103.23	200.00	3,305.40	12.28	19.75	1,467.06	500	1,967.06		
GM_0039	UCS	1:35	100.00	100.00	100.00	200.00	3,785.70	0.63	24.10	80.21	0	80.21	28	28
	1		105.29	102.32	103.81	200.00	3,784.70	2.37	22.36	279.47	100	379.47		
	2		103.59	104.70	104.15	200.00	3,851.30	5.25	22.61	615.85	300	915.85		
	3		104.58	102.41	103.50	200.00	3,794.20	8.03	22.55	954.06	500	1,454.06		
GM_0041	UCS	1:50	105.00	105.00	105.00	200.00	3,883.70	0.54	22.43	62.36	0	62.36	27	18
	1		105.38	108.81	107.10	200.00	3,879.50	1.67	21.53	184.90	100	284.90		
	2		107.1	106.00	106.55	200.00	3,947.60	2.99	22.14	335.67	300	635.67		
	3		107.08	106.94	107.01	200.00	3,917.60	4.77	21.78	530.56	500	1,030.56		
GM_0042	UCS	1:45	107.24	102.71	104.98	191.90	3,872.90	0.48	23.32	55.46	0	55.46	31	16
	1		108.47	105.15	106.81	200.00	3,962.30	2.17	22.11	241.75	100	341.75		
	2		109.21	106.75	107.98	200.00	3,952.40	1.86	21.58	203.35	300	503.35		
	3		106.81	104.77	105.79	200.00	3,912.90	4.37	22.26	497.11	500	997.11		
GM_0043	UCS	1:28	107.33	106.36	106.85	191.90	3,925.90	0.33	22.82	36.81	0	36.81	23	0
	1		101.49	106.44	103.97	200.00	3,958.10	0.49	23.31	57.77	100	157.77		
	2		107	100.06	103.53	200.00	3,802.60	0.35	22.59	41.85	300	341.85		
	3		104.88	104.05	104.47	200.00	3,953.00	0.39	23.06	45.99	500	545.99		
GM_0044	UCS	2:19	110.84	110.84	110.84	185.00	3,862.00	0.41	21.64	42.49	0	42.49	39	3
	1		107.61	107.61	107.61	195.00	3,902.40	1.31	22.00	143.56	100	243.56		
	2		105.58	106.12	105.85	192.00	3,785.60	1.00	22.41	113.82	300	413.82		
	3		106.74	106.53	106.64	193.00	3,807.70	1.17	22.09	130.94	500	630.94		
GM_0045	UCS	2:22	105.22	101.14	103.18	195.00	3,643.30	0.48	22.34	57.41	0	57.41	43	24
	1		103.73	104.20	103.97	198.00	3,920.90	4.04	23.33	476.27	100	576.27		
	2		104.72	103.98	104.35	198.00	3,900.80	2.43	23.04	284.63	300	584.63		
	3		105.31	101.50	103.41	198.00	3,856.30	7.54	23.19	897.91	500	1,397.91		

APPENDIX – C

INTERNATIONA PATENT APPLICATION No. PCT/AU2013/000310

METHOD AND APPARATUS FOR ASSESSING SHEAR STRENGTH DEVELOPMENT IN CEMENTITIOUS MATERIALS

Field of the Invention

The present invention relates to a method and apparatus for assessing strength development in cementitious materials, including, but not limited to shear strength development in sprayed cementitious materials.

Background of the Invention

Strength development is often a very important characteristic of cementitious materials used in civil and mining engineering. Cementitious materials comprise a combination of cement, sand, and water. Depending on the application at hand, aggregate and additives such as hardeners, accelerators, fillers and reinforcing fibres may also be incorporated. The provision of water in the cementitious material causes a reaction known as "hydration". Hydration involves many different chemical reactions resulting in the bonding together of individual sand and aggregate particles to form a solid mass. The process of strength growth during hydration is largely due to the formation of calcium silicate hydrate as the cementitious material continues to hydrate.

The hardening of cementitious material continues over a long period of time stretching to months and even years. One well known method of testing strength for cementitious material is to take a sample of the material being used for a particular application to form cylinders which are cured for specific times, for example 2, 7, 28 and 90 days at a set temperature such as 20°C. After reaching the required age for testing the cylinders are crushed in a press. The crushing pressure, measured in MPa, provides an indication of strength development after initial hardening.

In the context of civil and mining engineering excavations, it is common to spray

cementitious materials (typically known as shotcrete) onto an exposed rock face to form a protective canopy for personnel and equipment. A given level of strength is required before personnel can safely enter a shotcrete supported excavation. The shotcrete must be able to support its own mass and the mass of any small, loose rocks that may have not been removed, for example by hydro scaling, prior to the application of the shotcrete. The wait time required for a given level of hydration to be achieved places productivity and logistical constraints on the further development of the excavation. It is particularly advantageous for shotcrete to have early or very early strength development characteristics. Shotcrete strength development is often tested indirectly on samples within the excavation. This in itself may disregard early safe re-entry time rules for shotcreted excavations.

The present invention was developed in the context of considering the requirements for strength development in sprayed cementitious material (i.e. shotcrete). However embodiments of the present invention are not limited by the manner of application or placement of cementitious material and may, for example be applied equally to pumped or poured cementitious material.

Summary of the Invention

Aspects of the present invention are based on an observed correlation or relationship between electrical resistance and shear strength development of hydrating cementitious materials. Thus, in one aspect the invention may be considered as a method of assessing shear strength development in cementitious material by firstly obtaining empirical data correlating electrical resistance with shear strength development of a hydrating sample of the cementitious material; applying a batch of the cementitious material as required; and, during hydrating taking measurements of electrical resistance which can then be correlated to an estimated shear strength on the basis of the empirical data. This shear strength may also be related to a predetermined safe re-entry time in the event of the application of the cementitious material as shotcrete to excavation surfaces.

In an inter-related aspect, the present invention provides an electronic instrument for making electrical resistance measurements of hydrating cementitious material.
One aspect of the invention provides a method of assessing internal shear strength development in cementitious material comprising: measuring electrical resistance of a sample of cementitious material during hydration of the cementitious material to establish a correlation between electrical resistance and shear strength of the hydrating sample ;
applying a batch of the cementitious material in accordance with a desired purpose; measuring electrical resistance of the applied cementitious material in situ during hydration; and, using the measured electrical resistance of the applied cementitious material and the established correlation to assess the shear strength of the applied hydrating cementitious material.

In another aspect the invention provides a method of determining safe access time to excavation surfaces on which a cementitious material is sprayed, the method comprising: measuring electrical resistance of a sample of sprayed cementitious material during hydration of the sprayed cementitious material to establish a correlation between electrical resistance and internal shear strength of the hydrating sample; applying a batch of the cementitious material by spraying onto the excavation surfaces; measuring the electrical resistance of the applied cementitious material in situ during hydration; and, using the measured electrical resistance of the applied cementitious material and the established correlation to determine when the shear strength of the applied cementitious has reached a level deemed safe to allow re-entry to, or a location adjacent, the excavation.

In one embodiment, measuring the electrical resistance of the applied cementitious material comprises: measuring the electrical resistance between two or more electrical current paths in the cementitious material.

In one embodiment, measuring electrical resistance comprises: using an electrical resistance measurement probe with a first electrode of one polarity and two or more

second electrodes of an opposite polarity where the second electrodes are spaced an equal distance from the first electrode to measure the electrical resistance.

In one embodiment the method comprises using a probe wherein the two or more second electrodes are evenly spaced about the first electrode.

In one embodiment the method measuring the electrical resistance of the applied cementitious material comprises embedding the first and second electrodes in the applied cementitious material.

In one embodiment the determination of when the shear strength has reached the level deemed safe is made when the measured electrical resistance along each of the two or more paths correlate to the shear strength having reached the level deemed safe.

In one embodiment measuring the electrical resistance of the applied cementitious material comprises transmitting electrical resistance measurements to a location remote from that to which the cementitious material is applied.

A further aspect of the invention provides an electrical resistance measurement probe comprising: a first electrode; two or more second electrodes, the second electrodes being spaced an equal distance from the first electrodes; and, an electrical power source connected between the first electrode and each of the second electrodes.

In one embodiment the second electrodes are spaced evenly about the first electrode.

In one embodiment the probe comprises three second electrodes.

A further aspect of the invention provides an electrical resistance measurement probe

comprising:a first electrode; at least three second electrodes, wherein each of the

second electrodes are spaced an equal distance from the first electrodes and are evenly angularly spaced apart from each other about the first electrode; and, an electrical power source electrically connected between the first electrode and each of the second electrodes.

In one embodiment the probe comprises a body supporting the electrodes wherein the electrodes extend from a founding surface of the body.

In one embodiment the electrodes extend an equal distance from the founding surface.

In one embodiment the first electrode comprises one of the group comprising: a pin, a post and a rod.

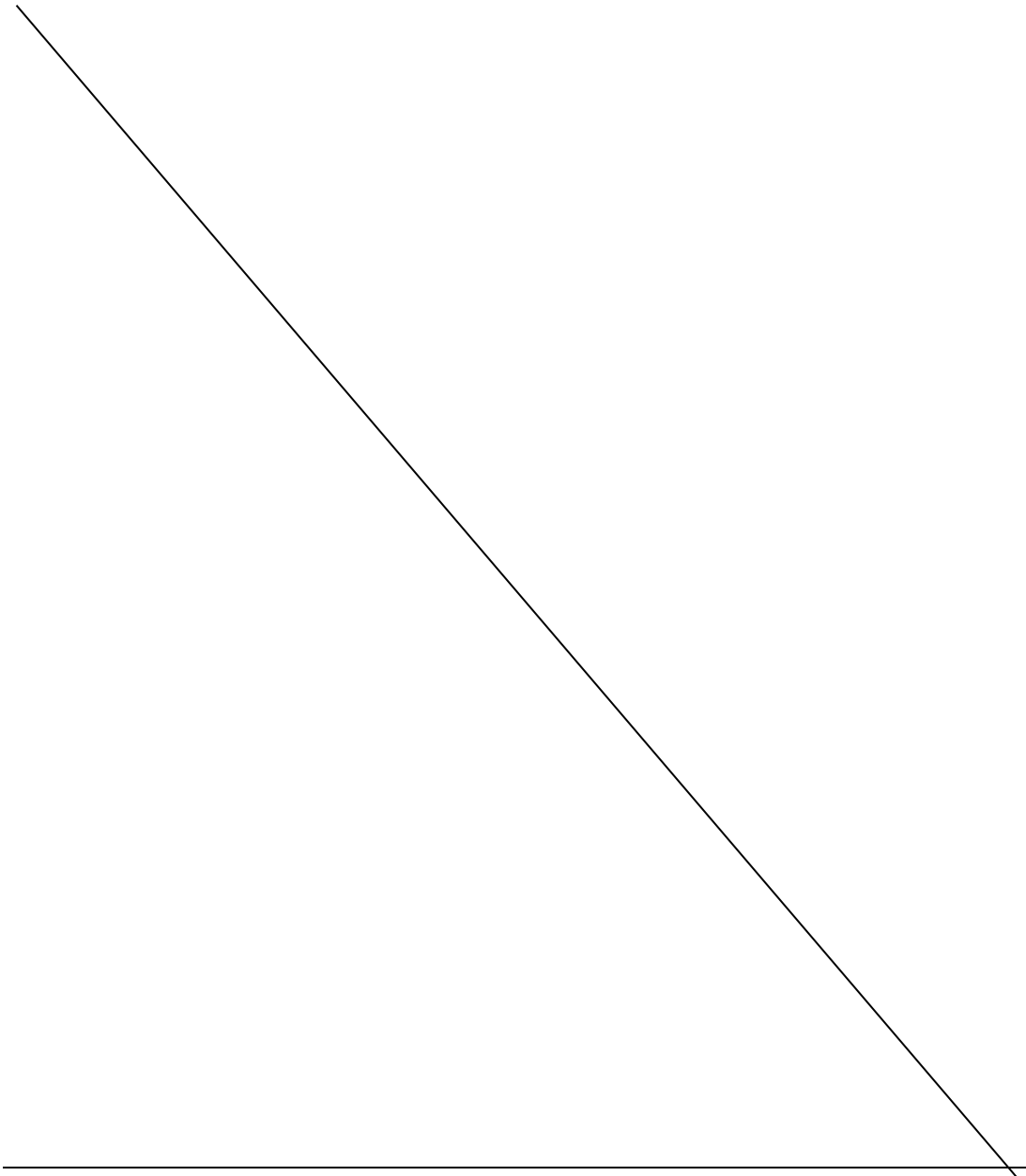

In one embodiment at least one of the second electrodes comprises a blade or plate like member.

In one embodiment each of the second electrodes comprises a blade or plate like member.

In one embodiment a voltmeter is arranged to measure voltage drop between the first electrode and one or more of the second electrodes, and an ammeter is arranged to measure current flow between the first electrode and one or more of the second electrodes; wherein electrical resistance measured by the probe is determined by dividing the measured voltage by the measured current.

In one embodiment the probe comprises a communications circuit arranged to communicate resistance measured by the probe to a location remote from the electrodes.

In one embodiment the communications circuit is a wireless communications circuit.

Brief Description of the Drawings

Embodiments of the present invention will now be described by way of example only with reference to the accompanying drawings in which:

Figure 1a is an elevation view of an electrical resistance measuring device in accordance with an embodiment of the present invention;

Figure 1b is a plan view of the electrical resistance measurement probe;

Figure 1c is an isometric view of the electrical resistance probe;

Figure 1d is an inverted isometric view of the electrical resistance probe;

Figure 2 is an electrical diagram of the electrical resistance measurement probe circuit;

Figure 3 is a graph illustrating a relationship between electrical resistance and shear strength development during the first eight hours of hydration of a cementitious material;

Figure 4 is a re-scaled version of the graph shown in Figure 3 in which the shear strength scale is magnified by a factor of 500;

Figure 5 is a graph showing a relationship between electrical resistance and shear strength development during the first four hours of hydration of a cementitious material for a given layer thickness of a different composition to that represented in Figure 3 and 4; and,

Figure 6 is a graph of minimum shear strength required to develop in a cementitious material of a given thickness in order to support a regular tetrahedral block of rock with one metre side lengths having a mass of approximately 400kg.

Detailed Description of Preferred Embodiments

The present embodiments are described in the context of preparation and use of shotcrete (i.e. sprayed cementitious material). Sprayed cementitious materials are based on hydraulic cements and pozzolanic materials that with time hydrate in the presence of water, transitioning from an initial fluid gel that may be sprayed, to a hardened solid that forms a structural or protective layer. As hydration proceeds water encapsulated in cementitious material is consumed in the chemical reactions that convert the fluid gel to a hardened solid. As the encapsulated water is consumed the electrical resistivity increases. Embodiments of the present invention correlate the increase in electrical resistivity to shear strength of sprayed cementitious material. Furthermore, as described herein below, an aspect of the present invention

provides an electrical resistance probe to enable electrical resistance measurement.

An instrument that may be used to measure the resistance of steel reinforced concrete for the purposes of assessing corrosion, rate of corrosion, and probability of corrosion is known as the Wenner linear 4-point instrument (Wenner instrument). The Wenner instrument was originally developed to measure resistivity of soil and, comprises four electrodes arranged along a common line. When the Wenner instrument is used to measure resistivity of steel reinforced concrete, it incorporates a mould into which the electrodes extend. Concrete is poured into the mould embedding the electrodes. Current is supplied to the concrete through each of the end electrodes and a potential difference is measured between the two inner electrodes. Knowing the potential difference and the current supplied, resistance can be calculated using Ohm's law and the "Wenner geometrical factor". The Wenner geometrical factor assumes a homogeneous, infinite, isotropic material; symmetrical current flows; and, uniform current density.

Typical shotcrete layer thickness for ground support ranges from 50mm to 200mm. Further, shotcrete is a heterogeneous mixture and electrical current flows are asymmetrical with non-uniform current density. Research conducted by the inventors shows that electrical current is greatly dissipated in a typical shotcrete layer rendering the Wenner probe unsuitable for practical use in assessing strength development of the cementitious materials and in particular in situ measurement of electrical resistance for the purposes of assessing shear strength development in sprayed cementitious materials.

Figures 1a – 2 illustrate an embodiment of an electrical resistance measurement probe 10 (hereinafter referred to in general as "probe 10"). The probe 10 is particularly well suited to in situ electrical resistance measurement of hydrating cementitious material. When used in relation to shotcrete one or more of the probes may be inserted into shotcrete sprayed within a standard mould set up within the excavation or alternately inserted into shotcrete sprayed onto the wall of the

excavation itself.

The probe 10 comprises a hollow cylindrical body 12, a first electrode 14, and two or more (in this instance three) second electrodes 16a, 16b and 16c (herein after referred to in general as "second electrodes 16"). Each of the second electrodes 16 is spaced in equal distance D from the first electrode 14. Moreover, the second electrodes 16 are evenly spaced about the first electrode 14. In the present instance, where the probe 10 comprises three second electrodes 16, the electrodes 16 are angularly spaced 120° apart about the first electrode 14.

The first electrode 14 is in the form of a pin, post or rod. Each of the second electrodes 16 however is in the form of a plate or blade like electrode. Electrodes 16 are orientated so that a corresponding plane in which they lie is substantially perpendicular to a line between the first electrode 14 and a midpoint of the corresponding second electrode 16. Also, each of the electrodes 14 and 16 extends for the same distance from a founding surface 18 of the body 12. Thus by maintaining the founding surface 18 substantially parallel to a surface of the body of cementitious material into which the probe 10 is pushed, each of the electrodes 14 and 16 will be embedded to substantially the same depth in a cementitious material.

Figure 2 illustrates a power source such as a battery 20; ammeter 22 and voltmeter 24 which are associated with the probe 10. A positive terminal 26 of battery 20 is connected to the second electrode 16a. However electrode 16a is also electrically connected to the electrode 16c and subsequently 16b via conductors 28a and 28b. Thus the second electrodes 16 are coupled in series to the positive terminal 26. Negative terminal 30 of the battery 20 is connected via the ammeter 22 to the first electrode 14. By virtue of this arrangement, the potential difference between any one of the second electrodes 16 and the first electrode 14 is the same. Voltmeter 24 is connected between the first electrode 14 and second electrode 16b.

The battery 20 may be disposed inside or outside of the body 12. It is however

envisaged that the battery 20, ammeter 22 and voltmeter 24 are all disposed outside of the body 12. In one example they may all be demountably supported on the probe or held on or in a plug that can be selectively plugged onto and removed from the probe 10. A benefit of this arrangement is that when probe 10 is in use in situ it generally cannot be, or in any event is not, removed until after hydration. However the battery 20, ammeter 22 and voltmeter 24 can be unplugged and thus removed and reused in association with other probes 10.

Optionally, the probe 10 may also incorporate a temperature sensor or probe and a transmitter or transponder. The temperature probe may be in the form of a thermocouple attached to or embedded in the first electrode 14. The transmitter or transponder may be arranged to transmit resistance data measured by the probe 10 to a remote location. However in an alternate arrangement, the temperature sensor or probe and a transmitter or transponder may be demountably supported on the body 12 as described above in relation to the battery 20, ammeter 22 and voltmeter 24.
Due to the configuration of the electrodes 14 and 16, the probe 10 provides electrical resistance measurement in multiple paths in a hydrating cementitious material. That is, when probe 10 has its electrodes 14 and 16 embedded in a hydrating cementitious material, current can flow along a path between the first electrode 14 and each of the electrodes 16a, 16b and 16c. Accordingly resistance measurement can be obtained for a substantial volume of the cementitious material bound by the second electrodes 16.

It is envisaged that in one embodiment the body 12 is made from a non-conductive polymeric material such as polyvinyl chloride and have a diameter of 130mm and height of 110mm. Body 12 comprises a base 32 and a demountable lid or water tight cap 34. Various components, parts or sensors of the probe may also be encapsulated within the body.

Each of the electrodes 14 and 16 may extend for a length of 50mm from the surface 18. It is further envisaged that the electrodes 14 and 16 are made from the same

highly conductive metallic material such as but not limited to, copper. The electrode 14 may have a diameter of 5mm, and is provided with a screw thread at a proximal end to facilitate coupling to the body 12.

Electrodes 16 are illustrated as being of an L-shape configuration with a thickness T of about 1mm and width of 30mm. A foot portion 36 of each electrode 16 is attached to the housing 12 via respective electrically conducting screws 38 which also enable electrical connection with electronic components of the probe 10 such as conductors 28a and 28b. In one example of the probe 10, the distance D between the electrode 14 and each second electrode 16 is approximately 50mm.

As shown in Figures 1c and 1d a braid of wires 40 passes through the housing 12 via a grommet 42. The wires 40 may be used to connect various components of the probe 10 such as the ammeter and voltmeter to a remote data logger or processor. Thus once the probe 10 has been put in place, monitoring of the electrical resistance and thus the development of shear strength can be monitored at a safe location. This avoids the need for people to enter an excavation at different times to take measurements.

In a variation measurements and data derived from electronic components of the probe 10 may be communicated wirelessly to a data logger or processor by incorporation of a transmitter or transponder within the body 12. In that event, the braid of wires 40 and grommet 42 may not be required.
One or more probes 10 can be inserted to a shotcreted surface by the people spraying the shotcrete. Alternately the probes 10 may be inserted by use of an elongated boom or a telescopic wand from outside of the excavation. The probes may be inserted into shotcrete sprayed within a standard mould set up within the excavation or alternately inserted into shotcrete sprayed onto the excavation surface.

In order to correlate the resistance of hydrating shotcrete to strength development and in particular shear strength development, tests are initially conducted on samples

of cementitious material. This provides empirical data that are subsequently used to estimate strength of the hydrating shotcrete and thus estimate safe re-entry time.

Figure 3 illustrates a typical relationship between electrical resistance and shear strength over time for a hydrating cementitious material. Resistance in Ohms is plotted on the left hand side vertical axis, time in hours is plotted on the horizontal axis, and shear strength in MPa is plotted on the right hand side vertical axis. Resistance is measured using the probe 10 inserted into a sample of hydrating cementitious material. Shear strength of a cementitious material when initially in a "fluid gel" state is measured by a rotational vane shear viscometer ("vane test"). The shear strength of a solidifying material "solid gel" is measured on multiple samples using triaxial tests. There is however a mix dependent transition period after the commencement of hydration in which the intrinsic shear strength of the cementitious material exceeds the capability of vane rotational shearing but is insufficient to maintain a free standing cylindrical form required for triaxial testing.

For the particular composition of the cementitious material measured in Figure 3, it is apparent that during the first four hours of hydration electrical resistance of the material increases by approximately 150%; and, by over 250% in the first eight hours. The non-linear rate of change of resistance and the significant magnitude of the change in time enable resistance to be used as a sensitive measure of shear strength development in time for that mix.

Shotcrete, like other cementitious materials, shows strength gain with hydration. Complete curing results in material with considerably greater strength than the 2.0 MPa maximum indicated by the scale of Figure 3. However, in application of the present invention to the determination of the safe re-entry time for shotcreted excavations, it is the shear strength development within the first few hours of hydration that is of interest.

Figure 4 shows the same data as Figure 3 but with the scale of the shear strength

magnified by a factor of 500 with maximum shear strength of 100kPa (i.e. 0.1MPa). From Figure 4 it can be seen for example that for the particular composition of the cementitious material tested, a resistance of 100 Ohms correlates to a shear strength of approximately 65kPa.

It must be recognised that the above empirical data is specific to the particular composition of cementitious material tested as well as the conditions under which hydration is occurring, e.g. temperature and humidity. For example, Figure 5 illustrates a further graph of resistance versus shear strength development over time but under different curing conditions. It should be noted that in Figure 5, the resistance scale on the left hand side is magnified by a factor of ten in comparison with that of Figures 3 and 4 and the time period is magnified by a factor of two.

In embodiments of the present invention samples of a cementitious material to be applied are first tested using the probe 10 and standard shear strength tests. The relationship between the resistance and shear strength in time is recorded and may be represented as a graph like Figures 3-5 or held as look up tables in a data file. The tests conducted to obtain these data are performed in conditions which replicate the conditions under which the same cementitious material (i.e. cementitious material with the same composition) is to be applied. With these data in hand, cementitious material is now applied as required, e.g. pumped, poured or sprayed. One or more of the probes 10 are embedded in the cementitious material and readings of resistance are continuously logged. This resistance is then used together with the previously derived empirical data to provide an indication of the shear strength of the hydrating cementitious material at any particular point in time. In relation to the application of shotcrete and the requirement to re-enter an excavation, the shear strength can be used to estimate a safe re-entry time to the excavation.
There are two structural requirements of a freshly sprayed shotcrete layer:

1. It must support its own mass immediately after being applied to the surface.
2. It must support the super-incumbent mass of an estimated unstable

volume of rock.

In the first instance, the shotcrete supports its own mass by development of a bond strength (comprising adhesion and mechanical interlock) between itself and the substrate and by development of an intrinsic shear strength. Consider a one metre square slab of shotcrete (unit weight of γ in kN/m^3 and of thickness't' in mm). In the case of zero shear strength, the bond strength must typically reach about ($\gamma t/1000$) kPa (or about 0.025t kPa). In the case of zero bond strength, the shear strength must typically reach ($\gamma/4$) kPa (or about 6.25 kPa). In almost all cases, where bond and shear strength development initiate simultaneously after spraying, both laboratory investigations and in situ experience have shown that the required strength levels for shotcrete to support itself are easily achieved.

In the second instance, the shotcrete must be capable of supporting the mass of loose rock blocks that may become unstable and represent a risk to personnel that enter the excavation. The volume of loose rock that may become unstable is minimised during blasting by waves that vibrate the excavation surfaces and by subsequent scaling (e.g. hydro-scaling) procedures that remove loose rocks from the excavation surfaces.

The specific arrangement of excavation span, stress and structural geology associated with each excavation will be different and the specification of a single or standard unstable volume of rock is not possible. However, an example calculation shows that within hours of spraying, shotcrete is quite capable of supporting a significant volume of unstable rock and that this volume or mass of rock may be calculated as a function of layer thickness and time after spraying.

Consider, the case of the minimum shear strength required to be developed within the shotcrete to support a regular tetrahedral block of rock with 1.0m side lengths. If this block existed in the roof of an underground excavation, its face triangle (i.e. the expression of its shape visible in the roof when viewed from beneath) would be an

equilateral triangle with side-lengths of 1m.

This example calculation is illustrated in Figure 6 which shows the shear strength required to be developed for different thickness layers of shotcrete and is computed for a rock with an average unit weight 27 kN/m^3 (this is a common assumption for most rock types) which results in a total mass of the block of 400 kg (i.e. equivalent to twenty, 20 kg bags of cement).

Figure 6 shows an average shotcrete layer of about 100mm thickness needs to develop a shear strength of about 7 kPa in addition to supporting its own mass. A longer re-entry is required for thinner layers of shotcrete.

Figure 6 also gives an indication of the time required to wait for a given layer thickness to develop the required shear strength to support the block, for a standard proportioned mix of cementitious material without accelerator or other admixtures, that has been placed on a granite rock slab and hydrated under laboratory conditions of temperature and humidity.

It is known that some combinations of additives and admixtures delay hydration and desensitise the resistance change in the first hours after mixing is complete. Consequently, the exact relationships between time, resistance and shear strength for a shotcrete mix comprising various additives and admixtures and sprayed onto various surfaces in various environmental conditions will be different.

Embodiments of the method and probe may be used to assist in the optimisation of a shotcrete or other cementitious material mix to address in situ conditions (such as rock substrate type, substrate dampness), environmental conditions (such as temperature and humidity) and logistic conditions (such as workability and strength development) specific to the site. A simple mix will comprise hydraulic cement, water and graded fractions of aggregates. However there are various additives and admixtures that can be used to assist in mixing, spraying or pumping, bonding,

curing and improving strength and stiffness of the cementitious material. By using embodiments of the method and probe it is possible to assess the in situ rate of

hydration (and strength development) as a consequence or function of varying the proportions of the mix constituents to suit a particular site.

For example a number of test shotcrete mixes can be prepared with known variations in mix composition and/or cured in different environmental conditions; with a probe 10 embedded in each batch. Resistance readings may be made at common time intervals for each batch with vane or triaxial tests performed at those time intervals to establish respective correlations between resistance and hydration for each batch. One can then assess the significance of the changes or differences in mix and/or environment conditions on hydration.

Modifications and variations that would be obvious to persons of ordinary skill in the art are deemed to be within the scope of the present invention the nature of which is to be determined from the above description and the appended claims.

CLAIMS:

1. A method of determining safe re-entry time to excavation surfaces on which a cementitious material is sprayed, the method comprising:

measuring electrical resistance of a sample of sprayed cementitious material during hydration of the sprayed cementitious material to establish a correlation between electrical resistance and internal shear strength of the hydrating sample;

applying a batch of the cementitious material by spraying on the excavation surfaces;

measuring the electrical resistance of the applied cementitious material in situ during hydration; and,

using the measured electrical resistance of the applied cementitious material and the established correlation to determine when the shear strength of the applied cementitious has reached a level deemed safe to allow re-entry to, or a location adjacent, the excavation.

2. The method according to claim 1 wherein measuring the electrical resistance of the applied cementitious material comprises measuring the electrical resistance between two or more electrical current paths in the cementitious material.

3. The method according to claim 1 or 2 wherein measuring electrical resistance comprises: using an electrical resistance measurement probe with a first electrode of one polarity and two or more second electrodes of an opposite polarity where the second electrodes are spaced an equal distance from the first electrode to measure the electrical resistance.

4. The method according to claim 3 comprising using a probe where the two or more second electrodes are evenly spaced about the first electrode.

5. The method according to claim 3 or 4 wherein measuring the electrical resistance of the applied cementitious material comprises embedding the first and

6. second electrodes in the applied cementitious material.

7. The method according to any one of claims 2 to 5 when dependent on claim 2, wherein the determination of when the shear strength has reached the level deemed safe is made when the measured electrical resistance along each of the two or more paths correlate to the strength having reached the level deemed safe.

8. The method according to any one of claims 1 to 6 wherein measuring the electrical resistance of the applied cementitious material comprises transmitting electrical resistance measurements to a location remote from that to which the cementitious material is applied.

9. An electrical resistance measurement probe comprising:

a first electrode;

at least three second electrodes, wherein each of the second electrodes are spaced an equal distance from the first electrodes and are evenly angularly spaced apart from each other about the first electrode; and,

an electrical power source electrically connected between the first electrode and each of the second electrodes.

10. The probe according to claim 8 comprising a body supporting the electrodes wherein the electrodes extend from a common surface of the body.

11. The probe according to claim 9 wherein the electrodes extend an equal distance from the common surface.

12. The probe according to any one of claims 8 to 10 wherein the first electrode comprises one of the group comprising: a pin, a post and a rod.

13. The probe according to any one of claims 8 to 11 wherein at least one of the second electrodes comprises a blade or plate like member.

14. The probe according to claim 12 wherein each of the second electrodes comprises a blade or plate like member.

15. The probe according to any one of claims 8 to 13 comprising a voltmeter arranged to measure voltage drop between the first electrode and one or more of the second electrodes, and an ammeter arranged to measure current flow between the first electrode and one or more of the second electrodes; wherein electrical resistance measured by the probe is determined by dividing the measured voltage by the measured current.

16. The probe according to any one of claims 8 to 14 comprising a communications circuit arranged to communicate resistance measured by the probe to a location remote from the electrodes.

17. The probe according to claim 14 wherein the communications circuit is a wireless communications circuit.

ABSTRACT

A method of assessing shear strength development in cementitious material involves measuring electrical resistance of a sample of cementitious material during hydration to establish a correlation between electrical resistance and shear strength of the hydrating sample, then applying the cementitious material in accordance with a desired purpose and measuring electrical resistance of the applied cementitious material in situ during hydration. The measured electrical resistance of the applied cementitious material and the established correlation is used to assess the shear strength of the applied hydrating cementitious material. Electrical resistance is measured by a probe 10 having a first electrode 14 and two or more second electrodes 16. The second electrodes 16 are spaced an equal distance from the first electrodes 14. An electrical power 20 source connected between the first electrode 14 and each of the second electrodes 16.

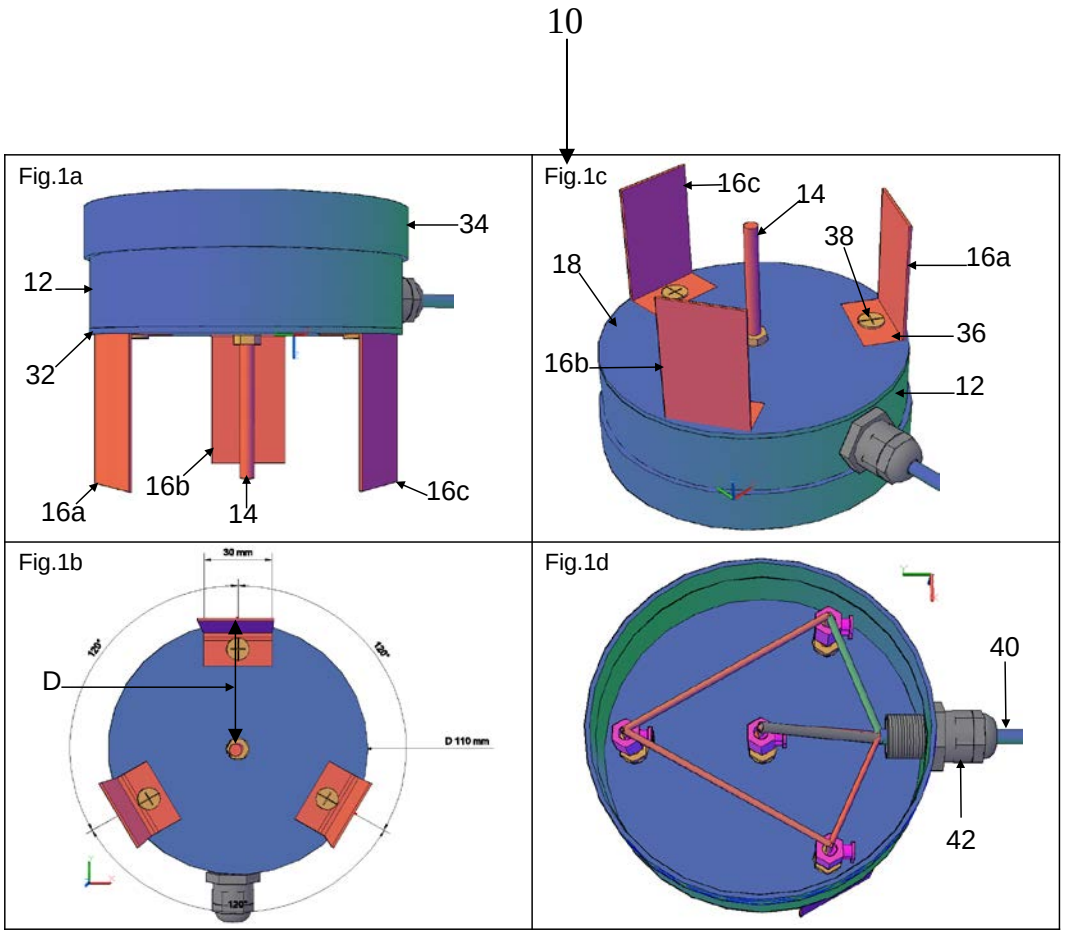
10
Fig.1a
34
12
32
16a
16b
14
16c
Fig.1c
16c
14
38
16a
18
36
16b
12
Fig.1b
30 mm
D
D 110 mm
Fig.1d
40
42

Figure 1.

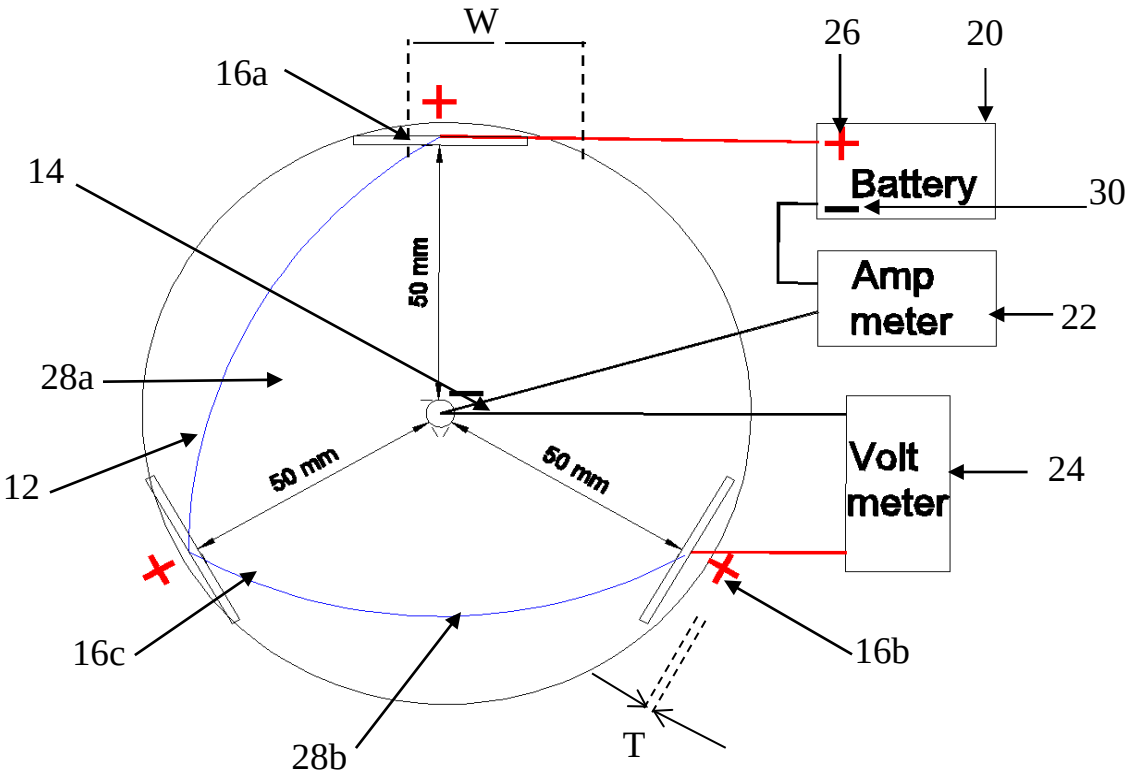
W
16a
26
20
14
Battery
30
50 mm
Amp
meter
22
28a
Volt
meter
24
12
50 mm
50 mm
16c
16b
28b
T

Figure 2.

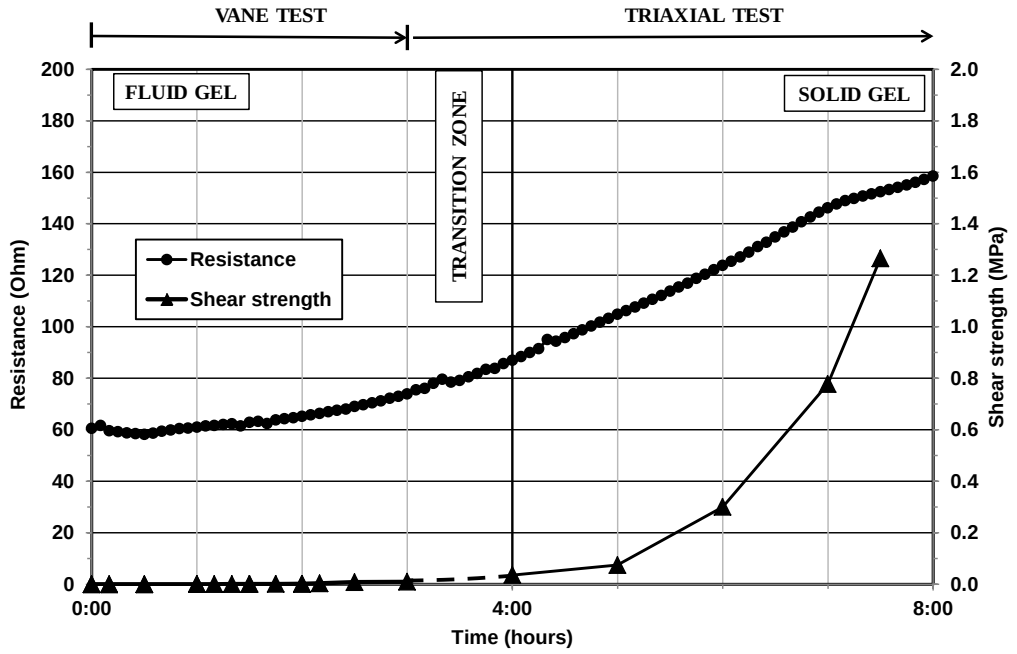

Figure 3.

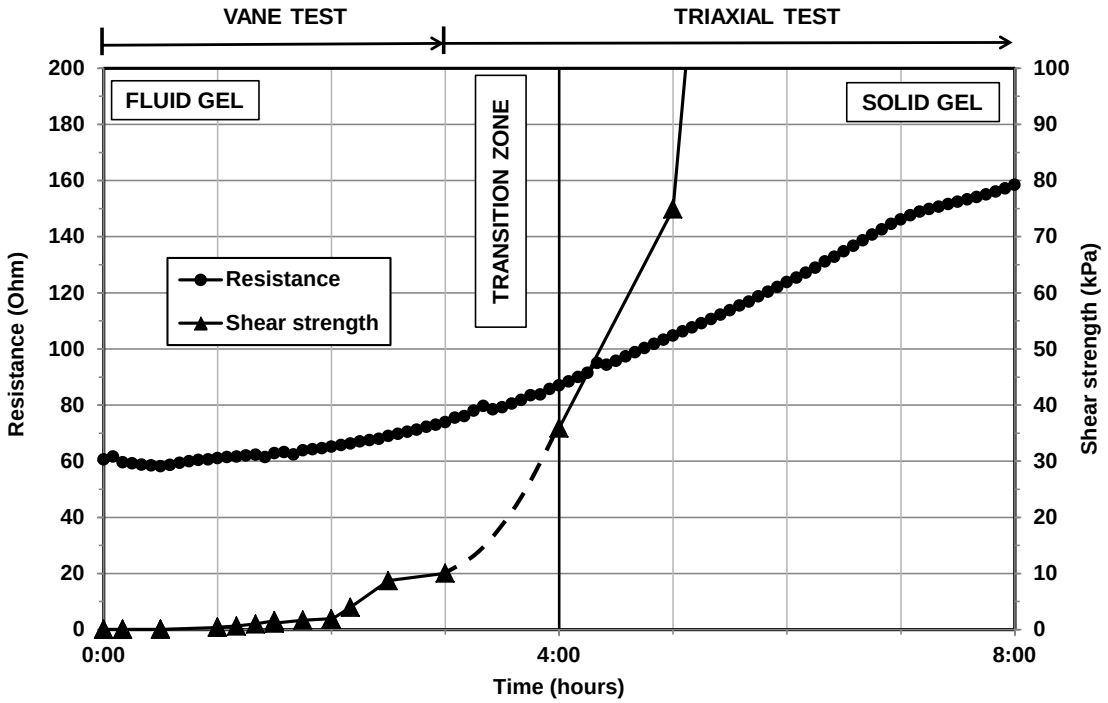

Figure 4.

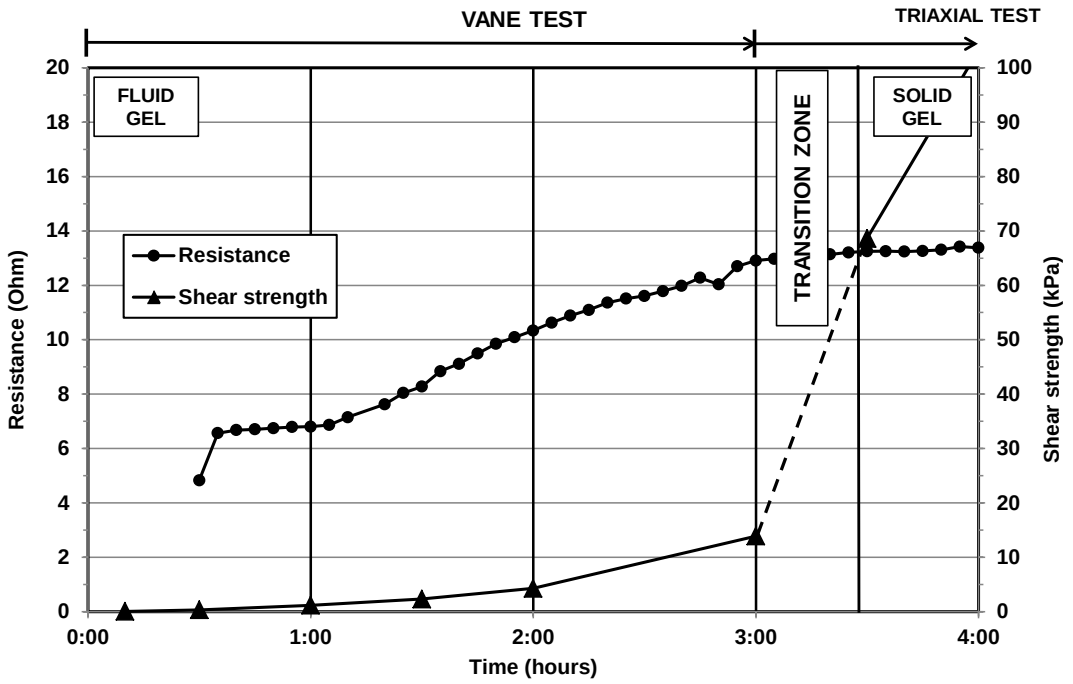

Figure 5.

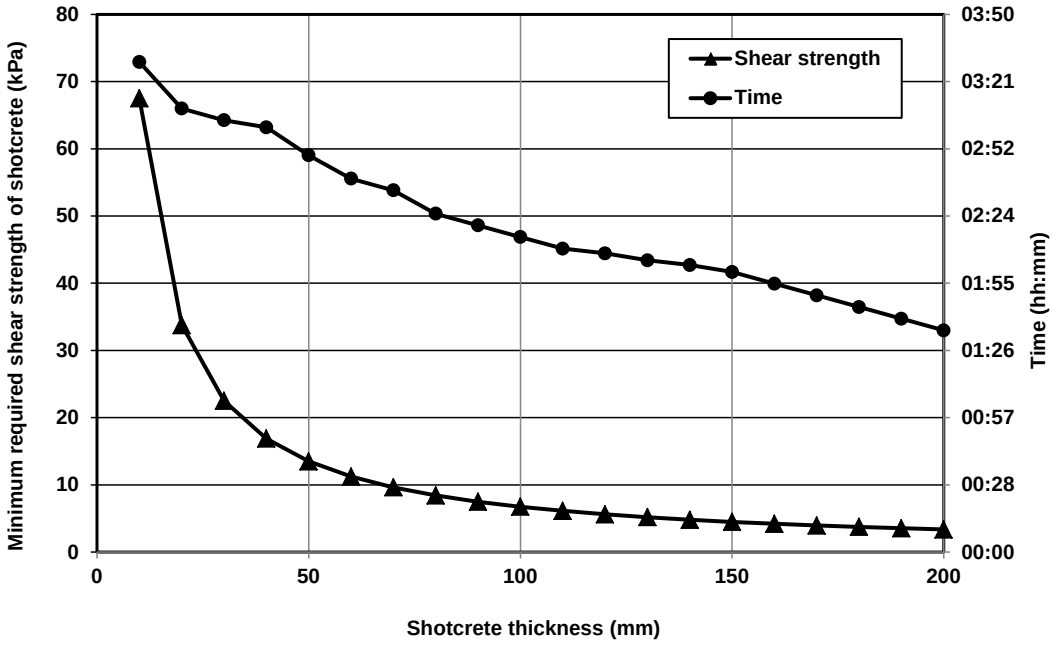

Figure 6.

APPENDIX – D

ELECTRICAL RESISTANCE MEASUREMENT WITH PROTOTYPE V2.1

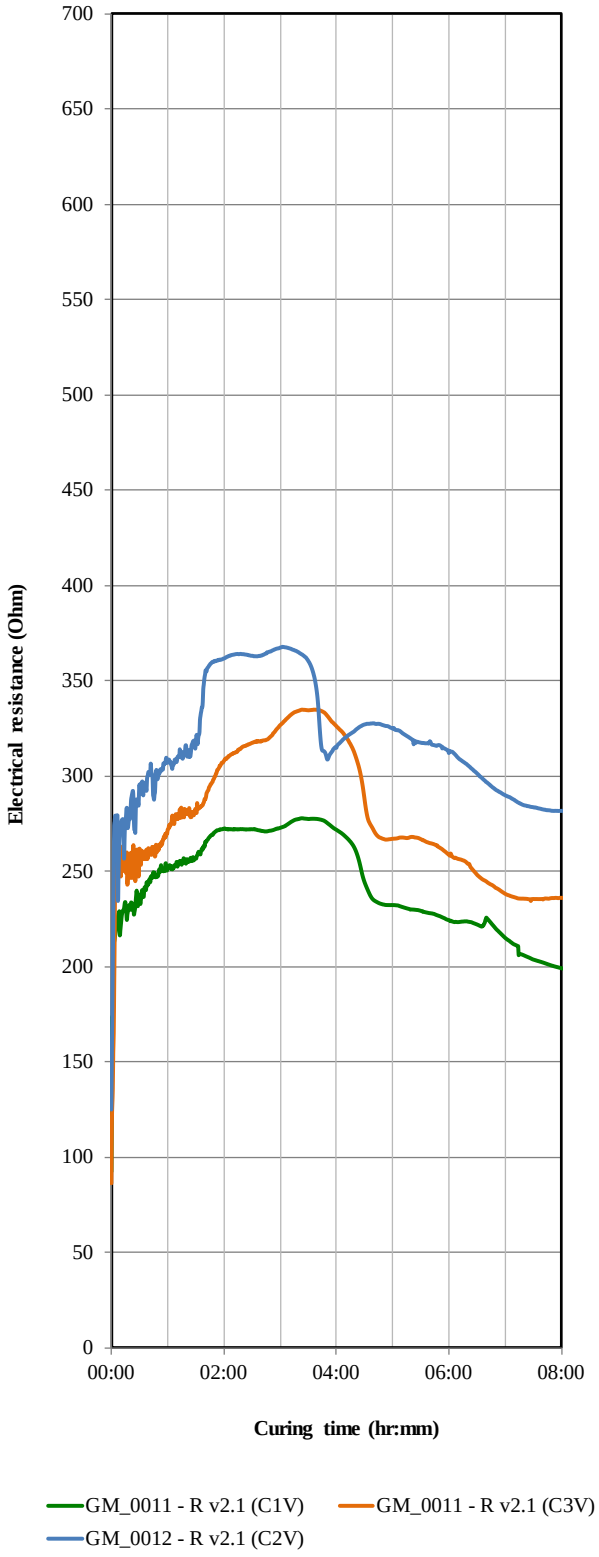

Figure D.1. Electrical resistance developments with time in shotcrete paste without chemical admixture (8 hours).

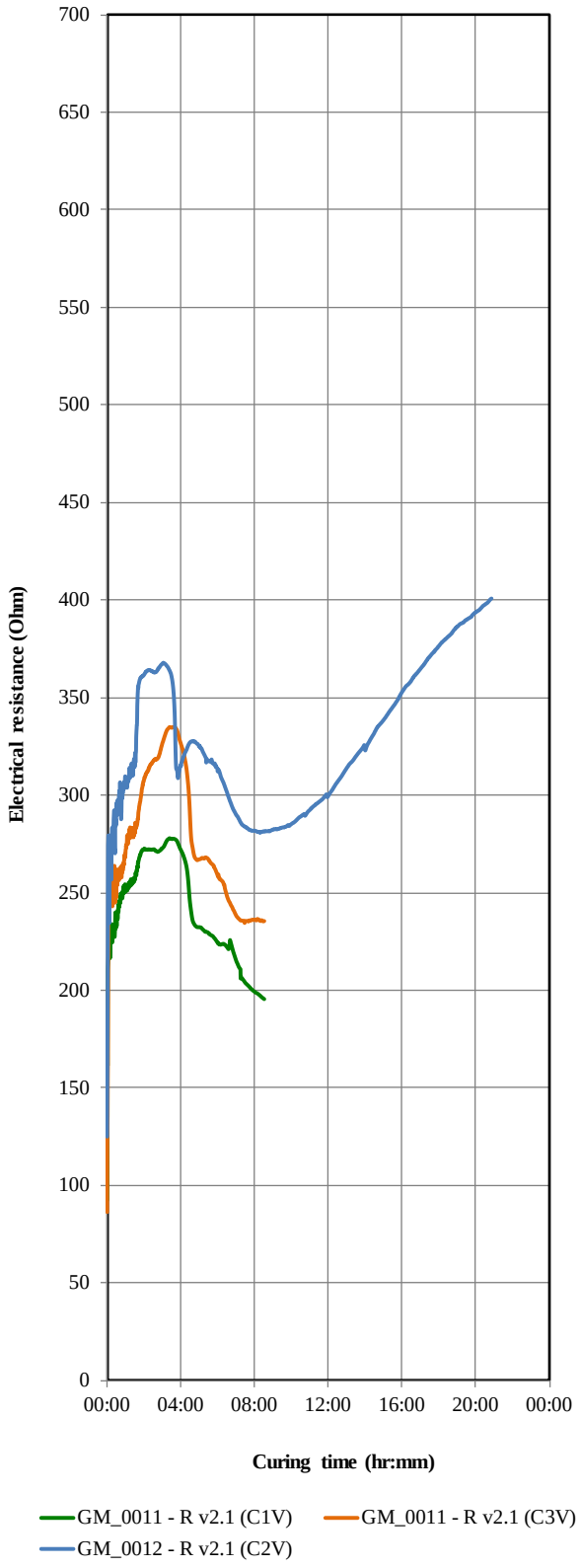

Figure D.2. Electrical resistance developments with time in shotcrete paste without chemical admixture (24 hours).

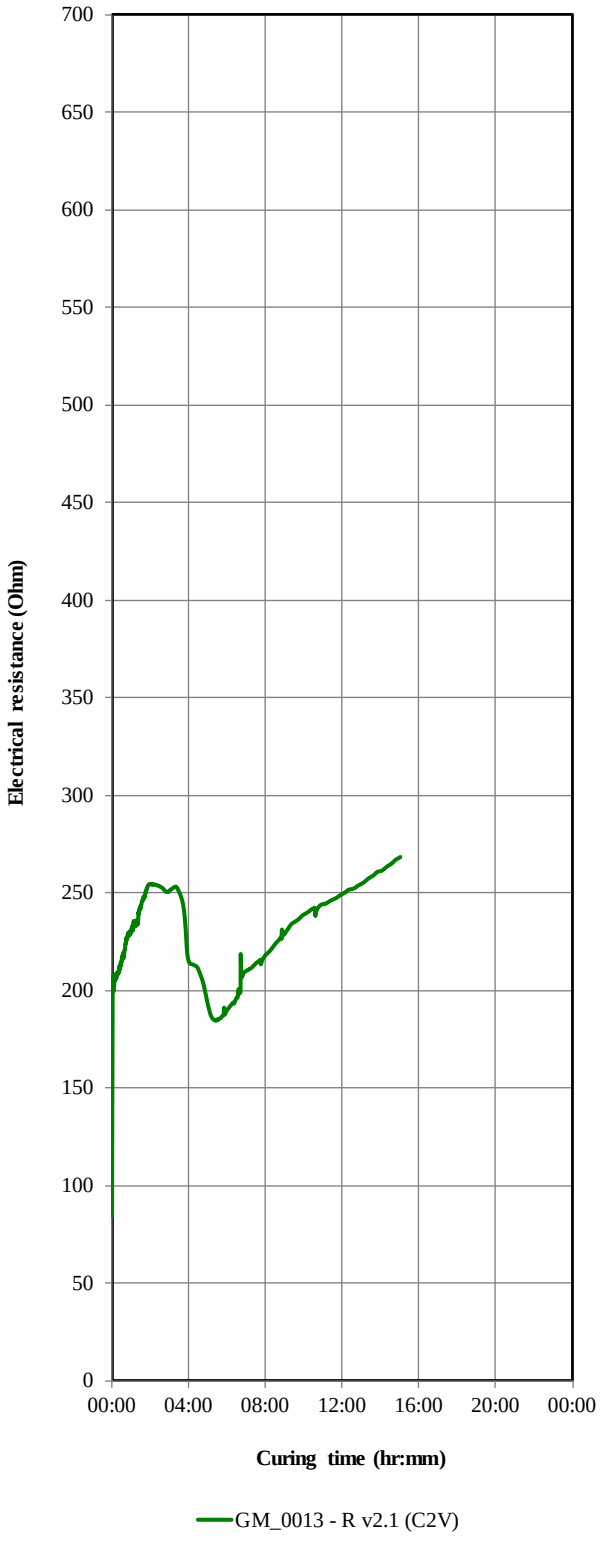

Figure D.3. Electrical resistance developments with time in shotcrete paste (8 hours).

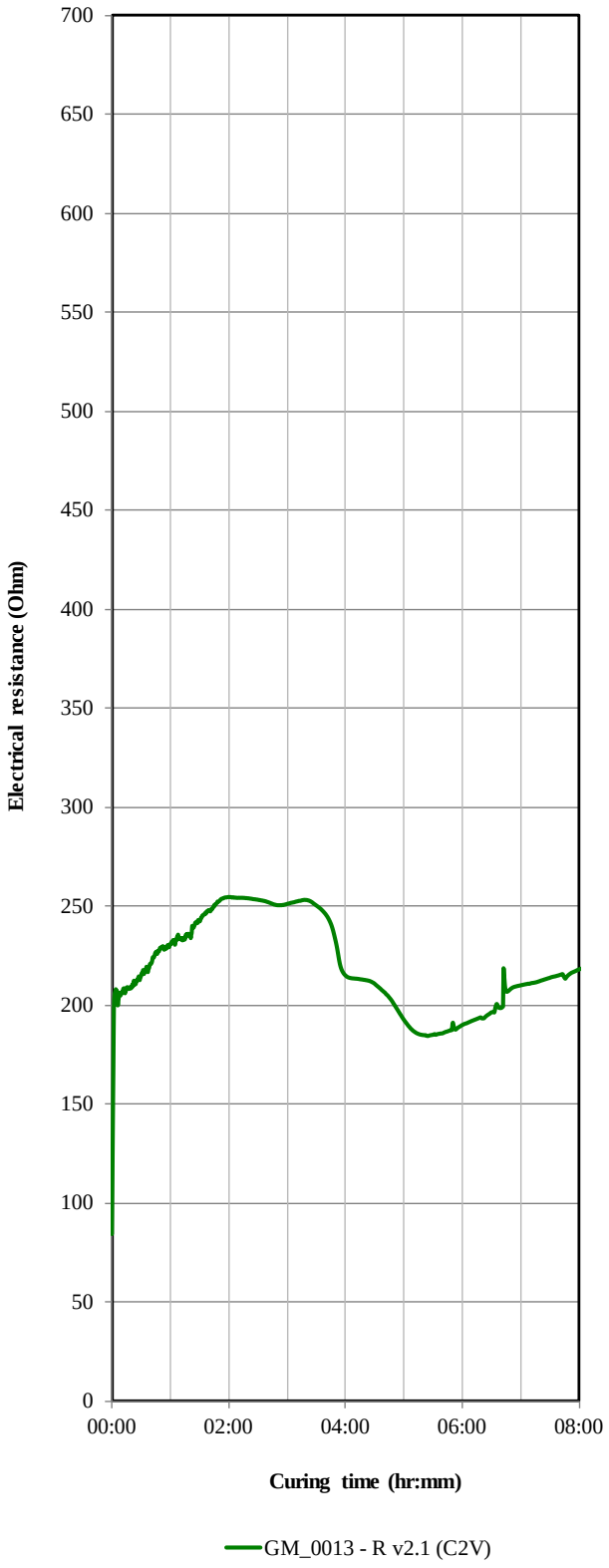

Figure D.4. Electrical resistance developments with time in shotcrete paste without chemical admixture (24 hours).

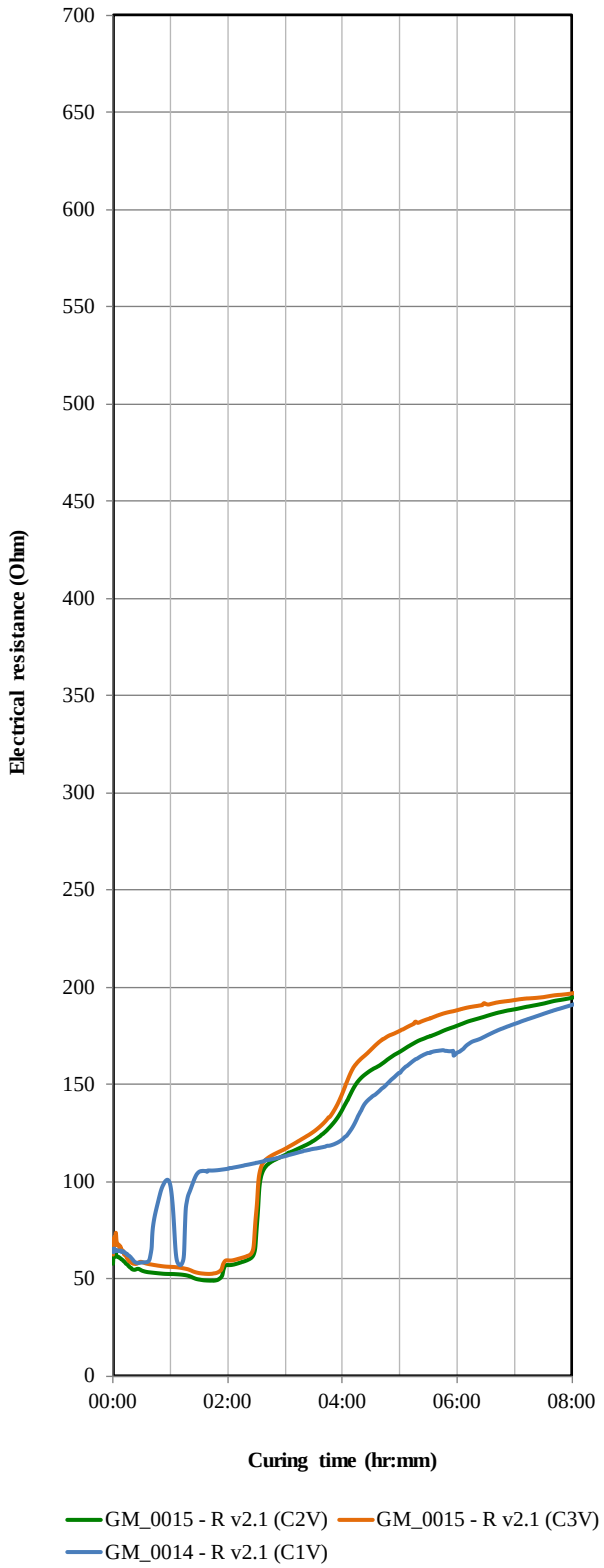

Figure D.5. Electrical resistance developments with time in shotcrete paste with accelearator (8 hours).

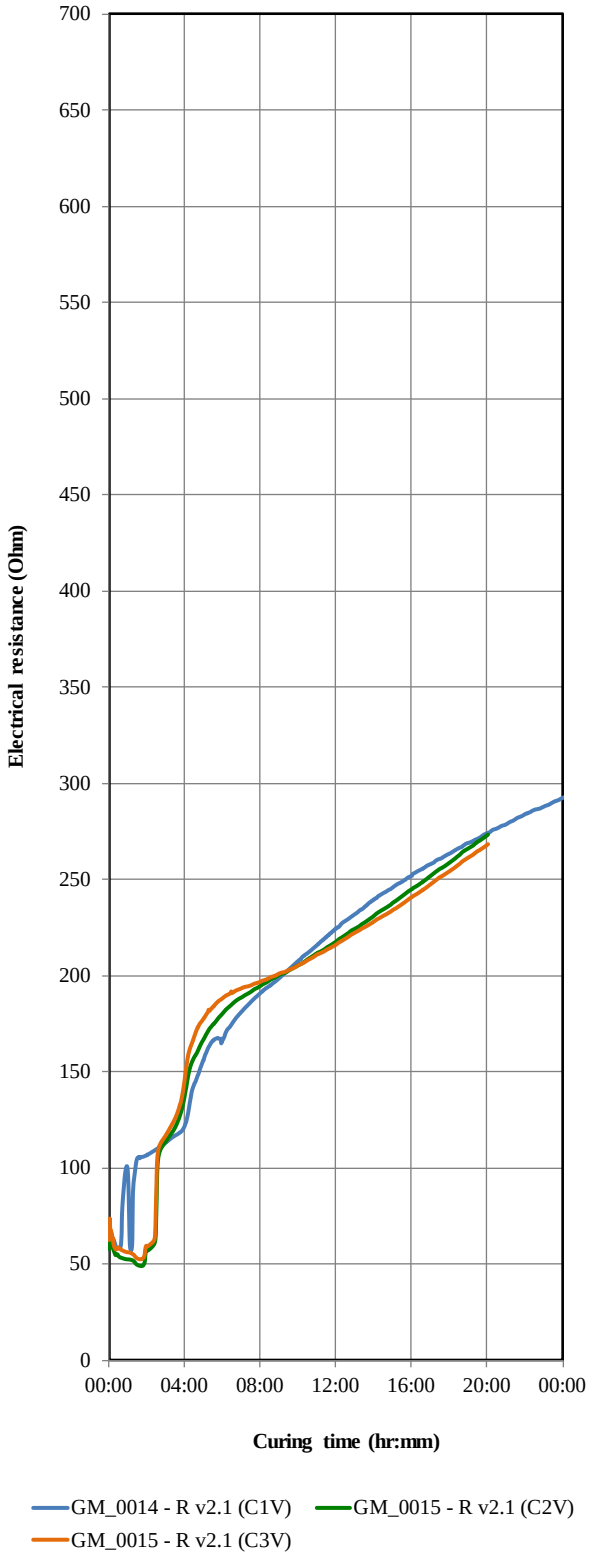

Figure D.6. Electrical resistance developments with time in shotcrete paste with accelearator (24 hours).

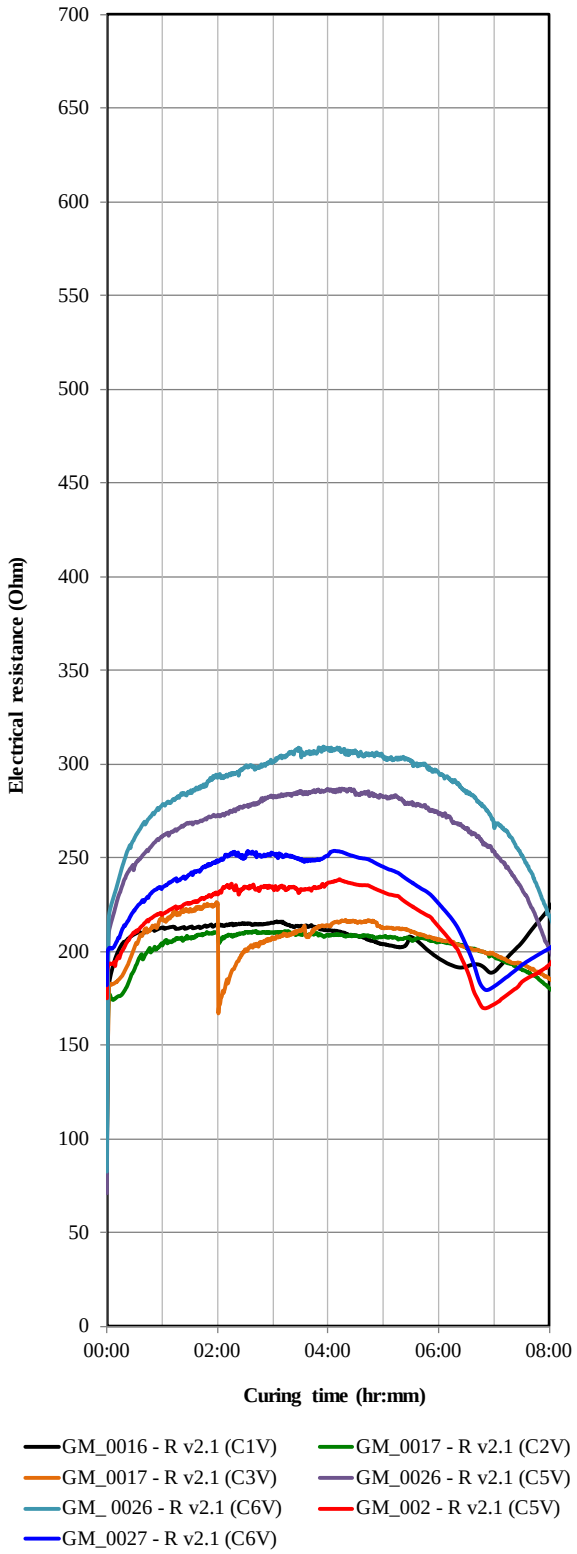

Figure D.7. Electrical resistance developments with time in shotcrete paste with superplasticier (8 hours).

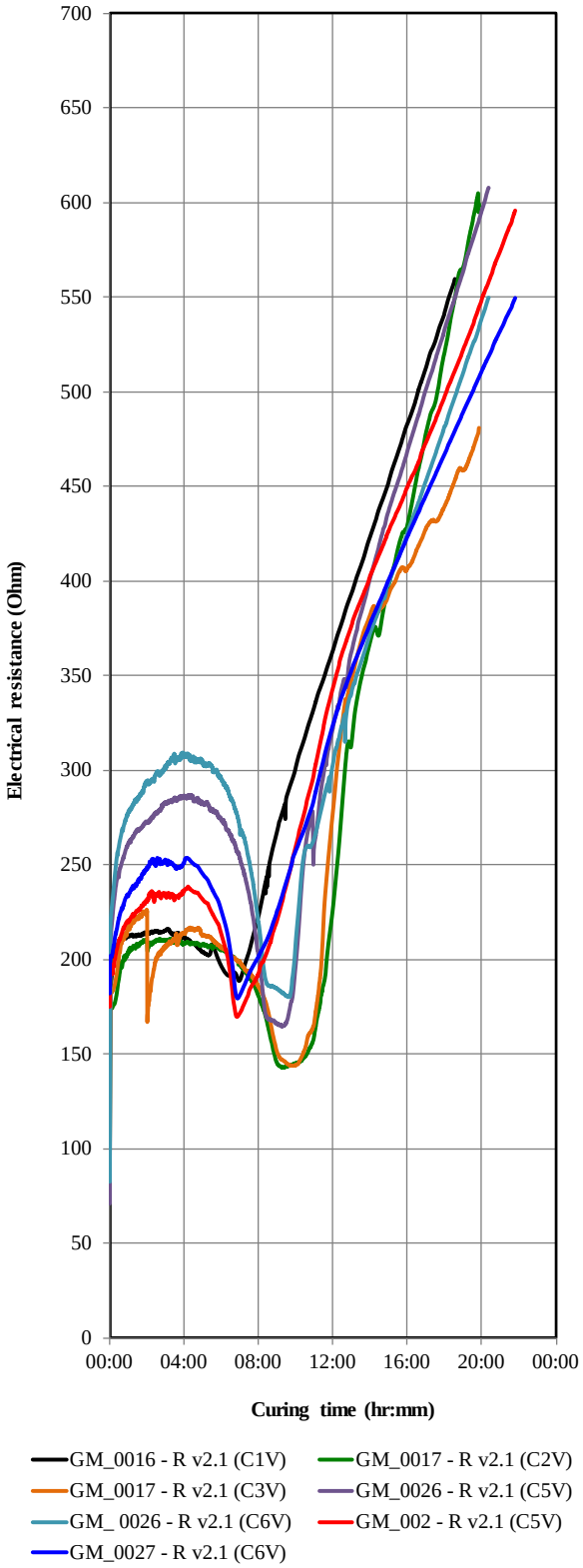

Figure D.8. Electrical resistance developments with time in shotcrete paste with superplasticier (24 hours).

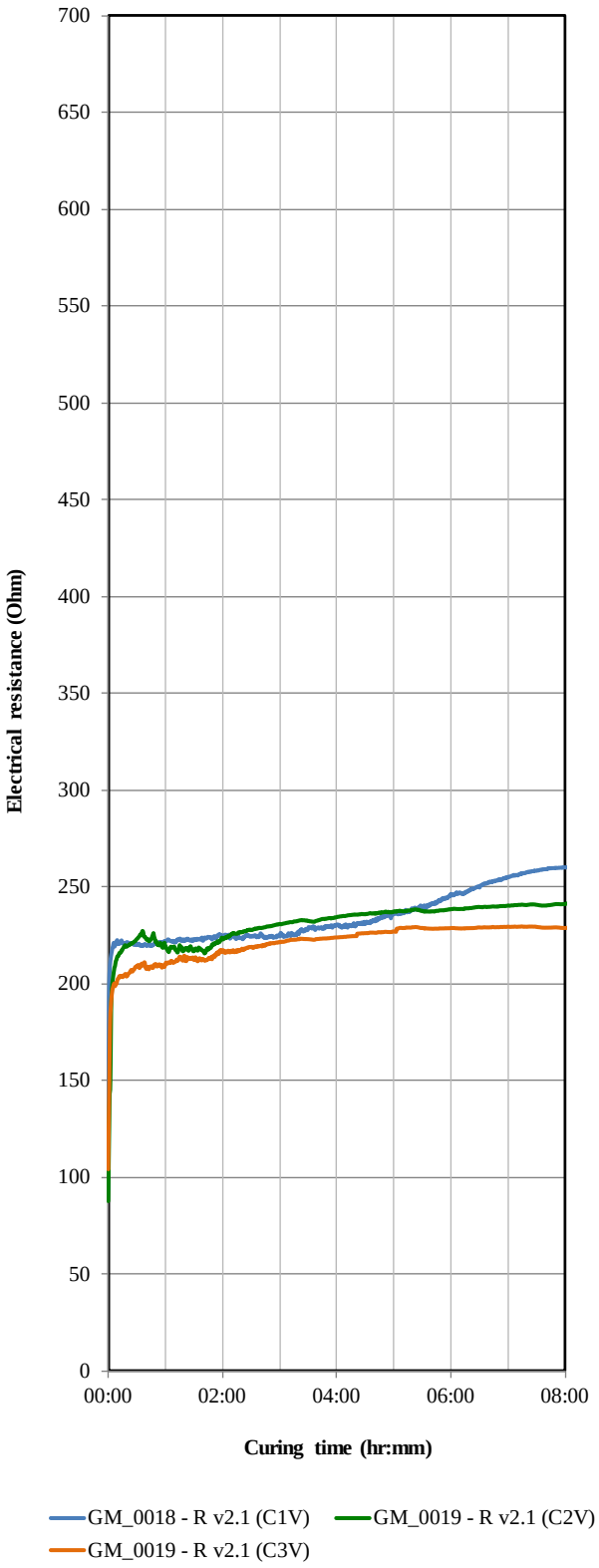

Figure D.9. Electrical resistance developments with time in shotcrete paste with hydration stabiliser (8 hours).

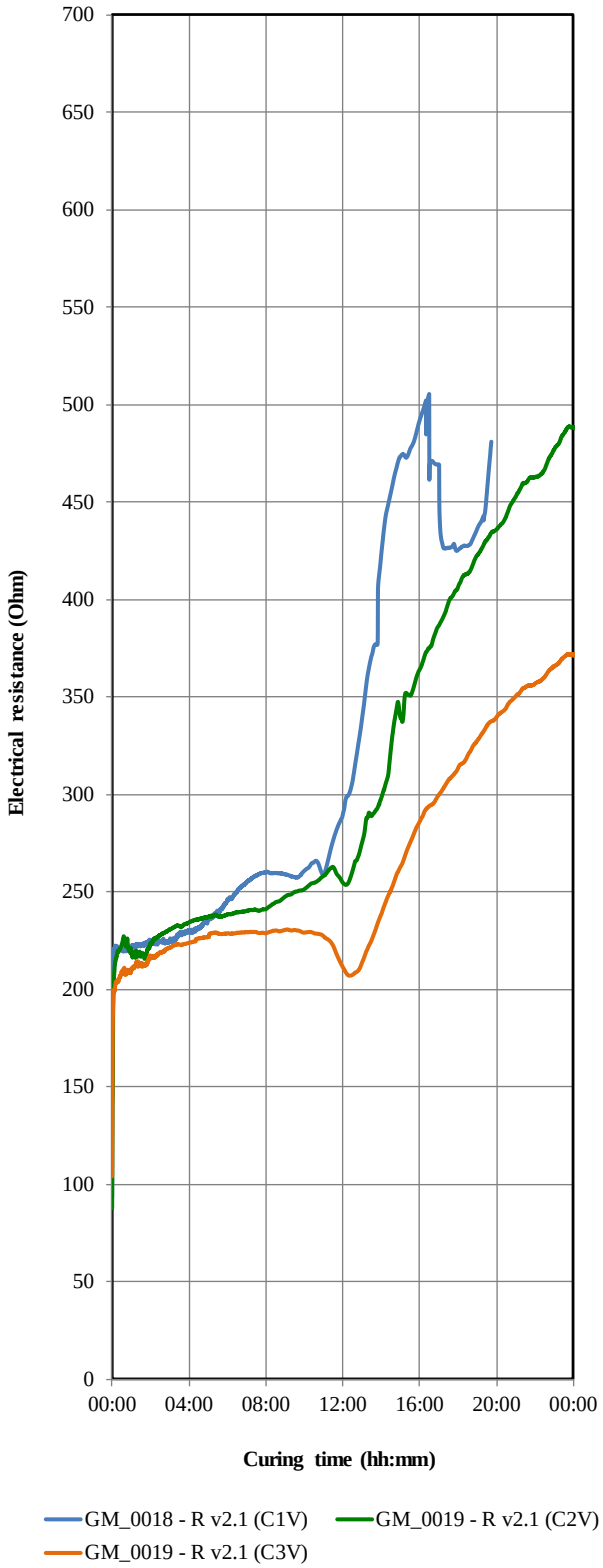

Figure D.10. Electrical resistance developments with time in shotcrete paste hydration stabiliser (24 hours).

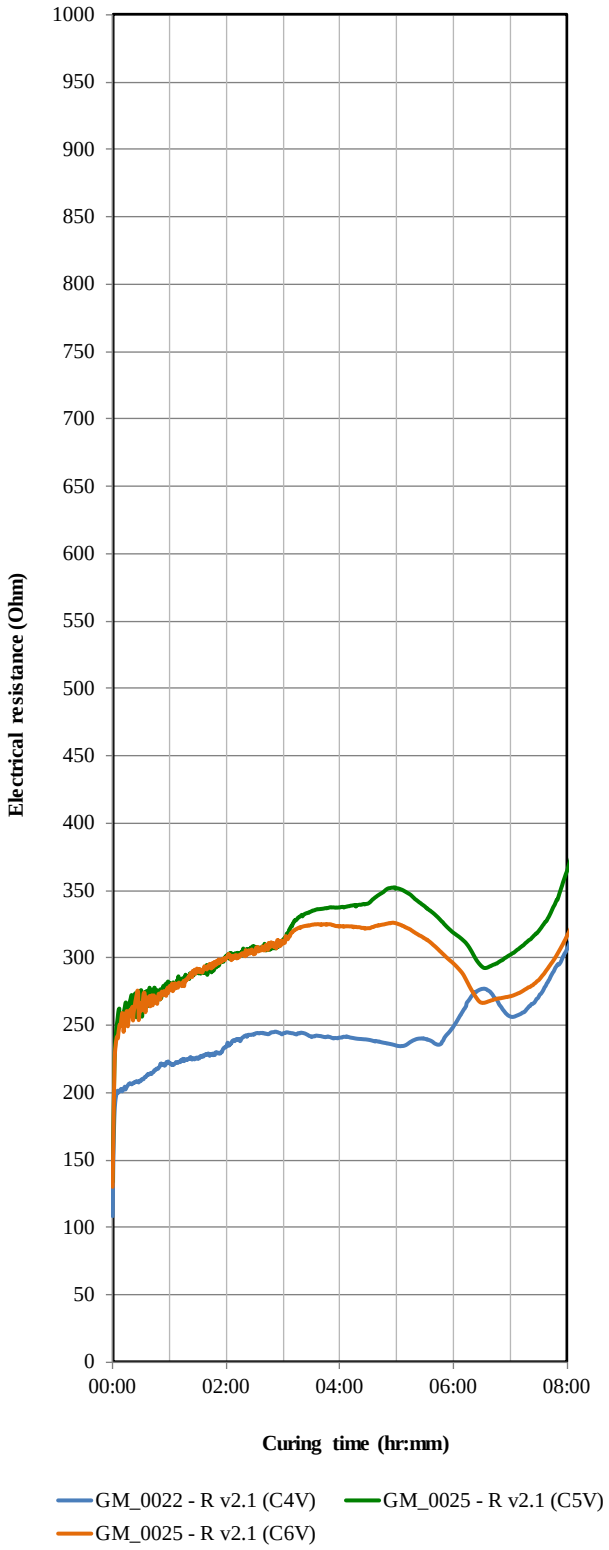

Figure D.11. Electrical resistance developments with time in shotcrete paste with water reducing admixture (8 hours).

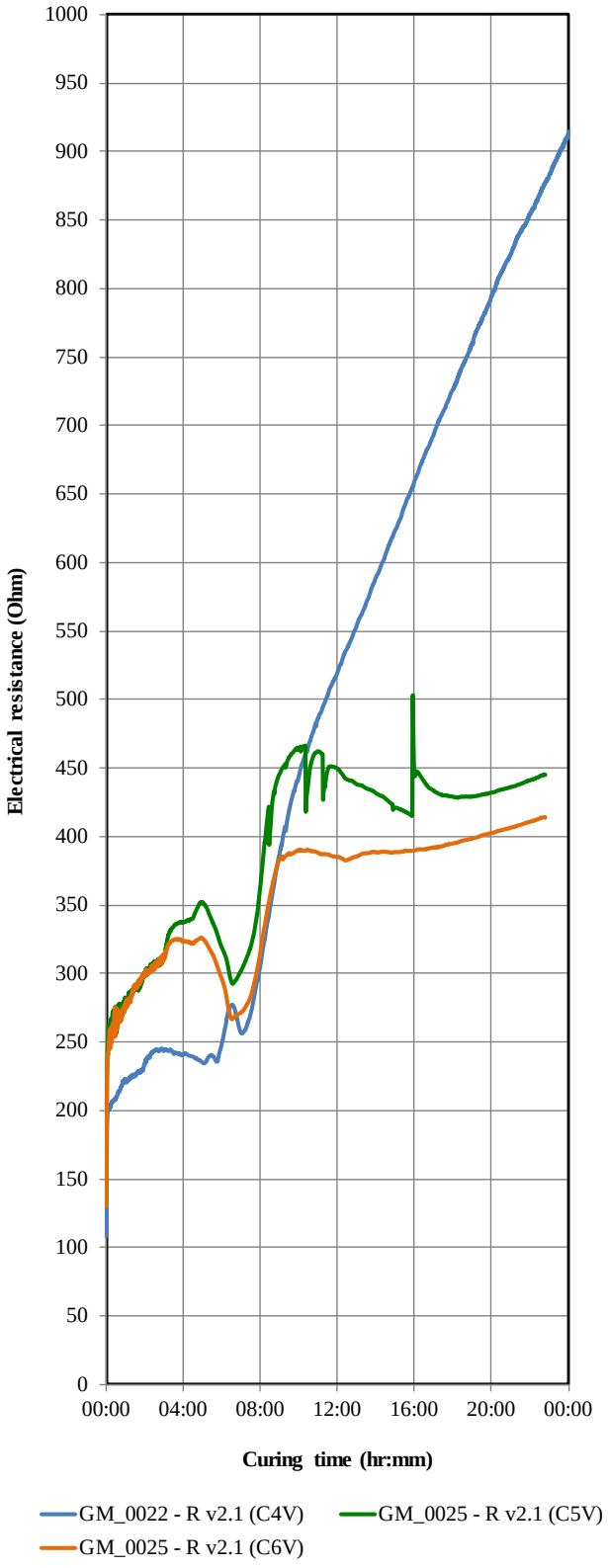

Figure D.12. Electrical resistance developments with time in shotcrete past with water reducing admixture (24 hours).

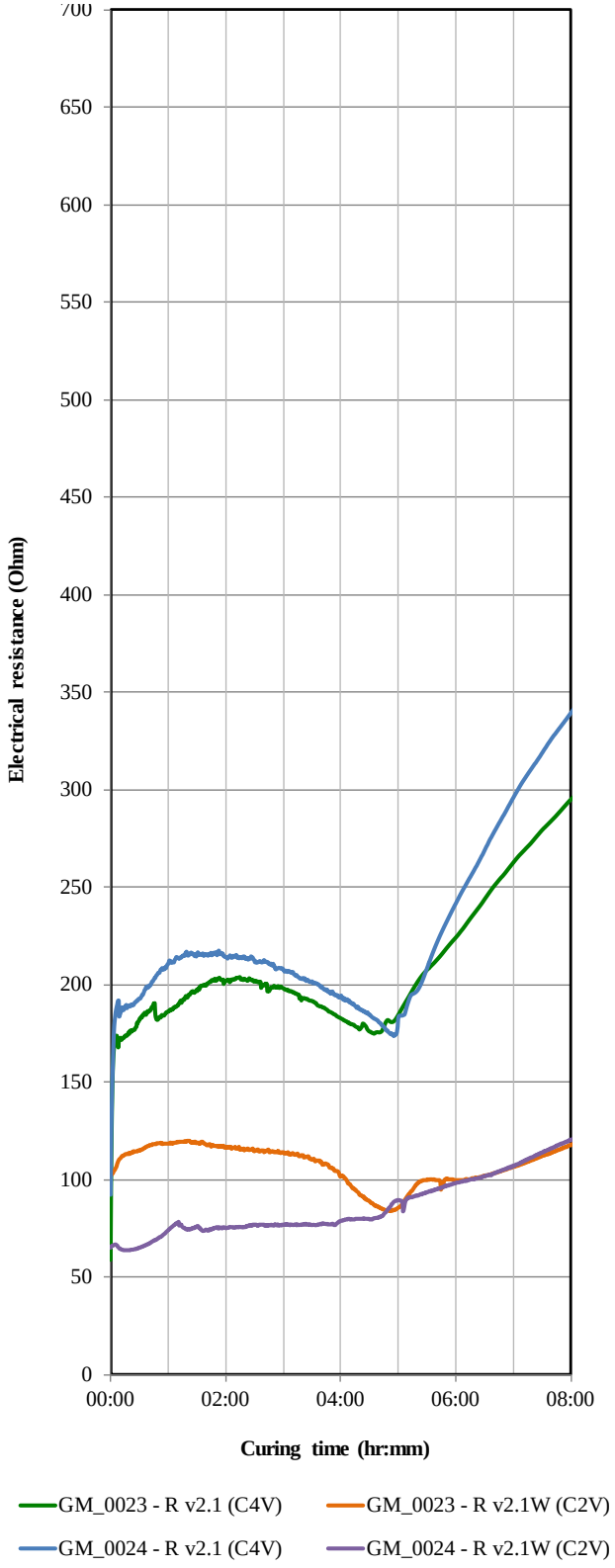

Figure D.13. Electrical resistance developments with time in shotcrete past without admixture (8 hours).

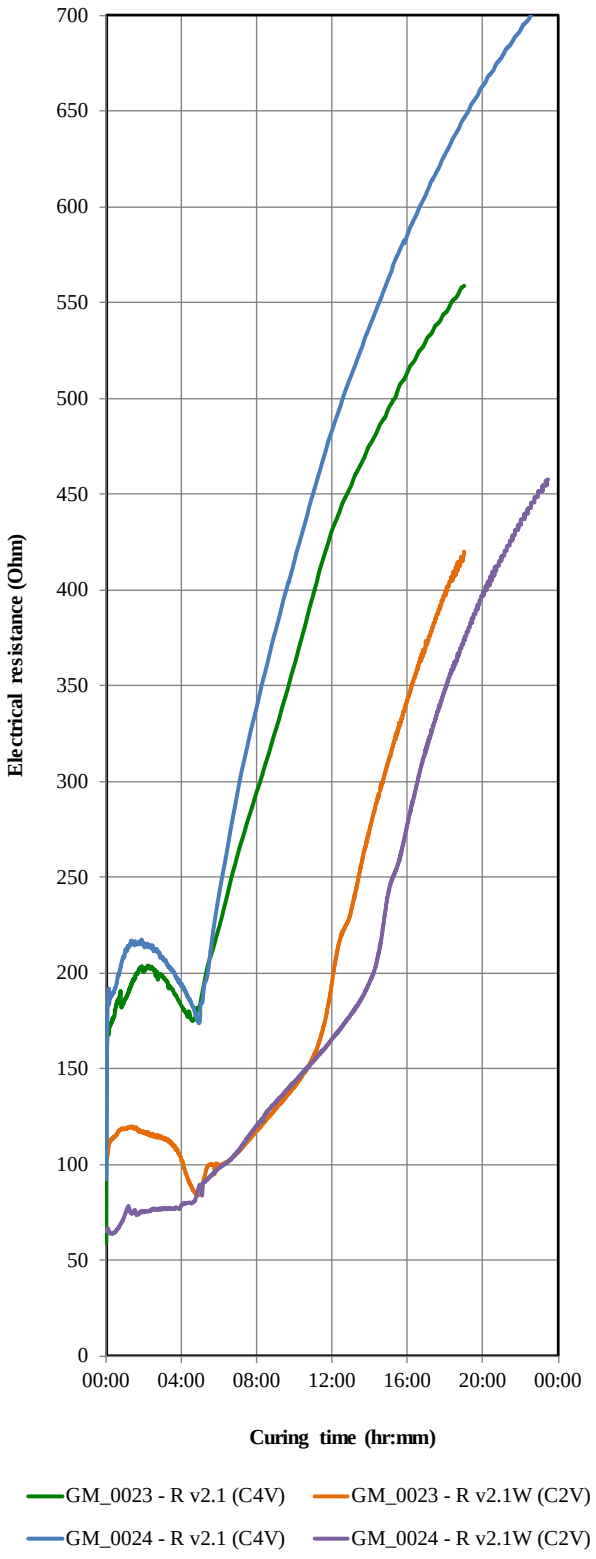

Figure D.14. Electrical resistance developments with time in shotcrete paste without admixture (24 hours).

APPENDIX – E

TRIAXIAL TEST RESULTS FOR STEEL FIBRE REINFORCED SHOTCRETE

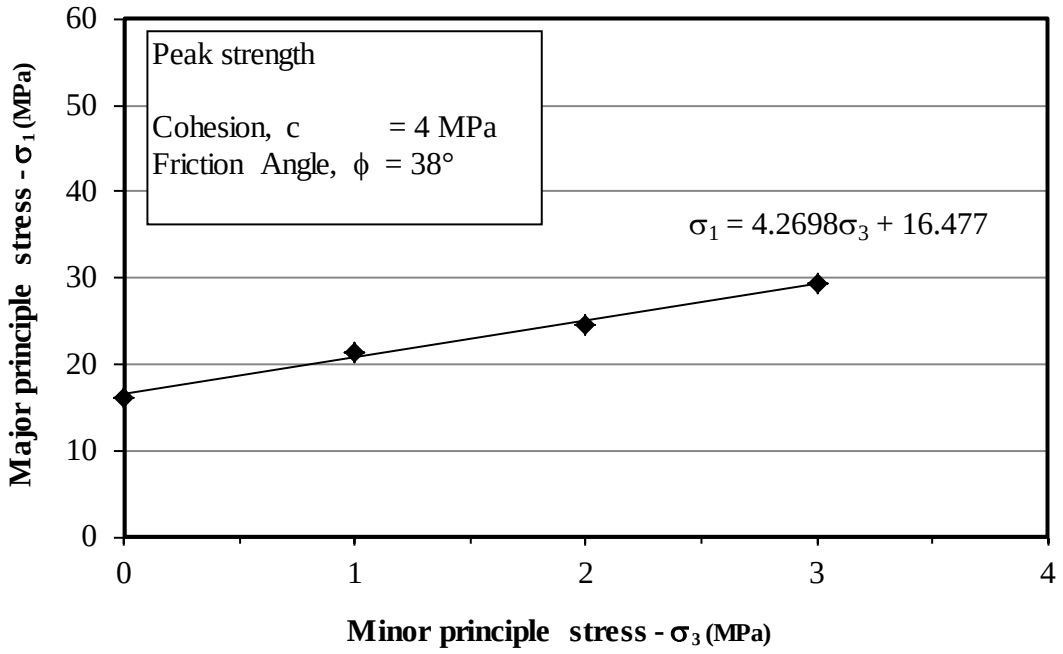

Figure E-1. Triaxial test result for shotcrete samples from batch No. 1– Peak strength (1 day curing).

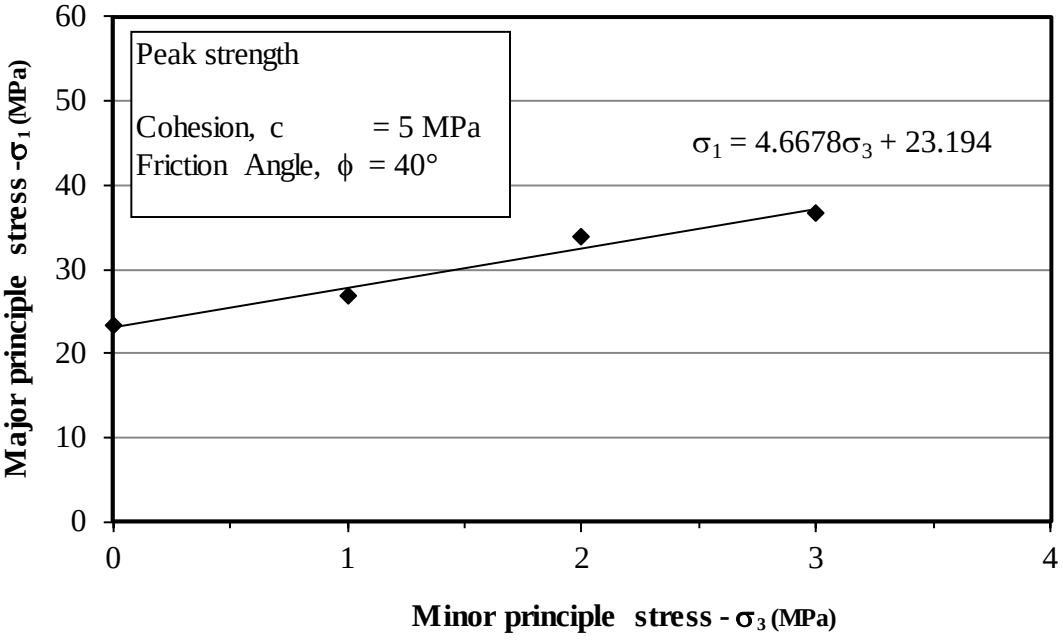

Figure E- 2. Triaxial test result for shotcrete samples from batch No. 1– Peak strength (3 days curing).

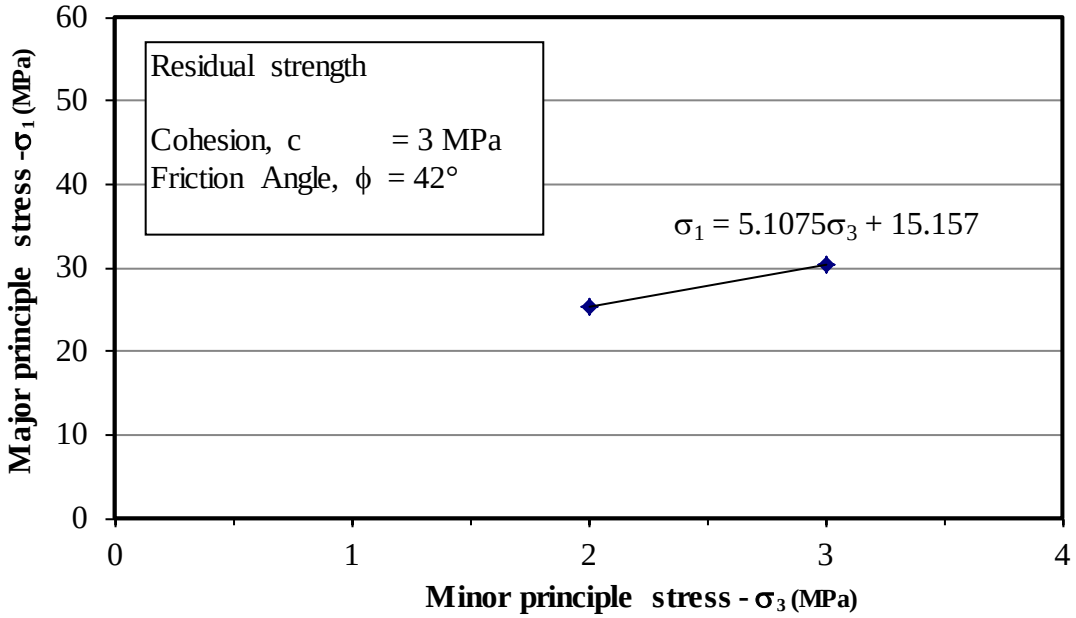

Figure E- 3. Triaxial test result for shotcrete samples from batch No. 1 – Residual strength (3 days curing).

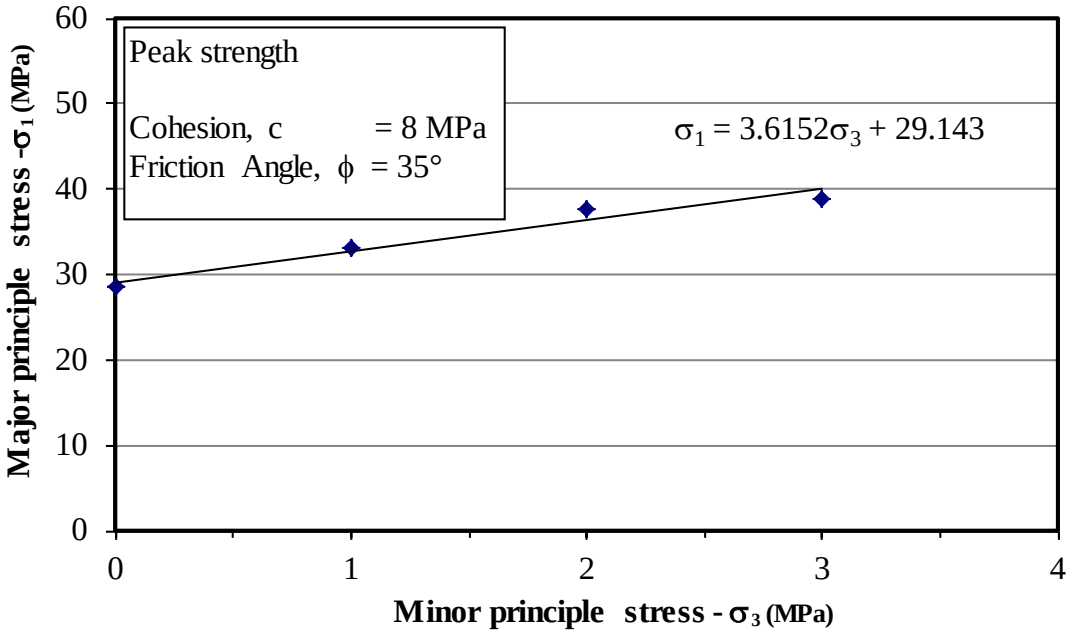

Figure E- 4. Triaxial test result for shotcrete samples from batch No. 1 – Peak strength (7 days curing).

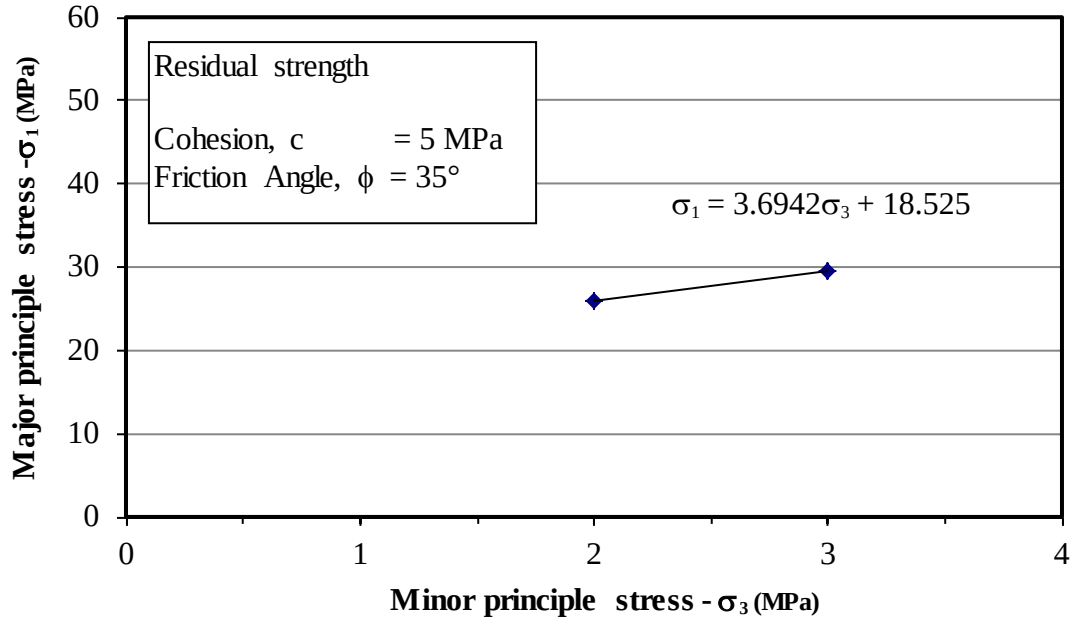

Figure E- 5. Triaxial test result for shotcrete samples from batch No. 1 – Residual strength (7 days curing).

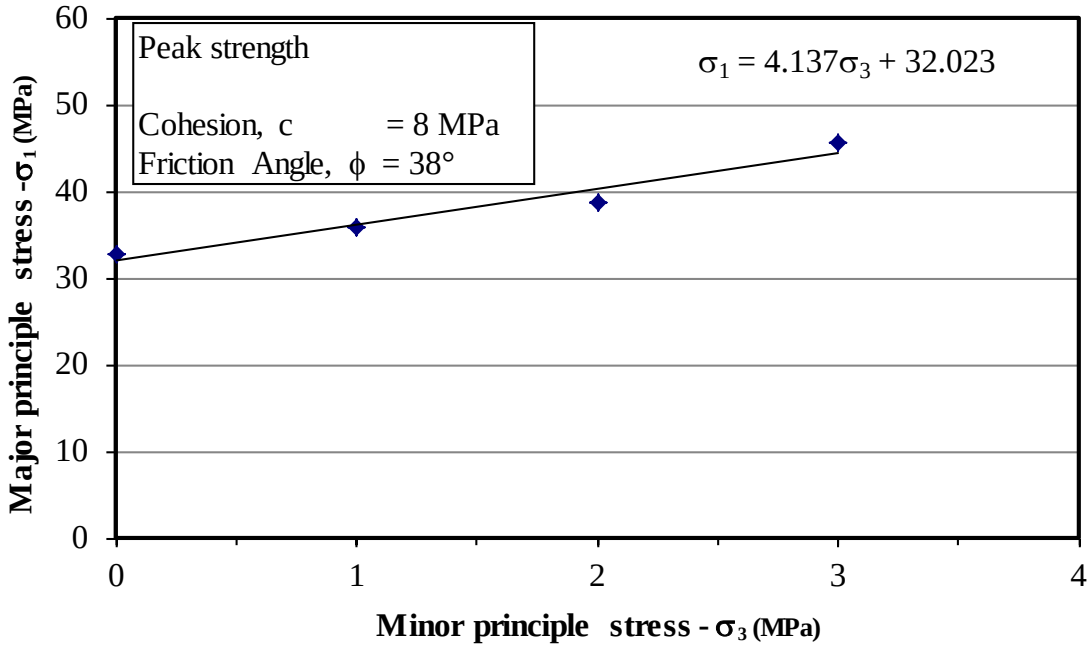

Figure E- 6. Triaxial test for shotcrete samples from batch No. 1– Peak strength (28 days curing).

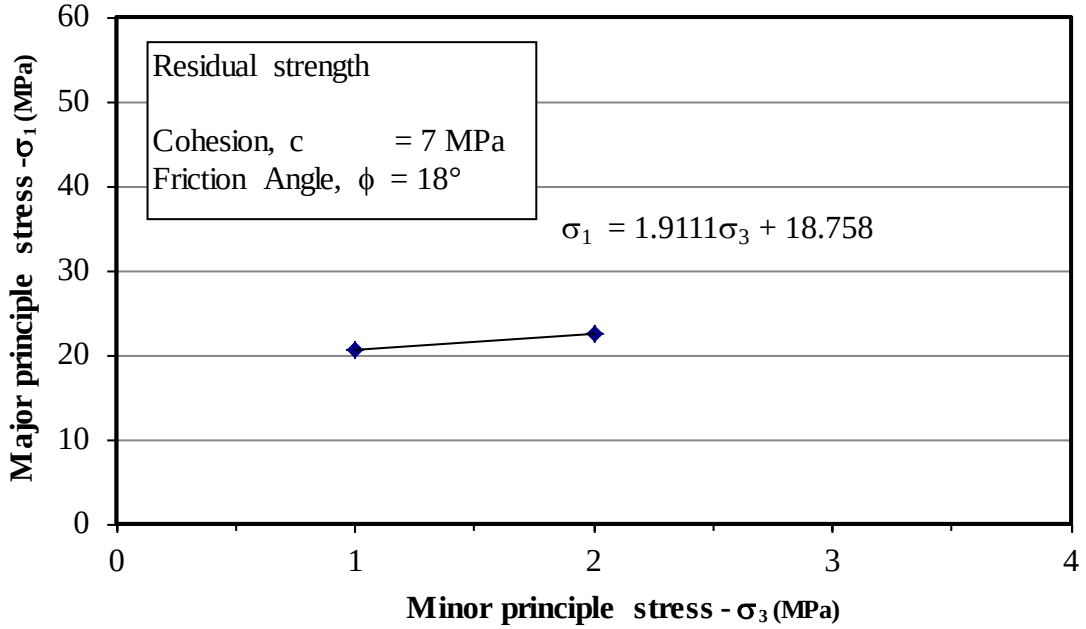

Figure E- 7. Triaxial test result for shotcrete samples from batch No.1– Residual strength (28 days curing).

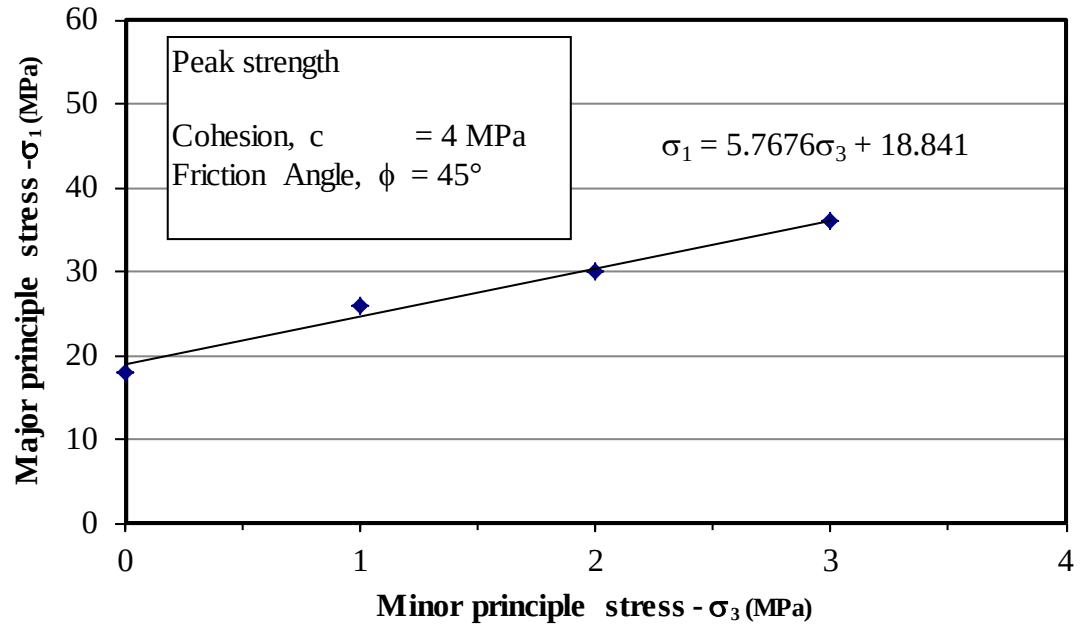

Figure E- 8. Triaxial test result for shotcrete samples from batch No.2– Peak strength (1 day curing).

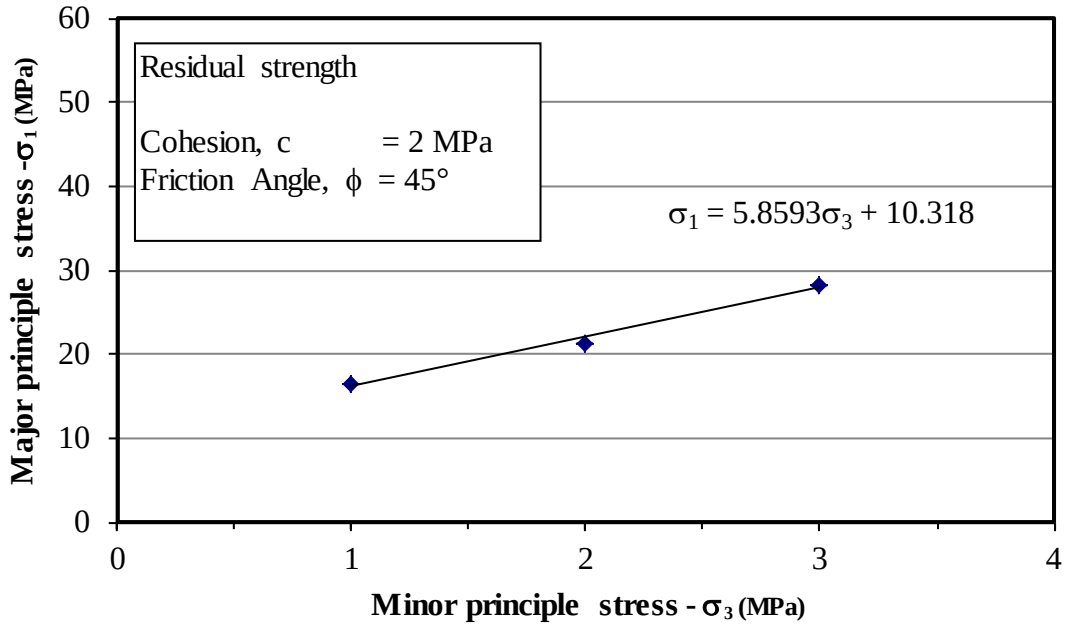

Figure E- 9. Triaxial test result for shotcrete samples from batch No. 2 – Residual strength (1 day curing).

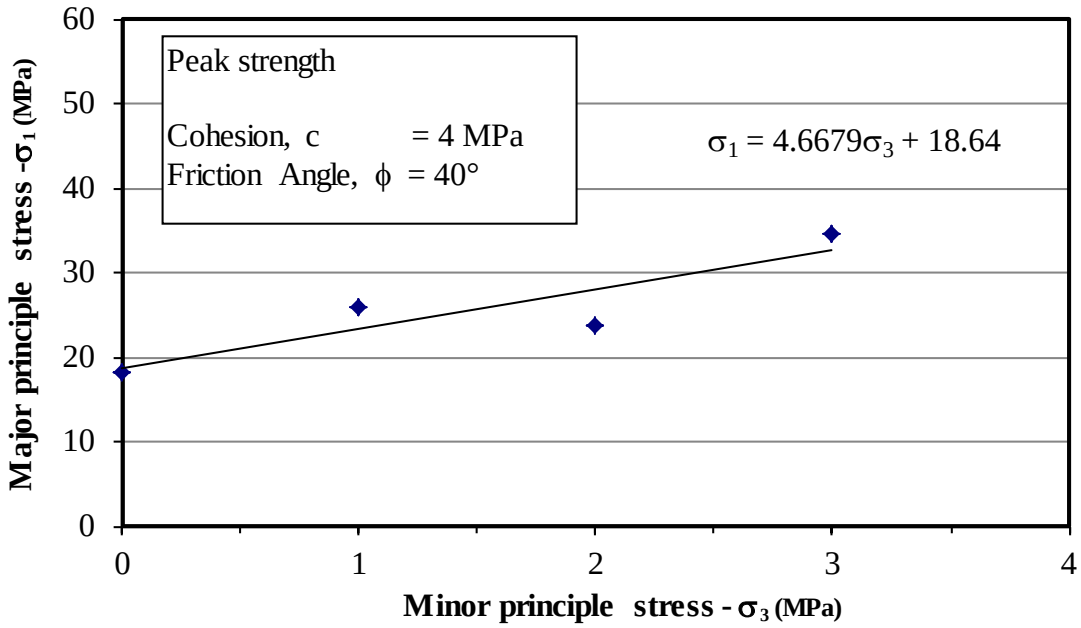

Figure E- 10. Triaxial test result for shotcrete samples from batch No. 2 – Peak strength (3 days curing).

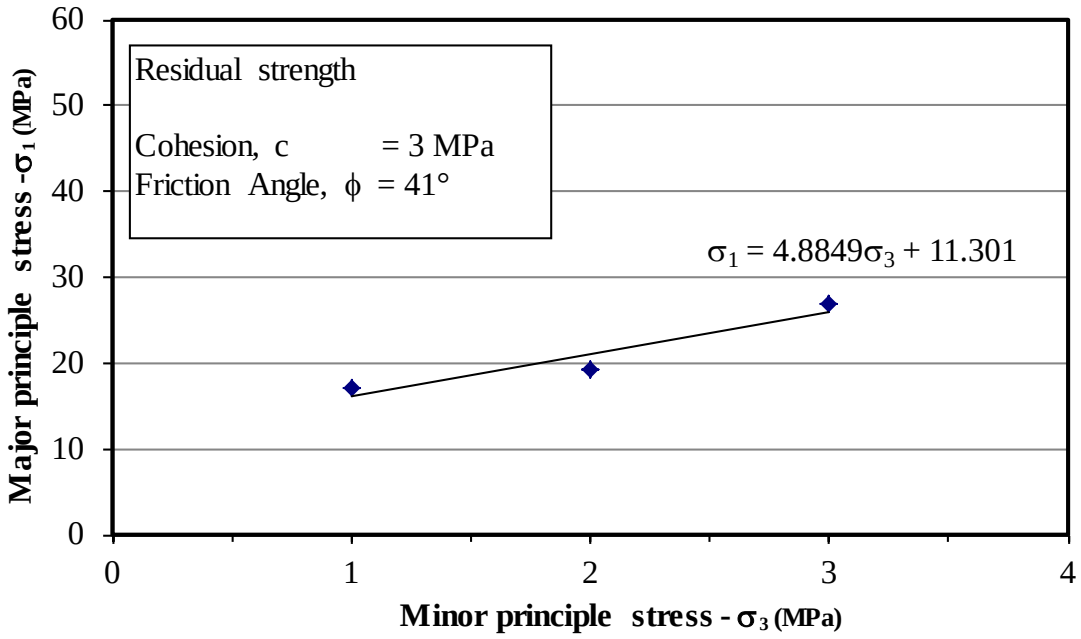

Figure E- 11. Triaxial test result for shotcrete samples from batch No. 2 – Residual strength (3 days curing).

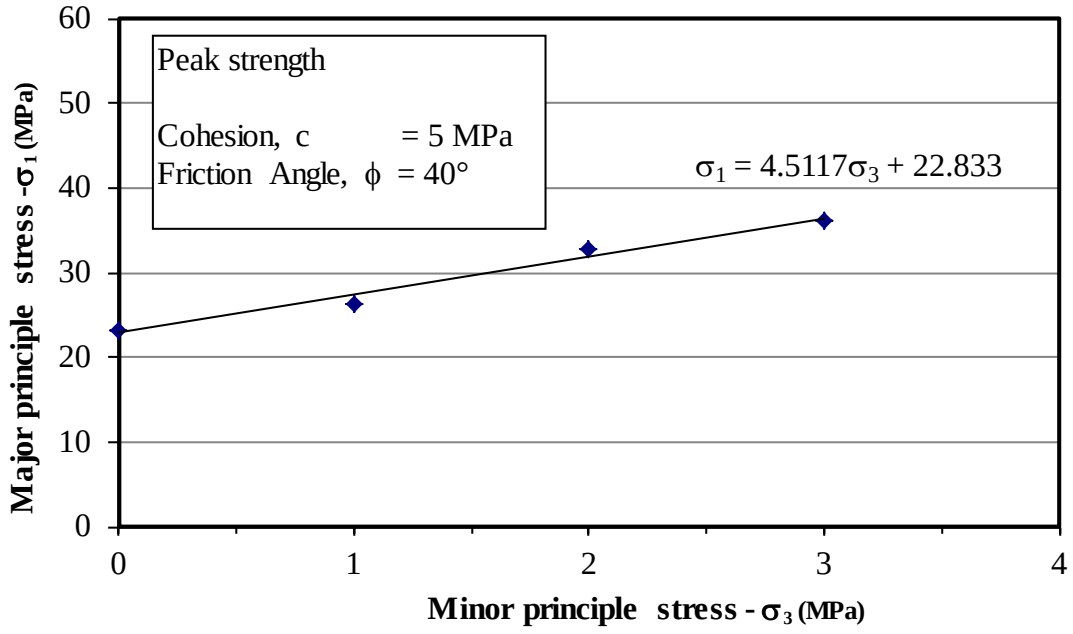

Figure E- 12. Triaxial test result for shotcrete samples from batch No.2– Peak strength (7 days curing).

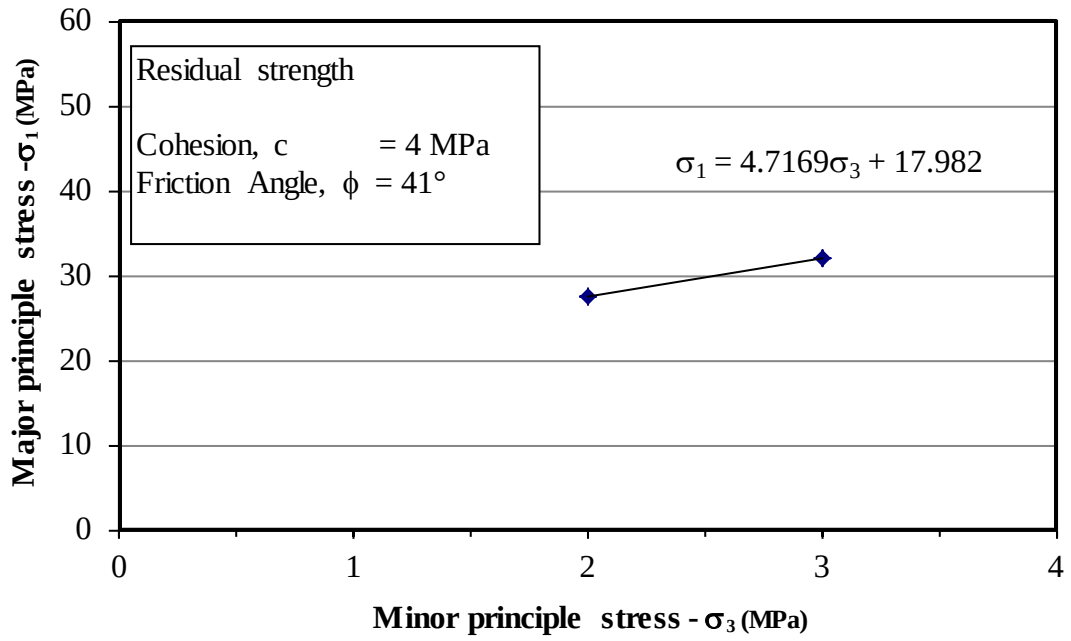

Figure E- 13. Triaxial test result for shotcrete samples from batch No.2 – Residual strength (7 days curing).

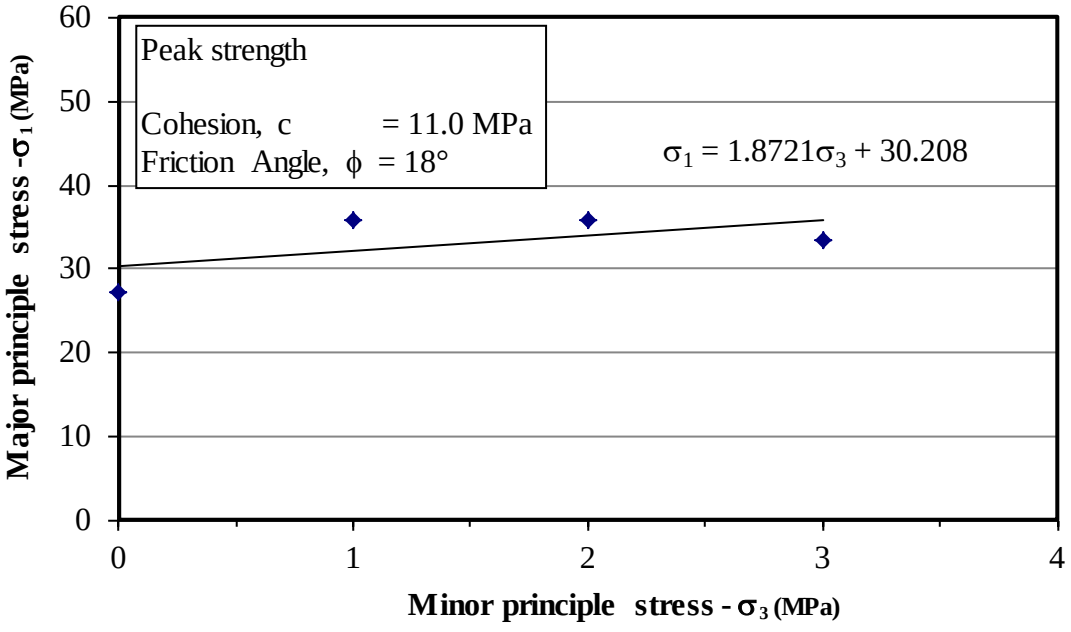

Figure E- 14. Triaxial test result for shotcrete samples from batch No.2 – Peak strength (28 days curing).

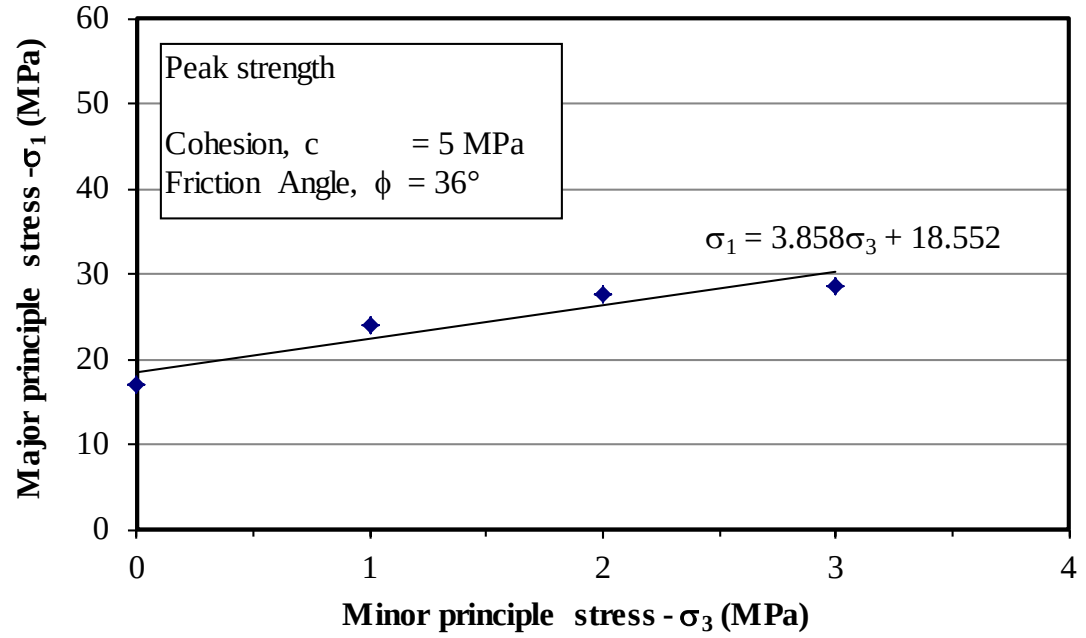

Figure E- 15. Triaxial test result for shotcrete samples from batch No.3– Peak strength (1 day curing).

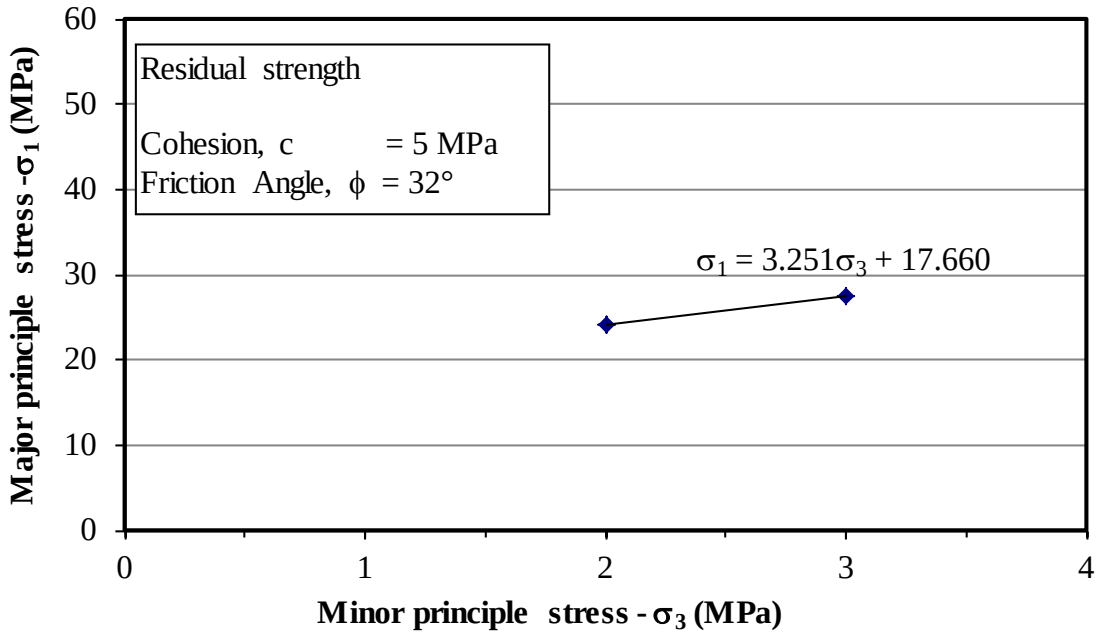

Figure E- 16. Triaxial test result for shotcrete samples from batch No.3– Residual strength (1 day curing).

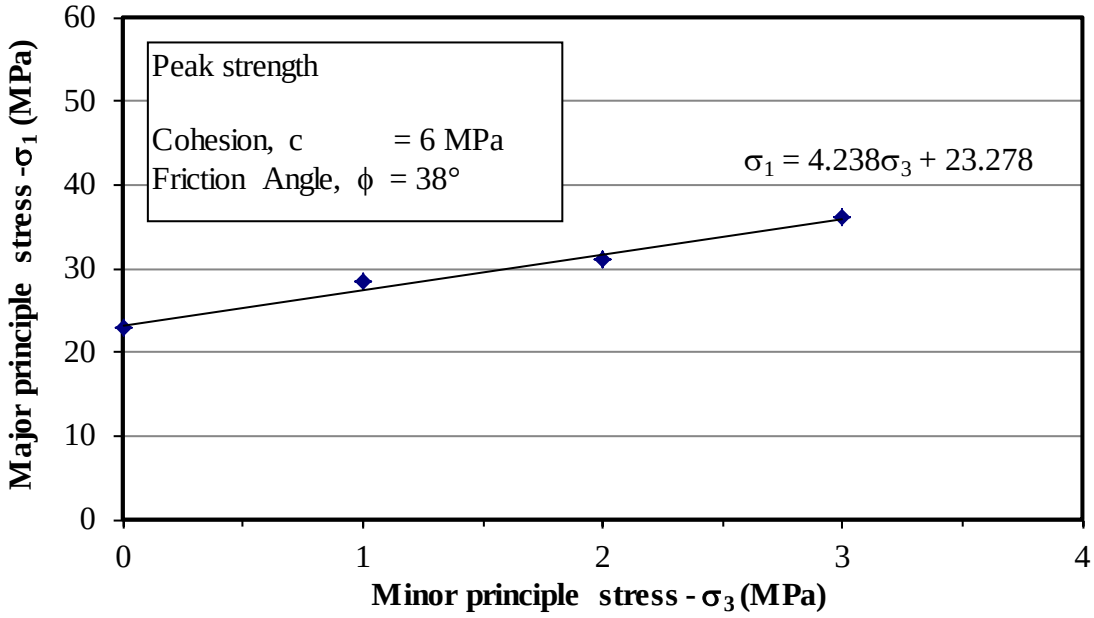

Figure E- 17. Triaxial test result for shotcrete samples from batch No.3– Peak strength (3 day curing).

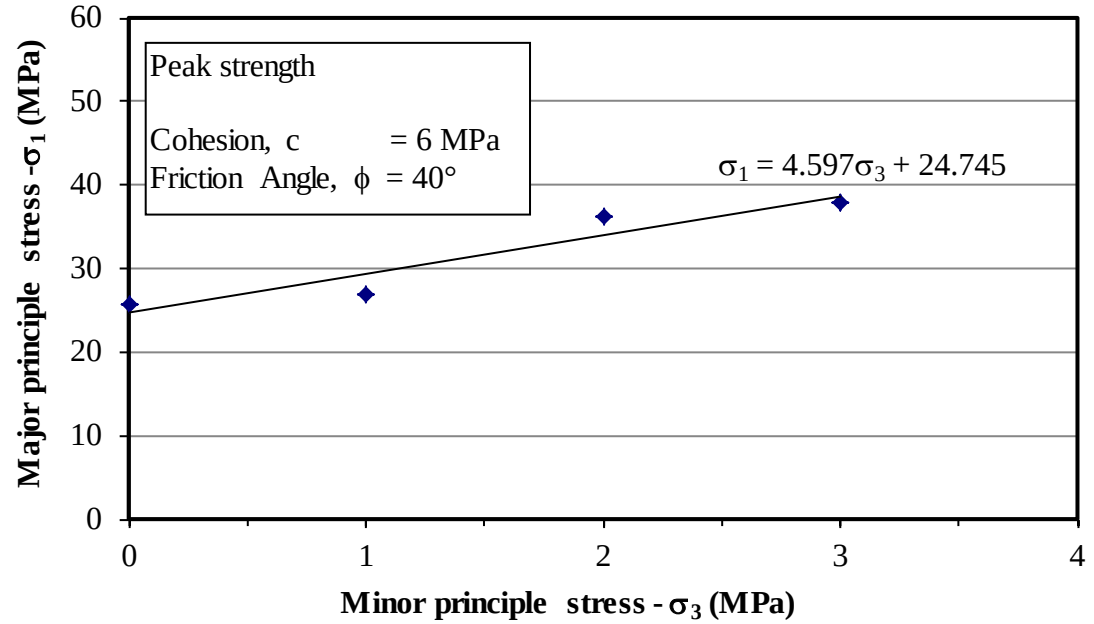

Figure E-18. Triaxial test result for shotcrete samples from batch No.3– Peak strength (7 day curing).

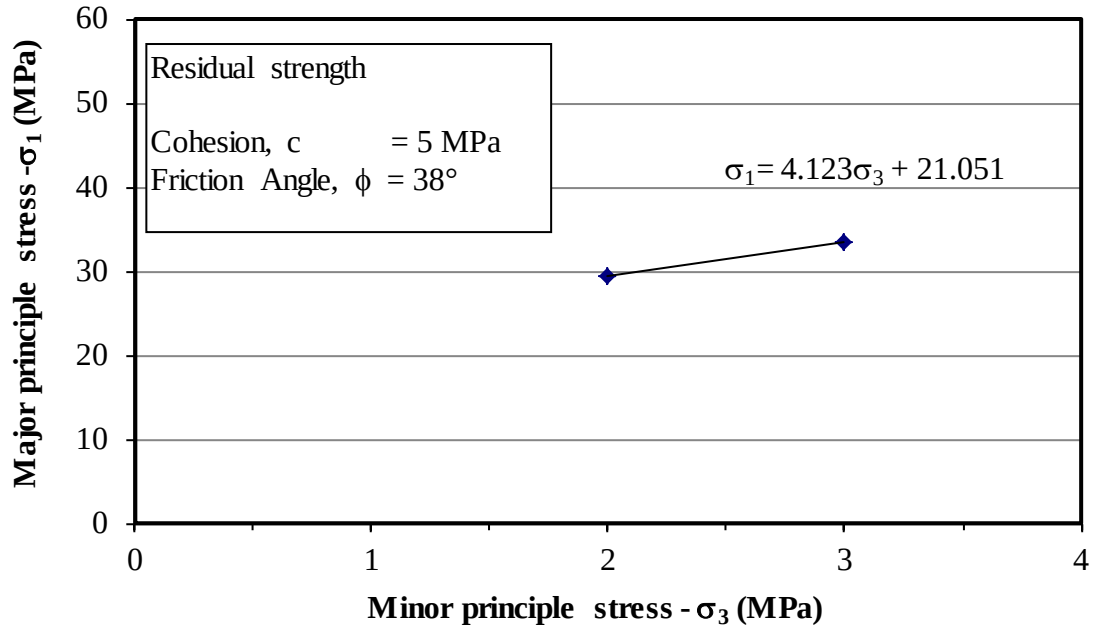

Figure E-19. Triaxial test result for shotcrete samples from batch No.3– Residual strength (7 day curing).

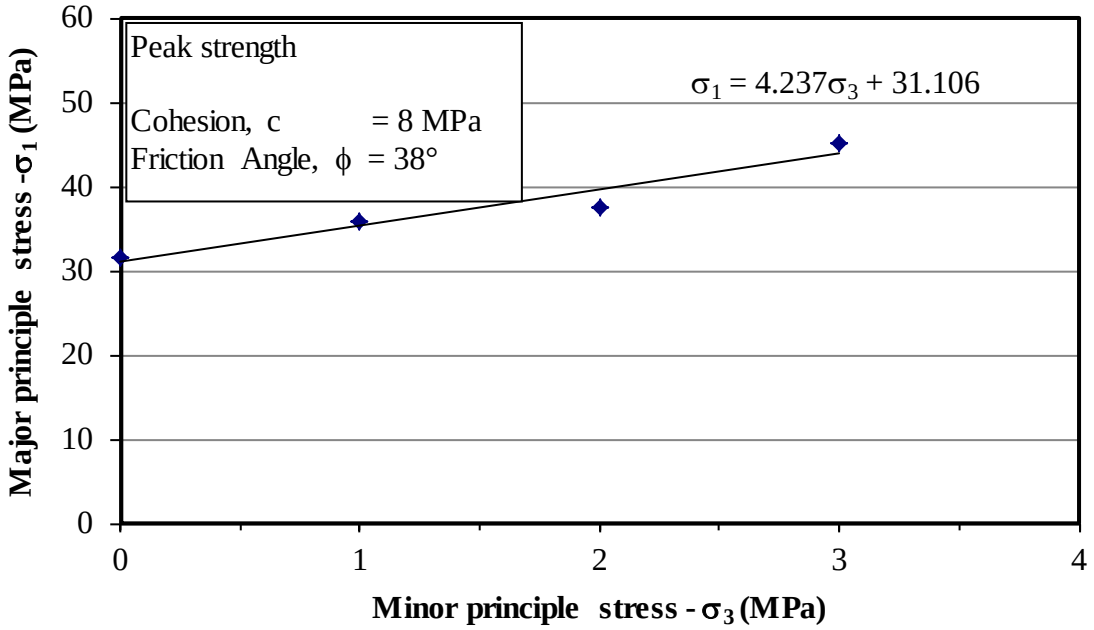

Figure E-20. Triaxial test result for shotcrete samples from batch No.3– Peak strength (28 day curing).